Structural Performance of Expanded Slate Lightweight Self-Consolidating Concrete Containing Polymeric Fibers

By

© Ahmed Taha Mohamed Omar, B.Sc., M.Sc.

A thesis submitted to

The School of Graduate Studies

in partial fulfillment of the requirements for the degree of

Doctor of Philosophy (Civil Engineering)

Faculty of Engineering and Applied Science

Memorial University of Newfoundland

May 2023

St. John's, Newfoundland, Canada

Abstract

This thesis investigates the possibility of using different polymeric fibers in the development of a number of successful lightweight self-consolidating concrete (LWSCC) and lightweight vibrated concrete (LWVC) mixtures with minimum possible density and improved mechanical properties. The investigation examines different replacement levels of normal-weight fine or coarse aggregates by fine and coarse lightweight expanded slate (Stalite) aggregates to optimize these mixtures. The research program was divided into four stages. The first stage aimed to develop and optimize a number of successful LWSCC and fiber-reinforced LWSCC (FRLWSCC) with minimum possible density, adequate mechanical properties and maximized impact resistance using expanded slate lightweight coarse (LC) and lightweight fine (LF) aggregate. The second stage evaluated the mechanical properties of these developed mixtures under cold temperatures. The effect of using different polymeric fibers' types, lengths, and volumes on enhancing the shear and flexural performance of large-scale reinforced LWSCC beams was investigated in the third stage of this program. Finally, the fourth stage examined the influence of combining PVA fibers and the maximum possible volume of Stalite aggregates on the structural performance of exterior beam-column joints (BCJs) under reversed cyclic loading.

The results indicated that it was possible to use up to 0.3% fraction volume of polymeric fibers with a binder content of 550 kg/m^3 to develop LWSCC mixtures with acceptable self-compactability. Increasing the binder content to 600 kg/m^3 allowed a maximum of 0.5% fibers and higher content of lightweight expanded slate aggregate to be used safely, achieving further reduction of the mixture density and better improvements in the tensile

strength. It was also concluded that, when comparing different lengths of polymeric fibers, the highest improvement in the impact resistance of tested FRLWSCC mixtures was observed when shorter fibers were used. Under sub-zero temperatures, the results revealed that increasing the volume of either LC or LF in the mixture showed more improvement in the mechanical properties and impact resistance under cold temperatures, however, the failure mode of these mixtures appeared to be more brittle.

Replacing normal-weight aggregates, in the third stage, with either LC or LF to reduce the mixtures' density by approximately 15% negatively affected the ultimate shear load, bending moment capacity, ductility, and energy absorption capacity of the tested beams. However, the use of 0.5% PVA fibers completely alleviated for these reductions in shear capacity and flexural strength of tested beams, and further helped the beams to achieve much higher ductility and absorbed energy. It was also found that using LF better improved the beams' load-carrying capacity, post-diagonal cracking resistance, deformability, ductility, and energy absorption capacity compared to using LC. Properly detailed LWSCC-BCJs (with sufficient hoops) showed slightly lower load-carrying capacity, ductility and dissipated energy, when compared to NWSCC specimen. The results also revealed that using high percentage of PVA fibers (1%) in the development of lightweight vibrated concrete (LWVC) compensated for the significant reduction in load-carrying capacity that resulted from using high Stalite content and helped improve the overall cyclic performance of BCJs. This improvement allowed to develop BCJ with significant enhancement in ductility, stiffness, and energy dissipation, while maintaining a considerable reduction in the self weight reached up to 28% lower than NWSCC.

Dedications

To the soul of my father, ***Taha Omar****,*

may Allah Almighty bless him.

To my mother and my brothers,

thank you for your constant love and support.

To my beloved wife, ***Nour****, who was always there for me,*

even on the tough days.

Acknowledgements

After thanking and praising Almighty "ALLAH" for his numerous blessings throughout my program of study and my entire life. I would like to express my sincere gratitude and deepest appreciation to my lovely wife, father, mother, and brothers for their endless support and inspiration throughout the course of my life.

This work would not have been made possible without the excellent guidance and assistance from my supervisor, Dr. Assem A. Hassan. Without your patient guidance, support, encouragement, valuable discussions, and great efforts, this project would not have been possible for me to complete so successfully.

As well, I would like to thank the highly respected supervisory committee members, Dr. Mohamed Ismail and Dr. Basem AbdelAleem, for their valuable discussions and recommendations. I would also like to extend my deepest gratitude to my colleague Mohamed Sadek for his help throughout the various stages of this work.

I would like to present my sincere thankfulness to my late father, who passed away during my preparation for this dissertation, for his great role in my life and his numerous sacrifices for me and for my brothers.

My deepest appreciation and love to my wife Nourhan for her infinite love and tender. She was always beside me supporting and encouraging me to complete this work. Without her in my life the completion of this research would not have been possible for me.

Ahmed Omar

Co-Authorship Statement

I, Ahmed Taha Omar, hold the principal author status for all the manuscript chapters (Chapters 2 - 8) in this dissertation. Chapter 2 was co-authored by my supervisor Prof. Assem Hassan and by the supervisory committee member Dr. Mohamed Ismail. Chapter 4 was co-authored by my co-researcher Mr. Mohamed Sadek and my supervisor Prof. Assem Hassan. Chapters 3, 5, and 6 were co-authored by my supervisor Prof. Assem Hassan. Chapters 7-8 were co-authored by my supervisor Prof. Assem Hassan and by the supervisory committee member Dr. Basem AbdelAleem. Co-authors contributions have facilitated the development of this work. Prof. Assem Hassan presented the idea for this project to me, and it was my task to carry out the work necessary to complete this manuscript and fulfill the requirements for PhD degree. In the papers presented in Chapters 2-8, I performed all experimental work including the development of concrete mixtures, casting small-scale and large-scale specimens, and the tests performed. I then collected the data obtained from those tests, analyzed the data, and formulated the results and conclusions presented in this thesis.

Described below is a detailed breakdown of the work facilitated by my team and me.

- Paper 1 in Chapter 2: Ahmed T. Omar, Mohamed K. Ismail, and Assem AA Hassan, "Use of polymeric fibers in the development of lightweight self-consolidating concrete containing expanded slate." Published in the Journal of Materials in Civil Engineering, ASCE.

I was the primary author, with the second and third authors contributing to the idea, its formulation, development, and refinement of the format in which it has been presented.

URL: https://doi.org/10.1061/(ASCE)MT.1943-5533.0003104

- Paper 2 in Chapter 3: Ahmed T. Omar, and Assem AA Hassan, “Use of polymeric fibers to improve the mechanical properties and impact resistance of lightweight SCC.” Published in Construction and Building Materials Journal.

I was the primary author, with the second author contributing to the idea, its formulation, development, and refinement of the format in which it has been presented.

URL: https://doi.org/10.1016/j.conbuildmat.2019.116944

- Paper 3 in Chapter 4: Ahmed T. Omar, Mohamed M. Sadek, and Assem AA Hassan, "Impact resistance and mechanical properties of lightweight SCC under cold temperatures." Published in ACI Materials Journal.

I was the primary author, with second and third authors contributing to the idea, its formulation, development, and refinement of the format in which it has been presented.

URL:
https://www.concrete.org/publications/internationalconcreteabstractsportal.aspx?m=details&id=51725975

- Paper 4 in Chapter 5: Ahmed T. Omar, and Assem AA Hassan, “Behavior of expanded slate lightweight SCC beams with improved cracking performance and shear capacity.” Published in Structures Journal.

I was the primary author, with the second author contributing to the idea, its formulation, development, and refinement of the format in which it has been presented.

URL: https://doi.org/10.1016/j.istruc.2021.03.108

- Paper 5 in Chapter 6: Ahmed T. Omar, and Assem AA Hassan, “Flexural performance of fiber-reinforced SCC beams containing expanded slate lightweight aggregates.” Submitted to Structures Journal.

I was the primary author, with the second author contributing to the idea, its formulation, development, and refinement of the format in which it has been presented.

- Paper 6 in Chapter 7: Ahmed T. Omar, Basem H. AbdelAleem, and Assem AA Hassan, "Performance of Stalite Lightweight SCC Beam-Column Joints under Reversed Cyclic Loading." Submitted to Engineering Structures Journal.

I was the primary author, with the second and third authors contributing to the idea, its formulation, development, and refinement of the format in which it has been presented.

- Paper 7 in Chapter 8: Ahmed T. Omar, Basem H. AbdelAleem, and Assem AA Hassan, "Cyclic behavior of expanded slate lightweight SCC beam-column joints containing different lengths of PVA fibers." Submitted to Engineering Structures Journal.

I was the primary author, with the second and third authors contributing to the idea, its formulation, development, and refinement of the format in which it has been presented.

Ahmed Omar

January 2023

Ahmed T. Omar

Date

Table of Contents

List of Tables

List of Figures

List of Symbols, Nomenclature or Abbreviations

ACI	American Concrete Institute
AS	Australian Standard
ASTM	American Society for Testing and Materials
BCJ	Beam-Column Joint
BI	Brittle Index
BS	British Standards
C/F	Coarse-to-Fine Aggregate
CSA	Canadian Standards Association
EC 2	Eurocode 2
EFNARC	European guidelines for Self-Consolidating Concrete
FA	Fly Ash
f_c'	Characteristic Compressive Strength of Concrete (MPa)
FRLWSCC	Fiber-Reinforced Lightweight Self-Consolidating Concrete
FS	Flexural Strength (MPa)
g	Acceleration due to gravity ($9{\cdot}81$ m/s^2)
h	Drop height in impact test
HRWRA	High-Range Water-Reducer Admixture
IE	Impact Energy
LC	Expanded slate lightweight coarse aggregate
LF	Expanded slate lightweight fine aggregate
l_f/d_f	Fiber aspect ratio
LWA	Lightweight aggregate
LWC	Lightweight Concrete
LWSCC	Lightweight self-consolidating concrete
LWVC	Lightweight vibrated concrete
m	Mass of drop hammer
M_{cr}^{exp}	Experimental First Cracking Moment

M_{cr}^{theo}	Theoretical First Cracking Moment Calculated by Design Codes
ME	Modulus of Elasticity
MK	Metakaolin
M_u^{exp}	Experimental Bending Moment Capacity
M_u^{theo}	Theoretical Bending Moment Capacity Calculated by Design Codes
N	Number of drops
N_1	Number of drops required to cause the first crack
N_2	Number of drops required to cause the failure crack
NC	Normal-weight coarse aggregate
NF	Normal-weight fine aggregate
NWC	Normal-Weight Concrete
NWSCC	Normal-Weight Self-Consolidating Concrete
PP	Polypropylene Fiber
PVA	Polyvinyl Alcohol Fiber
SCC	Self-Consolidating Concrete
SCMs	Supplementary Cementing Materials
STS	Splitting Tensile Strength of Concrete (MPa)
T_{50}	Time to reach a diameter of 500 mm in the slump flow test
$T_{50\text{-}J}$	Time to reach a diameter of 500 mm in the J-ring test
VC	Vibrated Concrete
V_{exp}	Experimental ultimate shear load
V_f	Volume Fraction of Fibres
V_{nz}	Normalized Shear Load
V_{pred}	Predicted shear load Calculated by design codes
V_u	Ultimate Shear Load
w/b	Water-to-Binder Ratio
β	Factor accounting for shear resistance of cracked concrete
μ	Ductility Index
λ	Modification factor for lightweight concrete

1. Introduction

1.1 Background and Research Motivation

The use of lightweight aggregates in modern construction industry has gained interest due to the global move towards developing sustainable structures. Using lightweight aggregates (LWAs) to produce structural lightweight concrete (LWC) can significantly reduce the self-weight of concrete structures, affording a considerable reduction in design loads. This contributes toward reaching a more economical design with minimized structural dimensions, providing a smaller seismic demand, and introducing potential savings in construction expenses (Mousa et al., 2018; Alqahtani et al., 2021). Moreover, LWC has the potential to reach relatively high strength levels, attaining a convenient strength-to-weight ratio and sustainability properties (Sari & Pasamehmetoglu, 2005). Consequently, this type of concrete has been widely adopted with great success in various structural applications including long-span bridges, high-rise buildings, and ocean platforms (Fernandez & Pardo, 2013; Chai, 2016). However, it is frequently pointed out that the mechanical characteristics and failure modes of LWC members are quite different from that of normal-weight concrete (NWC). Previous researchers report that, under similar loading conditions, LWC commonly exhibits lower modulus of elasticity, steeper descending portion of stress-strain curve, lower shear capacity, and more brittle fracture characteristics, when compared to counterpart NWC (Chi et al., 2003; Yang et al., 2014).

Lightweight self-consolidating concrete (LWSCC) is one of the latest innovations in concrete technology that combines the structural benefits of LWC and desired properties

of self-consolidating concrete (SCC). Properly designed LWSCC can spread readily under its own weight without segregation, completely fill the formwork, and encapsulate the reinforcement without the necessity of mechanical consolidation, which significantly reduces construction time and labor demand (Lotfy et al., 2016a). The application of LWSCC in construction projects has gradually increased, specifically in the area of offshore and marine structures, rehabilitation and strengthening of existing buildings, and precast industry (Shi et al., 2005; Azmee & Shafiq, 2018). Due to the growing interest towards using LWSCC in construction, several attempts have been made to investigate the influence of material properties and mix proportions on the rheological behavior and mechanical properties of LWSCC (Bogas et al., 2012; Abouhussien et al., 2015; Lotfy et al., 2016b). These attempts revealed that optimizing the flowability and stability of LWSCC is challenging due to the risk of aggregate floating in such flowable mixture and the high-water absorption of LWAs during mixing. However, using relatively high binder content that contains supplementary cementing materials (SCMs) in the production of LWSCC was found to enhance the mixture viscosity, providing higher particle suspension, and therefore reduce the chance of aggregate segregation (Cyr & Mouret, 2003; Hassan et al., 2015a).[17-18] Nevertheless, the limited information available regarding the structural performance and ductility of large-scale LWSCC members still possess concerns among designers/engineers to expand the use of LWSCC in construction practices, especially in seismically active regions.

Beam-column joints (BCJs) are one of the most crucial components in RC frame structures under seismic loading that plays a significant role in maintaining structural integrity of the

structural system. Under strong earthquake events, BCJs are typically subjected to horizontal and vertical shear forces accompanied by large deformations that may lead to serious damage or global collapse of the structures. Over the last decades, designers have paid a great deal of attention to ensuring proper ductility and damage tolerance of these joints in order to prevent sudden collapse of structures. Ductility is a key factor in seismic design that reflects the ability of any structure to undergo significant deformations and dissipate the earthquake's energy without a substantial loss of strength. In this regard, closely spaced stirrups are recommended by seismic design codes (ACI 352, 2002; Eurocode 8, 2005) to be provided within the joint core to prevent the early shear strength degradation and ensure adequate ductility of BCJs. Nevertheless, closely spaced hoops' detailing usually forms congested areas and interrupts placing and consolidating the concrete within the joint. SCC is an ideal choice in this situation that can overcome the compaction difficulties and reduce the risk of segregation in such highly congested regions (Paultre et al., 2005).

Another innovative solution to reduce the congestion of lateral reinforcement in BCJs is the use of fiber-reinforced concrete. Adding fibers into concrete has proven to significantly improve the shear strength, ductility, stiffness degradation, energy dissipation, and damage tolerance of BCJs subjected to reverse cyclic loading (Ganesan & Shashikala, 2013; AbdelAleem & Hassan, 2019; Cardoso et al., 2019). The fibers' bridging mechanism effectively helps to transfer stress across crack interferences, providing residual strength to the concrete composite in post-peak stage (Grabois et al., 2016; Cardoso et al., 2019; Çelik & Bingöl, 2020). Meanwhile, the stitching action of fibers plays an effective role in

arresting cracks, thus effectively delaying the initiation of cracks and limiting their propagation (AbdelAleem & Hassan, 2019). Among the different types of fibers, steel fibers have been primarily used by researchers to improve the ductility, toughness, and impact resistance of concrete members. However, the low density of polymeric fibers is supposed to further decrease the self-weight of concrete. Further, polymeric fibers were found to have higher corrosion and alkali resistance and better dispersion in the matrix, compared to steel fibers (Corinaldesi & Moriconi, 2015; Jun Li et al., 2016). Polyvinyl alcohol (PVA) fiber is a novel type of synthetic fiber that has been mainly used in fiber-reinforced concrete to control shrinkage and thermal cracking. The high modulus and high bonding strength of PVA fibers with concrete matrix significantly enhances the tensile strength, ductility, and energy absorption capacity of concrete (Jun Li et al., 2016; Bastami, 2019). Recently, PVA fibers have been used as the main constituent in the development of engineered cementitious composite (ECC), affording convenient strain-hardening response (Wang & Li, 2007; Singh et al., 2019).

Despite all advantages associated with the use of fibers in concrete, developing SCC with synthetic/polymeric fibers is a challenge and requires more investigation. Previous studies indicated that the inclusion of high volume of fibers in concrete may result in high interference and collision with coarse aggregates and hence reduce the workability of fresh concrete (Hossain et al., 2013; Aslani & Kelin, 2018). Moreover, adding relatively low-density synthetic fibers to highly flowable mixtures encourages segregation of the fibers. This adds another challenge to optimizing the flowability and stability of the mixture (Bogas et al., 2012).

In spite of the potential difficulties on optimizing the fresh properties of SCC with LWA and fibers, developing such composites is increasingly needed in order to produce new types of concrete with higher strength-to-weight ratio, impact resistance, ductility, and energy absorption. In addition, despite the relatively strong strength of expanded slate (Stalite) lightweight aggregate compared to other types of lightweight aggregates (Oti et al., 2010; Hassan et al., 2015b), insufficient studies have been conducted to evaluate the structure performance of large-scale concrete elements made with this type of aggregate. Moreover, investigations of shear performance of fiber reinforced LWSCC members is missing from the literature, despite the high potential of fibers to enhance ductility and post-cracking resistance of concrete. Hence, the proposed research attempted to fill this knowledge gap by presenting a comprehensive investigation that aimed to develop and optimize a number of LWSCC and fiber-reinforced lightweight self-consolidating concrete (FRLWSCC) mixtures with maximized volume of LWA and different types, lengths, and volumes of polymeric fibers. This research focus on the structural performance of beam-column joints subjected to reverse cyclic loading, as well as flexural and shear behavior of full-scale reinforced concrete beams developed with the optimized mixtures.

1.2 Research Objectives and Significance

Despite the outstanding performance of expanded slate (Stalite) lightweight aggregates compared to all other LWAs (Oti et al., 2010; Hassan et al., 2015b), insufficient studies were conducted to assess the fresh and mechanical properties of SCC mixtures containing this type of lightweight aggregate, especially when different types, lengths and volumes of fibers were introduced. In addition, by reviewing the current literature, it can be seen that

investigating the structural performance of full-scale elements made with FRLWSCC mixtures is missing. Therefore, the present study attempts to fill this knowledge gap by optimizing the fresh properties, stability, and strength of a number of structural LWSCC and FRLWSCC mixtures developed with both fine and coarse Stalite aggregates and reinforced with different polymeric fibers (polyvinyl alcohol [PVA] and polypropylene [PP] fibers). The study investigated different replacement levels of normal-weight fine or coarse aggregates by fine and coarse lightweight expanded slate aggregates in order to obtain LWSCC mixtures with minimum possible density and improved mechanical properties. In order to achieve the research objectives, different binder contents (550 kg/m^3 and 600 kg/m^3), coarse-to-fine aggregate (C/F) ratios (0.7 and 1.0), fiber types (PVA and PP fibers), fiber lengths (8 mm, 12 mm, and 19 mm), and fiber volumes (0.3%, 0.5%, and 1%) were used in this investigation.

The research also aims to investigate the effect of using different polymeric fibers' types, lengths, and volumes on enhancing the shear and flexural performance of large-scale reinforced-concrete beams made with these optimized mixtures. The research also focusses on examining the potential benefits resulting from combining PVA fibers and the maximum possible volume of Stalite aggregates on the behavior of exterior BCJs when subjected to reversed cyclic loads. I believe that this experimental research will be useful to help designers/engineers make appropriate decisions on using FRLWSCC in the construction industry.

1.3 Thesis Outline

This dissertation consists of nine chapters described as follows:

Chapter 1 describes the research background, motivation, objectives, significance, and scope of the research completed in the current thesis.

Chapter 2 highlights the challenges and difficulties while developing a number of LWSCC mixtures with minimum possible density (maximized volume of expanded slate aggregate) and minimized reduction in stability and fresh properties using different mixture compositions and various SCMs, different types, lengths, and volumes of polymeric fibers.

Chapter 3 discusses the advantages that can be obtained from adding different types, lengths, and volumes of polymeric fibers into LWSCC and lightweight vibrated concrete (LWVC) mixtures developed with minimum possible density. In this chapter, the author discusses the role of fibers in alleviating the reductions in mechanical properties resulted from using LWA and in enhancing the impact resistance and cracking behavior of concrete samples.

Chapter 4 investigates the performance of some optimized LWSCC and FRLWSCC mixtures under cold temperatures, which is considered an important factor for structures in Arctic regions subjected to continuous dynamic impact loads resulting from drifting ice sheets, high waves, or iceberg collisions.

Chapter 5 aims to alleviate the reduction in shear strength of large-scale concrete beams, which is anticipated from the use of low-density lightweight aggregates, by adding optimum type and volume of PVA fibers into LWSCC mixtures. The structural performance of tested beams was assessed based on cracking pattern, load-deflection

response, shear capacity, post-diagonal cracking resistance, and energy absorption capacity. The experimental results were also compared with several code-based equations and selected proposed models from the literature that predict the shear strength of reinforced concrete beams with and without fibers.

Chapter 6 presents an extensive investigation into the flexural performance and ductility of large-scale concrete beams cast with optimized FRLWSCC mixtures. The structural performance of the tested beam specimens was assessed in terms of load-deflection response, cracking behavior, energy absorption, displacement ductility, cracking moment, and ultimate flexural strength. The performance of design code provisions in predicting the cracking and ultimate moment capacities of all tested specimens was also evaluated.

Chapter 7 evaluates the structural performance of LWSCC beam-column joints made with coarse/fine expanded slate lightweight aggregates under reversed cyclic loading. The contribution of joint shear reinforcement on enhancing the performance of the tested LWSCC joints in terms of strength degradation, deformability, ductility, and energy dissipation capacity was also assessed. The accuracy of design code provisions in predicting the shear and flexural strength of BCJs was also ascertained.

Chapter 8 examines the potential benefits resulting from combining PVA fibers and the maximum possible volume of expanded slate aggregate on the behaviour of exterior BCJs under reversed cyclic loads. This chapter also compares the cyclic behavior of NWSCC beam-column joints to that of LWSCC/LWVC developed with minimum possible density.

Chapter 9 presents the conclusions drawn from the completed research.

1.4 References

AbdelAleem, B. H., & Hassan, A. A. (2019). Influence of synthetic fibers' type, length, and volume on enhancing the structural performance of rubberized concrete. *Construction and Building Materials*, *229*, 116861.

Abouhussien, A. A., Hassan, A. A., & Ismail, M. K. (2015). Properties of semi-lightweight self-consolidating concrete containing lightweight slag aggregate. *Construction and Building Materials*, *75*, 63-73.

ACI Committee 352. (2002). Recommendations for design of beam-column connections in monolithic reinforced concrete structures (ACI 352R-02). *American Concrete Institute*, Farmington Hills, MI.

Alqahtani, F. K., Abotaleb, I. S., & Harb, S. (2021). LEED Study of Green Lightweight Aggregates in Construction. *Sustainability*, 13(3), 1395.

Aslani, F., & Kelin, J. (2018). Assessment and development of high-performance fibre-reinforced lightweight self-compacting concrete including recycled crumb rubber aggregates exposed to elevated temperatures. *Journal of Cleaner Production*, *200*, 1009-1025.

Azmee, N. M., & Shafiq, N. (2018). Ultra-high performance concrete: From fundamental to applications. *Case Studies in Construction Materials*, *9*, e00197.

Bastami, R. (2019). *Structural Performance of High-Strength Reinforced Concrete Beams Built with Synthetic Fibers* (Doctoral dissertation, Université d'Ottawa/University of Ottawa).

Bogas, J. A., Gomes, A., & Pereira, M. F. C. (2012). Self-compacting lightweight concrete produced with expanded clay aggregate. *Construction and Building Materials*, *35*, 1013-1022.

Cardoso, D. C., Pereira, G. B., Silva, F. A., Silva Filho, J. J., & Pereira, E. V. (2019). Influence of steel fibers on the flexural behavior of RC beams with low reinforcing ratios: Analytical and experimental investigation. *Composite Structures*, *222*, 110926.

Çelik, Z., & Bingöl, A. F. (2020). Fracture properties and impact resistance of self-compacting fiber reinforced concrete (SCFRC). *Materials and Structures*, *53*(3), 1-16.

Chai, Y. H. (2016). Service performance of long-span lightweight aggregate concrete box-girder bridges. *Journal of Performance of Constructed Facilities*, *30*(1), 04014196.

Chi, J. M., Huang, R., Yang, C. C., & Chang, J. J. (2003). Effect of aggregate properties on the strength and stiffness of lightweight concrete. *Cement and Concrete Composites*, *25*(2), 197-205.

Code, P. (2005). Eurocode 8: Design of structures for earthquake resistance-part 1: general rules, seismic actions and rules for buildings. *European Committee for Standardization*, Brussels, Belgium.

Corinaldesi, V., & Moriconi, G. (2015). Use of synthetic fibers in self-compacting lightweight aggregate concretes. *Journal of Building Engineering*, 4, 247-254.

Cyr, M., & Mouret, M. (2003). Rheological characterization of superplasticized cement pastes containing mineral admixtures: consequences on self-compacting concrete design. *Proceedings of seventh CANMET/ACI International Conference on*

Superplasticizers and Other Chemical Admixtures in Concrete, American Concrete Institute, Farmington Hills, Michigan, USA.

Fernandez, R. P., & Pardo, M. L. (2013). Offshore concrete structures. *Ocean Engineering*, *58*, 304-316.

Ganesan, N., Raj, B., & Shashikala, A. P. (2013). Behavior of self-consolidating rubberized concrete beam-column joints. *ACI Materials Journal*, *110*(6), 697.

Grabois, T. M., Cordeiro, G. C., & Toledo Filho, R. D. (2016). Fresh and hardened-state properties of self-compacting lightweight concrete reinforced with steel fibers. *Construction and Building Materials*, *104*, 284-292.

Hassan, A. A., Ismail, M. K., & Mayo, J. (2015a). Mechanical properties of self-consolidating concrete containing lightweight recycled aggregate in different mixture compositions. *Journal of Building Engineering*, *4*, 113-126.

Hassan, A. A., Ismail, M. K., & Mayo, J. (2015b). Shear behavior of SCC beams with different coarse-to-fine aggregate ratios and coarse aggregate types. *Journal of Materials in Civil Engineering*, *27*(11), 04015022.

Hossain, K. M. A., Lachemi, M., Sammour, M., & Sonebi, M. (2013). Strength and fracture energy characteristics of self-consolidating concrete incorporating polyvinyl alcohol, steel and hybrid fibres. *Construction and Building Materials*, *45*, 20-29.

Jun Li, J., gang Niu, J., jun Wan, C., Jin, B., & liu Yin, Y. (2016). Investigation on mechanical properties and microstructure of high performance polypropylene fiber reinforced lightweight aggregate concrete. *Construction and Building Materials*, *118*, 27-35.

Lotfy, A., Hossain, K. M., & Lachemi, M. (2016a). Durability properties of lightweight self-consolidating concrete developed with three types of aggregates. *Construction and Building Materials*, *106*, 43-54.

Lotfy, A., Hossain, K. M., & Lachemi, M. (2016b). Mix design and properties of lightweight self-consolidating concretes developed with furnace slag, expanded clay and expanded shale aggregates. *Journal of Sustainable Cement-Based Materials*, *5*(5), 297-323.

Mousa, A., Mahgoub, M., & Hussein, M. (2018). Lightweight concrete in America: presence and challenges. *Sustainable Production and Consumption*, *15*, 131-144.

Oti, J. E., Kinuthia, J. M., Bai, J., Delpak, R., & Snelson, D. G. (2010). Engineering properties of concrete made with slate waste. *Proceedings of the Institution of Civil Engineers-Construction Materials*, *163*(3), 131-142.

Paultre, P., Khayat, K. H., Cusson, D., & Tremblay, S. (2005). Structural performance of self-consolidating concrete used in confined concrete columns. *ACI structural journal*, *102*(4), 560-568.

Sari, D., & Pasamehmetoglu, A. G. (2005). The effects of gradation and admixture on the pumice lightweight aggregate concrete. *Cement and concrete research*, *35*(5), 936-942.

Shi, C., Yang, X., Yu, Z., & Khayat, H. (2005). Design and application of self-compacting lightweight concretes. In *SCC'2005-China: 1st International Symposium on Design, Performance and Use of Self-Consolidating Concrete* (pp. 55-64). RILEM Publications SARL.

Singh, M., Saini, B., & Chalak, H. D. (2019). Performance and composition analysis of engineered cementitious composite (ECC)–A review. *Journal of Building Engineering*, *26*, 100851.

Wang, S., & Li, V. C. (2007). Engineered cementitious composites with high-volume fly ash. *ACI Materials journal*, *104*(3), 233.

Yang, K. H., Mun, J. H., & Lee, J. S. (2014). Flexural tests on pre-tensioned lightweight concrete beams. *Proceedings of the Institution of Civil Engineers-Structures and Buildings*, *167*(4), 203-216.

2. Use of polymeric fibers in the development of lightweight SCC containing expanded slate

2.1 Abstract

This chapter aims to evaluate and optimize a number of lightweight self-consolidating concrete (LWSCC) mixtures containing coarse and fine aggregates, lightweight expanded slate, and reinforced with different types of polymeric fiber. The fibers used were 8- and 12-mm polyvinyl alcohol (PVA8 and PVA12), and 19-mm polypropylene (PP19). The developed mixtures included different binder contents (550 kg/m^3 and 600 kg/m^3), fiber volumes (0.3% and 0.5%), and coarse-to-fine (C/F) aggregate ratios (0.7 and 1.0). Two normal-weight self-consolidating concrete (NWSCC) mixtures made with fine and coarse crushed granite aggregates were also tested in this investigation for comparison. Although the use of polymeric fibers negatively affected the fresh properties of the mixture, it was possible to develop successful LWSCC mixtures with significantly improved flexural strength using up to 0.5% fibers. LWSCC mixtures with shorter fibers (PVA8) had better fresh properties and strengths compared to mixtures with longer fibers (PVA12 and PP19). A minimum of 550 kg/m^3 binder content was required to develop LWSCC mixtures with acceptable self-compactability. However, using 600 kg/m^3 binder content contributed to improving the fresh properties of the mixture, which allowed using higher content of lightweight expanded slate aggregate, achieving further reduction of the mixture density. The results also showed that unlike the lightweight coarse aggregates, the use of lightweight

fine aggregates helped to develop mixtures with higher flowability, passing ability, and strengths.

2.2 Introduction

In the last few decades, using lightweight concrete in the construction industry has received a great amount of interest due to its economic and structural benefits. This type of concrete is typically developed by replacing conventional fine and/or coarse aggregates, entirely or partially, with lightweight aggregates. Such low-density aggregates play an effective role in reducing the self-weight of concrete, which helps to reach minimized structural dimensions and therefore a more economical design. Moreover, in some applications, such as precast concrete elements, the use of lightweight concrete substantially reduces the transportation and handling costs (Umehara et al., 1994; Shi & Yang, 2005; Yao & Gerwick, 2006), thus reducing overall construction expenses (Ko & Choi, 2013). A new direction of research attempts to utilize different types of lightweight aggregates in the development of self-consolidating concrete (SCC), aiming to present a promising concrete type characterized by low-density and superior ability to flow through congested reinforcement, as well as the ability to fill complex formwork under the effect of self-compaction. This can effectively contribute to the construction industry by offering cost-effective structures and an easy construction process.

However, the development of SCC incorporating lightweight aggregates is considered a big challenge due to the low density of aggregate particles, which may easily move upward during fresh state and increase the risk of segregation. This problem was highlighted by Bogas et al. (2012) in which the use of expanded clay aggregate showed greater tendency

(compared to normal-weight aggregate) to segregate, thus reducing the stability of mixtures. Other researchers also studied the effect of using lightweight slag aggregate to produce normal-to-high strength semi-lightweight self-consolidating concrete mixtures (Abouhussien et al., 2015a). They concluded that a limited volume of lightweight coarse aggregate should be used to achieve acceptable fresh properties. Further increases in the volume of lightweight coarse aggregate led to a reduction in the passing ability and increased the risk of segregation, which highlights a significant concern regarding the performance of the developed mixtures in applications with congested reinforcement. Another challenge was raised by Choi et al. (2006), who evaluated the use of rhyolitic origin lightweight aggregate in SCC as a replacement for either the coarse or fine normal-weight aggregates. This study showed that although the mixtures achieved acceptable results in the slump flow test, the use of rhyolitic lightweight aggregate led to a high blockage in the V-funnel and U-box tests, thus yielding unsatisfactory results. A similar problem in the V-funnel test was found by Wu et al. (2009), when expanded shale aggregates were used. In addition to the negative effects of lightweight aggregates on the fresh properties of SCC, using lightweight coarse or fine aggregates generally reduces the compressive and tensile strengths of concrete (Abouhussien et al., 2015b; Hossain et al., 2013).

One of the main approaches to overcome the production challenges of SCC mixtures containing lightweight aggregate is achieving a balanced mixture viscosity, which offers adequate particle suspension as well as provides reasonable flowability. This can be achieved by optimizing the binary material system used. For example, the use of

supplementary cementing materials (SCMs) such as metakaolin (MK) and/or silica fume (SF) commonly enhances the mixture's viscosity, which results in higher particle suspension and stability (Cyr & Mouret, 2003; Lachemi et al., 2003). Other SCMs such as fly ash (FA) can be used to help achieve adequate flowability without overdosing the high-range water-reducer admixture (HRWRA) (Marar & Eren, 2011). Increasing the binder content can also contribute to reducing the friction and blockage between aggregate particles, thus allowing for better flowability and passing ability (Ismail & Hassan, 2015). Using high pozzolanic SCMs (such as MK or SF) or increasing the binder content not only improves the fresh properties, but it also can effectively boost the compressive and tensile strengths of SCC made with lightweight aggregates, which achieves reasonable strengths for various structural purposes (Hassan et al., 2015; Madandoust & Mousavi, 2012).

The mechanical properties of lightweight concrete, in particular the tensile strength, toughness, impact strength, and energy absorption capacity can also be improved by using different types of fibers such as steel and/or polymeric fibers (Hossain et al., 2013; Choi & Yuan, 2005; Khayat et al., 2014). For instance, Libre et al. (2011) reported that using 0.4% polypropylene (PP) fiber in lightweight concrete made with natural pumice aggregate improved the splitting tensile strength up to 26%; however, the 28-day compressive strength decreased by 8.5%. Similarly, Mazaheripour et al. (2011) noticed a 14% increase in the splitting tensile strength when 0.3% PP was added to lightweight concrete developed with lightweight expanded clay aggregate, while the compressive strength was not affected. Other researchers utilized steel fibers to improve the tensile strength of lightweight concrete (Choi et al., 2014; Iqbal et al., 2015). Li et al. (2017) evaluated the flexural properties of

lightweight concrete mixtures developed with 38 mm steel fibers using the most common test to evaluate the performance of fiber reinforced concrete (ASTM C1609). The authors concluded that the post cracking ductility of lightweight concrete mixtures significantly improved due to inclusion of fibers. Other studies conducted on fibered-SCC indicated that the use of fibers resulted in a general decay in the fresh properties of SCC. Corinaldesi and Moriconi investigated the workability of lightweight SCC mixtures produced using expanded clay aggregate and reinforced with macro and micro synthetic fibers (Corinaldesi & Moriconi, 2015). The results of this study indicated that the use of fibers negatively affected the passing ability of the developed mixtures. Such problem in the passing ability was also highlighted by Aslani and Kelin who studied the effect of polypropylene fibers in rubberized SCC mixtures developed with scoria lightweight aggregates (Aslani & Kelin, 2018). The results obtained from this study indicated that increasing the volume/length of fibers worsens the fresh properties and caused an accumulation of the fibers behind the J-ring bars which further reduced the passing ability of the mixtures. The addition of fiber reduced the flowability and increased the segregation, especially when the normal-weight aggregates were totally replaced. This was also confirmed by Hossain et al. (2013), in which using polyvinyl alcohol and steel fibers generally decayed the flowability and passing ability of SCC. Similar results were reported by other researchers (AbdelAleem et al., 2017), in which the use of fibers represented a potential challenge for researchers to develop SCC mixtures with acceptable fresh properties.

This investigation evaluated the fresh properties, stability, and strength of a number of developed fibered-LWSCC mixtures containing expanded slate aggregates. The

experimental test parameters included (i) various combinations of fine and coarse lightweight expanded slate aggregates and normal-weight crushed granite aggregates, (ii) different types of fibers including 8 and 12 mm polyvinyl alcohol (PVA8 and PVA12) fibers, and 19 mm polypropylene (PP19) fibers, (iii) different binder contents (550 kg/m^3 and 600 kg/m^3), (iv) two fiber volumes (0.3% and 0.5%), and (v) two coarse-to-fine (C/F) aggregate ratios (0.7 and 1.0). Two normal-weight self-consolidating concrete (NWSCC) mixtures made with fine and coarse crushed granite aggregates were also tested in this investigation for comparison. The properties measured in this investigation were HRWRA demand, flowability, passing ability, and segregation resistance in the fresh state, while the hardened state was evaluated using compressive strength and flexural strength (FS).

2.3 Research Significance

By reviewing the current literature, it can be seen that the use of either fine or coarse expanded slate aggregates in the development of LWSCC is not well evaluated, especially when fibers were introduced. Therefore, the present study attempts to fill this knowledge gap by optimizing the fresh properties, stability, and strength of a number of fibered-LWSCC mixtures developed with both fine and coarse expanded slate aggregates and reinforced with different polymeric fibers (polyvinyl alcohol and polypropylene fibers). Developing and optimizing LWSCC mixtures combines the structural benefits of lightweight aggregate and the desirable properties of SCC, thus contributing to a more economical design and eliminating construction problems in multiple structural applications.

2.4 Experimental Program

2.4.1 Material Properties

Type GU Canadian Portland cement, MK, and FA conforming to ASTM C150 Type I (2012), ASTM C618 class N (2012), and ASTM C618 type F (2012), respectively, were used in the development of NWSCC and LWSCC mixtures. All cementitious materials were supplied by the Ornamental Concrete Ltd. (St John's, NL, CA), Different combinations of normal-weight and lightweight coarse and fine aggregates were used to develop the NWSCC and LWSCC mixtures. The normal-weight aggregates used were crushed granite sand and crushed granite stones with a specific gravity of 2.60 and absorption of 1%. The lightweight aggregates used were expanded slate coarse aggregate (LC) and expanded slate fine aggregate (LF) with a specific gravity of 1.53 and 1.80, respectively. The absorption of LC and LF was 7.1% and 10%, respectively conforming to ASTM C127 (2015). The gradation curves for both normal-weight and lightweight aggregates are shown in **Figure 2-1**.

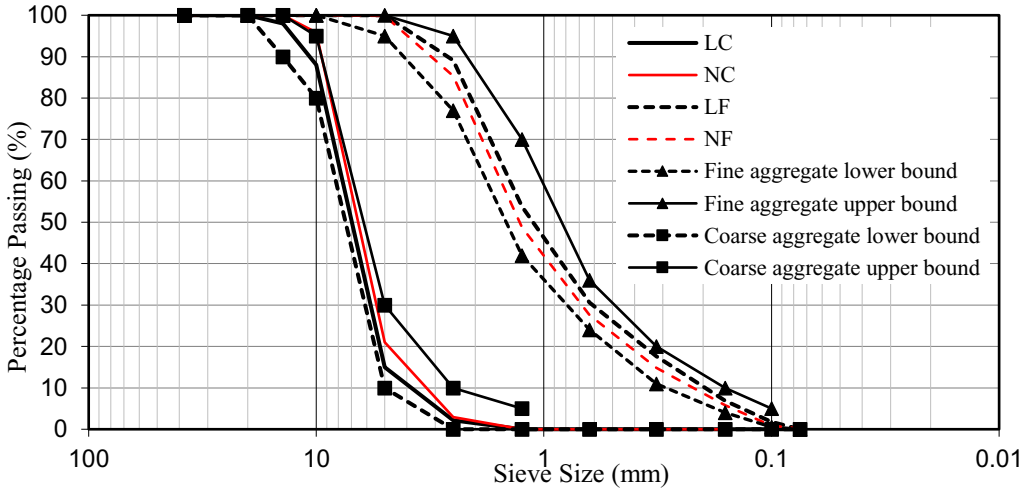

Figure 2-1: Gradation curves for fine and coarse normal-weight and lightweight aggregates.

Expanded slate (Stalite) aggregates were provided by the Carolina Stalite Company (Salisbury, NC, USA), which were prepared by expanding slate rocks in a rotary kiln at temperatures over 1000°C. Meanwhile, the crushed granite sand and crushed granite stones were supplied by City Sand & Gravel Ltd. (NL, Canada). Figure 2-2 indicates all cementitious materials and aggregates used in this study. Two types of polyvinyl alcohol (PVA) fibers (PVA8 and PVA12) and another polypropylene fiber (PP19) were used to reinforce the developed LWSCC mixtures. The physical and mechanical properties of these fibers are shown in Table 2-1 and Figure 2-3. The used fibers were provided by Nycon corporation (Fairless Hills, PA, USA). A polycarboxylate-based HRWRA similar to ASTM C494 Type F (2013) with a specific gravity, volatile weight, and pH of 1.20, 62%, and 9.5, respectively, was used to achieve the required flowability.

Figure 2-2: Cementitious materials and aggregates used.

Table 2-1: Physical and mechanical properties of the fibers used.

Fiber	Type	Length (mm)	Aspect Ratio	Specific Gravity	Tensile Strength (MPa)
PVA8	Polyvinyl Alcohol Fiber	8	210	1.3	1600
PVA12	Polyvinyl Alcohol Fiber	12	130	1.3	1200
PP19	Polypropylene Fiber	19	860	0.91	480

(a) (b) (c)

Figure 2-3: Fibers used (a) PVA8, (b) PVA12, (c) PP19.

2.4.2 Mixtures Development

The main objective of this stage was to develop a number of LWSCC mixtures reinforced with different types of polymeric fiber. This special type of concrete required a balanced viscosity, in which mixtures can achieve acceptable self-compactability, adequate particle suspension, and reduced risk of segregation. Therefore, I conducted a preliminary trial mixes stage to determine the minimum water-to-binder (w/b) ratio, total binder content, and optimal combination/type of binary materials that could be used to develop minimum density fibered-LWSCC mixtures with maximized compressive strength and having 700 ± 50 mm slump flow diameter with no visual sign of segregation. The results of the trial

mixes stage indicated that using a minimum w/b ratio of 0.4 and minimum binder content of 550 kg/m^3 allowed the mixtures to achieve the target flowability without overdosing the HRWRA. This stage also showed that using a w/b ratio lower than 0.4 required an excessive amount of HRWRA to achieve the required flowability, while using a binder content lower than 550 kg/m^3 negatively affected the stability and aggregate particle suspension. From the trial mixes stage, inclusion of FA in LWSCC was found to increase the flowability and reduce the amount of HRWRA added to the mixture. Also, the incorporation of MK helped improve the stability and particle suspension of LWSCC mixtures. Therefore, 20% MK and 30% FA were chosen in all LWSCC mixtures. With a w/b ratio of 0.4 and binder content of 550 kg/m^3, it was possible to develop successful LWSCCs with C/F aggregate ratio up to 0.7 in LWSCC-LC mixtures and up to 1.0 in LWSCC-LF mixtures. Increasing the content of LC in LWSCC-LC led to a reduction in its passing ability, while increasing the content of LF in LWSCC-LF reduced the mixture stability. In the trial mixes stage for LWSCC mixtures with 550 kg/m^3 binder content, the possible addition of fibers reached up to 0.3%. Further increase in the fiber content reduced the passing ability. Therefore, increasing the binder content to 600 kg/m^3 was found to be an alternative that allowed up to 0.5% fiber volume and higher contents of lightweight aggregates (achieving further reduction in the mixture's density) to be used safely in LWSCC.

It is worth noting that the target slump flow value of the developed mixtures (700 ± 50 mm) meets the specification of SF2 class, which is suitable for multiple structural applications according to the European Guidelines for Self-Compacting Concrete (EFNARC, 2005).

The experimental program included two normal-weight SCC (NWSCC) mixtures with a density of 2276 kg/m^3 and 14 LWSCC and fibered-LWSCC mixtures with a density ranging from 1838 kg/m^3 to 1942 kg/m^3, as follows (see **Table 2-2**):

- Mixtures 1 and 2 were developed as NWSCC with normal-weight crushed granite aggregates having a maximum size of 10 mm coarse aggregate and 4.75 mm fine aggregate. The C/F aggregate ratio was equal to 0.7 in mixture 1 (550-0.7NWSCC) and 1.0 in mixture 2 (550-1NWSCC). These mixtures were designed to be compared with their counterpart LWSCC mixtures (mixtures 3 and 10) in order to evaluate the influence of aggregate type on fresh properties and strengths of concrete.
- Mixtures 3 and 10 were developed as LWSCCs using total binder content, SCMs, w/b ratio, and C/F aggregate ratio similar to mixtures 1 and 2, respectively. In mixture 3, crushed granite sand was used as a fine aggregate while the coarse aggregate was totally replaced with LC. In this mixture, the C/F aggregate ratio was 0.7, which represented the maximum possible volume of LC that can be used to develop successful LWSCC. From the trial mixes stage, further increase in the C/F aggregate ratio caused a potential problem in the passing ability. Meanwhile, in mixture 10, crushed granite stone was used as a coarse aggregate while the fine aggregate was totally replaced with LF. In this mixture, the C/F aggregate ratio was 1, which represented the maximum possible volume of LF that can be used to produce successful LWSCC. From the trial mixes stage, increasing the C/F aggregate ratio more than 1 led to an increase in the risk of segregation. Mixtures 3 and 10 were developed for evaluating the effect of aggregate type (lightweight aggregates vs.

normal-weight aggregates). Mixtures 3 and 10 were also designed as reference mixtures for fibered-LWSCC mixtures (mixture 3 vs. mixtures 4-6 and mixture 10 vs. mixtures 11-13).

- Mixtures 4-6 were developed similar to mixture 3, and mixtures 11-13 were developed similar to mixture 10 but reinforced with different types of fiber (PVA8, PVA12, and PP19) at 0.3% fraction volume. These mixtures (mixtures 4-6 vs. mixture 3 and mixtures 11-13 vs. mixture 10) were designed to investigate the influence of using different types of polymeric fiber on both fresh properties and strengths of LWSCC made with either LC or LF.
- Mixtures 7 and 14 were LWSCC mixtures developed similar to mixtures 4 and 11, respectively, but with binder content of 600 kg/m^3 instead of 550 kg/m^3. These mixtures were designed to investigate the influence of using higher binder content on the behavior of LWSCC made with either LC or LF.
- Mixtures 8 and 15 were LWSCC mixtures developed similar to mixtures 7 and 14, respectively, but with higher volume of lightweight aggregates (taking advantage of using higher binder content). Mixture 8 was designed with C/F aggregate ratio equal to 1.0, while mixture 15 was designed with C/F aggregate ratio equal to 0.7. These mixtures were designed to study the benefits of increasing the binder content (from 550 kg/m^3 to 600 kg/m^3) on increasing the maximum possible amount of lightweight aggregate in LWSCC mixtures and its effects on the fresh properties and strengths.

Table 2-2: Mixture proportions for the developed mixtures.

		Designation	Cement kg/m^3	MK kg/m^3	FA kg/m^3	Aggregates					Fiber %	HRWRA L/m^3	Density kg/m^3
						C/F ratio	NC kg/m^3	NF kg/m^3	LC kg/m^3	LF kg/m^3			
NWSCC mixtures	1	550-0.7NWSCC	275	110	165	0.7	620	886	-	-	-	3.40	2276.4
	2	550-1NWSCC	275	110	165	1.0	753	753	-	-	-	3.10	2276.4
LWSCC (coarse aggregate slate & normal-weight sand)	3	550-0.7LC	275	110	165	0.7	-	689	482	-	-	3.67	1942
	4	550-0.7LC-0.3PVA8	275	110	165	0.7	-	686	480	-	0.3	4.10	1940
	5	550-0.7LC-0.3PVA12	275	110	165	0.7	-	686	480	-	0.3	4.30	1940
	6	550-0.7LC-0.3PP19	275	110	165	0.7	-	686	480	-	0.3	4.67	1938
	7	600-0.7LC-0.3PVA8	300	120	180	0.7	-	640	448	-	0.3	3.40	1933
	8	600-1LC-0.3PVA8	300	120	180	1.0	-	519	519	-	0.3	3.70	1883
	9	600-0.7LC-0.5PVA8	300	120	180	0.7	-	638	447	-	0.5	4.29	1931
LWSCC (normal-weight coarse aggregate & fine aggregate slate)	10	550-1LF	275	110	165	1.0	617	-	-	617	-	3.50	2005
	11	550-1LF-0.3PVA8	275	110	165	1.0	614	-	-	614	0.3	3.83	2002
	12	550-1LF-0.3PVA12	275	110	165	1.0	614	-	-	614	0.3	3.95	2002
	13	550-1LF-0.3PP19	275	110	165	1.0	614	-	-	614	0.3	4.22	2001
	14	600-1LF-0.3PVA8	300	120	180	1.0	574	-	-	574	0.3	3.30	1991
	15	600-0.7LF-0.3PVA8	300	120	180	0.7	458	-	-	654	0.3	3.60	1955
	16	600-1LF-0.5PVA8	300	120	180	1.0	571.4	-	-	571.4	0.5	4.30	1989

Note: All mixtures have a 0.4 w/b ratio; and HRWRA = high-range water-reducer admixture.

- Mixtures 9 and 16 were developed with the same proportions as mixtures 7 and 14, respectively, but with higher fiber volume of 0.5% (taking advantage of using higher binder content). These mixtures were designed to investigate the influence of changes in the fiber volume fraction on fresh properties and strengths of LWSCC made with either LC or LF.

The developed LWSCC mixtures were designated by the total binder content, C/F aggregate ratio, type of aggregate used (either LC or LF), fiber volume, and type (see **Table 2-2**). For example, an LWSCC mixture with 550 kg/m^3 binder content, 0.7 C/F aggregate ratio, LC instead of crushed granite aggregate, and 0.3% PVA8 fiber would be labeled as 550-0.7LC-0.3PVA8.

2.5 Testing Program

2.5.1 Fresh and Mechanical Properties Tests

The fresh properties of NWSCC and LWSCC mixtures were assessed according to the European Guidelines for Self-Compacting Concrete (2005). The flowability was evaluated by measuring the time to reach 500 mm slump flow diameter (T_{50}), time to reach 500 mm J-ring diameter ($T_{50\text{-}J}$), and the V-funnel time. The L-box ratio and the difference between slump flow and J-ring diameters were calculated to evaluate the mixtures' passing ability. The used apparatuses in the assessment of SCC fresh properties are shown in Figure 2-4. The segregation resistance of the NWSCC and LWSCC mixtures was evaluated by investigating the aggregates' distribution along a splitted 100 mm diameter x 200 mm high concrete cylinder (see Figure 2-5**a**). The segregation resistance was also assessed by

dividing a 200 mm high concrete cylinder into four equal segments, and then the relative density was calculated for each segment (density of segment/dry density of mixture) in order to assess the variation of aggregate distribution along the specimen height (see **Figure 2-5b**).

Slump Flow

V-funnel

L-box

J-ring

Figure 2-4: Fresh properties' tests as per EFNARC guidelines.

In this study, the stability of mixture was assumed to be in acceptable range if the maximum difference in the relative density between the top and the lowest segments does not exceed 10%. The percentage of the entrained air in all tested mixtures was measured by following a procedure given in ASTM C231 (2014). The compressive strength of the developed

mixtures was tested as per ASTM C39 (2011) using 100 mm diameter x 200 mm high cylinders, while the 28-day FS of 100 mm x 100 mm x 400 mm prisms was measured for all developed mixtures as per ASTM C78 (2018).

(a)

A sample of LWSCC-LC mixture

A sample of LWSCC-LF mixture

(b)

Figure 2-5: Evaluating the distribution of lightweight aggregates along hardened concrete cylinders.

2.6 Discussion of Test Results

2.6.1 Fresh Properties

2.6.1.1 HRWRA Demand

Table 2-3 shows the amount of HRWRA that was used to develop the NWSCC and LWSCC mixtures, achieving a slump flow diameter of 700 ± 50 mm. From the results, it can be seen that using lightweight aggregates (LC or LF) showed a slight increase in the HRWRA demand compared to normal-weight aggregate. This increase was 7.9% and 12.9% when LC and LF were used, respectively, as shown in mixture 3 compared to mixture 1 and mixture 10 compared to mixture 2. It should be noted that both lightweight and normal-weight aggregates were used as saturated surface dry in the mixture. Therefore, the slight increase in HRWRA demand may be attributed to the nature of the expanded slate aggregates compared to the crushed granite aggregates and/or the difference in the particle size between the two aggregates (Figure 2-1).

Using fibers in LWSCC demanded a higher dosage of HRWRA to obtain the target slump flow compared to mixtures without fibers. For example, using 0.3% PVA8 increased the HRWRA demand by 11.7% and 9.4% as shown in mixtures 4 and 11 compared to mixtures 3 and 10, respectively. Increasing the length of PVA fibers from 8 mm to 12 mm resulted in slight increases in the HRWRA demand by an average of 4% (mixtures 5 and 12 vs. mixtures 4 and 11, respectively). Further increase in the length of fibers resulted in a further increase in HRWRA demand. As shown in mixture 6 and 13 (mixtures with PP19), the HRWRA demand was 27.2% and 20.6% higher than that of mixtures 3 and 10, respectively (mixtures with no fibers). The results also showed that in LWSCC mixtures, increasing the

fiber volume from 0.3% to 0.5% significantly raised the HRWRA demand by 26.2% in LC mixtures (mixture 9 vs. mixture 7) and 30.3% in LF mixtures (mixture 16 vs. mixture 14). Table 2-3 also shows that increasing the binder content reduced the HRWRA demand required to achieve the desired flowability. As seen in mixtures 4 and 11 compared to mixtures 7 and 14, respectively, increasing the binder content from 550 kg/m^3 to 600 kg/m^3 led to a reduction in the amount of HRWRA used by an average of 15.5%. This result agrees with previous work from the authors in their research findings (Ismail & Hassan, 2015). In LWSCC mixtures, the HRWRA demand increased as the volume of lightweight aggregates (either LC or LF) increased. As seen in mixture 7 compared to mixture 8, increasing the C/F aggregate ratio from 0.7 to 1.0 (increasing the volume of LC) resulted in an 8.8% increase in the HRWRA demand. A similar result was observed in mixtures with LF (mixture 14 vs. mixture 15), in which decreasing the C/F aggregate ratio from 1.0 to 0.7 (increasing the volume of LF) required a 9.1% increase in the HRWRA.

2.6.1.1 Flowability

The flowability of all developed NWSCC and LWSCC mixtures was evaluated by T_{50}, $T_{50\text{-}J}$, and V-funnel times. From Table 2-3 and Figure 2-6**a**, it was found that replacing crushed granite stones with LC led to a reduction in the flowability. As seen in mixture 3 compared to mixture 1, the T_{50}, $T_{50\text{-}J}$, and V-funnel time increased by 34.1%, 44%, and 57.4%, respectively. This finding can be attributed to the low density of LC that results in the presence of a higher number of aggregate particles, compared to crushed granite's particles (at the same C/F aggregate ratio). This increases the friction and collision between particles during mixture spreading, which, in turn, limits the flowability of LWSCC-LC mixtures.

On the other hand, using LF as a replacement for crushed granite sand (mixture 10 vs. mixture 2) was found to decrease the T_{50}, $T_{50\text{-}J}$, and V-funnel time by 8.7%, 7.2%, and 31.2%, respectively, indicating a higher mixture flowability. Such results are due to the higher volume of LF compared to crushed granite sand (at the same C/F aggregate ratio), which offers a larger mortar volume and then reduces the inter-particle friction and collision between crushed granite stones.

The results indicated that the flowability of LWSCC mixtures was negatively affected by the inclusion of fibers, as shown in Table 2-3 and Figure 2-6 (**b** and **c**). In LWSCC-LC mixtures, using 0.3% PVA8 increased the T_{50}, $T_{50\text{-}J}$, and V-funnel time by 26.5%, 30.9%, and 4.6%, respectively, as shown in mixture 4 compared to mixture 3. Such findings could be attributed to the interference and blockage induced by fibers and aggregates, which decreased the ability of mixtures to flow freely under their own weight. A higher reduction in the flowability was observed when the length of PVA fibers increased from 8 mm to 12 mm (mixture 4 vs. mixture 5), in which the T_{50}, $T_{50\text{-}J}$, and V-funnel time increased by 13.8%, 6.6%, and 16.2%, respectively (see Figure 2-6**b**). Using PP19 (19 mm) appeared to have the greatest effect on decaying the flowability of mixtures, in which the use of 0.3% PP19 raised the T_{50}, $T_{50\text{-}J}$, and V-funnel time by 70.6%, 62.9%, and 49.1%, respectively, as shown in mixture 6 compared to mixture 3. The higher negative impact of PP19 (compared to PVA8 and PVA12) is attributed to the greater length of PP19, which heightened the blockage and inter-particle friction during mixture spreading.

Table 2-3: Fresh properties of tested mixtures.

Mix. #	Designation	T_{50} (s)	$T_{50\text{-}J}$ (s)	Slump – J-ring diameter (mm)	L-box (H2/H1) (%)	V-funnel (s)	Segregation resistance	Air %	HRWR L/m^3
1	550-0.7NWSCC	2.05	2.43	10	0.97	6.86	NS	1.5	3.40
2	550-1NWSCC	2.30	2.90	25	0.91	7.80	NS	2.1	3.10
3	550-0.7LC	2.75	3.50	30	0.92	10.80	NS	3.1	3.67
4	550-0.7LC-0.3PVA8	3.48	4.58	45	0.82	11.30	NS	3.5	4.10
5	550-0.7LC-0.3PVA12	3.96	4.88	50	0.80	13.13	NS	3.7	4.30
6	550-0.7LC-0.3PP19	4.69	5.70	70	0.76	16.10	NS	4.0	4.67
7	600-0.7LC-0.3PVA8	3.20	3.90	25	0.91	9.48	NS	3.3	3.40
8	600-1LC-0.3PVA8	3.48	4.52	40	0.81	11.20	NS	3.5	3.70
9	600-0.7LC-0.5PVA8	4.12	5.35	50	0.82	12.48	NS	3.5	4.29
10	550-1LF	2.10	2.69	15	0.95	5.37	NS	3.2	3.50
11	550-1LF-0.3PVA8	2.41	3.22	35	0.85	6.25	NS	3.5	3.83
12	550-1LF-0.3PVA12	2.80	3.80	45	0.82	7.12	NS	3.5	3.95
13	550-1LF-0.3PP19	3.38	4.72	65	0.77	8.55	NS	3.7	4.22
14	600-1LF-0.3PVA8	2.10	2.60	30	0.88	4.86	NS	4.0	3.30
15	600-0.7LF-0.3PVA8	1.70	2.30	20	0.91	4.05	NS	3.5	3.60
16	600-1LF-0.5PVA8	2.70	3.53	45	0.83	6.75	NS	3.6	4.30

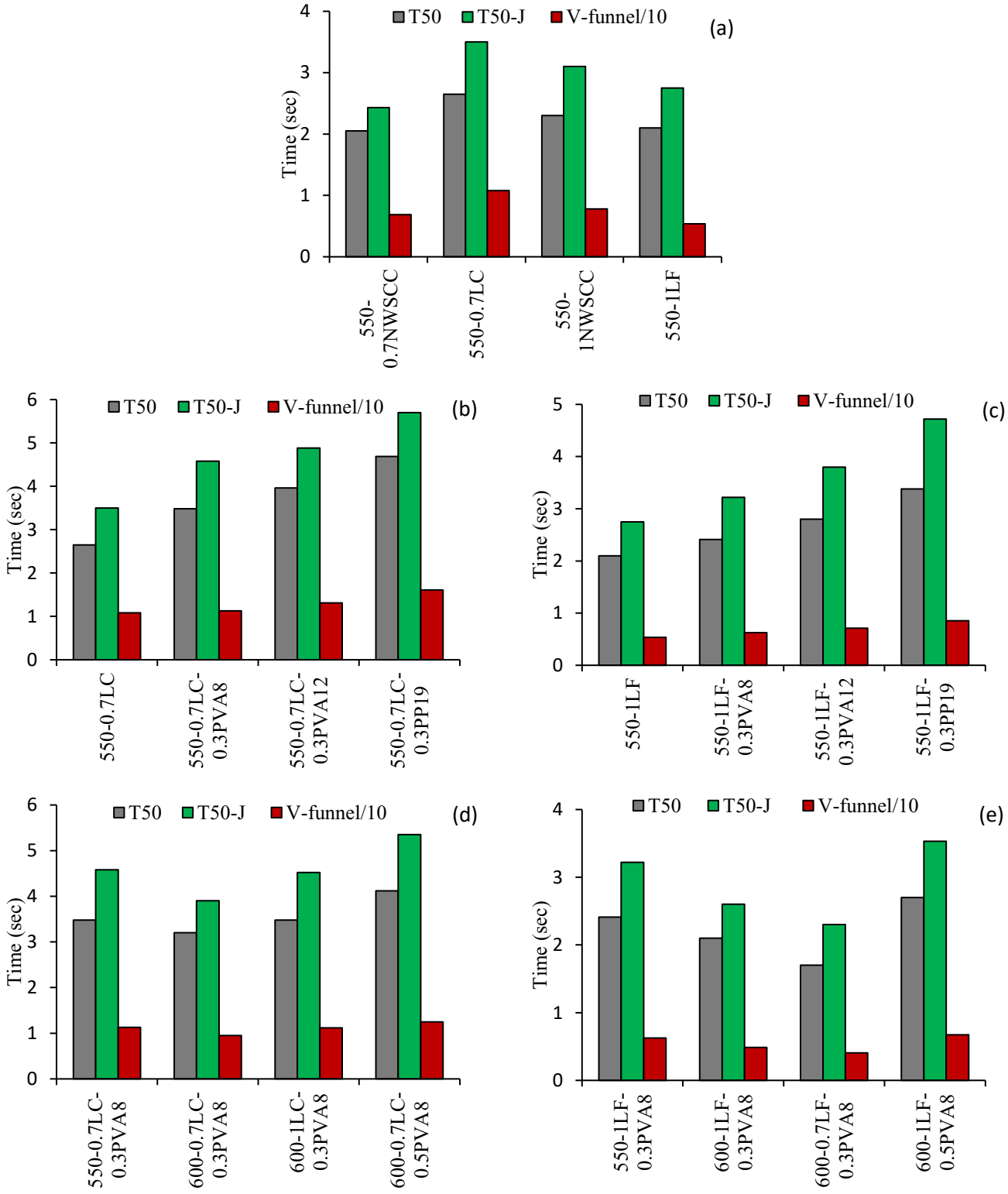

Figure 2-6: Flowability of the developed mixtures.

The results of LWSCC made with LF also confirmed the negative effect of fibers on the flowability. For example, the inclusion of 0.3% PVA8 increased the T_{50}, $T_{50\text{-}J}$, and V-funnel time by an average of 14.8%, 19.7%, and 16.4%, respectively, as shown in mixture 11 compared to mixture 10. The T_{50}, $T_{50\text{-}J}$, and V-funnel time were found to have increased by 16.2%, 18.8%, and 13.9%, respectively, when the length of fibers increased from 8 mm to 12 mm (mixture 11 vs. mixture 12). The inclusion of 0.3% PP19 (mixture 13) exhibited the maximum reduction in flowability as the T_{50}, $T_{50\text{-}J}$, and V-funnel time rose by an average of 61%, 75.5%, and 59.2%, respectively, compared to the non-fibered LWSCC-LF mixture (mixture 10).

Increasing the fiber volume from 0.3% to 0.5% also showed a reduction in the mixture flowability. It should be noted that it was not possible to develop LWSCC mixtures with 0.5% fibers without increasing the binder content from 550 kg/m^3 to 600 kg/m^3. In LWSCC mixtures with 600 kg/m^3 binder content, increasing the fiber volume resulted in higher aggregate-fiber interference, which extends the time needed for the mixture to spread. For example, including 0.5% PVA8 in the LWSCC-LC mixture (mixture 9) raised the T_{50}, $T_{50\text{-}J}$, and V-funnel time of by 28.8%, 37%, and 31.6%, respectively, compared to the mixture with 0.3% PVA8 (mixture 7). Also, when the same fraction volume of PVA8 was employed in LWSCC-LF (mixture 16), the T_{50}, $T_{50\text{-}J}$, and V-funnel time increased by 29%, 36%, and 39%, respectively, compared to the mixture with 0.3% PVA8 (mixture 14).

Table 2-3 and Figure 2-6 (**d** and **e**) indicate that increasing the total binder content improved the flowability of LWSCC mixtures. This may be due to the increase in the volume of cement paste, which can result in better distribution for both coarse aggregate

particles and fibers and also allow for smoother flow. The LWSCC-LC mixture developed with 600 kg/m^3 binder content (mixture 7) showed a lower T_{50}, $T_{50\text{-}J}$, and V-funnel time by 8%, 14.8%, and 16.1%, respectively, compared to mixture 4 (with 550 kg/m^3 binder content). Similarly, increasing the binder content from 550 kg/m^3 to 600 kg/m^3 in the LWSCC-LF mixture reduced the T_{50}, $T_{50\text{-}J}$, and V-funnel time by 13%, 19%, and 22%, respectively, as shown in mixture 11 compared to mixture 14.

The results in Table 2-3 and Figure 2-6**d** showed that in LWSCC-LC mixtures, increasing the C/F aggregate ratio (increasing the volume of LC) adversely affected the flowability. As the C/F aggregate ratio increased from 0.7 (mixture 7) to 1.0 (mixture 8) the T_{50}, $T_{50\text{-}J}$, and V-funnel time increased by 9%, 16%, and 18%, respectively. This could be attributed to the increase in the inter-particle friction and collision when a higher volume of coarse aggregate was used. This trend of results was confirmed in LWSCC-LF mixtures, in which mixture 14 with higher normal-weight coarse aggregate (C/F aggregate ratio of 1.0) compared to mixture 15 with less normal-weight coarse aggregate (C/F aggregate ratio of 0.7) had higher T_{50}, $T_{50\text{-}J}$, and V-funnel time by 23.5%, 13%, and 20%, respectively. By comparing mixture 8 to mixture 14, it can be observed that at a C/F aggregate ratio of 1.0, using LF can help to develop mixtures with lower T_{50}, $T_{50\text{-}J}$, and V-funnel time (higher flowability) than that of the mixture with LC.

2.6.1.2 Passing Ability

The passing ability of all developed mixtures was evaluated by measuring the L-box (H2/H1) ratio and the difference between the slump flow and J-ring diameters. Table 2-3 and Figure 2-7**a** show that in LWSCC mixtures, using LC as a replacement for crushed

granite stones exhibited a reduction in the passing ability of mixtures. As shown in mixture 3 compared to mixture 1, when LC was used, the H2/H1 ratio decreased from 0.97 to 0.92 and the difference between slump flow and J-ring diameters increased from 10 mm to 30 mm, indicating a lower passing ability. This can be attributed to the higher volume (more aggregate particles) of LC compared to the crushed granite stones (at the same C/F aggregate ratio), which, in turn, increased the blockage and constricted the mixture from passing through limited spaces between the steel bars of the L-box and/or J-ring device. On the other hand, replacing crushed granite sand with LF improved the passing ability of the mixture (mixture 2 vs. mixture 10), in which the H2/H1 ratio increased from 0.91 to 0.95 and the difference between slump flow and J-ring diameters decreased from 25 mm to 15 mm. Such results can be related to the higher volume of LF (compared to crushed granite sand), which offers higher mortar volume and can provide a better distribution for coarse aggregate particles, easing the mixture's movement through the steel bars of the L-box and/or J-ring device.

Table 2-3 and Figure 2-7**b** show the passing ability results of LWSCC-LC reinforced with polymeric fibers. Adding fibers to the mixture significantly increased the interference between fibers and coarse aggregates, resulting in high blockage at the openings between vertical bars of both the J-ring and L-box devices, thus decreasing the passing ability. When 0.3% PVA8 was added to the LWSCC-LC mixture, the H2/H1 ratio was dropped from 0.92 to 0.82 and the difference between the slump flow and J-ring diameters was raised from 30 mm to 45 mm (see mixture 4 compared to mixture 3). Increasing the length of PVA fiber from 8 mm to 12 mm (mixture 4 vs. mixture 5) slightly reduced the H2/H1ratio

from 0.82 to 0.80 and increased the difference between the slump flow and J-ring diameters from 45 mm to 50 mm. This indicates that the possibility of blockage occurring through the vertical steel bars may increase as the fiber length is increased. The maximum reduction in the passing ability was found in the LWSCC-LC mixture reinforced with 0.3% PP19, in which the H2/H1 ratio decreased from 0.92 to 0.76 and the difference between the slump flow and J-ring diameters increased from 30 mm to 70 mm, as shown in mixture 6 compared to mixture 3 (non-fibered LWSCC-LC mixture). Although the LWSCC-LC reinforced with PP19 exhibited a potential blockage in the L-box test, the mixture was still satisfied the minimum acceptable value of H2/H1 (0.75 or greater), as per the criteria given by the European Guidelines for Self-Compacting Concrete and the Interim Guidelines for the Use of Self-Consolidating Concrete (EFNARC, 2005).

Similarly, the passing ability of LWSCC-LF mixtures was negatively affected by the inclusion of fiber (see Figure 2-7**c**). By comparing mixture 11 (with 0.3% PVA8) to mixture 10 (non-fibered mixture), it was found that the addition of PVA8 significantly decreased the H2/H1 ratio from 0.95 to 0.85 and increased the difference between the slump flow and J-ring diameters from 15 mm to 35 mm. Using PVA12 (mixture 12) compared to PVA8 (mixture 11) led to a slight reduction in the H2/H1 and a relative increase in the difference between the slump flow and J-ring diameters. Further decay in the passing ability was achieved when PP19 was added to the LWSCC-LF mixtures, in which the H2/H1 decreased from 0.95 to 0.77, and the difference between the slump flow and J-ring diameters increased from 15 mm to 65 mm, as shown in mixture 13 compared

to mixture 10 (non-fibered LWSCC-LF mixture). These results are attributed to the same reasons explained earlier for the fibered LWSCC-LC mixtures.

Table 2-3 and Figure 2-7 **(d** and **e)** also show that increasing the fiber volume yielded a significant reduction in the passing ability of LWSCC mixtures. In LWSCC-LC mixtures, the H2/H1 ratio decreased from 0.91 to 0.82 and the difference between the slump flow and J-ring diameters rose from 25 mm to 50 mm when the fiber volume increased from 0.3% to 0.5%, as seen in mixture 7 compared to mixture 9. Similarly, in LWSCC-LF mixtures, changing the fiber volume from 0.3% (mixture 14) to 0.5% (mixture 16) showed a drop in the H2/H1 ratio from 0.88 to 0.83 and an increase in the difference between the slump flow and J-ring diameters from 30 mm to 45 mm.

As seen in Table 2-3, using higher binder content appeared to improve the passing ability of LWSCC mixtures. In LWSCC-LC mixtures (mixture 4 vs. mixture 7), the H2/H1 ratio increased from 0.82 to 0.91 while the difference between the slump flow and J-ring diameters dropped from 45 mm to 25 mm when the binder content increased from 550 kg/m^3 to 600 kg/m^3. Similarly, as the binder content increased, the passing ability of LWSCC-LF mixtures improved but at a lower rate. For the same increase in the binder content (550 kg/m^3 to 600 kg/m^3), the H2/H1 ratio increased from 0.85 to 0.88 while the difference between the slump flow and J-ring diameters decreased from 35 mm to 30 mm, as seen in mixture 14 compared to mixture 11. These results indicated the benefit of using higher binder content to increase the cement paste volume, thus limiting the friction between coarse aggregate particles and achieving a higher ability to pass through limited spaces.

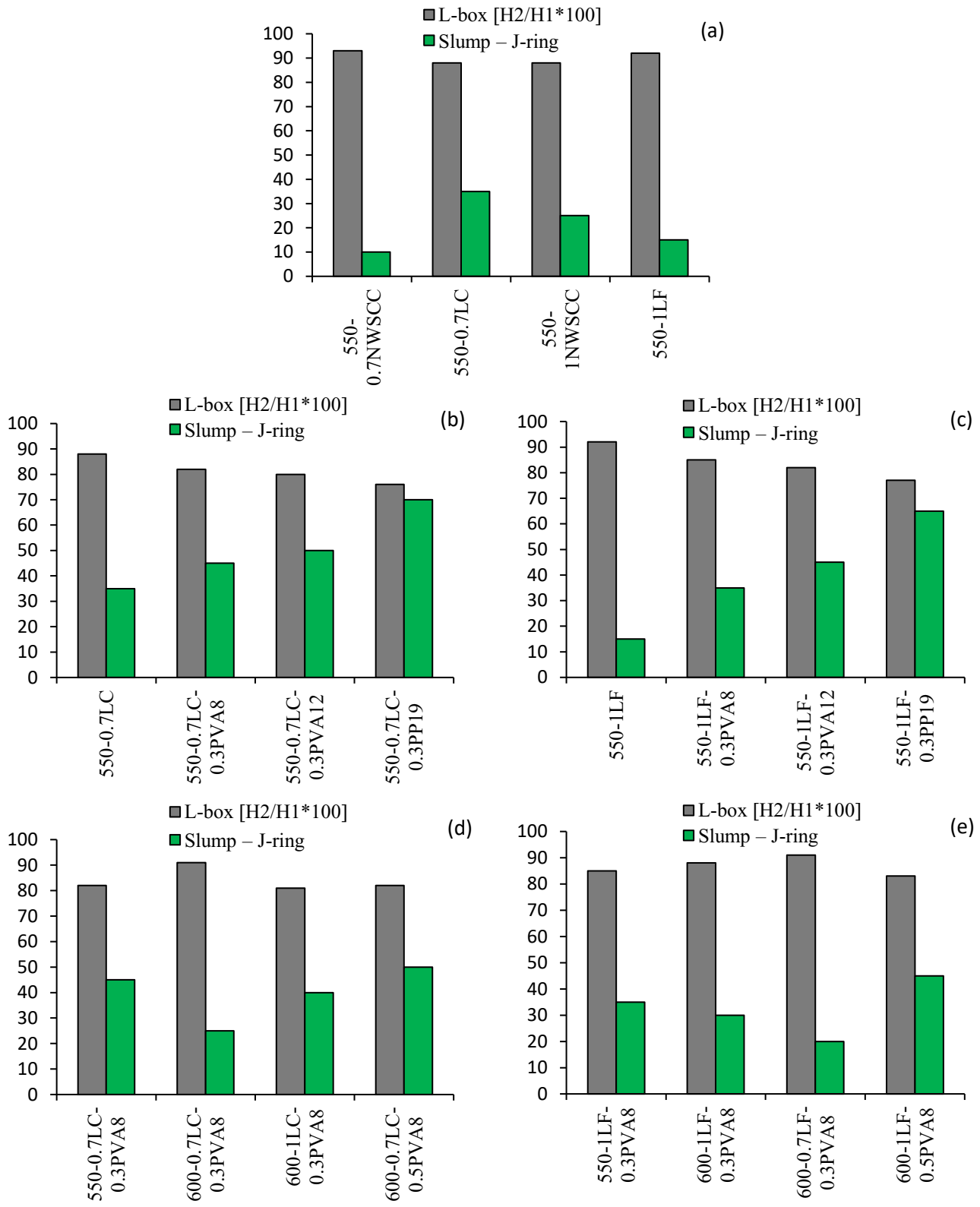

Figure 2-7: Passing ability of the developed mixtures.

Increasing the coarse aggregate content resulted in higher levels of blockage, inter-particle friction, and interference with fibers, which, in turn, negatively affected the passing ability of fibered-LWSCC mixtures, as seen in Table 2-3 and Figure 2-7 (**d** and **e**). In LWSCC-LC mixtures, by comparing mixture 8 to mixture 7, it can be seen that as the C/F aggregate ratio was increased from 0.7 to 1.0 the H2/H1 ratio decreased from 0.91 to 0.81, while the difference between the slump flow and J-ring diameters increased from 25 mm to 40 mm. In LWSCC-LF mixtures, the mixture with higher C/F aggregate ratio yielded a lower passing ability, as shown in mixture 14 compared to mixture 15. At C/F aggregate ratio of 1.0, the mixture with LF (mixture 14) exhibited better passing ability results than the mixture with LC (mixture 8).

2.6.1.3 Segregation Resistance

The segregation resistance of developed mixtures was evaluated by using two methods. In the first method, the stability of LWSCC mixtures was visually evaluated by investigating the distribution of both LC and LF particles along hardened splitted cylinders (see Figure 2-5**a**). As mentioned earlier, the low density of the LC and LF may facilitate the movement of aggregate particles toward the concrete surface in fresh state. From Table 2-3, it can be observed that all developed mixtures achieved a good distribution of lightweight aggregate particles and no visual sign of segregation (denoted by NS in Table 2-3). This indicates that the ternary material system used efficiently provided adequate mixture viscosity, which reduced the risk of segregation and improved the particle suspension.

In the second method, the segregation resistance was assessed for each mixture by dividing the 200 mm high hardened concrete cylinder into four equal discs (see Figure 2-5**b**). For

each disc, the relative dry density (the dry density of each disc / the dry density of the mixture) was measured and calculated as presented in Table 2-4. From the table, the differences between the relative dry densities at the bottom compared to the top were insignificant in all mixtures. As seen from Table 2-4, the maximum differences in the relative density between the upper and lower segments did not exceed 3.8%, which indicated acceptable stability for all developed mixtures.

Table 2-4: Relative dry density of the developed LWSCC mixtures along the height of concrete cylinders.

Mix. #	Designation	Unit Weight Ratios			
		Bottom segment	Middle segments		Top Segment
			1	2	
3	550-0.7LC	1.016	1.012	0.992	0.980
4	550-0.7LC-0.3PVA8	1.017	1.000	1.002	0.980
5	550-0.7LC-0.3PVA12	1.009	0.997	1.000	0.994
6	550-0.7LC-0.3PP19	1.006	1.005	0.998	0.990
7	600-0.7LC-0.3PVA8	1.010	0.999	1.001	0.989
8	600-1LC-0.3PVA8	1.009	1.000	0.998	0.994
9	600-0.7LC-0.5PVA8	1.008	1.007	0.997	0.988
10	550-1LF	1.005	1.000	1.002	0.994
11	550-1LF-0.3PVA8	1.014	1.000	0.996	0.990
12	550-1LF-0.3PVA12	1.003	1.004	1.002	0.991
13	550-1LF-0.3PP19	1.022	0.997	0.996	0.985
14	600-1LF-0.3PVA8	1.006	1.000	1.001	0.996
15	600-0.7LF-0.3PVA8	1.005	1.000	1.000	0.996
16	600-1LF-0.5PVA8	1.005	1.003	0.998	0.995

2.6.2 Mechanical Properties

Figure 2-8 shows the results of the 28-day compressive strength and FS of all developed mixtures. These results indicated that using lightweight aggregates (either LC or LF)

obviously decreased the compressive strength and FS of the composite. The LWSCC mixture with LC (mixture 3) had a compressive strength and FS of 28.2% and 27.3%, respectively, lower than that of the NWSCC mixture made with crushed granite stones (mixture 1). Similarly, the use of LF (mixture 10) exhibited a reduction in the compressive strength and FS of 40.1% and 29.6%, respectively, compared to the mixture with crushed granite sand (mixture 2). As is well-known, the strength of concrete composite is affected by strength of mortar, coarse aggregate, and cement paste-aggregate interface. Consequently, using lightweight aggregates that typically have lower strength, compared to either crushed granite aggregates or cement paste, can effectively reduce the overall strengths of concrete composite.

From **Figure 2-8** (**b** and **c**), it can be seen that the use of fibers did not significantly affect the compressive strength of LWSCC mixtures while the FS of the composite improved. In LWSCC-LC mixtures, using 0.3% fibers (mixtures 4-6) slightly reduced the compressive strength by 1.2%, 3.7%, and 4.7%, respectively, compared to non-fibered LWSCC-LC (mixture 3). This slight reduction can be attributed to the higher air content in mixtures with fibers compared to non-fibered mixtures. In addition, the low stiffness of polymeric fibers decreased the overall stiffness of composite, which limits the ability to carry high compressive loading. Similar results were observed when fibers were used in LWSCC-LF mixtures. The addition of 0.3% PVA8, PVA12, and PP19 (mixtures 11-13) caused an insignificant decrease in the compressive strength, reaching up to 3.3%, 4.2%, and 3.4%, respectively, compared to LWSCC-LF with no fibers (mixture 10).

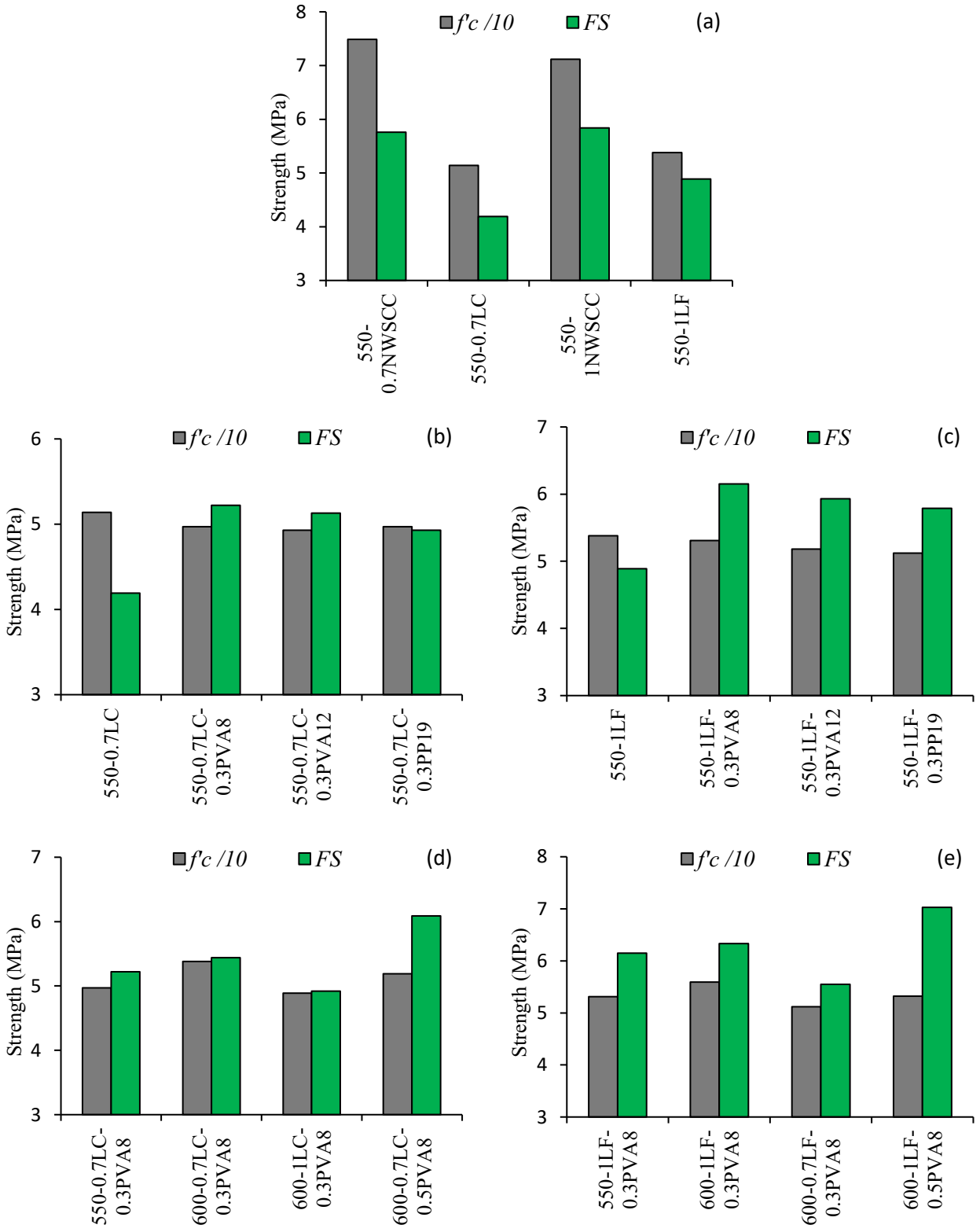

Figure 2-8: 28-day strengths of tested mixtures.

On the other hand, an obvious improvement in the FS of LWSCC mixtures was observed. Adding 0.3% of PVA8, PVA12, and PP19 to LWSCC-LC mixtures (mixtures 4-6) revealed higher FS of the composite by about 24.6%, 22.4%, and 17.7%, respectively, compared to LWSCC-LC with no fibers (mixture 3). Similarly, LWSCC-LF mixtures with 0.3% PVA8, PVA12, and PP19 showed increases in the FS reached up to 25.8%, 21.3%, and 18.4%, respectively, compared to non-fibered LWSCC-LF mixture (mixture 10).

The results of mixtures 4-6 compared to mixtures 11-13 confirmed the effect of PVA and PP fibers on the mechanical properties of LWSCC, in which incorporating fibers had a non-considerable impact on the compressive strength, but the FS was increased. In LWSCC-LC mixtures with 600 kg/m^3 binder, increasing the PVA8 fraction volume from 0.3% (mixture 7) to 0.5% (mixture 9) led to a reduction in the compressive strength up to 4.9%, while the FS increased by 11.9%. At the same level of volume change, the compressive strength of LWSCC-LF decreased by 3.5%, while the FS increased by 11.1% (mixture 14 vs. mixture 16).

The test results showed that the compressive strength and FS of the composite slightly increased as the binder content increased. As shown in Figure 2-8**d**, increasing the binder content from 550 kg/m^3 to 600 kg/m^3 in LWSCC-LC mixtures improved the compressive strength and FS by 5.3% and 4.2%, respectively (mixture 4 vs. mixture 7). The same increase in the binder content, in LWSCC-LF mixtures, led to an improvement in the compressive strength and increases in FS up to 8.1% and 2.9%, respectively (mixture 11 vs. mixture 14). This is attributed to the improvement in the strength of mortar as a result

of increasing the binder content, which, in turn, boosts the overall strength of concrete composite.

The results also showed that increasing the binder content from 550 kg/m^3 to 600 kg/m^3 achieved a maximum FS reaching up to 16.7% compared to the maximum FS achieved with 550 kg/m^3 binder (mixture 9 compared to mixture 4). Figure 2-8 (**d** and **e**) also illustrate that the compressive strength and FS decreased as the lightweight aggregate content (component with weaker strength) increased in the concrete composite. Varying the C/F aggregate ratio in LWSCC-LC mixtures from 0.7 to 1.0 decreased the compressive strength and FS by about 8.4% and 9.6%, respectively, as shown in mixture 7 compared to mixture 8. Increasing the content of LF in LWSCC mixtures also decayed their mechanical properties. When the C/F aggregate ratio changed from 1.0 to 0.7 (mixture 14 vs. mixture 15) the compressive strength and FS decreased by 9.1% and 12.3%, respectively. At the same C/F aggregate ratio, developing LWSCC with LF achieved higher compressive strength and FS than can be achieved using LC, as shown in mixture 14 vs. mixture 8.

2.7 Conclusions

In this investigation, fourteen LWSCC mixtures were produced, using either LC or LF, and reinforced with different types of polymeric fibers. The fiber types used were PVA8, PVA12, and PP19. The fresh properties, compressive strength, and FS of the developed mixtures were tested. Two NWSCC mixtures were cast for comparison. Based on the results obtained from this stage, the following conclusions can be drawn:

1. It was not possible to develop SCC mixtures with either LC or LF with binder content less than 550 kg/m^3. Using less than 550 kg/m^3 binder content made it very difficult to achieve acceptable SCC flowability with no sign of segregation. Also, it was not possible to use less than 0.4 w/b ratio to develop SCC mixtures with either LC or LF. The trial mixes stage indicated that mixtures with w/b ratio less than 0.4 required excessive HRWRA to achieve the required flowability.
2. At w/b ratio of 0.4 and binder content of 550 kg/m^3, the maximum possible percentage of LC to normal-weight sand that achieved acceptable SCC fresh properties was 0.7. Using a higher amount of LC noticeably reduced the passing ability of the mixture. Also, at the same binder content and w/b ratio, the maximum possible percentage of LF to normal-weight coarse aggregate that achieves acceptable SCC fresh properties was 1.0. Increasing this percentage resulted in increased risk of segregation.
3. At 550 kg/m^3 binder content, the maximum possible percentage of either PVA or PP fibers that can be used to develop LWSCC mixtures with acceptable self-compactability was limited to 0.3%. A higher volume of fiber led to potential problems in the passing ability of the mixtures. Increasing the binder content to 600 kg/m^3 improved the flowability and passing ability of the developed mixtures and allowed a maximum of 0.5% fibers to be used safely with acceptable fresh properties.
4. LWSCC with either expanded slate coarse or fine aggregates required slightly higher HRWRA demand compared to that required by NWSCC mixtures made

with normal-weight aggregates. Inclusion of either PVA or PP fibers led to an increase in the HRWRA demand, and as the fiber content increased the required HRWRA increased. On the other hand, increasing the binder content decreased the dosage of HRWRA required to achieve the target flowability.

5. The inclusion of PVA8 fiber showed better results in terms of flowability and passing ability than that showed by PVA12 and PP19 at the same volume of fiber content. Furthermore, LWSCC mixtures developed with PVA8 fibers exhibited the highest increase in the FS without considerable reduction in compressive strength compared to other mixtures developed with PVA12 and PP19.
6. Increasing the binder content from 550 kg/m^3 to 600 kg/m^3 improved the stability of LWSCC mixtures and allowed for a higher content of lightweight aggregates and higher content of fibers (0.5% compared to 0.3%) to be used in the mixture. The higher contents of lightweight aggregates achieved a minimum concrete density, reaching 1883 kg/m^3 compared to a 1938 kg/m^3 minimum density achieved with 550 kg/m^3 binder. Also, the increased percentage of fibers used with 600 kg/m^3 allowed for up to 16.7% higher FS to be achieved compared to the maximum FS achieved with 550 kg/m^3.
7. At the same C/F aggregate ratio, using LF exhibited better results compared to LC in terms of flowability, passing ability, compressive strength, and the FS, which indicates promising potential for the use of lightweight expanded slate aggregates as a fine aggregate rather than coarse aggregate to develop LWSCC mixtures.

2.8 References

AbdelAleem, B. H., Ismail, M. K., & Hassan, A. A. (2017). Properties of self-consolidating rubberised concrete reinforced with synthetic fibres. *Magazine of Concrete Research,* 69(10), 526-540.

Abouhussien, A. A., Hassan, A. A. A., & Ismail, M. K. (2015a). Properties of semi-lightweight self-consolidating concrete containing lightweight slag aggregate. *Construction and Building Materials*, 75, 63-73.

Abouhussien, A. A., Hassan, A. A. A., & Hussein, A. A. (2015b). Effect of expanded slate aggregate on fresh properties and shear behaviour of lightweight SCC beams. *Magazine of Concrete Research*, 67(9), 433-442.

Aslani, F., & Kelin, J. (2018). Assessment and development of high-performance fibre-reinforced lightweight self-compacting concrete including recycled crumb rubber aggregates exposed to elevated temperatures. *Journal of Cleaner Production*, 200, 1009-1025.

ASTM C39 / C39M. (2011). Standard Test Method for Compressive Strength of Cylindrical Concrete Specimens. *ASTM International*, West Conshohocken, PA, USA.

ASTM C78 / C78M. (2018). Standard Test Method for Flexural Strength of Concrete (Using Simple Beam with Third-point Loading). *ASTM International*, West Conshohocken, PA, USA.

ASTM C127. (2015). Standard test method for relative density (specific gravity) and absorption of fine aggregate. *ASTM International*, West Conshohocken, PA, USA.

ASTM C150 / C150M. (2012). Standard Specification for Portland Cement. *ASTM International*, West Conshohocken, PA, USA.

ASTM C231 / C231M. (2014). Standard Test Method for Air Content of Freshly Mixed Concrete by the Pressure Method. *ASTM International*, West Conshohocken, PA, USA.

ASTM C494 / C494M. (2013). Standard Specification for Chemical Admixtures for Concrete. *ASTM International*, West Conshohocken, PA, USA.

ASTM C618. (2012). Standard Specification for Coal Fly Ash and Raw or Calcined Natural Pozzolan for Use in Concrete. *ASTM International*, West Conshohocken, PA, USA.

ASTM C1609 / C1609M. (2012). Standard Test Method for Flexural Performance of Fiber-Reinforced Concrete (Using Beam with Third-Point Loading). *ASTM International*, West Conshohocken, PA, USA.

Bogas, J. A., Gomes, A., & Pereira, M. F. C. (2012). Self-compacting lightweight concrete produced with expanded clay aggregate. *Construction and Building Materials*, 35, 1013-1022.

Choi, J., Zi, G., Hino, S., Yamaguchi, K., & Kim, S. (2014). Influence of fiber reinforcement on strength and toughness of all-lightweight concrete. *Construction and Building Materials*, 69, 381-389.

Choi, Y., & Yuan, R. L. (2005). Experimental relationship between splitting tensile strength and compressive strength of GFRC and PFRC. *Cement and Concrete Research*, 35(8), 1587-1591.

Choi, Y. W., Kim, Y. J., Shin, H. C., & Moon, H. Y. (2006). An experimental research on the fluidity and mechanical properties of high-strength lightweight self-compacting concrete. *Cement and Concrete Research*, 36(9), 1595-1602.

Corinaldesi, V., & Moriconi, G. (2015). Use of synthetic fibers in self-compacting lightweight aggregate concretes. *Journal of Building Engineering*, 4, 247-254.

Cyr, M., & Mouret, M. (2003). Rheological characterization of superplasticized cement pastes containing mineral admixtures: consequences on self-compacting concrete design. *Proceedings of seventh CANMET/ACI International Conference on Superplasticizers and Other Chemical Admixtures in Concrete, American Concrete Institute*, Farmington Hills, Michigan, USA.

EFNARC. (2005). The European Guidelines for Self-Compacting Concrete Specification, Production and Use. *European Federation for Specialist Construction Chemicals and Concrete Systems*, English ed. Norfolk, UK.

Hassan, A. A. A., Ismail, M. K., & Mayo, J. (2015). Mechanical Properties of Self-Consolidating Concrete Containing Lightweight Recycled Aggregate in Different Mixture Compositions. *Journal of Building Engineering*, 4, 113-126.

Hossain, K. M. A., Lachemi, M., Sammour, M., & Sonebi, M. (2013). Strength and fracture energy characteristics of self-consolidating concrete incorporating polyvinyl alcohol, steel and hybrid fibres. *Construction and Building Materials*, 45, 20-29.

Iqbal, S., Ali, A., Holschemacher, K., & Bier, T. A. (2015). Mechanical Properties of Steel Fiber Reinforced High Strength Lightweight Self-Compacting Concrete (SHLSCC). *Construction and Building Materials*, 98, 325-333.

Ismail, M. K., & Hassan, A. A. A. (2015). Influence of mixture composition and type of cementitious materials on enhancing the fresh properties and stability of self-consolidating rubberized concrete. *Journal of Materials in Civil Engineering*, 28(1), 04015075.

Khayat, K. H., Kassimi, F., & Ghoddousi, P. (2014). Mixture Design and Testing of Fiber-Reinforced Self-Consolidating Concrete. *ACI Materials Journal*, 111(2), 143-151.

Ko, D., & Choi, H. (2013). Truss rail method for punching shear strength of flat-plate slab-column using high-strength lightweight concrete. *Magazine of Concrete Research*, 65(10), 589–599.

Lachemi, M., Hossain, K. M., Lambros, V., & Bouzoubaa, N. (2003). Development of cost-effective self-consolidating concrete incorporating fly ash, slag cement, or viscosity-modifying admixtures. ACI Materials Journal, 100(5), 419-425.

Libre, N. A., Shekarchi, M., Mahoutian, M., & Soroushian, P. (2011). Mechanical properties of hybrid fiber reinforced lightweight aggregate concrete made with natural pumice. *Construction and Building Materials*, 25(5), 2458-2464.

Li, J., Wan, C., Niu, J., Wu, L., & Wu, Y. (2017). Investigation on flexural toughness evaluation method of steel fiber reinforced lightweight aggregate concrete. *Construction and Building Materials*, 131, 449-458.

Madandoust, R., & Mousavi, S. Y. (2012). Fresh and Hardened Properties of Self-Compacting Concrete Containing Metakaolin. Construction and Building Materials, 35, 752-760.

Marar, K., & Eren, O. (2011). Effect of Cement Content and Water/ Cement Ratio on Fresh Concrete Properties without Admixtures. International Journal of Physical Sciences, 6(24), 5752-5765.

Mazaheripour, H., Ghanbarpour, S., Mirmoradi, S. H., & Hosseinpour, I. (2011). The effect of polypropylene fibers on the properties of fresh and hardened lightweight self-compacting concrete. *Construction and Building Materials*, 25(1), 351-358.

Shi, C., & Yang, X. (2005). Design and application of self-consolidating lightweight concretes. *Proceedings of 1st Int. RILEM Symp. on design, performance and use of self-consolidating concrete*. RILEM Publication SARL, Paris, France, 55-64.

Umehara, H., Uehara, T., Enomoto, Y., & Oka, S. (1994). Development and usage of lightweight high-performance concrete. Proceedings of International Conference on high Performance Concrete (supplementary papers), Singapore, *American Concrete Institute,* Detroit, USA, 339-53.

Wu, Z., Zhang, Y., Zheng, J., & Ding, Y. (2009). An experimental study on the workability of self-compacting lightweight concrete. *Construction and Building Materials*, 23(5), 2087-2092.

Yao, S. X., & Gerwick, B. C. (2006). Development of Self-Compacting Lightweight Concrete for RFP Reinforced Floating Concrete Structures. Technical Report, California, USA.

3. Use of polymeric fibers to improve the mechanical properties and impact resistance of lightweight SCC

3.1 Abstract

This chapter aims to evaluate the impact resistance and mechanical properties of a number of lightweight self-consolidating concrete (LWSCC) mixtures containing coarse and fine lightweight expanded slate aggregates and reinforced with different types of polymeric fibers. The investigation covered different binder contents (550 kg/m^3 and 600 kg/m^3), coarse-to-fine aggregate (C/F) ratios (0.7 and 1.0), fiber types (polyvinyl alcohol and polypropylene fibers), fiber lengths (8 mm, 12 mm, and 19 mm), and fiber volumes (0.3%, 0.5%, and 1%). Two normal-weight self-consolidating concrete (NWSCC) mixtures containing coarse and fine crushed granite aggregates were also tested for comparison. The results indicated that the addition of shorter fibers showed more pronounced improvement of the impact resistance compared to longer fibers. Mixtures developed with expanded slate fine aggregate exhibited better strength-to-weight ratio in terms of splitting tensile strength (STS), flexural strength (FS), and energy absorption capacity compared to their counterpart mixtures containing expanded slate coarse aggregate. With the absence of self-compactability restrictions (especially the passing ability), it was possible to develop vibrated concrete mixtures with higher content of lightweight aggregate and polymeric fibers, achieving lightweight concrete with lower density and higher STS, FS, ductility, and energy absorption capacity.

3.2 Introduction

Lightweight concrete is a preferred choice in some applications of the concrete industry as it allows for reduced weight of structural elements, which offers a prospective reduction in construction expenses (Kim et al., 2012; Ko & Choi, 2013). Using lightweight concrete can also lower transportation costs when used in the precast industry. The density of lightweight concrete is normally less than 1850 kg/m^3. This concrete is a favorable alternative in different structural applications, such as long-span bridges and post-tensioned concrete ceiling due to its higher strength-to-weight ratio and better sustainability properties compared to conventional concrete (Melby et al., 1996; Raithby & Lydon, 1981; Szydlowki & Mieszcak, 2017). Lightweight concrete is also characterized by a decreased shrinkage cracking and superior fire resistance (Uygunoğlu & Topçu, 2009; Mousa et al., 2018). It is widely used in marine areas and offshore structures due to its acceptable durability performance (Haug & Fjeld, 1996).

Lightweight self-consolidating concrete (LWSCC) is a new type of innovative concrete that combines the beneficial effects of lightweight concrete and the desired properties of SCC (Kim et al., 2010; Hassan et al., 2015). Recently, LWSCC has been applied in a number of structural applications related to the precast industry, such as thin concrete walls and sections (Shi et al., 2005). Developing LWSCC mixtures is challenging due to the low density of lightweight aggregates, which increases the chance of segregation. However, optimizing the mixture proportions and using supplementary cementing materials in LWSCC was found to improve the mixture viscosity, enhance the particle suspension, and reduce the probability of aggregate segregation (Lachemi et al., 2003; Hassan et al., 2012;

AbdelAleem & Hassan, 2018). Bogas et al. (2012) studied the effect of different mixture compositions on the fresh properties of LWSCC developed with expanded clay lightweight aggregate. Their research concluded that with 33% fly ash by weight and a total binder content of between 490 kg/m^3 and 599 kg/m^3, it was possible to develop LWSCC between 1724 kg/m^3 and 1947 kg/m^3 with successful fresh properties and reduced risk of segregation. Abouhussien et al. (2015) investigated the fresh properties of semi-lightweight concrete mixtures (density ranging from 1850 to 2150 kg/m^3, based on CSA's classification) made with expanded slag aggregates. They found that using a high binder content (above 500 kg/m^3) is necessary to develop successful LWSCC with acceptable fresh properties. They also found that using metakaolin (MK) appeared to improve the viscosity and particle suspension of SCC mixtures and greatly enhanced the compressive strength.

The use of fibers proved to greatly improve the ductility, tensile strength, toughness, impact strength, and energy absorption capacity of concrete (Balendran et al., 2002; Hossain et al., 2013; Ismail & Hassan 2017; AbdelAleem et al., 2017). However, the use of fibers in LWSCC adds more challenge in optimizing the fresh properties of the mixture. Previous studies concluded that the addition of fibers significantly reduced the flowability and passing ability of SCC. The high flowability of SCC mixtures also increased the chance of fiber segregation. Wang and Wang (Wang & Wang, 2013) investigated the influence of using different volumes of steel fibers on the impact resistance and mechanical properties of lightweight vibrated concrete (LWVC) mixtures containing expanded shale lightweight aggregate. They reported that the addition of steel fibers generally improved the impact

resistance and post-cracking behavior, attributing that to the bridging effect of fibers. The authors also suggested a volume ratio of 1%–1.5% for the highest improvement in the strength and fracture toughness.

Compared to all other types of fiber, steel fibers were found to have higher improvements on the mechanical properties, ductility, and impact strength. However, steel fibers showed some negative effects on the fresh properties, density, and corrosion resistance of concrete (Wu & Li, 1994; Shafigh et al., 2011; Hassanpour et al., 2012). Kayali et al. (2003) studied the effect of polypropylene (PP) and steel fibers on the mechanical properties of LWVC developed with sintered fly ash aggregates (Lytag). The authors found that the inclusion of steel fibers showed better improvement in terms of the splitting tensile strength (STS) and flexural strength (FS) compared to PP fibers. However, the mixtures containing steel fibers exhibited lower modulus of elasticity (ME) and higher concrete density. Using synthetic fibers in concrete showed some advantages in terms of density and corrosion resistance. Synthetic fibers also improved the post-cracking behavior and concrete ductility (AbdelAleem et al., 2018). Corinaldesi and Moriconi investigated the mechanical properties of LWSCC mixtures reinforced with synthetic fibers. They found that the inclusion of synthetic macro-fibers significantly improved the post-cracking behavior of LWSCC mixtures and provided the same strain-hardening response obtained by steel fibers, but with lower concrete density and higher corrosion resistance (Corinaldesi & Moriconi, 2015).

This chapter aims to develop a number of successful LWSCC mixtures with different types of polymeric fibers having minimum possible density and maximized impact resistance.

The chapter also included the development of lightweight vibrated concrete (LWVC) mixtures with maximum possible content of lightweight aggregates and fibers. In addition, normal-weight self-consolidating concrete (NWSCC) mixtures were poured for comparison. The experimental test parameters included type of lightweight aggregates (either fine or coarse expanded slate aggregates), type of polymeric fibers, fiber volume, fiber length, lightweight aggregate content, and binder content.

3.3 Research Significance

LWSCC is a very promising material used in applications that require both high compactability and lightweight concrete. The development of LWSCC, however, is challenging as the high flowability of SCC mixtures increases the risk of segregation. The low density of lightweight coarse aggregate used in LWSCC also has a negative effect on the flowability and passing ability of the mixture. Using fibers in LWSCC significantly improves the STS, FS, and ductility and alleviates the reduction in the mechanical properties from using lightweight aggregates (LWA). However, the use of fibers in LWSCC adds additional challenge in optimizing the mixture since fibers negatively affect the fresh properties of SCC. By reviewing the literature, it was found that only a few studies have investigated the development of LWSCC with fibers. In addition, investigating fiber-reinforced LWSCC with expanded slate is missing from the literature despite the high quality and strength of this aggregate compared to other types of LWA. Therefore, this chapter aimed to cover this knowledge gap by highlighting the key factors that impact the development of successful fiber-reinforced LWSCC with expanded slate. The influence of using different types, volumes, and lengths of fibers—and the influence of using different

mixture compositions on improving the mechanical properties and impact resistance of the developed mixtures are also covered in this stage. Moreover, this chapter exclusively presents the advantages/disadvantages of using expanded slate coarse aggregates compared to expanded slate sand on the fresh/mechanical properties and impact resistance of the developed mixtures.

3.4 Experimental Program

3.4.1 Concrete mixtures

In this stage, Two NWSCC, fourteen LWSCC and fibered-LWSCC, and two lightweight vibrated concrete (LWVC) mixtures were developed and tested. All SCC mixtures were previously developed in Chapter 2. While mixtures 10 and 18 were designed as fiber-reinforced LWVC to investigate the advantage of using a higher volume of LWA and higher fiber content (1%) on reducing the mixture density and possibly improving the impact resistance of the developed mixtures. It should be noted that it was possible to use the highest percentages of LWA and the highest fiber volume (1%) in LWVC only because of the absence of the fresh properties' restrictions of LWSCC.

All developed mixtures were designated by total binder content, C/F ratio, type of lightweight aggregate used (either LC or LF), fraction volume of fiber, and type of fiber (see **Table 3-1**). For example, an LWSCC mixture with 550 kg/m^3 binder content, 0.7 C/F aggregate ratio, LC, and 0.3% PVA8 fiber has a designation of 550-0.7LC-0.3PVA8. While a LWVC mixture with a 600 kg/m^3 binder content, 0.5 C/F ratio, LF, and 1% PVA8 fiber has a designation of 600-0.5LF-1PVA8-VC.

Table 3-1: Mixture proportions for the developed mixtures.

	Mix. #	Designation	Cement (kg/m^3)	MK (kg/m^3)	FA (kg/m^3)	Aggregates					Fiber (%)
						C/F aggregate ratio	NC (kg/m^3)	NF (kg/m^3)	LC (kg/m^3)	LF (kg/m^3)	
NWSCC mixtures	1	550-0.7NWSCC	275	110	165	0.7	620.3	886.1	-	-	-
	2	550-1NWSCC	275	110	165	1.0	753.2	753.2	-	-	-
LWSCC (coarse aggregate slate & normal-weight sand)	3	550-0.7LC	275	110	165	0.7	-	689.2	482.4	-	-
	4	550-0.7LC-0.3PVA8	275	110	165	0.7	-	685.6	480.0	-	0.3
	5	550-0.7LC-0.3PVA12	275	110	165	0.7	-	685.6	480.0	-	0.3
	6	550-0.7LC-0.3PP19	275	110	165	0.7	-	685.6	480.0	-	0.3
	7	600-0.7LC-0.3PVA8	300	120	180	0.7	-	640.3	448.2	-	0.3
	8	600-1LC-0.3PVA8	300	120	180	1.0	-	519.4	519.4	-	0.3
	9	600-0.7LC-0.5PVA8	300	120	180	0.7	-	638.0	446.6	-	0.5
	10	600-1.5LC-1PVA8-VC	300	120	180	1.5	-	389.9	584.9	-	1.0
LWSCC (normal-weight coarse aggregate & fine aggregate slate)	11	550-1LF	275	110	165	1.0	617.3	-	-	617.3	-
	12	550-1LF-0.3PVA8	275	110	165	1.0	614.1	-	-	614.1	0.3
	13	550-1LF-0.3PVA12	275	110	165	1.0	614.1	-	-	614.1	0.3
	14	550-1LF-0.3PP19	275	110	165	1.0	614.1	-	-	614.1	0.3
	15	600-1LF-0.3PVA8	300	120	180	1.0	573.6	-	-	573.6	0.3
	16	600-0.7LF-0.3PVA8	300	120	180	0.7	457.7	-	-	653.8	0.3
	17	600-1LF-0.5PVA8	300	120	180	1.0	571.4	-	-	571.4	0.5
	18	600-0.5LF-1PVA8-VC	300	120	180	0.5	355.9	-	-	711.7	1.0

Note: All mixtures have a 0.4 w/b ratio.

3.5 Testing Program

3.5.1 Fresh and mechanical properties tests

The fresh properties of NWSCC and LWSCC mixtures were assessed according to the European Guidelines for Self-Compacting Concrete (2005) using slump flow, V-funnel, J-ring, and L-box tests. The flowability of mixtures was assessed by measuring the time to reach 500 mm slump flow diameter (T_{50}), time to reach 500 mm J-ring diameter ($T_{50\text{-}J}$), and V-funnel time. In addition, the difference between slump flow and J-ring diameters and the ratio of L-box test (H2/H1) were also determined to evaluate the passing ability of mixtures. The segregation resistance of the developed NWSCC and LWSCC mixtures was evaluated by splitting a 100 mm diameter x 200 mm high concrete cylinder vertically into two halves and then observing the distribution of the aggregate along the cylinder's broken section. On the other hand, the slump test was performed to evaluate the workability of LWVC mixtures as per ASTM C143 (2015). Table 3-2 presents the fresh properties of all developed mixtures.

Table 3-2: Fresh properties of tested mixtures.

Mix. #	Designation	T_{50} (s)	$T_{50\text{-}J}$ (s)	Slump – J-ring diameter (mm)	L-box (H2/H1) (%)	V-funnel (s)	Segregation resistance	Air (%)	HRWR (L/m^3)
1	550-0.7NWSCC	2.05	2.43	10	0.97	6.86	NS	1.5	3.40
2	550-1NWSCC	2.30	2.90	25	0.91	7.80	NS	2.1	3.10
3	550-0.7LC	2.75	3.50	30	0.92	10.80	NS	3.1	3.67
4	550-0.7LC-0.3PVA8	3.48	4.58	45	0.82	11.30	NS	3.5	4.10
5	550-0.7LC-0.3PVA12	3.96	4.88	50	0.80	13.13	NS	3.7	4.30
6	550-0.7LC-0.3PP19	4.69	5.70	70	0.76	16.10	NS	4.0	4.67
7	600-0.7LC-0.3PVA8	3.20	3.90	25	0.91	9.48	NS	3.3	3.40
8	600-1LC-0.3PVA8	3.48	4.52	40	0.81	11.20	NS	3.5	3.70
9	600-0.7LC-0.5PVA8	4.12	5.35	50	0.82	12.48	NS	3.5	4.29
10	600-1.5LC-1PVA8-VC	Slump value = 175 mm						3.2	3.25
11	550-1LF	2.10	2.69	15	0.95	5.37	NS	3.2	3.50
12	550-1LF-0.3PVA8	2.41	3.22	35	0.85	6.25	NS	3.5	3.83
13	550-1LF-0.3PVA12	2.80	3.80	45	0.82	7.12	NS	3.5	3.95
14	550-1LF-0.3PP19	3.38	4.72	65	0.77	8.55	NS	3.7	4.22
15	600-1LF-0.3PVA8	2.10	2.60	30	0.88	4.86	NS	4.0	3.30
16	600-0.7LF-0.3PVA8	1.70	2.30	20	0.91	4.05	NS	3.5	3.60
17	600-1LF-0.5PVA8	2.70	3.53	45	0.83	6.75	NS	3.6	4.30
18	600-0.5LF-1PVA8-VC	Slump value = 190 mm						3.3	3.15

The mechanical properties tests included compressive strength (f_c'), STS, FS, and modulus of elasticity (ME). The compressive strength and STS were determined using 100 mm diameter x 200 mm high cylinders, as per ASTM C39 (2011) and C496 (2011), respectively. The FS of 100 mm x 100 mm x 400 mm prisms was measured for all developed mixtures as per ASTM C78 (2010). The ME of all mixtures was measured using a strain gauge attached to a 150 mm diameter x 300 mm high concrete cylinder tested under compressive loading. All mechanical properties tests were performed using three identical specimens that had been moist-cured until the age of testing (7 and 28 days).

3.5.2 Impact resistance tests

Two different tests were carried out to evaluate the impact resistance of the developed mixtures, as follows:

A. Drop-weight test: This test was conducted according to the recommendation of the ACI Committee 544 (1999) using three identical 150 mm diameter x 63.5 mm thick cylindrical specimens from each mixture. In this test, a 4.45-kg hammer was dropped from a height of 457 mm onto a 63.5-mm steel ball located at the center of the top surface of the cylindrical specimen (as per ACI 544, 1999), as shown in Figure 3-1**a**. The number of blows needed to produce the first visible crack (N1) was recorded. Also, the ultimate crack resistance was determined by recording the number of blows needed to cause failure (N2). The ultimate crack resistance was recorded when the cracked disc touched the lugs on the baseplate of the test apparatus (ACI 544, 1999).

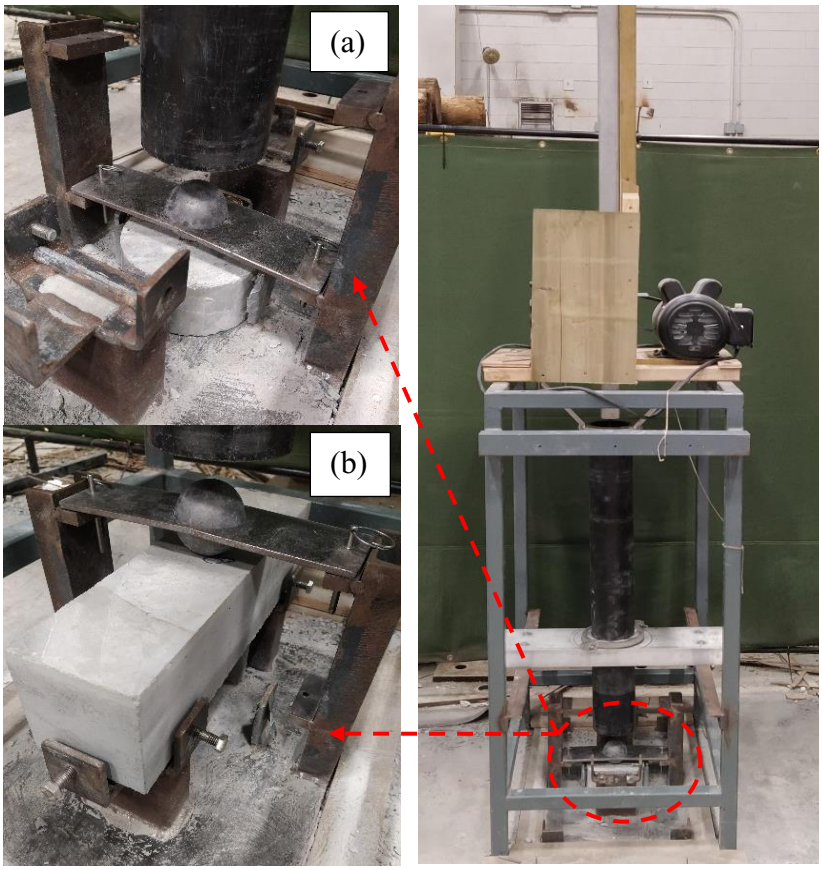

Figure 3-1: Impact resistance tests: (a) ACI drop-weight test; and (b) flexural impact loading test.

B. Flexural impact loading test: This test was performed on beams using a three-point loading setup to assess the energy absorption capacity of the developed mixtures. For each of the developed mixtures, three identical 100 mm x 100 mm x 400 mm beam samples were tested with an effective loading span of 350 mm. The specimens were subjected to repeated impact loading generated by dropping a 4.45-kg hammer from a height of 150 mm onto a 63.5-mm steel ball placed at the mid-span of the tested beams (see Figure 3-1**b**). Due to the difficulty of determining the first crack, especially in

non-fibered NWSCC/LWSCC mixtures, only the number of blows that cause failure was recorded to calculate the ultimate impact energy of all developed mixtures.

In general, the impact energy for both tests was calculated according to Eq. (1):

$$IE = Nmgh \quad (1)$$

Where N = number of blows at crack level; m = mass of the dropped hammer (4.45 kg); g = gravity acceleration (9.81 m/s^2); and h = drop height (457 mm or 150 mm).

3.6 Results and Discussion

3.6.1 Compressive strength

3.6.1.1 Effect of lightweight aggregate

The 7- and 28-day compressive strengths for all developed mixtures are presented in Table 3-3 and Figure 3-2 (**a** and **b**). Using either coarse or fine LWA showed an obvious reduction in the compressive strength. By comparing mixtures 1 to 3, it can be seen that substituting normal-weight coarse aggregate with expanded slate coarse aggregate, to reduce the density by 15.5%, decreased the 28-day compressive strength by 28.2%. Similarly, replacing normal-weight fine aggregate (mixture 2) by expanded slate fine aggregate (mixture 11) to reduce the density by 12.3%, decreased the 28-day compressive strength by 27.8%. This reduction in compressive strength was expected due to replacing stronger crushed granite aggregate by relatively weaker expanded slate aggregate.

Table 3-3: Mechanical properties of tested mixtures.

Mix. #	Mixture designation	f'_c (MPa)		*STS* (MPa)		*FS* (MPa)		*ME* (GPa)	*Dry density*
		7-days	28-days	7-days	28-days	7-days	28-days	28-days	(kg/m^3)
1	550-0.7NWSCC	59.7	74.9	3.82	4.38	5.04	5.76	30.57	2259.4
2	550-1NWSCC	65.3	71.2	4.09	4.29	5.84	5.84	30.41	2261.2
3	550-0.7LC	41.6	53.8	2.54	2.87	3.58	4.19	23.21	1909.1
4	550-0.7LC-0.3PVA8	40.6	53.1	3.21	3.76	4.42	5.22	22.58	1904.2
5	550-0.7LC-0.3PVA12	39.6	51.8	3.09	3.59	4.31	5.13	21.83	1907.8
6	550-0.7LC-0.3PP19	39.0	51.2	2.97	3.48	4.10	4.93	21.05	1905.9
7	600-0.7LC-0.3PVA8	42.4	55.9	3.33	3.89	4.58	5.44	22.34	1898.1
8	600-1LC-0.3PVA8	39.1	51.2	3.02	3.54	4.07	4.92	20.13	1836.7
9	600-0.7LC-0.5PVA8	40.1	53.2	3.64	4.33	5.08	6.09	20.35	1893.2
10	600-1.5LC-1PVA8-VC	31.9	44.2	3.24	3.92	4.51	5.24	18.11	1734.6
11	550-1LF	40.5	51.4	2.63	3.10	4.21	4.89	24.87	1982.8
12	550-1LF-0.3PVA8	39.8	49.7	3.39	4.17	5.23	6.15	23.89	1979.7
13	550-1LF-0.3PVA12	39.1	49.3	3.24	3.98	5.03	5.93	23.46	1978.2
14	550-1LF-0.3PP19	38.3	49.7	3.12	3.81	4.85	5.79	22.36	1975.6
15	600-1LF-0.3PVA8	42.5	53.8	3.53	4.30	5.41	6.33	23.91	1970.6
16	600-0.7LF-0.3PVA8	38.5	48.9	3.07	3.79	4.60	5.55	21.72	1922.3
17	600-1LF-0.5PVA8	40.7	51.9	3.92	4.88	5.97	7.03	22.04	1965.3
18	600-0.5LF-1PVA8-VC	35.6	47.8	3.48	4.36	5.45	6.12	20.84	1868.6

3.6.1.2 Effect of fiber type, length, and content

The inclusion of polymeric fibers in lightweight concrete (containing either LC or LF) slightly reduced the compressive strength. In LWSCC-LC mixtures, adding 0.3% PVA8, PVA12, or PP19 (mixtures 4-6) slightly decreased the 7- and 28-day compressive strength by an average of 4.5% and 3.2%, respectively, compared to mixture 3 with no fibers. Similarly, LWSCC-LF mixtures with 0.3% fibers (mixtures 12-14) showed insignificant reduction in the 7- and 28-day compressive strength by an average of 3.5% and 3.6%, respectively, compared to the non-fibered LWSCC-LF mixture (mixture 11). The results also showed that mixtures 9 and 17 exhibited further reduction in the compressive strength compared to mixtures 7 and 15, respectively. This reduction was obvious due to using a higher percentage of fibers (0.5%).

3.6.1.3 Effect of binder content

As mentioned before, it was possible to improve the compressive strength of the developed LWSCC mixtures by using higher binder content (600 kg/m^3 compared to 550 kg/m^3) without affecting the mixtures' density. As seen in Table 3-3, increasing the binder content in LWSCC-LC mixtures from 550 kg/m^3 (mixture 4) to 600 kg/m^3 (mixture 7) enhanced the 7- and 28-day compressive strength by an average of 4.3% and 5.3%, respectively, while the density of the mixture was not significantly affected. Similar results were observed in LWSCC-LF mixtures with the same increase in binder content. The 7- and 28-day compressive strength in LWSCC-LF mixtures were improved by an average of 6.9% and 3.4%, respectively (mixture 15 compared to mixture 12).

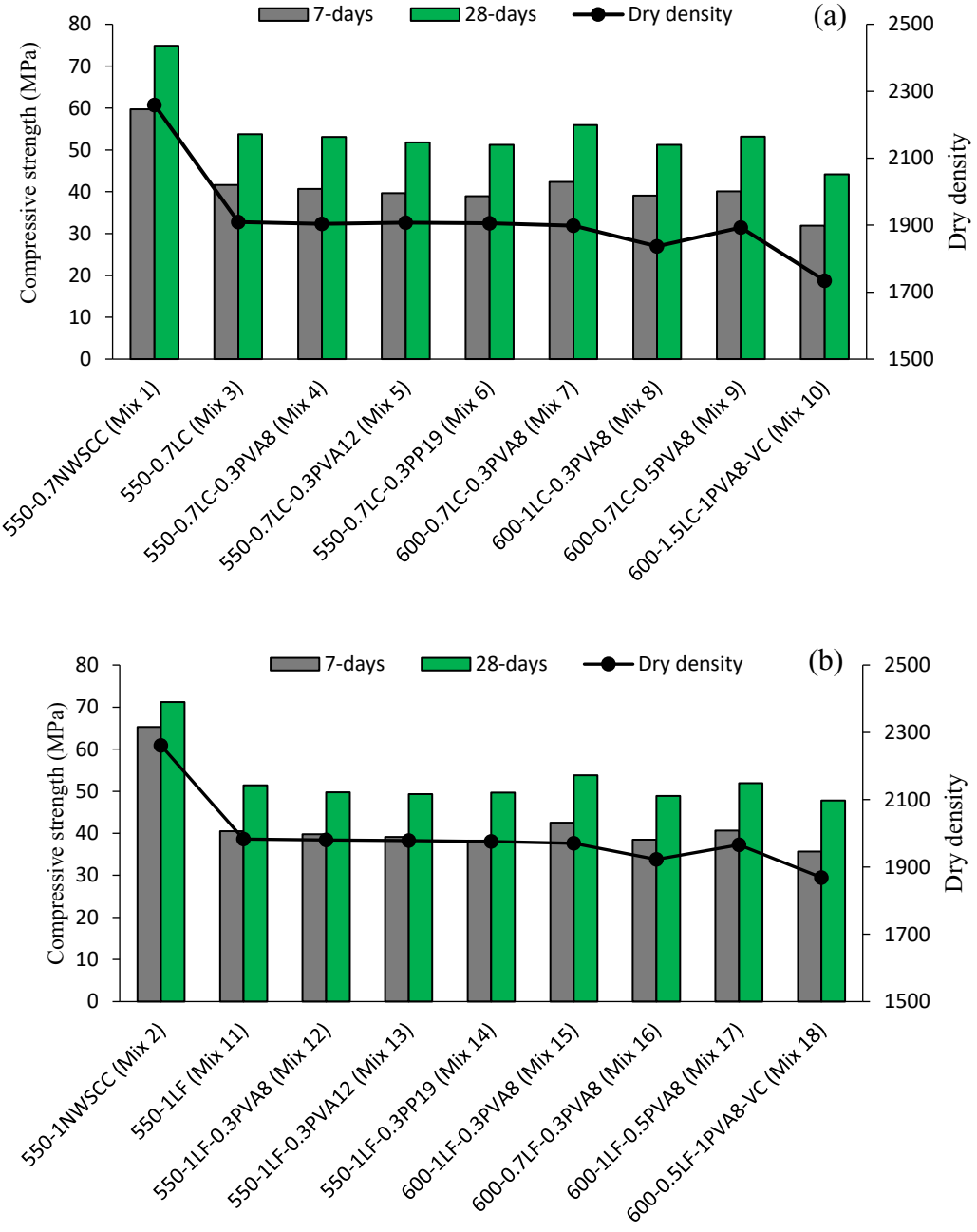

Figure 3-2: 7- and 28-day compressive strengths for (a) mixtures with LC, (b) mixtures with LF.

3.6.1.4 Comparison of LWVC and LWSCC mixtures

Without the fresh properties restrictions of SCC (mainly passing ability and segregation), it was possible to develop vibrated concrete mixtures with up to 1.5 C/F aggregate ratio of coarse aggregate expanded slate and 0.5 C/F aggregate ratio of expanded slate fine aggregate (compared to 1.0 and 0.7 C/F aggregate ratio, maximum contents of expanded slate aggregates in LWSCC mixtures). This increase in the LWA contents allowed to develop LWVC mixtures with a minimum density of 1734.6 and 1868.6 kg/m^3 compared to 1836.7 and 1922.3 kg/m^3, the minimum density achieved in the development of SCC mixtures with LC and LF, respectively (mixtures 10 and 18 compared to mixtures 8 and 16, respectively). This reduction in the density (4.2% on average) of LWVC mixtures showed a slight decrease in the 28-day compressive strength by an average of 8% (for both LF and LC mixtures) compared to the compressive strengths of the minimum-density counterpart mixtures developed in SCC.

3.6.2 Splitting tensile and flexural strengths and modulus of elasticity

3.6.2.1 Effect of lightweight aggregate

Table 3-3 shows the STS and FS results of all tested mixtures. It can be noticed that the STS, FS, and ME were negatively affected by using LWA. For example, in the LWSCC-LC mixture (mixture 3), a 15.5% reduction in the density resulted in a reduction in the STS, FS, and ME of 34.4%, 27.3%, and 24.1%, respectively, compared to mixture 1 with normal-weight aggregate. Similarly, a 12.3% reduction in the density of LWSCC-LF mixtures resulted in a reduction in the STS, FS, and ME of 27.7%, 16.3%, and 18.2%,

respectively (mixture 11 compared to mixture 2). These reductions may be attributed to the weak strength and stiffness of LWA compared to normal-weight aggregate, which is also reported by other researchers (Floyd et al., 2015; Lotfy et al., 2015; Grabois et al., 2016). Figure 3-3 shows the ratios of STS/weight and FS/weight of all tested mixtures. In general, it can be observed from these figures that using LF in LWSCC/LWVC mixtures showed higher strength-to-weight ratios in terms of splitting and flexural strengths compared to those obtained when using LC. This is related to the higher volume of internal pores in LC compared to LF, which caused more reduction in the strength of the mixture.

3.6.2.2 Effect of fiber type, length, and content

Table 3-3 shows that the inclusion of polymeric fibers greatly improved the STS and FS and slightly decreased the ME of the developed LWSCC mixtures. For example, by comparing mixtures 4-6 to mixture 3 (which have comparable densities), it can be noticed that using 0.3% polymeric fibers improved the 28-day STS and FS by an average of 25.3% and 22.1%, respectively (see Table 3-3) and decreased the ME by an average of 6% (Figure 3-4**a**). The improvements in the STS and FS can be attributed to the bridging action of fibers, which contributes to restricting the propagation of cracks and transferring the tensile stress across crack faces, providing residual strength to the concrete composite (Jun Li et al., 2016). Meanwhile, the reduction in the ME is due to the low modulus of elasticity of polymeric fibers, which contributes to decreasing the overall stiffness of the composite and in turn reduces the overall ME (AbdelAleem et al., 2018). Similar results were also confirmed in LWSCC-LF mixtures (mixtures 12-14 compared to mixture 11).

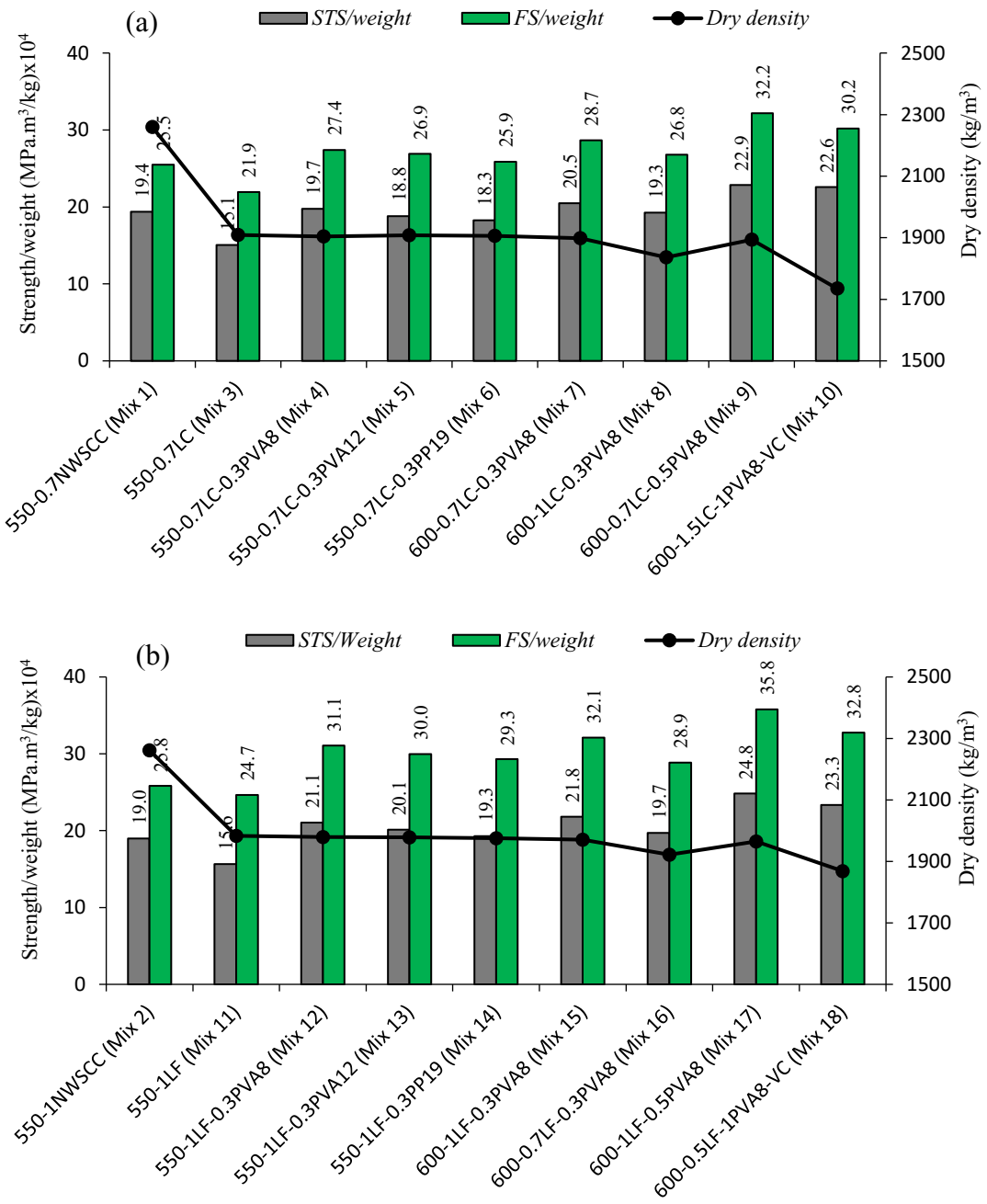

Figure 3-3: 28-day strength-to-weight ratio in terms of STS and FS for (a) mixtures with LC, (b) mixtures with LF.

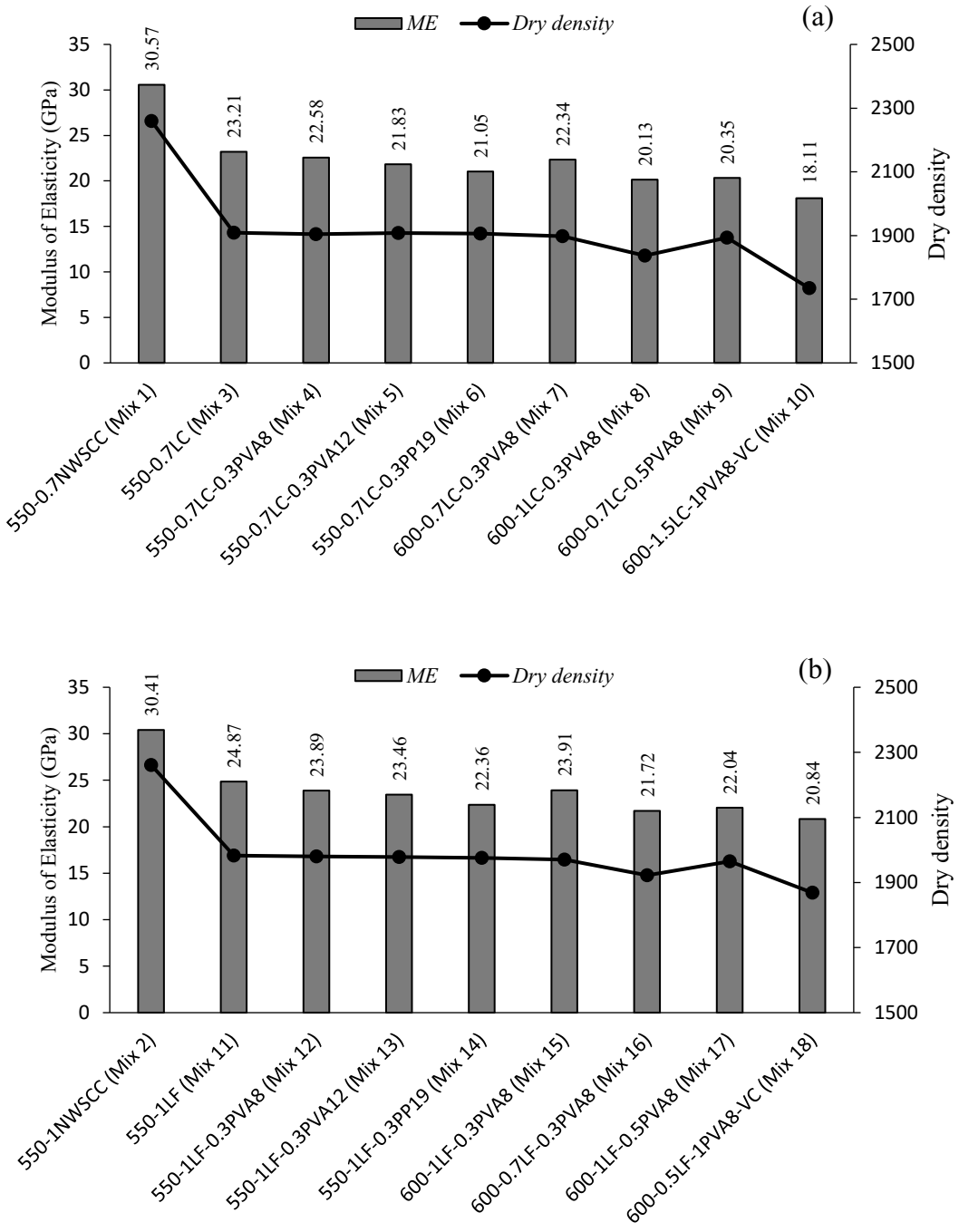

Figure 3-4: 28-day ME results for (a) mixtures with LC, (b) mixtures with LF.

The results shown in Table 3-3 also indicated that PVA8 showed the highest improvement in the STS and FS, and the lowest reduction in the ME followed by PVA12 and then PP19. For example, by looking at mixtures 4-6 (which had the same density and volume of fibers), using PVA8 increased the 28-day STS by 30.8% compared to 24.9% and 21.1% increase in PVA12 and PP19, respectively. A similar trend was also observed with LWSCC-LF mixtures, indicating better improvement in the STS and FS with the use of PVA8 compared to the other tested fiber types (mixtures 12-14 compared to mixture 11). The better improvement of PVA fibers compared to PP fibers may be related to the higher tensile strength of PVA fibers, while the higher results achieved by PVA8 compared to PVA12 can be attributed to the shorter length of PVA8 compared to PVA12, which provided a higher number of single fibers (at the same fiber volume) dispersed in the concrete matrix, allowing better crack widening control and better tensile stress transfer across crack faces (Passuello et al., 2009; Ismail et al., 2018). **Figure 3-4a** also indicates that using PVA8 in LWSCC-LC mixtures at the same level of fiber content showed a reduction in the ME by 2.7% compared to a 5.9% and 9.3% decrease when using PVA12 and PP19, respectively (mixtures 4-6 compared to mixture 3).

The results also indicated that using higher fiber content (0.5% compared to 0.3%) showed further improvement in the STS and FS results of LWSCC mixtures, but with extra reduction in the ME. For example, in LWSCC-LC mixtures, increasing the fiber content from 0.3% to 0.5% (mixture 7 compared to mixture 9) increased the 28-day STS and FS by 11.3% and 11.9%, respectively, and decreased the ME by 8.9% (see **Table 3-3**).

3.6.2.3 Effect of binder content

Increasing the binder content from 550 kg/m^3 to 600 kg/m^3 showed higher ratios of STS/weight and FS/weight, indicating better mechanical properties at the same density level. However, the results of ME were insignificantly affected. For example, by looking at mixture 15, with a total binder content of 600 kg/m^3 compared to mixture 12 with 550 kg/m^3, it can be seen that the ratio of STS/weight increased from 21.1 to 21.8 Mpa.m^3/kg x10^4, and the ratio of the FS/weight increased from 31.1 to 32.1 Mpa.m^3/kg x10^4 (Figure 3-3**b**), while the results of ME were not affected (Figure 3-4**b**). It should be noted that by increasing the binder content from 550 kg/m^3 to 600 kg/m^3 and using 0.5% PVA fibers, it was possible to fully compensate for the reductions in the STS and FS resulting from using LWA and achieve LWSCC mixtures with slightly higher STS and FS compared to NWSCC mixtures (see Table 3-3).

3.6.2.4 Comparison of LWVC and LWSCC mixtures

Since the passing ability is not a factor in developing VC mixtures, it was possible to incorporate higher content of PVA8 fiber (up to 1%) and higher content of LWA in mixtures 10 and 18. These two mixtures were achieved with densities less than those obtained when using SCC, and with even better STS and FS results. Table 3-3 shows that the inclusion of 1% of PVA8 in LWVC mixtures improved the 28-day STS and FS by 12.9% and 8.4% (on average), respectively, compared to what mixtures with minimum possible density achieved when using SCC (mixtures 10 and 18 compared to mixtures 8 and 16). Despite, the improvements achieved in the STS and FS, it was observed that LWVC mixtures showed slightly lower ME results (by an average of 7%) than those

obtained in LWSCC mixtures (mixtures 10 and 18 compared to mixtures 8 and 16, respectively) (see Table 3-3). This reduction was obvious due to the reduction in density, which was achieved after employing higher LWA content (see Figure 3-4**a** and **b**).

3.6.3 Impact resistance under drop-weight test

3.6.3.1 Effect of lightweight aggregate

The results of impact resistance under the drop-weight test for all tested mixtures are summarized in Table 3-4 and Figure 3-5 (**a** and **b**). The substitution of normal-weight aggregate with expanded slate aggregate adversely affected the impact resistance of the tested specimen in terms of number of blows required for initiating visible crack (N1) and number of blows required for ultimate failure (N2). By comparing mixture 3 to mixture 1 it can be seen that employing LC decreased N1 and N2 by 37.3% and 37.7%, respectively. Whereas using LF instead of crushed granite sand decreased N1 and N2 by 25.4% and 26.7%, respectively. These results can be attributed to the low density and compressive strength of lightweight mixtures compared to normal-weight mixtures. Also, mixtures 8 and 16, with minimum possible density achieved in SCC (higher LWA content with 600 kg/m^3 binder), showed a reduction in N1 and N2 by an average of 21.3% and 21.1%, respectively, compared to their counterpart mixtures with lower LWA content (mixtures 7 and 15). The results also indicated that, in general, mixtures with LF showed higher energy absorption compared to mixtures with LC (see Table 3-4), indicating favorable use of LF in LWSCC and LWVC mixtures.

Table 3-4: Results of impact resistance for tested mixtures.

Mix. #	Mixture designation	Drop-Weight Test					Flexural Impact Loading	
		Number of blows			IE (J)		Number of blows	IE (J)
		N_1	N_2	N_2-N_1	Initial	Failure		
1	550-0.7NWSCC	59	61	2	1177	1217	38	249
2	550-1NWSCC	56	59	3	1117	1177	36	236
3	550-0.7LC	37	38	1	738	758	23	151
4	550-0.7LC-0.3PVA8	51	59	8	1017	1177	37	242
5	550-0.7LC-0.3PVA12	46	52	6	918	1037	34	223
6	550-0.7LC-0.3PP19	43	46	3	858	918	29	190
7	600-0.7LC-0.3PVA8	61	70	9	1217	1397	45	295
8	600-1LC-0.3PVA8	48	55	7	958	1097	33	216
9	600-0.7LC-0.5PVA8	85	97	12	1696	1935	65	426
10	600-1.5LC-1PVA8-VC	41	54	13	818	1077	35	229
11	550-1LF	43	45	2	858	898	27	177
12	550-1LF-0.3PVA8	62	72	10	1237	1436	45	295
13	550-1LF-0.3PVA12	56	65	9	1117	1297	41	268
14	550-1LF-0.3PP19	54	60	6	1077	1197	36	236
15	600-1LF-0.3PVA8	75	86	11	1496	1716	53	347
16	600-0.7LF-0.3PVA8	59	68	9	1177	1357	42	275
17	600-1LF-0.5PVA8	109	122	13	2175	2434	79	517
18	600-0.5LF-1PVA8-VC	47	62	15	938	1237	41	268

3.6.3.2 Effect of fiber type, length, and content

Table 3-4 shows that the addition of polymeric fibers significantly alleviated the reduction in the impact resistance that resulted from using lightweight expanded slate aggregate in LWSCC mixtures. By looking at mixtures 4-6 and mixtures 12-14, it is obvious that adding 0.3% polymeric fibers increased N1 and N2 by an average of 29.7% and 41.8%, respectively, over the non-fibered mixtures (mixtures 3 and 11). Also, the difference between the number of blows for ultimate failure and initial crack (N2-N1) obviously increased, indicating a significant improvement in the ductility and post-cracking behavior of concrete (see **Figure 3-5a** and **b**). Such findings may be related to the role of fiber in restricting the cracks and transferring stresses through a bridging mechanism.

It is worth noting that the improvement in the impact resistance provided by PVA8 fiber was more pronounced compared to that induced by other types of polymeric fibers. For example, by evaluating the fiber-reinforced LWSCC-LC mixtures (mixtures 4-6), it can be noticed that at the same level of fiber content, the inclusion of PVA8 fibers significantly increased the absorbed energy at failure crack by 55.3% compared to 36.8% and 21.1% increase when PVA12 and PP19 were used, respectively (Figure 3-5**a**). Similar performance was confirmed in fiber-reinforced LWSCC-LF mixtures (see Figure 3-5**b**). The results also indicated that the inclusion of 0.5% fiber volume instead of 0.3% improved the N1 and N2 by an average of 42% and 40.2%, respectively (mixtures 9 and 17 compared to mixtures 7 and 15). Figure 3-6 shows the failure pattern of the tested specimens. It can be observed from the figure that the inclusion of polymeric fibers changed the failure pattern from one single wide crack (**Figure 3-6a**) to three or more intersecting smaller

cracks (Figure 3-6**b**). This confirms the favorable effect of polymeric fibers on enhancing the ductility and post-cracking performance of lightweight concrete under impact loading.

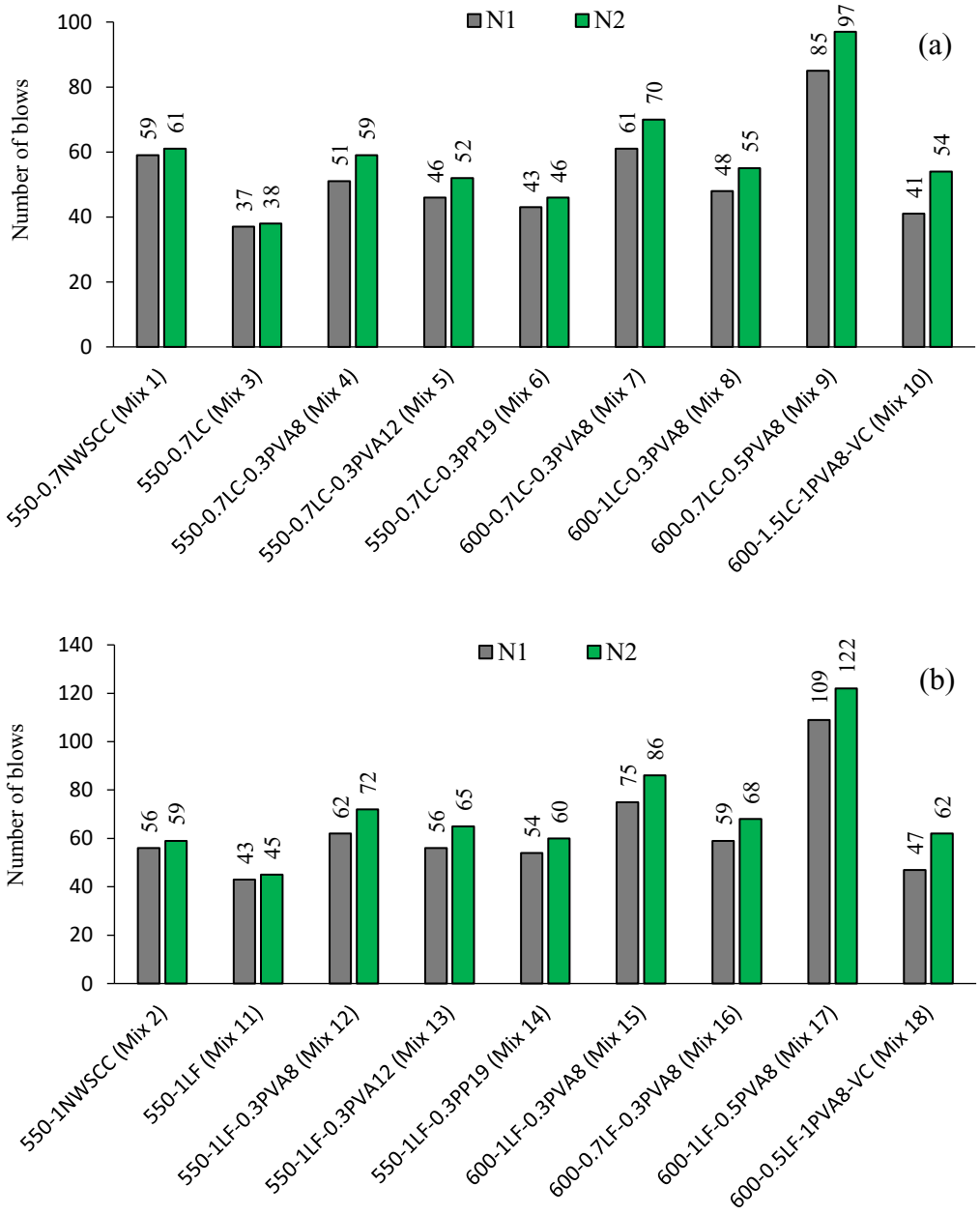

Figure 3-5: Results of impact resistance for the cylindrical specimens under drop-weight test: (a) mixtures with LC, (b) mixtures with LF.

(a) (b)

Figure 3-6: Failure pattern of tested specimens under drop-weight test: (a) non-fibered specimen, (b) specimen with polymeric fiber.

3.6.3.3 Effect of binder content

As shown in Table 3-4 and Figure 3-5 (**a** and **b**), increasing the binder content from 550 kg/m^3 to 600 kg/m^3 maintained similar concrete density and also improved the impact resistance of LWSCC mixtures. For example, increasing the binder content by 50 kg/m^3 in LWSCC-LC mixtures showed relatively higher number of blows at first and failure cracks, by 19.6% and 18.6%, respectively (mixture 7 compared to mixture 4) (see Figure 3-5**a**). Similar results were observed in LWSCC-LF mixtures as shown in Figure 3-5**b**. This increase can be related to the higher compressive strength of mixtures with binder content of 600 kg/m^3.

3.6.3.4 Comparison of LWVC and LWSCC mixtures

Using a higher amount of LWA and fiber volume in LWVC mixtures contributed to developing concrete with a density less than that obtained in SCC, and with comparable

impact resistance. For example, using LC with 1.5 C/F aggregate ratio and incorporating 1% PVA8 fiber in mixture 10 allowed a reduction in the concrete density by about 5.6% and allowed the mixture to endure similar impact energy compared to the minimum possible density obtained with SCC (mixture 8), as shown in **Figure 3-5a**. Also, the difference between the number of blows for ultimate failure and initial crack (N2 − N1) increased by 1.9 times in the LWVC compared to the LWSCC mixture (mixture 10 compared to mixture 8), indicating better post-cracking behavior. This is due to the absence of fresh properties restrictions of SCC, which allowed the introduction of a higher amount of polymeric fibers, up to 1%.

3.6.4 Impact resistance under flexural loading

It can be observed that the reduction that occurred in concrete density due to using expanded slate aggregate resulted in a drop in the ultimate impact energy of the developed LWSCC mixtures. By comparing mixtures 3 and 11 to their counterpart mixtures in NWSCC (mixtures 1 and 2), it can be seen that replacing crushed granite stones by either coarse or fine expanded slate aggregate reduced the impact energy by an average of 32.2%. Further increase in LWA content, which was used to develop LWSCC mixtures with minimum possible density (with 600 kg/m^3 binder), showed extra reduction in the energy absorption of concrete, as seen in mixtures 8 and 16 compared to mixtures 7 and 15, respectively. This reduction in impact resistance was obvious due to the decrease in compressive strength and density.

Optimizing the mixtures shows that it was possible to compensate for the reduction in the ultimate impact energy of LWSCC mixtures by using polymeric fibers without affecting the concrete density. For example, including PVA8 fiber in LWSCC-LC mixtures significantly improved the impact resistance of the tested prisms by 60.9% compared to the control mixture without fiber (mixture 4 compared to mixture 3) and reached an impact energy comparable to NWSCC (mixture 1). Using PVA12 and PP19 also exhibited improvements in the absorbed energy by 47.8% and 26.1%, respectively, higher than that obtained by the non-fibered mixture (mixtures 5-6 compared to mixture 3). Such behavior may be related to the same reasons previously explained for impact resistance under the drop-weight test. Mixtures 9 and 17, which contained the maximum possible fiber volume of fibers (0.5%) that can be used to develop successful LWSCC (using 600 kg/m^3 binder), showed an improvement in the ultimate impact energy of tested beams by an average of 46.8% compared to counterpart mixtures with 0.3% PVA8 (mixtures 7 and 15).

LWVC mixtures containing higher amounts of LWAs and polymeric fibers exhibited ultimate impact results comparable to those obtained in SCC, and with even lower concrete density. For example, combining 1% PVA8 and LC with 1.5 C/F aggregate ratio in mixture 10 showed a reduction in concrete density by about 5.6% and almost similar ultimate energy absorption compared to that obtained in the LWSCC-LC mixture with minimum possible density (mixture 8) (see Table 3-4).

3.7 Conclusions

This chapter focused on evaluating the mechanical properties and impact resistance of LWSCC mixtures reinforced with polymeric fibers. Expanded slate (fine/coarse) aggregates were employed to develop fourteen LWSCC mixtures and two LWVC mixtures reinforced with different types of polymeric fibers (PVA8, PVA12, and PP19). Two NWSCC mixtures were cast for comparison. Based on the results presented in this chapter, the following conclusions can be drawn:

1. It was possible to develop LWSCC mixtures with a dry density ranging from 1836 kg/m^3 to 1982 kg/m^3 and LWVC with a dry density ranging from 1734.6 kg/m^3 to 1868.6 kg/m^3 using either fine or coarse expanded slate lightweight aggregate. These densities achieved a 28-day compressive strength ranging from 48.9 MPa to 55.9 MPa in LWSCC mixtures and 44.2 MPa to 47.8 MPa in LWVC mixtures.
2. Using polymeric fibers greatly improved the STS and FS of LWSCC mixtures; however, the compressive strength and ME were insignificantly affected. The highest improvements in the STS and FS were achieved when PVA8 fiber was used, followed by PVA12 and then PP19.
3. The use of polymeric fibers in LWSCC mixtures significantly improved the impact resistance under drop-weight and flexural loading. This improvement was more pronounced when shorter PVA fibers (PVA8) were used, reaching up to 64% compared to a 50% and 30% increase (on average) when using PVA12 and PP19, respectively.

4. The use of polymeric fibers greatly increased the difference between the number of blows for ultimate failure and initial cracks, indicating higher ductility compared to non-fibered LWSCC mixtures. Also, fibered-LWSCC mixtures showed higher number of cracks at failure under drop-weight test compared to non-fibered LWSCC, indicating higher post- cracking resistance compared to non-fibered LWSCC.
5. It was possible to use up to a maximum of 0.7 C/F aggregate ratio of expanded slate coarse aggregate to develop LWSCC with 550 kg/m^3 binder content. Further increase in the coarse aggregate slate significantly reduced the passing ability. Also, it was possible to use up to 1 C/F aggregate ratio of expanded slate sand with 550 kg/m^3 binder content. Further increase in expanded slate sand resulted in an increased risk of segregation. Increasing the binder content from 550 kg/m^3 to 600 kg/m^3, however, allowed further increase to the amount of LWA in the mixture, achieving concrete with lower density and with improvements in the compressive strength, STS, FS, and impact resistance.
6. With the absence of the fresh properties' restrictions (especially the passing ability), it was possible to develop LWVC mixtures with maximized percentage of LWA (minimum density) and maximized percentage of fibers (1%). Although the compressive strengths of these mixtures were slightly reduced, they showed a significant improvement in their STS, FS, and impact resistance compared to the minimum-density mixtures developed as SCC.

7. It was observed that LWSCC/LWVC mixtures developed with expanded slate fine aggregate showed higher strength-to-weight ratios in terms of STS, FS, and ultimate energy absorption compared to their counterpart mixtures developed with expanded slate coarse aggregate.

3.8 References

AbdelAleem, B. H., & Hassan, A. A. (2018). Development of self-consolidating rubberized concrete incorporating silica fume. *Construction and Building Materials*, *161*, 389-397.

AbdelAleem, B. H., Ismail, M. K., & Hassan, A. A. (2017). Properties of self-consolidating rubberised concrete reinforced with synthetic fibres. *Magazine of Concrete Research*, *69*(10), 526-540.

AbdelAleem, B. H., Ismail, M. K., & Hassan, A. A. (2018). The combined effect of crumb rubber and synthetic fibers on impact resistance of self-consolidating concrete. *Construction and Building Materials*, *162*, 816-829.

Abouhussien, A. A., Hassan, A. A., & Ismail, M. K. (2015). Properties of semi-lightweight self-consolidating concrete containing lightweight slag aggregate. *Construction and Building Materials*, *75*, 63-73.

ACI 544.2R-89 (1999) Measurement of properties of fiber reinforced concrete. *ACI Committee 544*, West Conshohocken, PA, USA.

ASTM C127. (2015). Standard test method for relative density (specific gravity) and absorption of fine aggregate. *ASTM International*, West Conshohocken, PA, USA.

ASTM C150 / C150M. (2012). Standard Specification for Portland Cement. *ASTM International*, West Conshohocken, PA, USA.

ASTM C231 / C231M. (2014). Standard Test Method for Air Content of Freshly Mixed Concrete by the Pressure Method. *ASTM International*, West Conshohocken, PA, USA.

ASTM C39 / C39M. (2011). Standard Test Method for Compressive Strength of Cylindrical Concrete Specimens. *ASTM International*, West Conshohocken, PA, USA.

ASTM C494 / C494M. (2013). Standard Specification for Chemical Admixtures for Concrete. *ASTM International*, West Conshohocken, PA, USA.

ASTM C618. (2012). Standard Specification for Coal Fly Ash and Raw or Calcined Natural Pozzolan for Use in Concrete. *ASTM International*, West Conshohocken, PA, USA.

ASTM C78 / C78M. (2018). Standard Test Method for Flexural Strength of Concrete (Using Simple Beam with Third-point Loading). *ASTM International*, West Conshohocken, PA, USA.

Balendran, R. V., Zhou, F. P., Nadeem, A., & Leung, A. Y. T. (2002). Influence of steel fibres on strength and ductility of normal and lightweight high strength concrete. *Building and environment*, *37*(12), 1361-1367.

Bogas, J. A., Gomes, A., & Pereira, M. F. C. (2012). Self-compacting lightweight concrete produced with expanded clay aggregate. *Construction and Building Materials*, *35*, 1013-1022.

Corinaldesi, V., & Moriconi, G. (2015). Use of synthetic fibers in self-compacting lightweight aggregate concretes. *Journal of building engineering*, *4*, 247-254.

EFNARC. (2005). The European Guidelines for Self-Compacting Concrete Specification, Production and Use. *European Federation for Specialist Construction Chemicals and Concrete Systems*, English ed. Norfolk, UK.

Floyd, R. W., Hale, W. M., & Bymaster, J. C. (2015). Effect of aggregate and cementitious material on properties of lightweight self-consolidating concrete for prestressed members. *Construction and Building Materials*, *85*, 91-99.

Grabois, T. M., Cordeiro, G. C., & Toledo Filho, R. D. (2016). Fresh and hardened-state properties of self-compacting lightweight concrete reinforced with steel fibers. *Construction and Building Materials*, *104*, 284-292.

Hassan, A. A., Ismail, M. K., & Mayo, J. (2015). Mechanical properties of self-consolidating concrete containing lightweight recycled aggregate in different mixture compositions. *Journal of Building Engineering*, *4*, 113-126.

Hassan, A. A., Lachemi, M., & Hossain, K. M. (2012). Effect of metakaolin and silica fume on the durability of self-consolidating concrete. *Cement and concrete composites*, *34*(6), 801-807.

Hassanpour, M., Shafigh, P., & Mahmud, H. B. (2012). Lightweight aggregate concrete fiber reinforcement–A review. *Construction and Building Materials*, *37*, 452-461.

Haug, A. K., & Fjeld, S. (1996). A floating concrete platform hull made of lightweight aggregate concrete. *Engineering Structures*, *18*(11), 831-836.

Hossain, K. M. A., Lachemi, M., Sammour, M., & Sonebi, M. (2013). Strength and fracture energy characteristics of self-consolidating concrete incorporating polyvinyl alcohol, steel and hybrid fibres. *Construction and Building Materials*, *45*, 20-29.

Ismail, M. K., & Hassan, A. A. (2016). Use of metakaolin on enhancing the mechanical properties of self-consolidating concrete containing high percentages of crumb rubber. *Journal of Cleaner Production*, *125*, 282-295.

Ismail, M. K., & Hassan, A. A. (2017). Use of Steel Fibers to Optimize Self-Consolidating Concrete Mixtures Containing Crumb Rubber. *ACI Materials Journal*, *114*(4).

Ismail, M. K., Hassan, A. A., & Lachemi, M. (2018). Effect of Fiber Type on Impact and Abrasion Resistance of Engineered Cementitious Composite. *ACI Materials Journal*, *115*(6).

Jun Li, J., gang Niu, J., jun Wan, C., Jin, B., & liu Yin, Y. (2016). Investigation on mechanical properties and microstructure of high performance polypropylene fiber reinforced lightweight aggregate concrete. *Construction and Building Materials*, *118*, 27-35.

Kayali, O., Haque, M. N., & Zhu, B. (2003). Some characteristics of high strength fiber reinforced lightweight aggregate concrete. *Cement and Concrete Composites*, *25*(2), 207-213.

Kim, H. K., Jeon, J. H., & Lee, H. K. (2012). Workability, and mechanical, acoustic and thermal properties of lightweight aggregate concrete with a high volume of entrained air. *Construction and Building Materials*, *29*, 193-200.

Kim, Y. J., Choi, Y. W., & Lachemi, M. (2010). Characteristics of self-consolidating concrete using two types of lightweight coarse aggregates. *Construction and Building Materials*, *24*(1), 11-16.

Ko, D., & Choi, H. (2013). Truss rail method for punching shear strength of flat-plate slab-column using high-strength lightweight concrete. *Magazine of concrete research*, *65*(10), 589-599.

Lachemi, M., Hossain, K. M., Lambros, V., & Bouzoubaa, N. (2003). Development of cost-effective self-consolidating concrete incorporating fly ash, slag cement, or viscosity-modifying admixtures. *Materials Journal*, *100*(5), 419-425.

Lotfy, A., Hossain, K. M., & Lachemi, M. (2016). Mix design and properties of lightweight self-consolidating concretes developed with furnace slag, expanded clay and expanded shale aggregates. *Journal of Sustainable Cement-Based Materials*, *5*(5), 297-323.

Madandoust, R., & Mousavi, S. Y. (2012). Fresh and hardened properties of self-compacting concrete containing metakaolin. *Construction and building materials*, *35*, 752-760.

Melby, K., Jordet, E. A., & Hansvold, C. (1996). Long-span bridges in Norway constructed in high-strength LWA concrete. *Engineering structures*, *18*(11), 845-849.

Mousa, A., Mahgoub, M., & Hussein, M. (2018). Lightweight concrete in America: presence and challenges. *Sustainable Production and Consumption*, *15*, 131-144.

Passuello, A., Moriconi, G., & Shah, S. P. (2009). Cracking behavior of concrete with shrinkage reducing admixtures and PVA fibers. *Cement and Concrete Composites*, *31*(10), 699-704.

Raithby, K. D., & Lydon, F. D. (1981). Lightweight concrete in highway bridges. *International Journal of Cement Composites and Lightweight Concrete*, *3*(2), 133-146.

Shafigh, P., Mahmud, H., & Jumaat, M. Z. (2011). Effect of steel fiber on the mechanical properties of oil palm shell lightweight concrete. *Materials & Design*, *32*(7), 3926-3932.

Shi, C., Yang, X., Yu, Z., & Khayat, H. (2005, May). Design and application of self-compacting lightweight concretes. In *SCC'2005-China: 1st International Symposium on Design, Performance and Use of Self-Consolidating Concrete* (pp. 55-64). RILEM Publications SARL.

Szydlowki, R., & Mieszcak, M. (2017). Study of application of lightweight aggregate concrete to construct post-tensioned long-span slabs. *Procedia Engineering*, *172*, 1077-1085.

Uygunoğlu, T., & Topçu, İ. B. (2009). Thermal expansion of self-consolidating normal and lightweight aggregate concrete at elevated temperature. *Construction and Building Materials*, *23*(9), 3063-3069.

Wang, H. T., & Wang, L. C. (2013). Experimental study on static and dynamic mechanical properties of steel fiber reinforced lightweight aggregate concrete. *Construction and Building Materials*, *38*, 1146-1151.

Wu, H. C., & Li, V. C. (1994). Trade-off between strength and ductility of random discontinuous fiber reinforced cementitious composites. *Cement and concrete composites*, *16*(1), 23-29.

4. Impact resistance and mechanical properties of lightweight SCC under cold temperatures

4.1 Abstract

This chapter aims to evaluate the impact resistance and mechanical properties of a number of developed lightweight self-consolidating concrete (LWSCC) mixtures under cold temperatures. In order to achieve LWSCC mixtures with minimum possible density, this investigation explored different replacement levels of normal-weight fine or coarse aggregates by lightweight fine and coarse expanded slate aggregates. The studied parameters included testing temperature (+20°C, 0°C, and -20°C), type of lightweight aggregate (either fine or coarse expanded slate aggregates), binder content (550 kg/m^3 and 600 kg/m^3), coarse-to-fine (C/F) aggregate ratio (0.7 and 1.0), and the use of polyvinyl alcohol (PVA) fibers (fibered and nonfibered mixtures). The results indicated that for all tested mixtures, decreasing the temperature of concrete below room temperature significantly improved the mechanical properties and impact resistance. Increasing the percentage of lightweight fine or coarse aggregate in the mixture showed more improvement in the mechanical properties and impact resistance under cold temperatures. However, the failure mode of all tested specimens appeared to be more brittle under subzero temperatures. It was also observed that the inclusion of PVA8 fibers helped compensate for the brittleness that resulted from decreasing the temperature, and it further enhanced the impact resistance and mechanical properties under low temperatures.

4.2 Introduction

Lightweight self-consolidating concrete (LWSCC) is one of the latest innovations in the concrete industry. It combines the benefits of lightweight concrete (LWC) and the favorable properties of self-consolidating concrete (SCC) (Kim et al., 2010; Karahan et al., 2012; Hassan et al., 2015). This type of concrete is a favorable concrete in different structural applications due to its higher strength-to-weight ratio, superior fire resistance, low thermal conductivity, and good fluidity (Uygunoğlu & Topçu, 2009; Papanicolaou & Kaffetzakis, 2011; Andiç-Çakır & Hızal, 2012; Mousa et al., 2018). Over the last few decades, a number of studies investigated the fresh and mechanical properties of LWSCC using different types of lightweight aggregates (LWA). These studies indicated that achieving the desired flowability, passing ability, and segregation resistance of LWSCC is a challenge, often requiring high binder content and the use of supplementary cementing materials (SCMs) to optimize the mixture flowability and stability. However, the specific gravity, nominal size, shape, surface texture, and water absorption of LWA have a significant effect on the fresh and hardened properties of LWSCC mixtures (Bogas et al., 2012; Abouhussien et al., 2015a & 2015b; Lotfy et al., 2016; Ting et al., 2019).

Lightweight concrete is commonly used in offshore structural applications in Arctic areas, especially in ocean platforms (Jiang et al., 2004). These structures are exposed to harsh environmental conditions such as impact loads under very low temperatures. The continuous striking of high waves or ice sheets on offshore structures in Arctic areas may eventually develop cracks in the structure and cause the strength to deteriorate over time. Moreover, the low temperature in Arctic areas was found to have a significant effect on the

properties of concrete, in which its failure mode became more brittle (Rostasy & Wiedemann, 1980). This behavior can greatly affect the overall ductility, toughness, and impact resistance of the whole structure. Unfortunately, no information on the impact resistance and mechanical properties of LWSCC under cold temperature conditions is currently available in the literature.

Previous research has been conducted to evaluate the mechanical properties of normal-weight concrete under cold temperatures (Yamane et al., 1978; Lee et al., 1988; Liu, 2011). Most of these studies indicated that the mechanical properties of concrete were significantly affected when concrete is cooled below the freezing point. The compressive strength, splitting tensile strength (STS), and modulus of elasticity (ME) of concrete showed a noticeable improvement at low temperature compared to normal temperature (Miura, 1989; Dahmani et al., 2007; Xie & Yan, 2018). The main reason for this improvement under cold temperature conditions has been attributed to the formation of ice within the pores and micro-cracks of concrete, which increase the strength of the composite. In addition, decreasing the temperature below room temperature led to a shrinkage in concrete, which can increase the attractive force between atoms and in turn contribute to the enhancement of concrete strength. Most of the past research focused on assessing the behavior of concrete in cryogenic environments (liquefied natural gas storages). However, a limited number of studies were conducted to study the behavior of concrete under terrestrial temperatures in cold regions. Lee et al. (1988) investigated the performance of normal-strength concrete when the temperature dropped from 20° C to -70° C. They reported that the corresponding compressive strength and STS showed a

significant increase under cold conditions, reaching up to 201% and 207%, respectively. Montejo et al. (2008) studied the influence of cold temperature on the seismic behavior of concrete columns under reversed cyclic loading. The results of this study showed that, when the temperature decreased from 20° C to -40° C, flexural strength and elastic stiffness of concrete members increased up to 15% and 90%, respectively. The results also showed that a 20% reduction in the displacement capacity was observed in the tested joints, indicating more brittle failure under cold temperatures.

Despite the noticeable improvement in the mechanical properties of concrete under cold temperatures, many researchers have found that concrete became more brittle under subzero temperatures (Montejo et al., 2008; Kim et al., 2018). For example, Rostasy and Wiedemann (1980) studied the stress-strain behavior of concrete under compression loading at low temperatures. Their study indicated that when the temperature went down to -170° C, the slope of the stress-strain curve increased more than twice the value at room temperature and behaved purely elastic, with no descending branch at failure, indicating an increase in the brittleness.

The inclusion of fibers has proven to greatly improve the ductility, tensile strength, toughness, impact strength, and energy absorption capacity of concrete under normal temperatures (Balendran et al., 2002; Hossain et al., 2013; Ismail & Hassan, 2017; AbdelAleem et al., 2017). Such improvements were related to the role of fibers in transferring the tensile stress across crack faces, providing residual strength to the concrete composite (Jun Li et al., 2016; Jun Li et al., 2017; AbdelAleem & Hassan, 2019). Therefore, the use of fibers can also be an effective way to compensate for the brittleness

of concrete under low temperatures. Moreover, the decreased distance between atoms under cold temperatures contributes to increasing the grip around fibers, which helps increase the bonding strength of fibers and, hence, provides further improvement in the performance of fibers under cold temperatures (Pigeon & Cantin, 1998; Kim et al., 2018; Beirnes et al., 2019).

Similar to steel fibers, synthetic fibers also contribute to improving the post-cracking behavior and ductility of concrete (Malhotra et al., 1994; Pigeon & Cantin, 1998; Banthia & Gupta, 2006; Hassanpour et al., 2012; Kim et al., 2018; AbdelAleem et al., 2018; Beirnes et al., 2019). However, the inclusion of synthetic fibers in concrete mixtures proved to have some advantages over steel fibers. Synthetic fibers have lower density, higher corrosion resistance, and reduced shrinkage compared to steel fibers (Malhotra et al., 1994; Banthia & Gupta, 2006; Hassanpour et al., 2012). In addition, synthetic fibers are produced with different rigidities (semi-rigid and flexible), which may be more suitable in some applications (AbdelAleem et al., 2017). Corinaldesi and Moriconi (2015) studied the effect of using synthetic micro- and macro-fibers on the mechanical properties of LWSCC mixtures. The results indicated that adding synthetic macro-fibers strongly improved the post-cracking behavior of LWSCC mixtures and provided the same strain-hardening response obtained by steel fibers, but with lower concrete density and higher corrosion resistance.

In this chapter, the mechanical properties and impact resistance of a number of successful LWSCC mixtures were evaluated under cold temperatures. The effect of using polyvinyl alcohol (PVA) fibers to compensate for the brittleness of concrete under cold temperatures

was also investigated. The experimental test parameters included three testing temperatures (+20° C, 0° C and -20° C), type of lightweight aggregate (either fine or coarse expanded slate aggregates), C/F aggregate ratio (0.7 and 1.0), the use of fibers in the mixture, and the total binder content used (550 kg/m^3 and 600 kg/m^3).

4.3 Research Significance

Previous research studies indicated that reducing the temperature increased the compressive strength, tensile strength and brittleness of normal concrete. However, because of the porous nature of LWA, lightweight concrete is expected to perform differently under cold temperatures compared to normal concrete. By reviewing the literature, it can be seen that no available studies have investigated the mechanical properties and impact strength of lightweight concrete under cold temperatures. This chapter aimed to cover this knowledge gap by presenting the performance of some developed LWSCC under two degrees of cold temperature compared to normal temperature. The investigation highlights the effect of cold temperature on impact resistance of lightweight concrete, which is considered an important factor for structures in Arctic regions subjected to continuous dynamic impact loads resulting from drifting ice sheets, high waves, or iceberg collisions. Despite the high quality and strength of expanded slate lightweight aggregate compared to other types of LWA, very few studies have investigated this LWA in lightweight concrete. In this stage, LWSCC with both lightweight coarse and fine expanded slate aggregates were developed and investigated to help designers/engineers to make a decision about choosing the best type of expanded slate aggregates that gives better mechanical properties and greater impact resistance. This

chapter also investigated the performance of some optimized LWSCC mixtures with PVA fibers in an attempt to overcome the problems resulting from the increased brittleness of concrete under cold temperatures.

4.4 Experimental Program

4.4.1 Concrete mixtures

The study aimed to investigate the effect of cold temperatures on the mechanical properties and impact resistance of concrete mixtures containing expanded slate lightweight aggregates and reinforced with polymeric fibers. The tested mixtures consisted of three LWSCC mixtures developed with LC, two LWSCC mixtures developed with LF, and two LWSCC mixtures reinforced with PVA8 fibers (one developed with LC and the other with LF). The development of LWSCC mixtures was a big challenge in this investigation due to the low density and high porosity of lightweight aggregates, which increase the risk of segregation and water absorption. Therefore, a preliminary trial mixtures stage was performed to determine the optimum mixture proportions that could be used to develop minimum-density LWSCC mixtures having 700 ± 50 mm slump flow diameter with no visual sign of segregation and without overdosing the HRWRA. To achieve this target, different approaches were considered as follows:

(a) In order to avoid absorbing any mixing water, the lightweight aggregates were pre-soaked in water for 48 hours prior to mixing.

(b) A ternary material system of cement, FA, and MK was used to achieve a balanced viscosity and improve the particle suspension in order to decrease the risk of segregation.

(c) Relatively low water-to-binder (w/b) ratio, high binder content, and large amounts of SCMs were used to achieve LWSCC mixtures with maximized strength, sufficient flowability, and improved particle suspension.

The preliminary trial mixtures stage attempted to determine the optimum volume of lightweight aggregates in the mixture (to achieve minimum possible density of LWSCC mixtures), the minimum water-to-binder (w/b) ratio, the total binder content, and the optimal combination of SCMs that could be used to develop minimum-density fibered-LWSCC mixtures with maximized compressive strength and with acceptable fresh properties according to the European Guidelines for Self-Consolidating Concrete (EFNARC, 2005).

In total, seven mixtures were selected from the mixtures developed in the previous stage as follows (see Table 4-1):

a) Mixtures 1 and 2 were selected as LWSCC to represent the minimum possible density (maximum volume of LWA) that could be obtained by the author, using either LC or LF with 550 kg/m^3 binder content.

b) Mixture 3 was selected to be compared with mixture 1, in which LC and normal-weight sand were used with a C/F aggregate ratio of 0.7. This mixture was developed to study the effect of cold temperature on the impact resistance and mechanical properties of LWSCC mixtures with different contents of LWA (different mixture densities).

c) Mixtures 4 and 5 were LWSCC mixtures developed similarly to mixtures 1 and 2, respectively, but with binder content of 600 kg/m^3. These mixtures were optimized to study the effect of cold temperature on the mechanical properties and impact resistance of LWSCC mixtures with different binder content.

d) Mixtures 6 and 7 were developed similarly to mixtures 4 and 5, respectively, but reinforced with PVA8 fibers at 0.3% fraction volume. These two mixtures were selected to investigate the influence of using polymeric fiber on the impact resistance and mechanical properties of concrete under cold temperatures.

All tested mixtures were designated according to the total binder content (either 550 kg/m^3 or 600 kg/m^3), C/F ratio, and type of lightweight aggregate used (LC or LF) (see **Table 4-1**). For example, an LWSCC mixture with 550 kg/m^3 binder content, 0.7 C/F aggregate ratio, and containing LC has a designation of 550-0.7LC. A fiber-reinforced LWSCC mixture with 600 kg/m^3 binder content, 1.0 C/F ratio, LF, and 0.3% PVA8 fiber has a designation of 600-1LF-0.3PVA8.

Table 4-1: Mixture proportions for the developed mixtures.

Mix. #	Designation	Cement (kg/m^3)	MK (kg/m^3)	FA (kg/m^3)	Aggregates					Fiber (%)
					C/F aggregate ratio (by weight)	NC (kg/m^3)	NF (kg/m^3)	LC (kg/m^3)	LF (kg/m^3)	
1	550-1LC	275	110	165	1.0	-	559.0	559.0	-	-
2	550-1LF	275	110	165	1.0	617.3	-	-	617.3	-
3	550-0.7LC	275	110	165	0.7	-	689.2	482.4	-	-
4	600-1LC	275	110	165	1.0	-	522.3	522.3	-	-
5	600-1LF	300	120	180	1.0	576.8	-	-	576.8	-
6	600-1LC-0.3PVA8	300	120	180	1.0	-	519.4	519.4	-	0.3
7	600-1LF-0.3PVA8	300	120	180	1.0	573.6	-	-	573.6	0.3

Note: All mixtures have a 0.4 w/b ratio; MK = metakaolin; FA = fly ash; NC = normal-weight coarse aggregate; NF = normal-weight fine aggregate; LC = expanded slate coarse aggregate; and LF = expanded slate fine aggregate.

4.4.2 Fresh and mechanical properties tests

The fresh properties of LWSCC mixtures were assessed according to the self-compactability criteria given by the European Guidelines for Self-Compacting Concrete (EFNARC, 2005), including slump flow, V-funnel, L-box, and J-ring. The segregation resistance of the LWSCC mixtures was evaluated by investigating the aggregates' distribution along a splitted 100 mm diameter x 200 mm high concrete cylinder. The percentage of air in all tested mixtures was measured by following ASTM C231 (2014). The results of the fresh properties for all tested mixtures are included in Table 4-2.

The mechanical performance of tested mixtures including compressive strength (f_c'), splitting tensile strength (STS), flexural strength (FS), and modulus of elasticity (ME) was determined at room temperature (+20° C) and cold temperatures of 0° C and -20° C. The compressive strength and STS were determined using 100 mm diameter x 200 mm high concrete cylinders as per ASTM C39 (2011) and ASTM C496 (2011), respectively. The FS of 100 mm x 100 mm x 400 mm prisms was measured for all developed mixtures as per ASTM C78 (2010). The ME of all mixtures was measured using a 150 mm diameter x 300 mm high concrete cylinder. All mechanical properties tests were performed using three identical specimens. The impact resistance of studied mixtures was assessed using the same tests adopted in Chapter 3.

The specimens were demolded after 24 hours of casting, moist-cured for 28 days, and then left in air for three days. After the three days in air environment, the densities of all mixtures were measured and then the specimens were divided into three groups (at least three

specimens for each group) based on the desired temperature at the time of testing. The first group tested at room temperature conditions (+20°C) while the remaining two groups were placed in cold room (7m long x 4m wide) for three days, to ensure stabilization of the required temperature (either 0° C or -20° C), and then tested inside the cold room.

Table 4-2: Fresh properties of tested mixtures.

Mix #	Mixture designated	T_{50} (s)	$T_{50\text{-}J}$ (s)	V-funnel (s)	L-box (H2/H1)	Segregation resistance	Air %	HRWRA kg/m^3
1	550-1LC	3.36	4.67	11.13	0.80	NS	3.5	4.15
2	550-1LF	2.15	2.70	5.45	0.90	NS	3.3	3.50
3	550-0.7LC	2.78	3.50	10.30	0.87	NS	3.2	3.78
4	600-1LC	3.02	3.96	8.77	0.89	NS	3.2	3.48
5	600-1LF	1.70	2.33	4.81	0.94	NS	3.0	3.22
6	600-1LC-0.3PVA8	4.09	5.12	12.24	0.78	NS	3.6	4.28
7	600-1LF-0.3PVA8	2.65	3.48	6.82	0.85	NS	3.3	3.85

Note: NS = no segregation observed; and HRWRA = high-range water-reducer admixture.

4.5 Results and Discussion

4.5.1 Compressive Strength and ME

4.5.1.1 Behavior of LWSCC mixtures at room temperature

The 28-day compressive strength and ME for all tested mixtures are presented in Table 4-3. It can be seen that the developed LWSCC mixtures in this investigation containing 600 kg/m^3 binder and effective ternary system of cement, FA, and MK with 0.3 PVA fibers allowed a minimum density to be reached up to 1836.7 kg/m^3 (52.1 MPa 28-day compressive strength) using LC (mixture 6) and 1968.8 kg/m^3 (57.3 MPa 28-day compressive strength) using LF (mixture 7). The results also showed that increasing the compressive strength by increasing the binder content from 550 kg/m^3 to 600 kg/m^3 did not

have a significant effect on the developed mixtures' density. Increasing the binder content from 550 kg/m^3 to 600 kg/m^3 showed an average increase in the compressive strength of 8% while the average reduction in the density was only 0.5% (mixtures 4, 5 compared to 1, 2). It should be noted that the effect of entrapped air on the compressive strength was not significant in this investigation as all mixtures showed comparable air contents (see Table 4-2).

Figure 4-1 shows the strength-to-weight ratios for all developed mixtures. It can be noticed that mixtures with LF showed higher strength-to-weight ratios compared to mixtures with LC. For example, mixture 5 with LF and C/F aggregate ratio of 1.0 (minimum possible density SCC obtained by the author with 600 kg/m^3 binder content) showed a strength-to-weight ratio of 29.93 MPa.m^3/kg x10^3 compared to 28.88 MPa.m^3/kg x10^3 obtained in counterpart mixture with LC (mixture 4). The results also showed that the inclusion of PVA fibers with a volume of 0.3% showed insignificant reduction in the compressive strength and ME of the developed LWSCC mixtures.

Table 4-3: Results of compressive strength and modulus of elasticity at different temperatures.

Mix #	Mixture designated	*f'c (MPa)*			*ME (GPa)*			28-day density (kg/m^3)
		+20° C	*0° C*	*-20° C*	*+20° C*	*0° C*	*-20° C*	
1	550-1LC	49.1	59.9	66.8	21.8	22.9	23.8	1848.4
2	550-1LF	55.1	65.1	71.8	23.7	24.8	24.9	1979.1
3	550-0.7LC	52.1	61.4	69.2	22.9	23.8	24.5	1910.3
4	600-1LC	53.2	62.9	70.0	21.8	23.3	24.0	1840.5
5	600-1LF	59.0	68.4	75.3	23.5	24.8	25.2	1970.1
6	600-1LC-0.3PVA8	52.1	65.2	71.4	21.3	22.5	22.9	1836.7
7	600-1LF-0.3PVA8	57.3	69.7	76.9	22.8	23.6	23.5	1968.8

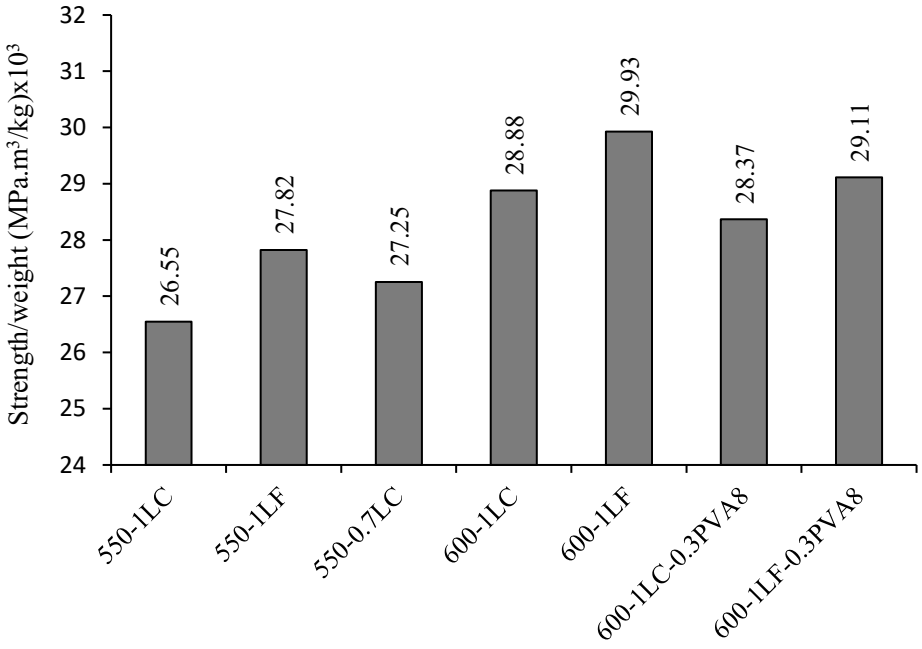

Figure 4-1: Strength-to-weight ratio for all tested mixtures.

4.5.1.2 Effect of low temperatures on the compressive strength and ME of the developed mixtures

Table 4-3 shows the results of 28-day compressive strength and ME at room temperature (+20° C) and cold temperatures (0° C and -20° C). It can be seen that the compressive strength of LWSCC mixtures was improved when the temperature of concrete decreased below room temperature (Figure 4-2). For example, in mixture 2 with LF and a C/F aggregate ratio of 1.0, decreasing the temperature from +20° C to 0° C and -20° C showed an increase in the compressive strength reaching up to 18.3% and 30.3%, respectively. This can be attributed to the formation of ice in the mixtures' pores and in the interference between cement mortar and coarse aggregates, which provide denser and harder cement matrix and help to fill the micro-cracks with ice at cold temperatures, contributing to

improving the interfacial zone between aggregates and cement matrix (Lee et al., 1988; Montejo et al., 2008). Increasing the compressive strength at low temperatures can also be related to the decrease in atomic distance due to concrete shrinkage, which can increase the attractive force between atoms and in turn help improve the concrete strength (Pigeon & Cantin, 1998; Yang et al., 2001).

It is noteworthy that LWSCC mixtures containing LC showed more pronounced increase in the compressive strength at cold temperatures compared to LWSCC mixtures with LF. As seen in mixture 1 (mixture with LC), decreasing the temperature from +20° C to 0° C and -20° C improved the compressive strength by 22.1% and 36.2%, respectively (see Table 4-3 and Figure 4-2) whereas these increases were 18.3% and 30.3% in mixture 2 (mixture with LF). Such findings may be attributed to the fact that LC has higher internal pores compared to LF, which is obvious from the difference between their specific gravities (1.53 for LC compared to 1.8 for LF). This LC with more pores, which are filled with water (as they were prepared in surface-saturated condition), becomes stronger at cold temperatures after the water in their pores turns into ice (Liu et al., 2016). It should be noted that, different types of LWA (other than expanded slate aggregate) with different internal pores, may also show different performance under cold temperature.

The results also indicated that LWSCC mixtures with higher LWA content exhibited higher increase in the compressive strength at low temperatures. As seen in LWSCC-LC mixtures (Figure 4-2), mixture 3 with a C/F aggregate ratio of 0.7 showed a 17.9% and 32.9% increase in compressive strength when the temperature decreased to 0° C and -20° C, respectively. These increases reached up to 22.1% and 36.2% in mixture 1 with a C/F

aggregate ratio of 1.0 (higher LWA content). This is due to the higher total volume of pores in mixtures with higher LWA content. It was also observed that mixtures with lower binder content showed a noteworthy improvement in the compressive strength under cold temperatures compared to mixtures with higher binder content. For instance, mixture 4 with 600 kg/m^3 binder content exhibited an increase in the compressive strength at 0° C and -20° C up to 18.3% and 31.7%, respectively, while this improvement reached up to 22.1% and 36.2%, respectively, in the mixture with 550 kg/m^3 binder content (mixture 1). As mentioned earlier, at low temperatures, the water in concrete pores changes into ice and improves the strength of concrete. Increasing the cement content increases the hydration products and creates denser concrete matrix, leaving less room for the ice to form in the pores and thus increases the strength under cold temperatures.

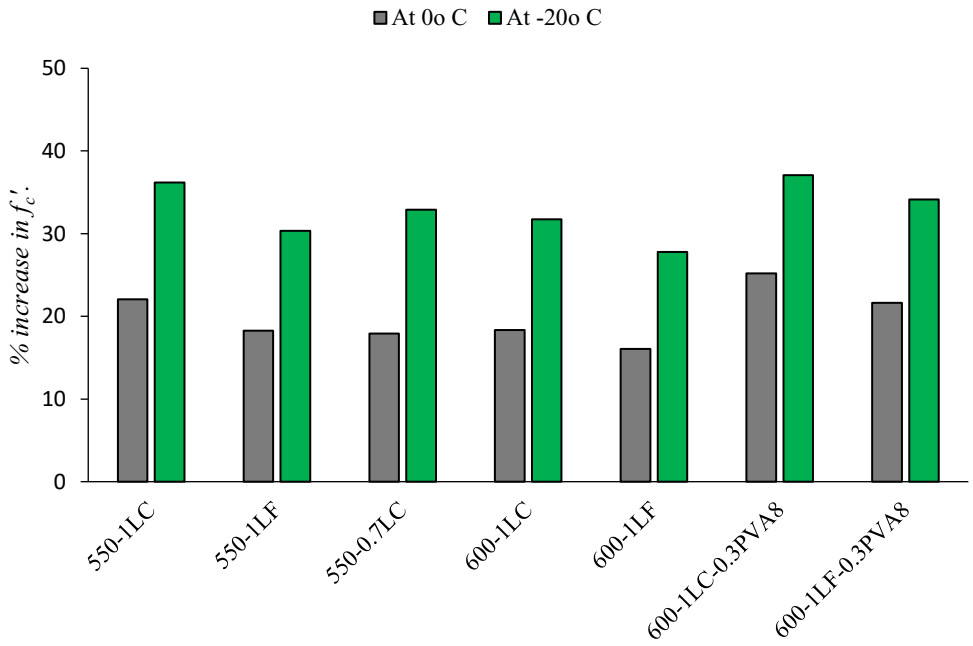

Figure 4-2: Effect of cold temperatures on the compressive strength of tested mixtures.

Figure 4-2 also showed that the inclusion of polymeric fibers (PVA8) in LWSCC mixtures, in general, further improved the compressive strength under cold temperatures. For example, adding 0.3% PVA8 to LWSCC mixtures enhanced the compressive strength by 21.6% and 34.1% under 0° C and -20° C, respectively, compared to a 16.1% and 27.8% increase in the nonfibered mixture (mixture 7 compared to mixture 5). This could be related to the fact that concrete shrinks at cold temperatures, which increases the gripping around the fibers and in turn increases the bonding strength of PVA fibers, leading to higher concrete strength.

The ME of LWSCC mixtures also showed a slight increase at low temperature compared to normal temperature. However, the increase of the compressive strength at low temperature was more pronounced compared to the increase in the ME at low temperature. Changing the binder content and using PVA fibers in LWSCC mixtures under cold temperatures also showed the same effects as those presented for the compressive strength.

4.5.2 Splitting tensile and flexural strengths

4.5.2.1 Evaluating the tensile and flexural strengths of LWSCC mixtures at room temperature

The results of the STS and FS of all tested mixtures are presented in Table 4-4. In this investigation, a reduction of 3.3% in the mixture density resulted in a slight reduction in the 28-day STS and FS by 6.6% and 5.2%, respectively. This was clear from comparing mixture 3 to mixture 1, in which increasing the C/F aggregate ratio of LC from 0.7 to 1.0 negatively affected the STS and FS. Such results were obvious due to the weak strength

and stiffness of LWA. It was also observed that increasing the binder content from 550 kg/m^3 to 600 kg/m^3 resulted in an improvement in the STS and FS of the developed mixtures between 5.3% -7.2% (mixture 4 compared to 1 and mixture 5 compared to mixture 2) (see Table 4-4).

Table 4-4: Results of splitting and flexural tensile strengths at different temperatures.

Mix #	Mixture designated	*STS (MPa)*			*FS (MPa)*		
		+20° C	*0° C*	*-20° C*	*+20° C*	*0° C*	*-20° C*
1	550-1LC	2.8	3.6	4.2	4.4	6.1	7.0
2	550-1LF	3.3	4.2	4.9	4.9	6.7	7.7
3	550-0.7LC	3.0	3.7	4.4	4.6	6.1	7.2
4	600-1LC	2.9	3.7	4.3	4.7	6.4	7.3
5	600-1LF	3.5	4.3	5.1	5.2	7.0	8.0
6	600-1LC-0.3PVA8	3.7	5.0	6.0	5.8	8.6	9.8
7	600-1LF-0.3PVA8	4.5	6.0	7.1	6.3	9.2	10.6

The results also indicated that the inclusion of PVA fibers greatly improved the STS and FS of LWSCC mixtures. In LWSCC-LC mixtures, adding 0.3% PVA8 fibers (mixture 6) showed an improvement in the STS and FS by 25.8% and 23.8%, respectively, compared to the nonfibered mixture (mixture 4). This enhancement in the STS and FS can be related to the bridging action of fibers, which contributes to transferring the tensile stress across the crack section, providing residual strength to the concrete composite (Corinaldesi & Moriconi, 2015). Similar improvements were observed in LWSCC-LF mixtures (mixture 7 compared to mixture 5).

4.5.2.2 Effect of low temperatures on the tensile and flexural strengths of the LWSCC mixtures

The results of STS and FS at room temperature (+20° C) and cold temperatures (0° C and -20° C) for all tested mixtures are presented in Table 4-4. All tested mixtures exhibited an increase in the STS and FS under cold temperatures. Figure 4-3 (**a** and **b**) shows the percentages of increase in the STS and FS of all tested mixtures under the effect of cold temperatures. As seen in mixture 1, for example, decreasing the temperature of concrete to 0° C and -20° C increased the STS by 29.9% and 52.5%, respectively, and increased the FS by 40.4% and 60.6%, respectively. These results can be related to the same reasons explained earlier in increasing the compressive strength with decreasing the temperature. It is also observed from the figure that LWSCC mixtures developed with LC showed more significant improvements compared to mixtures with LF. For example, the minimum possible density of LWSCC-LC mixture (mixture 1) showed an improvement in the STS at 0° C and -20° C up to 29.9% and 52.2%, respectively, while this improvement reached up to 25.5% and 47.2%, respectively, in mixture 2 (minimum possible density LWSCC-LF mixture) (Figure 4-3**a**). For the same reason, increasing the amount of lightweight coarse aggregate content showed further increase in the STS and FS of mixtures (mixture 1 compared to mixture 3).

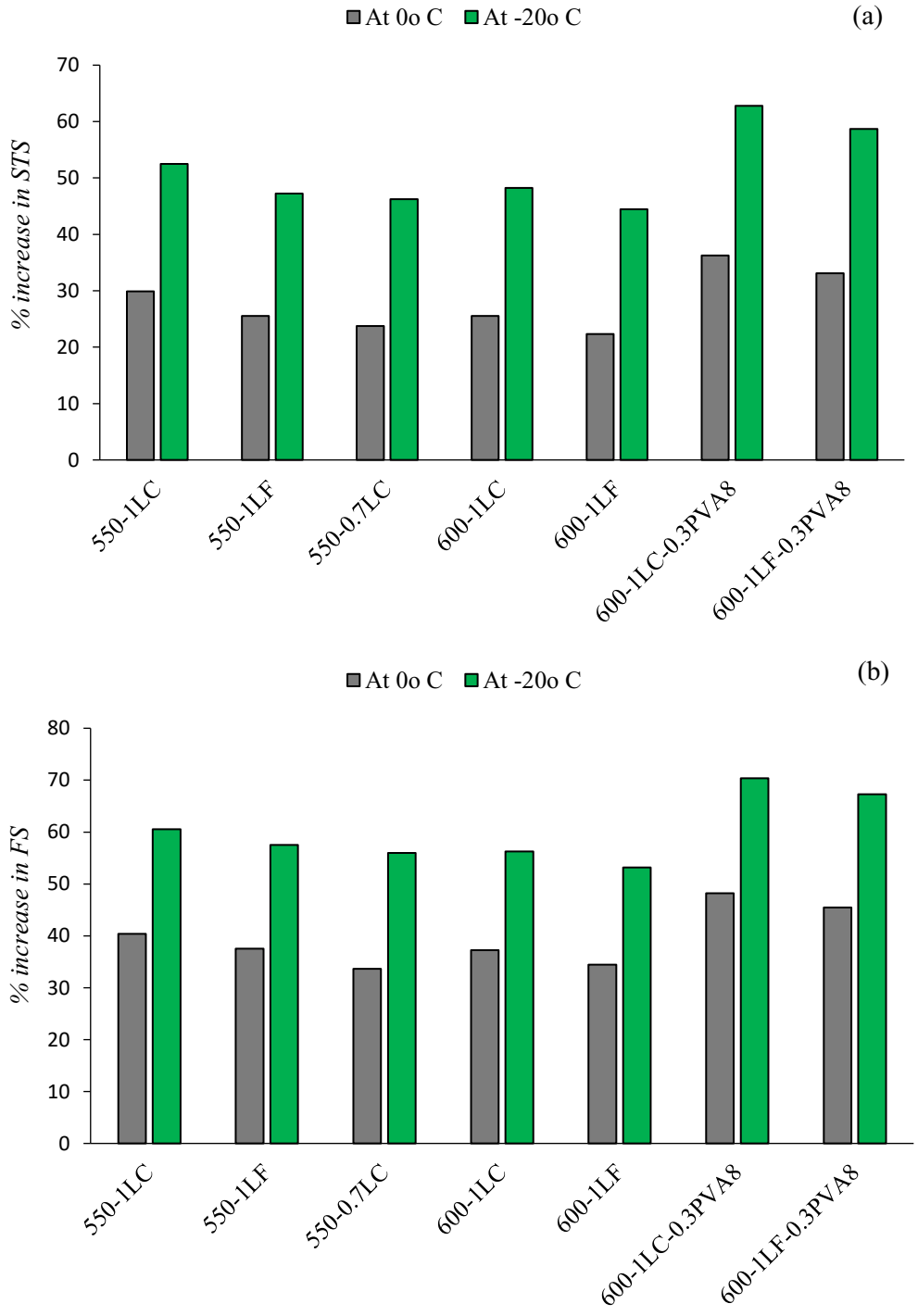

Figure 4-3: Effect of cold temperatures on the (a) STS, (b) FS for all tested mixtures.

Similar to the case of compressive strength, the STS and FS results at low temperatures also showed more pronounced enhancement in mixtures with total binder content of 550 kg/m^3 compared to mixtures with total binder content of 600 kg/m^3. For example, mixture 2 with 550 kg/m^3 binder content exhibited an increase in the STS at 0^o C and -20^o C, reaching up to 25% and 47.2%, respectively, compared to 22.3% and 44.5%, respectively, in mixture 5 with 600 kg/m^3 binder content (**Figure 4-3**a). Compared to the compressive strength, adding PVA fibers showed more pronounced improvements in the STS and FS of LWSCC mixtures under low temperatures. This can be attributed to the increased gripping force around the fibers at cold temperatures (increased the energy required for fiber pull-out), which has more effect in STS and FS compared to compressive strength.

4.5.3 Evaluation of impact resistance of LWSCC mixtures

4.5.3.1 Impact resistance under room temperature

The results of cylindrical specimens' impact resistance and flexural impact resistance tests for all tested mixtures are summarized in Table 4-5. It can be observed that the minimum possible density LWSCC mixture developed with LF showed higher impact resistance compared to the minimum possible density mixture developed with LC (in terms of number of drops required to initiate visible crack (N1) and number of drops required for ultimate failure (N2)). Mixture 2, developed with LF and with a C/F aggregate ratio of 1.0 (minimum possible density achieved in SCC), exhibited higher values of N1 and N2 by 22.2% and 25% respectively, compared to its counterpart mixture with LC (mixture 1). Similar performance was observed in the flexural impact loading test, in which the same mixture (mixture 2) showed an ultimate impact energy higher than that obtained in the

minimum possible density LWSCC-LC (mixture 1) by 31.3% (see Table 4-5). This can be related to the lower specific gravity of LC compared to LF (1.53 for LC compared to 1.8 for LF) due to the higher volume of internal pores in lightweight coarse aggregate. The results also indicated that a 3.3% reduction in the density of the developed mixture showed reductions in N1 and N2 of 6.9% and 9.7%, respectively, and an 11.1% reduction in the ultimate impact energy of tested prisms (mixture 3 with 0.7 C/F aggregate ratio compared to mixture 1 with 1.0 C/F aggregate ratio). Increasing the compressive strength by 8.3% due to using extra binder content of 50 kg/m^3 in LWSCC mixtures increased the number of blows at first and failure cracks by 18.5% and 17.9%, respectively, and increased the ultimate impact energy of tested prisms by 18.8% (mixture 4 compared to mixture 1).

It is also noteworthy that the inclusion of PVA fibers significantly enhanced both cylindrical specimens' impact resistance and flexural impact resistance of prism specimens. However, the improvement in the flexural impact resistance of prism specimens (due to addition of fibers) appeared to be more significant compared to the improvement in the impact resistance of cylindrical specimens. This can be attributed to the fact that the drop-weight impact of cylindrical specimens is more affected by the compressive strength while the flexural loading impact is more affected by the FS. And because the FS showed more improvement with the addition of fibers (compared to the improvement in the compressive strength), the improvement in the flexural impact resistance of prism was more pronounced compared to the improvement in the impact resistance of cylindrical specimens. The results also showed that the difference between the number of drops for ultimate failure and initial crack (N2-N1) in drop-weight cylindrical specimens test

obviously increased, indicating a significant improvement in the ductility and post-cracking behavior of concrete (see Table 4-5). Such findings may be related to the role of fibers in (1) enhancing the tensile strength of concrete, which can delay the initiation of cracks, and (2) restricting the cracks and transferring stresses through a bridging mechanism.

Table 4-5: Impact resistance results at different temperatures.

Mix #	Mixture designation	Drop-Weight Test					Flexural Impact Loading	
		Number of blows			IE (J)		Number of blows	IE (J)
		N_1	N_2	N_2-N_1	E1	E2		
Room temperature (+20° C)								
1	550-1LC	27	28	1	539	559	16	105
2	550-1LF	33	35	2	658	698	21	138
3	550-0.7LC	29	31	2	579	618	18	118
4	600-1LC	32	33	1	638	658	19	124
5	600-1LF	40	42	2	798	838	25	164
6	600-1LC-0.3PVA8	41	49	8	818	978	29	190
7	600-1LF-0.3PVA8	55	63	8	1097	1257	39	255
0° C								
1	550-1LC	41	42	1	818	838	25	164
2	550-1LF	49	50	1	978	998	31	203
3	550-0.7LC	43	44	1	858	878	26	170
4	600-1LC	47	48	1	938	958	28	183
5	600-1LF	57	59	2	1137	1177	36	236
6	600-1LC-0.3PVA8	77	86	9	1536	1716	51	334
7	600-1LF-0.3PVA8	99	109	10	1975	2175	67	439
-20° C								
1	550-1LC	76	76	0	1516	1516	42	275
2	550-1LF	90	90	0	1796	1796	51	334
3	550-0.7LC	73	74	1	1456	1476	43	282
4	600-1LC	84	84	0	1676	1676	46	301
5	600-1LF	102	102	0	2035	2035	58	380
6	600-1LC-0.3PVA8	139	152	13	2773	3032	87	570
7	600-1LF-0.3PVA8	173	187	14	3451	3731	110	720

4.5.3.2 Impact resistance of LWSCC mixtures under cold temperatures

Table 4-5 and Figure 4-4 (**a** and **b**) show the results of cylindrical specimens' impact resistance and flexural impact resistance of all tested mixtures at different temperatures. It can be seen from the results that decreasing the temperature of concrete specimens below room temperature greatly enhanced the impact resistance of LWSCC mixtures under both cylindrical specimens and flexural loading tests. For instance, decreasing the temperature of concrete specimens in mixture 1 below room temperature to 0^{o} C and -20^{o} C increased the impact resistance of the cylindrical specimens by 50% and 171%, respectively (Figure 4-4**a**), and also improved the impact resistance of the tested prisms by 56.3% and 162.5%, respectively (see Figure 4-4**b**). However, the mode of failure for all tested specimens was more brittle under cold temperatures compared to room temperature. This was confirmed by investigating the difference between energy absorption at failure (E2) and initial crack (E1) under room temperature and cold temperatures. For example, under room temperature (+20° C), the difference between E2 and E1 of mixture 2 was 40 kN.mm (see Table 4-5). This difference almost disappeared when the temperature was reduced to -20° C, indicating more brittle failure.

It is worth noting that LWSCC-LC mixtures exhibited more significant improvement at cold temperatures compared to counterpart mixtures developed with LF. By comparing mixture 1 with LC to mixture 2 with LF (with the same C/F aggregate ratio of 1.0), decreasing the temperature of concrete to 0^{o} C and -20^{o} C appeared to increase N2 of mixture 1 by 50% and 171%, respectively, compared to 42.9% and 157% increases in mixture 2. This is due to the same reason explained earlier in the compressive strength, in

which the LC mixture showed more improvement under cold temperatures than the LF mixture.

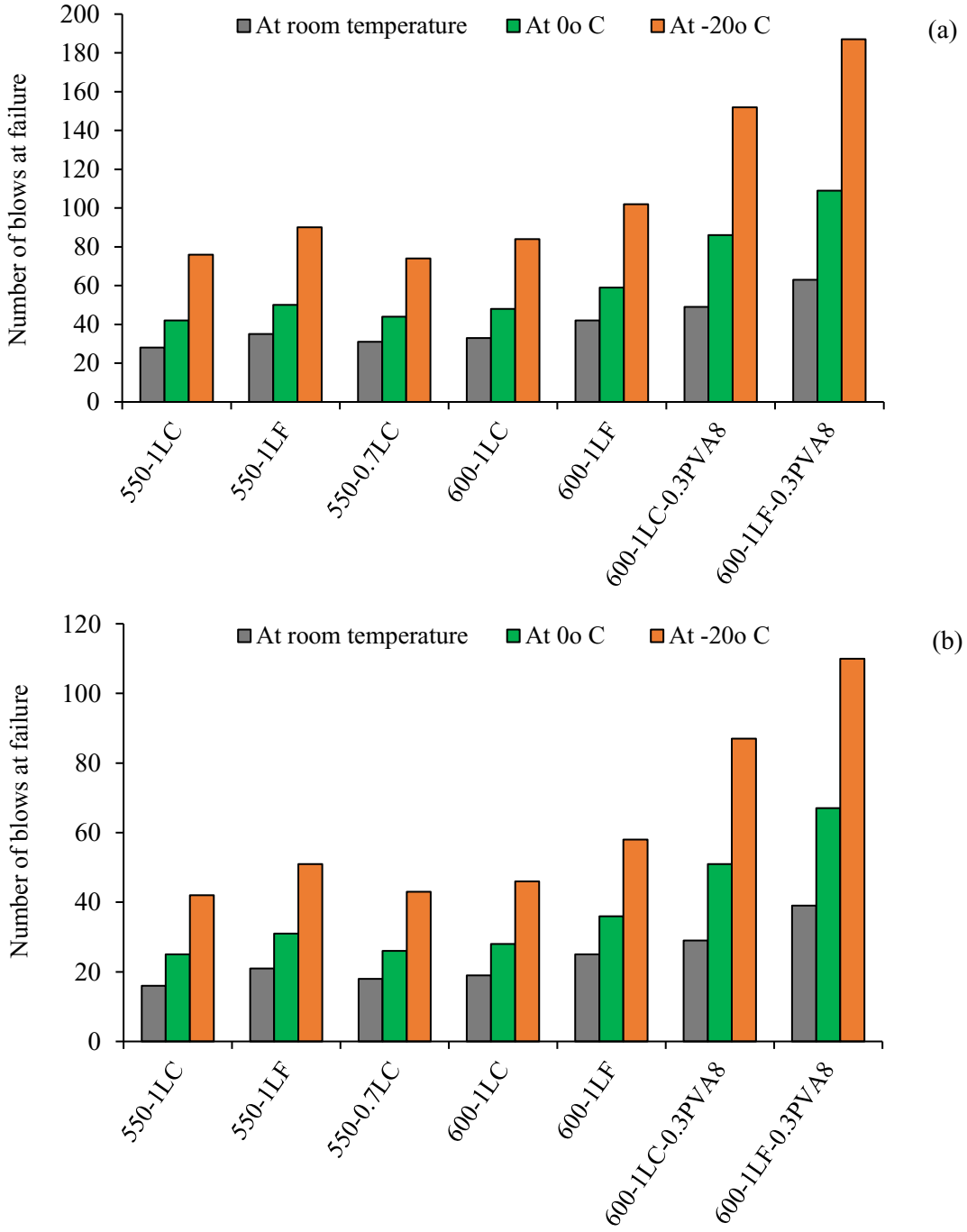

Figure 4-4: Impact resistance results for (a) drop-weight test, (b) flexural impact loading test at different temperatures.

Figure 4-4 also indicates that using higher binder content in LWSCC mixtures showed lower enhancements in the impact resistance of tested mixtures compared to mixtures with lower binder content. For example, LWSCC-LC mixture with 550 kg/m^3 binder content (mixture 1) showed an increase of 171% in the ultimate energy absorption at -20^o C compared to an increase of 154.6% in mixture 4 with 600 kg/m^3 binder content. Also, the flexural impact resistance of mixture 1 increased by 162.5% compared to by 142% in mixture 4 (see Figure 4-4**b**). This can be attributed to the significant effect of cold temperatures on the compressive strength of the mixture with low binder content compared to the mixture with high binder content.

The results also indicated that fiber-reinforced LWSCC mixtures exhibited further enhancement in the impact resistance under cold temperatures compared to nonfibered mixtures. By comparing mixtures 6 and 7 (developed with 0.3% PVA8 fibers) to mixtures 4 and 5 (nonfibered mixtures), it can be observed that decreasing the temperature from room temperature (+20° C) to -20^o C significantly increased N2 by 3 times (on average) and increased the impact resistance of tested prisms by 2.9 times (on average). It should be noted that decreasing the temperature of prism specimens reinforced with PVA fibers increased the difference between E2 and E1, indicating more ductile failure (compared to nonfibered mixtures). This can be clearly observed by examining the difference between E2 an E1 of mixture 7 (LWSCC-LF with 0.3% PVA8) under room temperature, which was 160 kN.mm; meanwhile, reducing the temperature to -20° C showed an increase in this difference up to 279 kN.mm (Table 4-5). Such findings can be attributed to the role of cold temperature in improving the bond between polymeric fibers and concrete matrix, which

helps to enhance the concrete tensile strength and in turn significantly improve the impact resistance of concrete.

4.6 Conclusions

This stage focused on assessing the mechanical properties and impact resistance of LWSCC mixtures under cold temperatures. Expanded slate (fine/coarse) aggregates were employed to develop LWSCC mixtures, including two mixtures reinforced with PVA8 fibers. Based on the results presented in this chapter, the following conclusions can be drawn:

1. It was possible to develop LWSCC mixtures with a minimum density of 1836.7 kg/m^3 and compressive strength of 52.1 MPa using LC, and a minimum density of 1968.8 kg/m^3 and compressive strength of 57.3 MPa using LF. LWSCC mixtures with LF showed higher strength-to-weight ratios than those obtained with LC, indicating favorable use of fine lightweight expanded slate aggregate.

2. A noticeable enhancement was observed in the mechanical properties and impact resistance of all tested mixtures when they were tested under cold temperatures. As the temperature decreased, greater enhancement was observed. However, the mode of failure for all tested specimens appeared to be more brittle under cold temperatures compared to room temperature.

3. LWSCC mixtures with a higher percentage of expanded slate LWA showed more improvement in the mechanical properties and impact resistance under cold temperatures (compared to mixture with lower percentage of expanded slate LWA).

This is due to the pores in expanded slate LWA being filled with water (as they were prepared in surface-saturated condition), which makes them become stronger in cold temperatures after the water in their pores turns into ice.

4. The effect of cold temperatures on improving the mechanical properties and impact resistance appeared to be more pronounced in LWSCC mixtures developed with expanded slate coarse aggregate compared to counterpart mixtures developed with expanded slate fine aggregate, indicating favorable use of coarse lightweight aggregate under cold temperatures.

5. The effect of cold temperatures appeared to be more significant at enhancing the mechanical properties of mixtures with low binder content (550 kg/m^3) compared to mixtures with higher binder content (600 kg/m^3). Also, using PVA fibers in LWSCC mixtures helped to boost the enhancing effect of cold temperatures on the mechanical properties and impact resistance of the developed mixtures.

4.7 References

AbdelAleem, B. H., & Hassan, A. A. (2019). Cyclic Behavior of Rubberized Beam-Column Joints Reinforced with Synthetic Fibers. *ACI Materials Journal*, *116*(2), 105-118.

AbdelAleem, B. H., Ismail, M. K., & Hassan, A. A. (2017). Properties of self-consolidating rubberised concrete reinforced with synthetic fibres. *Magazine of Concrete Research*, *69*(10), 526-540.

AbdelAleem, B. H., Ismail, M. K., & Hassan, A. A. (2018). The combined effect of crumb rubber and synthetic fibers on impact resistance of self-consolidating concrete. *Construction and Building Materials*, *162*, 816-829.

Abouhussien, A. A., Hassan, A. A., & Hussein, A. A. (2015). Effect of expanded slate aggregate on fresh properties and shear behaviour of lightweight SCC beams. *Magazine of Concrete Research*, *67*(9), 433-442.

Abouhussien, A. A., Hassan, A. A., & Ismail, M. K. (2015). Properties of semi-lightweight self-consolidating concrete containing lightweight slag aggregate. *Construction and Building Materials*, *75*, 63-73.

ACI 544.2R-89. (1999). Measurement of properties of fiber reinforced concrete. *ACI Committee 544*, West Conshohocken, PA, USA.

Andiç-Çakır, Ö., & Hızal, S. (2012). Influence of elevated temperatures on the mechanical properties and microstructure of self consolidating lightweight aggregate concrete. *Construction and building materials*, *34*, 575-583.

Assaad, J. J., & Issa, C. A. (2018). Stability and Bond Properties of Latex-Modified Semi-Lightweight Flowable Concrete. *ACI Materials Journal*, *115*(4).

ASTM C127. (2015). Standard test method for relative density (specific gravity) and absorption of fine aggregate. *ASTM International*, West Conshohocken, PA, USA.

ASTM C150 / C150M. (2012). Standard Specification for Portland Cement. *ASTM International*, West Conshohocken, PA, USA.

ASTM C231 / C231M. (2014). Standard Test Method for Air Content of Freshly Mixed Concrete by the Pressure Method. *ASTM International*, West Conshohocken, PA, USA.

ASTM C39 / C39M. (2011). Standard Test Method for Compressive Strength of Cylindrical Concrete Specimens. *ASTM International*, West Conshohocken, PA, USA.

ASTM C494 / C494M. (2013). Standard Specification for Chemical Admixtures for Concrete. *ASTM International*, West Conshohocken, PA, USA.

ASTM C618. (2012). Standard Specification for Coal Fly Ash and Raw or Calcined Natural Pozzolan for Use in Concrete. *ASTM International*, West Conshohocken, PA, USA.

ASTM C78 / C78M. (2018). Standard Test Method for Flexural Strength of Concrete (Using Simple Beam with Third-point Loading). *ASTM International*, West Conshohocken, PA, USA.

Balendran, R. V., Zhou, F. P., Nadeem, A., & Leung, A. Y. T. (2002). Influence of steel fibres on strength and ductility of normal and lightweight high strength concrete. *Building and environment*, *37*(12), 1361-1367.

Banthia, N., & Gupta, R. (2006). Influence of polypropylene fiber geometry on plastic shrinkage cracking in concrete. *Cement and concrete Research*, *36*(7), 1263-1267.

Beirnes, M., Dagenais, M. A., & Wight, G. (2019). Cold temperature effects on the impact resistance of thin, lightweight UHPFRC panels. *International Journal of Impact Engineering*, *127*, 110-121.

Bogas, J. A., Gomes, A., & Pereira, M. F. C. (2012). Self-compacting lightweight concrete produced with expanded clay aggregate. *Construction and Building Materials*, *35*, 1013-1022.

Corinaldesi, V., & Moriconi, G. (2015). Use of synthetic fibers in self-compacting lightweight aggregate concretes. *Journal of building engineering*, *4*, 247-254.

Dahmani, L., Khenane, A., & Kaci, S. (2007). Behavior of the reinforced concrete at cryogenic temperatures. *Cryogenics*, *47*(9-10), 517-525.

EFNARC. (2005). The European Guidelines for Self-Compacting Concrete Specification, Production and Use. *European Federation for Specialist Construction Chemicals and Concrete Systems*, English ed. Norfolk, UK.

Hassan, A. A., Ismail, M. K., & Mayo, J. (2015). Mechanical properties of self-consolidating concrete containing lightweight recycled aggregate in different mixture compositions. *Journal of Building Engineering*, *4*, 113-126.

Hassan, A. A., Lachemi, M., & Hossain, K. M. (2012). Effect of metakaolin and silica fume on the durability of self-consolidating concrete. *Cement and concrete composites*, *34*(6), 801-807.

Hassanpour, M., Shafigh, P., & Mahmud, H. B. (2012). Lightweight aggregate concrete fiber reinforcement–A review. *Construction and Building Materials*, *37*, 452-461.

Hossain, K. M. A., Lachemi, M., Sammour, M., & Sonebi, M. (2013). Strength and fracture energy characteristics of self-consolidating concrete incorporating polyvinyl alcohol, steel and hybrid fibres. *Construction and Building Materials*, *45*, 20-29.

Ismail, M. K., & Hassan, A. A. (2017). Use of Steel Fibers to Optimize Self-Consolidating Concrete Mixtures Containing Crumb Rubber. *ACI Materials Journal*, *114*(4).

Jiang, D., Wang, G., Montaruli, B. C., & Richardson, K. L. (2004, May). Concrete offshore LNG terminals-A viable solution and technical challenges. In *Offshore Technology Conference*. OnePetro.

Jun Li, J., gang Niu, J., jun Wan, C., Jin, B., & liu Yin, Y. (2016). Investigation on mechanical properties and microstructure of high performance polypropylene fiber reinforced lightweight aggregate concrete. *Construction and Building Materials*, *118*, 27-35.

Jun Li, J., jun Wan, C., gang Niu, J., feng Wu, L., & chao Wu, Y. (2017). Investigation on flexural toughness evaluation method of steel fiber reinforced lightweight aggregate concrete. *Construction and Building Materials*, *131*, 449-458.

Karahan, O., Hossain, K. M., Ozbay, E., Lachemi, M., & Sancak, E. (2012). Effect of metakaolin content on the properties self-consolidating lightweight concrete. *Construction and Building Materials*, *31*, 320-325.

Kim, M. J., Yoo, D. Y., Kim, S., Shin, M., & Banthia, N. (2018). Effects of fiber geometry and cryogenic condition on mechanical properties of ultra-high-performance fiber-reinforced concrete. *Cement and Concrete Research*, *107*, 30-40.

Kim, Y. J., Choi, Y. W., & Lachemi, M. (2010). Characteristics of self-consolidating concrete using two types of lightweight coarse aggregates. *Construction and Building Materials*, *24*(1), 11-16.

Lachemi, M., Hossain, K. M., Lambros, V., & Bouzoubaa, N. (2003). Development of cost-effective self-consolidating concrete incorporating fly ash, slag cement, or viscosity-modifying admixtures. *Materials Journal*, *100*(5), 419-425.

Lee, G. C., Shih, T. S., & Chang, K. C. (1988). Mechanical properties of concrete at low temperature. *Journal of cold regions engineering*, *2*(1), 13-24.

Liu, C. (2011). Experimental investigation on mechanical property of concrete exposed to low temperatures. *master's thesis, Tsinghua University, Beijing, PR China*.

Liu, X., Zhang, M. H., Chia, K. S., Yan, J., & Liew, J. R. (2016). Mechanical properties of ultra-lightweight cement composite at low temperatures of 0 to− 60° C. *Cement and Concrete Composites*, *73*, 289-298.

Lotfy, A., Hossain, K. M., & Lachemi, M. (2016). Mix design and properties of lightweight self-consolidating concretes developed with furnace slag, expanded clay and expanded shale aggregates. *Journal of Sustainable Cement-Based Materials*, *5*(5), 297-323.

Malhotra, V. M., Carette, G. G., & Bilodeau, A. (1994). Mechanical properties and durability of polypropylene fiber reinforced high-volume fly ash concrete for shotcrete applications. *Materials Journal*, *91*(5), 478-486.

Miura, T. (1989). The properties of concrete at very low temperatures. *Materials and Structures*, *22*(4), 243-254.

Montejo, L. A., Sloan, J. E., Kowalsky, M. J., & Hassan, T. (2008). Cyclic response of reinforced concrete members at low temperatures. *Journal of Cold Regions Engineering*, *22*(3), 79-102.

Mousa, A., Mahgoub, M., & Hussein, M. (2018). Lightweight concrete in America: presence and challenges. *Sustainable Production and Consumption*, *15*, 131-144.

Papanicolaou, C. G., & Kaffetzakis, M. I. (2011). Lightweight aggregate self-compacting concrete: state-of-the-art & pumice application. *Journal of Advanced Concrete Technology*, *9*(1), 15-29.

Pigeon, M., & Cantin, R. (1998). Flexural properties of steel fiber-reinforced concretes at low temperatures. *Cement and Concrete Composites*, *20*(5), 365-375.

Reda Taha, M. M., El-Dieb, A. S., Abd El-Wahab, M. A., & Abdel-Hameed, M. E. (2008). Mechanical, fracture, and microstructural investigations of rubber concrete. *Journal of materials in civil engineering*, *20*(10), 640-649.

Rostasy, F. S., & Wiedemann, G. (1980). Stress-strain-behaviour of concrete at extremely low temperature. *Cement and concrete research*, *10*(4), 565-572.

Ting, T. Z. H., Rahman, M. E., Lau, H. H., & Ting, M. Z. Y. (2019). Recent development and perspective of lightweight aggregates based self-compacting concrete. *Construction and Building Materials*, *201*, 763-777.

Uygunoğlu, T., & Topçu, İ. B. (2009). Thermal expansion of self-consolidating normal and lightweight aggregate concrete at elevated temperature. *Construction and Building Materials*, *23*(9), 3063-3069.

Xie, J., & Yan, J. B. (2018). Experimental studies and analysis on compressive strength of normal-weight concrete at low temperatures. *Structural Concrete*, *19*(4), 1235-1244.

Yamane, S., Kasami, H., & Okuno, T. (1978). Properties of concrete at very low temperatures. *Special Publication*, *55*, 207-222.

Yang, L. H., Han, Z., & Li, C. F. (2011). Strengths and flexural strain of CRC specimens at low temperature. *Construction and Building Materials*, *25*(2), 906-910.

5. Behavior of expanded slate lightweight SCC beams with improved cracking performance and shear capacity

5.1 Abstract

This chapter investigated the behavior of lightweight self-consolidating concrete (LWSCC) and lightweight vibrated concrete (LWVC) beams developed with improved shear capacity and cracking behavior. Fourteen concrete beams were cast with different types of lightweight aggregates (either fine or coarse expanded slate aggregates), total binder contents (550 kg/m^3 and 600 kg/m^3), fiber lengths (8 mm and 12 mm), and different fiber volume fractions (0.3%, 0.5%, and 1%). The experimental results were also compared with several code-based equations and selected proposed models from the literature that predict the shear strength of reinforced concrete beams with and without fibers. The inclusion of shorter polyvinyl alcohol (PVA) fibers appeared to have more influence on improving the shear performance and cracking behavior of LWSCC beams compared to longer fibers. It was also found that using expanded slate fine aggregate exhibited better results in terms of the beams' load-carrying capacity, post-diagonal cracking resistance, and energy absorption capacity compared to using expanded slate coarse aggregate. The highest increases in the shear capacity, deformation capacity, post-diagonal cracking resistance, and energy absorption capacity were observed in LWVC beams, as it was possible to use a higher percentage of PVA fibers (1%) because of the absence of self-compactability restrictions.

5.2 Introduction

Using lightweight concrete (LWC) in the construction industry offers significant advantages over conventional normal-weight concrete (NWC) in terms of unit weight and thermal insulation (Topçu & Uygunoğlu, 2010). The low density of such concrete allows for a significant reduction in self-weight of concrete structures, resulting in a smaller seismic demand (Kowalsky et al., 1999). The low density also helps to minimize structural dimensions, thus offering potential savings in construction expenses (NRMCA, 2003). Furthermore, LWC can reach high strength-to-weight ratio and sustainability properties (Kılıç et al., 2003). It has been successfully applied in several structural applications, specifically in the construction of high-rise buildings, post-tensioned concrete ceilings, and long-span bridges (Chai, 2016; Szydlowki & Mieszcak, 2017). The acceptable durability performance of LWC also extends its possible use to marine areas and offshore structures (Haug & Fjeld, 1996).

Lightweight self-consolidating concrete (LWSCC) is one of the latest innovations in concrete technology that combines the beneficial effects of LWC and self-consolidating concrete (SCC). Well-designed LWSCC can spread readily into place without segregation and encapsulate congested reinforcement without the necessity of mechanical consolidation, which can substantially reduce construction time and labor demand (Khayat et al., 2001). Over the last few decades, a number of investigations have been conducted to evaluate the rheological behavior and mechanical properties of LWSCC using different types of LWA (Bogas et al., 2012; Hassan et al., 2015; Abouhussien et al., 2015; Lotfy et al., 2016). Most of these investigations revealed that minimizing the coarse aggregate

fraction, using high binder content, and employing high-reactivity supplementary cementing materials were essential for optimizing the mixture flowability and stability of LWSCC. In contrast, uncertainties about the shear performance of LWSCC members still raise some concerns among designers/engineers regarding the feasibility of using this material in structural applications (Dymond et al., 2010; Yang & Ashour, 2011).

Shear failure in concrete members is undesirable due to its catastrophic nature, one that does not show any warnings or visible signs of disintegration prior to failure. The characteristic factors affecting this brittle failure have been investigated over the last several decades (Taylor, 1974; Sherwood et al., 2007; Campana et al., 2013). The interlocking action of aggregates along the diagonal fractured surface is one of the main factors influencing the shear transfer in concrete beams, which contributes to transferring up to 50% of the applied shear force (MacGregor & Wight, 2005; Hassan et al., 2008). The use of low-density coarse aggregates is assumed to reduce the degree of interlocking, in which the failure crack passes through the aggregate particles, resulting in a reduction in the interlocking resistance along the diagonal shear cracks (Yang & Ashour, 2011). On the other hand, the production of SCC usually involves using minimized volume of coarse aggregate in the mixture, which also contributes to reducing the aggregate interlock mechanism (Khayat et al., 2001; Yang et al., 2012). This highlights a concern regarding the shear capacity of structural elements constructed with LWSCC compared to structural elements made from traditional vibrated concrete (VC). Hassan et al. (2015) investigated the influence of mixture composition and coarse aggregate type/density on the structural performance of SCC beams. Their study included the use of slag, expanded slate, and

crushed stones coarse aggregate in the development of a number of non-fibered SCC mixtures with a density range of 1848 kg/m^3 to 2286 kg/m^3. Their study revealed that increasing the C/F aggregate ratio generally increased the load-carrying capacity of SCC beams, regardless of the aggregate type. Slag and expanded slate lightweight coarse aggregates were found to have better cracking characteristics compared to most common lightweight aggregates, since they were not entirely fractured along the diagonal crack surface.

Adding randomly distributed fibers into LWSCC is an effective approach, not only to compensate for the lower fracture toughness from using low-density aggregates but also to improve the ductility, impact resistance, energy absorption capacity, and cracking resistance of concrete (Hossain et al., 2013; Afroughsabet et al., 2016). The strengthening effect of fibers is related to the role fibers play in delaying the growth of cracks, limiting their propagation, and transferring the tensile stresses at crack interfaces via bridging action, affording residual strength to the concrete composite (Jung Li et al., 2016; AbdelAleem & Hassan, 2019). Over the past decades, steel fibers have been primarily used by researchers to improve the shear behavior of concrete members. Very few studies, however, have investigated the structural behavior of concrete containing synthetic fibers despite the advantage these fibers have over steel fibers (Corinaldesi & Moriconi, 2015; AbdelAleem, 2017). Synthetic fibers were found to have higher corrosion and alkali resistance, better dispersion in the matrix, and lower density compared to steel fibers (Corinaldesi & Moriconi, 2015; Jung Li et al., 2016).

Polyvinyl alcohol (PVA) fiber is a novel type of synthetic fiber that has been mainly used in fiber-reinforced concrete to control shrinkage and thermal cracking. The high modulus and high bonding strength of PVA fibers with concrete matrix significantly enhances the tensile strength, ductility, and energy absorption capacity of concrete (Arain et al., 2019; Hossain et al., 2020). Recently, PVA fibers have been used as the main constituent in the development of engineered cementitious composite (ECC), affording convenient strain-hardening response (Ismail & Hassan, 2019). Behrooyan and Ahmadian (2013) compared the impact resistance and mechanical properties of concrete containing PVA and steel fibers. Their results indicated that, when compared to steel fibers, PVA fibers exhibited better performance in transferring the tensile stresses along the crack interfaces prior to failure. The researchers attributed this result to the better bonding between PVA fibers and cementitious matrix.

Developing SCC with synthetic fibers is a challenge and requires more investigation. Previous studies indicated that the type and volume of the fiber significantly affected the properties of the developed mixture. The inclusion of synthetic fibers increases the interference and collision between fibers and coarse aggregates, resulting in high reductions in the passing ability of the mixture (Corinaldesi & Moriconi, 2015; Aslani & Kelin, 2018). Moreover, adding relatively low-density synthetic fibers to highly flowable mixtures encourages segregation of the fibers. This adds another challenge to optimizing the flowability and stability of the mixture. However, some researchers have recommended that a successful fiber-reinforced SCC can be obtained when the fiber volume does not exceed 0.5% (Nehdi & Ladanchuk, 2004).

This chapter investigates the shear resistance, cracking behavior, and energy absorption capacity of a number of lightweight self-consolidating concrete (LWSCC) beams (made with an air-dry density range of 1850 kg/m^3 to 2150 kg/m^3 as per CSA A23.3-14 (2014). The experimental test parameters included type of lightweight aggregates (either fine or coarse expanded slate aggregates), binder content (550 kg/m^3 and 600 kg/m^3), PVA fiber lengths (8 mm and 12 mm), fiber volume fractions (0.3%, 0.5%, and 1%), and type of concrete (SCC or VC).

5.3 Research Significance

Using lightweight aggregates in the development of SCC allows researchers to obtain a sustainable material for use in applications that require both high workability and reduced self-weight. However, by reviewing the literature, it was found that limited studies have investigated the structural performance and in-situ properties of lightweight self-consolidating concrete (LWSCC) members, which raises concerns among designers/engineers regarding the feasibility of using this material in structural applications. In addition, despite the relatively strong strength of expanded slate lightweight aggregate compared to other types of lightweight aggregates (Hassan et al., 2015), insufficient studies have been conducted to evaluate the structure performance of concrete members made with this type of aggregate. Moreover, investigations of shear performance of fiber-reinforced LWSCC members is missing from the literature, despite the high potential of fibers to enhance ductility and post-cracking resistance of concrete. Hence, this chapter attempted to fill this knowledge gap by presenting a comprehensive investigation that aimed to alleviate the reduction in shear strength, which is anticipated

from the use of low-density lightweight aggregates, by adding optimum type and volume of PVA fibers into LWSCC mixtures. In this study, the authors also highlighted the expected challenges and benefits of combining PVA fibers and expanded slate lightweight aggregates in the development of LWSCC. In addition, as the coarse aggregates play an important role in the shear transfer in beams, this chapter exclusively compares the shear and cracking behavior of fiber-reinforced beams made with lightweight coarse aggregates compared to beams made with lightweight fine aggregates to aid designers/engineers select the best strategy in developing optimized LWSCC.

5.4 Experimental Program

5.4.1 Materials Properties

The investigated mixtures were optimized using a ternary blended cementitious system containing 50% general use (GU) cement, 30% fly ash (FA), and 20% metakaolin (MK). Locally available natural sand with a nominal maximum grain size of 4.75 mm and 10 mm crushed granite stones were used as normal-weight fine (NF) and coarse (NC) aggregates, respectively. The saturated surface dry specific gravity of both fine and coarse aggregates was 2.6. Lightweight concrete (LWC) mixtures were proportioned using either expanded slate coarse aggregate (LC) or expanded slate fine aggregate (LF) with a specific gravity of 1.53 and 1.80, respectively. A polycarboxylate-based high-range water-reducing admixture (HRWRA) was utilized to adjust the flowability of the developed LWSCC mixtures. It had a specific gravity, volatile weight, and pH of 1.20, 62%, and 9.5, respectively. Two types of commercial polyvinyl alcohol (PVA) fibers were provided by a private American company (Nycon Corporation). Deformed steel bars with two different

diameters (10 mm and 25 mm) were used, designated as #10 and #25, respectively. Details of the longitudinal and transverse reinforcements used in the beam specimens are shown in Figure 5-1. The reinforcing bars and stirrups had an average yield strength of 480 MPa and an average tensile strength of 725 MPa.

5.4.2 Concrete mixtures

A total of 14 mixtures were selected from the previous stages (Omar & Hassan, 2019; Omar et al., 2020), aimed at optimizing the fresh and mechanical properties of LWSCC with different types and volumes of polymeric fibers. The author succeeded in obtaining a number of successful LWSCC mixtures, with minimum possible density and maximized compressive strength, using expanded slate aggregates. A ternary blended cementitious system including 50% cement, 30% FA, and 20% MK, was necessary to develop LWSCC mixtures having acceptable slump flow with no visual sign of segregation. FA helped improve the flowability and reduce the amount of HRWRA added to the mixture. Meanwhile, the incorporation of MK provided a good particle suspension due to its clay-like consistency and thus improved the stability of LWSCC mixtures (Ahari et al., 2015). In addition, the use of high pozzolanic activity of MK greatly enhanced the compressive strength and the mechanical properties of the developed mixtures (Wild et al., 1996; Ding & Li, 2002).

The concrete mixtures selected from the first stage were used to cast 14 beams without shear reinforcement (one beam was cast from each of the fourteen mixtures), to investigate their cracking behavior, shear strength, and post-diagonal cracking resistance in structural elements. In total, two normal-weight self-consolidating concrete (NWSCC), ten LWSCC

and fibered-LWSCC, and two lightweight vibrated concrete (LWVC) mixtures were selected as follows (see Table 5-1):

- Two NWSCC mixtures (mixtures 1 and 2) were developed with different coarse-to-fine (C/F) aggregate ratios (0.7 and 1.0, respectively). These two mixtures were selected to be compared with their counterpart LWSCC mixtures developed with either LC or LF (mixtures 3 and 8) in order to assess the influence of replacing normal-weight aggregates with lightweight aggregates (LWA) on shear behavior of concrete beams.
- Mixtures 3 and 8 were developed as LWSCC to represent the minimum possible density (without fiber) that could be obtained by the author using either LC or LF with 550 kg/m^3 binder content. In mixture 3, LC and normal-weight sand were used with a maximum possible C/F aggregate ratio of 0.7, representing the maximum possible volume of LC that can be used to develop successful SCC. Further increase in the volume of LC (to further reduce the density of mixture 3) reduced the passing ability of mixtures due to an increase in the inter-particle friction. On the other hand, in mixture 8, normal-weight stones and LF were used with a minimum possible C/F aggregate ratio of 1.0 to represent the maximum possible volume of LF that can be used to obtain successful SCC mixtures, as per recommendations of the European Guidelines for Self-Consolidating Concrete (EFNARC, 2005). It should be noted that further increasing the amount of LF in the development of mixture 8 (less than 1.0 C/F aggregate ratio) reduced the mixture's stability and increased the risk of segregation.
- Mixtures 4-5 were developed similar to mixture 3, and mixtures 9-10 were developed similar to mixture 8 but reinforced with fibers (PVA8 and PVA12 at 0.3% fraction

volume). This set of mixtures was selected to evaluate the effect of adding PVA fibers on the shear and cracking behavior of LWSCC beams. These mixtures were developed with the maximum percentage of polymeric fibers that could be used safely in SCC mixtures at that level of binder content (550 kg/m^3). Using more than 0.3% fiber content significantly reduced the flowability and passing ability of mixtures, as shown in the previous stages.

- Mixtures 6-7 and mixtures 11-12 were designed with 600 kg/m^3 binder content to allow a higher fraction volume of PVA fibers (up to 0.5%) to be used safely in SCC mixtures. This set of mixtures was selected to assess the influence of increasing the fiber content on the shear capacity and cracking behavior of LWSCC beams.
- Two lightweight vibrated concrete (LWVC) and fibered-LWVC mixtures (mixtures 13-14 in Table 5-1) were developed to investigate the advantage of using both coarse and fine expanded slate aggregates together with higher fiber content (1%) on reducing the density of mixtures and the possibility of enhancing the shear behavior of concrete. With the absence of fresh properties restrictions of SCC (mainly passing ability and segregation), it was possible to develop LWVC mixtures containing coarse and fine expanded slate aggregate with a C/F aggregate ratio of 1.5, contributing to producing an all-lightweight vibrated concrete mixture (All-LWVC) with minimum concrete density of 1714 kg/m^3. Furthermore, it was only possible to use up to 1% PVA fibers in mixture 14 due to the absence of the fresh properties' restrictions of SCC.

All tested mixtures were designated according to the total binder content (either 550 kg/m^3 or 600 kg/m^3), C/F ratio, type of lightweight aggregate (LC or LF), fiber volume fractions,

and type of PVA fiber. For example, a fibered-LWSCC mixture with 550 kg/m^3 binder content, 0.7 C/F aggregate ratio, lightweight coarse aggregate (LC), and containing 0.3% PVA8 fiber was designated 550-0.7LC-0.3PVA. Whereas, a fibered-LWVC mixture with 550 kg/m^3 binder content, 1.5 C/F ratio, with both coarse and fine expanded slate aggregates, and 1% PVA8 was designated 5501.5All-LWVC-1PVA8.

The slump flow, V-funnel, and L-box tests were conducted according to the EFNARC (2005) to assess the fresh properties of NWSCC and LWSCC mixtures. Meanwhile, the slump test was conducted to evaluate the workability of LWVC mixtures as per ASTM C143. After 28 days, the compressive strength (f'_c) and splitting tensile strength (*STS*) tests were conducted for all tested mixtures according to ASTM C39 and C496, respectively. In both tests, three identical 100 mm diameter x 200 mm height concrete cylinders, which had been exposed to a curing condition similar to that of the tested beams, were tested. The results of the fresh properties, 28-day compressive strength, and splitting tensile strength of the tested mixtures are included in Table 5-2.

Table 5-1: Mixture proportions for tested beams.

Mix. #	Designation	Cement (kg/m^3)	MK (kg/m^3)	FA (kg/m^3)	Aggregates					Fiber (%)	Fresh Density (kg/m^3)
					C/F ratio	Normal-weight Aggregates		Lightweight Aggregates			
						NC (kg/m^3)	NF (kg/m^3)	LC (kg/m^3)	LF (kg/m^3)		
NWSCC mixtures											
1	550-0.7NWSCC	275	110	165	0.7	620	886	-	-	-	2278.7
2	550-1NWSCC	275	110	165	1.0	753	753	-	-	-	2278.7
LWSCC-LC mixtures											
3	550-0.7LC	275	110	165	0.7	-	689	482	-	-	1941.7
4	550-0.7LC-0.3PVA8	275	110	165	0.7	-	686	480	-	0.3	1939.5
5	550-0.7LC-0.3PVA12	275	110	165	0.7	-	686	480	-	0.3	1939.5
6	600-0.7LC-0.3PVA8	300	120	180	0.7	-	640	448	-	0.3	1932.5
7	600-0.7LC-0.5PVA8	300	120	180	0.7	-	638	447	-	0.5	1931.1
LWSCC-LF mixtures											
8	550-1LF	275	110	165	1.0	617	-	-	617	-	2004.7
9	550-1LF-0.3PVA8	275	110	165	1.0	614	-	-	614	0.3	2002.2
10	550-1LF-0.3PVA12	275	110	165	1.0	614	-	-	614	0.3	2002.2
11	600-1LF-0.3PVA8	300	120	180	1.0	574	-	-	574	0.3	1991.0
12	600-1LF-0.5PVA8	300	120	180	1.0	571	-	-	571	0.5	1989.4
All-LWVC mixtures											
13	550-1.5All-LWVC	275	110	165	1.5	-	-	567	378	-	1714.7
14	550-1.5All-LWVC-1PVA8	275	110	165	1.5	-	-	557	371	1.0	1711.4

Note: All mixtures have a 0.4 w/b ratio; MK = metakaolin; FA = fly ash; C/F = coarse-to-fine aggregate ratio (by weight); NC = normal-weight coarse aggregate; NF = normal-weight fine aggregate; LC = expanded slate coarse aggregate; and LF = expanded slate fine aggregate.

Table 5-2: Fresh and hardened properties of tested mixtures.

Beam/ Mix #	NWSCC/LWSCC mixtures	T_{50} (s)	$T_{50\text{-}J}$ (s)	V-funnel (s)	Slump – J-ring diameter (mm)	L-box ratio (H2/H1)	f'_c (MPa)	*STS* (MPa)
1	550-0.7NWSCC	2.05	2.43	6.86	10	0.97	68.9	4.08
2	550-1NWSCC	2.30	2.90	7.80	25	0.91	67.1	3.97
3	550-0.7LC	2.75	3.50	10.80	30	0.92	51.6	2.90
4	550-0.7LC-0.3PVA8	3.48	4.58	11.30	45	0.82	50.3	3.61
5	550-0.7LC-0.3PVA12	3.96	4.88	13.13	50	0.80	48.9	2.42
6	600-0.7LC-0.3PVA8	3.20	3.90	9.48	25	0.91	52.6	3.69
s7	600-0.7LC-0.5PVA8	4.12	5.35	12.48	50	0.82	49.3	4.11
8	550-1LF	2.10	2.69	5.37	15	0.95	52.1	3.06
9	550-1LF-0.3PVA8	2.41	3.22	6.25	35	0.85	50.4	3.93
10	550-1LF-0.3PVA12	2.80	3.80	7.12	45	0.82	49.0	3.73
11	600-1LF-0.3PVA8	2.10	2.60	4.86	30	0.88	51.9	4.05
12	600-1LF-0.5PVA8	2.70	3.53	6.75	45	0.83	48.7	4.45
Beam/ Mix #	LWVC mixtures	Slump value (mm)					f'_c (MPa)	STS (MPa)
13	550-1.5All-LWVC	180					42.1	2.51
14	550-1.5All-LWVC-1PVA8	120					34.7	3.50

5.4.3 Specimen details, test setup, instrumentation and loading procedure

The experimental investigation was conducted on 14 beams that were constructed from the same developed mixtures. All beams had a similar cross-section of 250 x 250 mm and a total length of 1500 mm as shown in Figure 5-1**a**. Two hot-rolled deformed bars with 25 mm diameter (25M) were placed in the tension zone, with a clear concrete cover of 40 mm, providing an effective depth (d) of 197.5 mm. Also, two 10M steel bars (10 mm diameter) were used in the compression zone. All beam specimens were cast without shear reinforcement; however, only six stirrups with 10 mm diameter were used to support the steel bars in the compression zone. These stirrups were placed away from the shear failure zone as shown in Figure 5-1. The four-point symmetrical loading configuration shown in Figure 5-1 was used to investigate the shear performance of the beams. A shear span-to-effective depth (a/d) ratio of 2.5 was kept constant for all tested beams to ensure shear failure before bending failure (Cho & Kim, 2003; Ismail & Hassan, 2019). A single vertical load was applied using a hydraulic jack (500 kN capacity) and then distributed into two-points acting on the beam surface using a rigid steel beam. The corresponding mid-span deflection was monitored with a linear variable differential transducer (LVDT) that was placed beneath the tension side of each beam. A gradually increasing monotonic load was applied on each beam specimen at a constant loading rate through three stages until failure (50%, 75%, and 100% of the theoretically calculated failure load). At each load stage, the developed cracks were marked, their widths were accurately measured using a crack detection microscope (with a minimum resolution of 0.01 mm) and photographed. The applied load and deflection readings were continuously recorded with a computer-

controlled data acquisition system throughout the loading history. The overall behavior of the beam specimens, including the failure mechanism and cracking characteristics (patterns, widths, heights, and angles), was observed and sketched for all beams (see Figure 5-2). The results obtained from shear testing of the 14 tested beams are presented in Table 5-3.

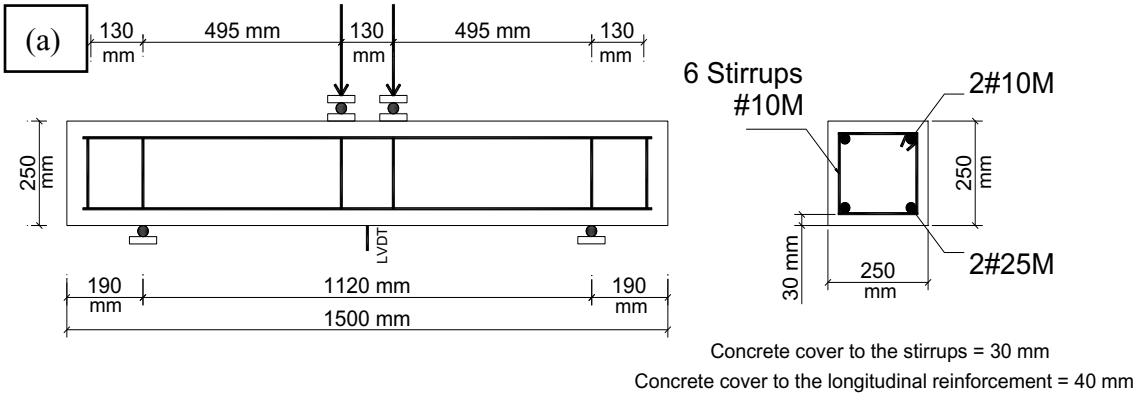

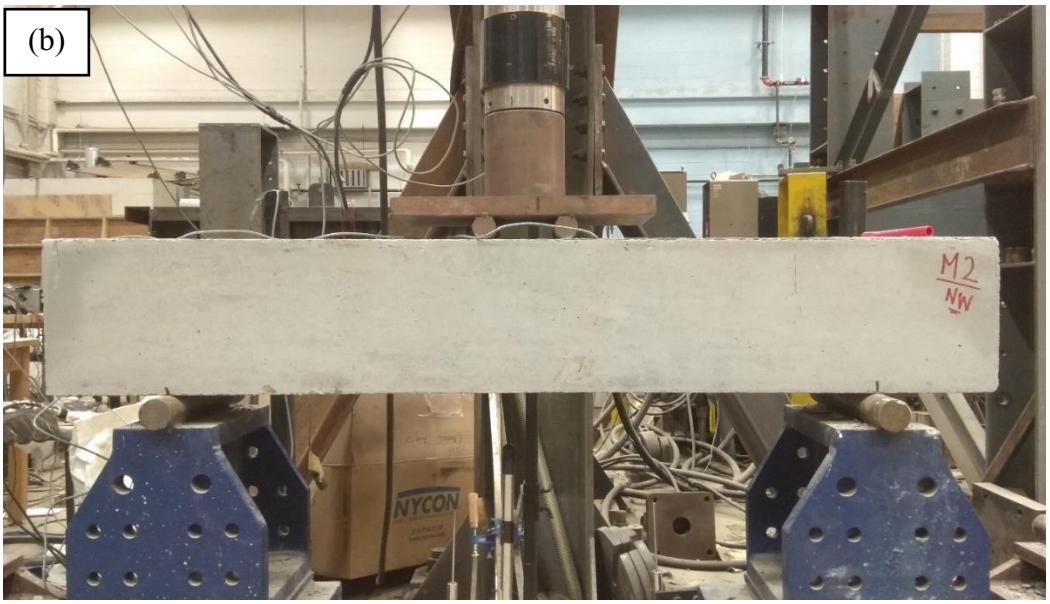

Figure 5-1: Tested beams: (a) Details of beam geometry and reinforcement, (b) test setup.

Failure Load (B1) = 242.8 kN

Failure Load (B2) = 252.4 kN

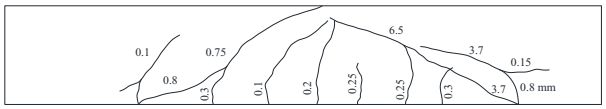

Failure Load (B3)= 161.9 kN

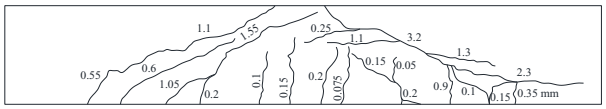

Failure Load (B4) = 192.1 kN

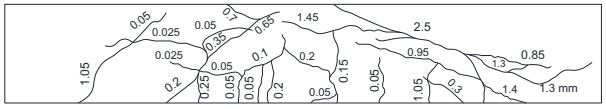

Failure Load (B5) = 185.4 kN

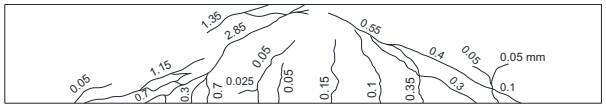

Failure Load (B6) = 198.7 kN

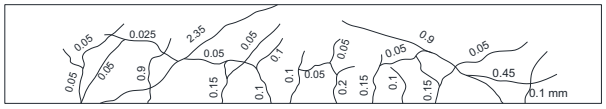

Failure Load (B7) = 219.5 kN

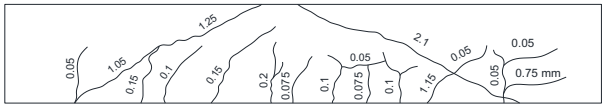

Failure Load (B8) = 202.2 kN

Failure Load (B9) = 241.4 kN

Failure Load (B10) = 230.1 kN

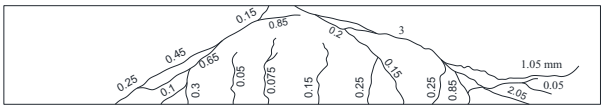

Failure Load (B11) = 244 kN

Failure Load (B12) = 264.9 kN

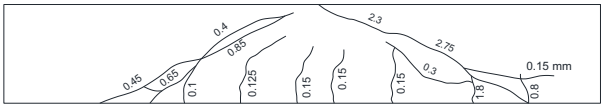

Failure Load (B13) = 178.2 kN

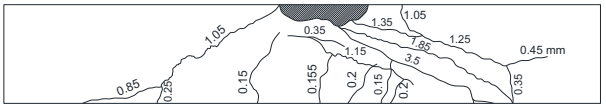

Failure Load (B14) = 223.5 kN

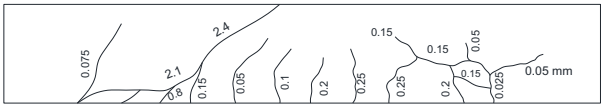

Figure 5-2: Crack patterns of tested beams at failure (crack widths in mm).

Table 5-3: Experimental results for tested shear beams.

Beam #	Beam/Mixture	1st Diagonal cracking load (kN)	Ultimate shear load, V_u (kN)	Normalized shear load, V_{nz}	Post-diagonal cracking (%)	Energy absorption (kN.mm)	At failure			
							No. of cracks	Max. crack width (mm)	Crack angle (deg.)	Deflection (mm)
B1	550-0.7NWSCC	128.4	121.4	14.62	47.1	522.3	12	6.80	28	3.00
B2	550-1NWSCC	131.9	126.2	15.40	47.7	498.4	11	6.50	27	2.95
B3	550-0.7LC	112.3	81.0	11.27	30.7	340.9	16	3.20	26	3.09
B4	550-0.7LC-0.3PVA8	120.8	96.0	13.54	37.1	539.4	21	2.50	22	3.87
B5	550-0.7LC-0.3PVA12	118.5	92.7	13.26	36.1	418.2	18	2.85	32	3.38
B6	600-0.7LC-0.3PVA8	121.8	99.4	13.70	38.7	487.4	18	2.35	29	3.72
B7	600-0.7LC-0.5PVA8	123.6	109.7	15.63	43.7	702.3	16	2.10	24	4.63
B8	550-1LF	109.5	101.1	14.00	45.8	433.6	14	3.55	29	3.28
B9	550-1LF-0.3PVA8	116.0	120.7	16.99	51.9	703.9	17	2.90	33	4.32
B10	550-1LF-0.3PVA12	114.3	115.0	16.43	50.3	576.3	15	3.00	22	3.80
B11	600-1LF-0.3PVA8	118.7	122.0	16.93	51.4	664.4	15	2.75	34	4.17
B12	600-1LF-0.5PVA8	121.2	132.5	18.99	54.2	946.1	14	2.30	25	5.07
B13	550-1.5All-LWVC	107.3	89.1	13.74	39.8	512.7	11	3.50	29	4.34
B14	550-1.5All-LWVC-1PVA8	109.7	111.8	18.96	50.9	1010.0	14	2.40	33	6.03

5.5 Results and Discussion

5.5.1 Hardened concrete properties

The 28-day compressive strength and STS results of all tested mixtures are shown in Table 5-2. From the table, it can be noted that the 28-day compressive strength and STS of the NWSCC mixtures (M1 and M2) were 68 MPa and 4.03 MPa, respectively (on average). Substituting normal-weight aggregates with either coarse or fine expanded slate lightweight aggregates in order to produce LWSCC mixtures with density ranging from 1941 kg/m^3 to 2004 kg/m^3 showed an expected reduction in compressive strength and STS by an average of 23.8% and 26%, respectively, as shown in M3 and M8 compared to M1 and M2, respectively. When attempting to further reduce the density of the mixture to reach 1714 kg/m^3 (by using both LC and LF) (M13/550-1.5All-LWVC), the 28-day compressive strength and STS reduced to 42.1 MPa and 2.51 MPa, respectively.

The inclusion of polymeric fibers with a fraction volume of 0.3% insignificantly affected the compressive strength, but it helped to greatly enhance the STS of tested mixtures. For example, using 0.3% PVA8 fibers with LWSCC mixtures increased the STS by an average of 26.7% (M4 and M9 compared to M3 and M8, respectively). This improvement in the STS can be attributed to the significant role of fibers in restricting the propagation of cracks and transferring the tensile stress across crack faces by bridging mechanism. Although further improvement in the STS of LWSCC mixtures was observed with the increase in fiber volume, a slight reduction in the compressive strength was observed. For example, by comparing M7 to M6, it can be noticed that increasing the fiber content from 0.3% to 0.5% increased the STS by 11.2% and decreased the 28-day compressive strength by 6.4%.

Furthermore, using up to 1% PVA8 fibers with the all-LWVC mixture significantly increased the STS by 41%, while the compressive strength decreased by 17.6% (M14 compared to M13).

5.5.2 General cracking and failure behavior

Figure 5-2 illustrates the crack patterns of all tested beams at the failure stage. It can be seen from the figure that all beam specimens exhibited the same failure mode, which was characterized by the formation of a single major inclined crack starting from the loading point and propagating downwards with angles ranging from 22^{o} to 34^{o}. For all tested beams, the first crack was visually observed at an early stage of loading on the tension side of the beam between the loading points (maximum moment region). During the first stage of loading, fine vertical flexural cracks appeared within the mid-span section of the beam. Their width at this stage was about 0.05 mm, as measured by the crack detection microscope. By increasing the applied load, the vertical flexural cracks within the mid-span section propagated toward the top fiber of the beam; in addition, more flexural cracks were formed away from the mid-span region on both sides of the beam specimen. With further increase in load afterwards, these cracks increased in number along the beam span, and the first diagonal shear crack was visually detected closer to the support in the middle third of the beam's height. The shear cracks proceeded to spread diagonally towards the loading point and simultaneously downward to the support zone, until the beam suddenly failed along one large shear crack (Figure 5-2).

Figure 5-2 and Table 4-5 show the crack pattern and crack numbers/widths of all tested beams at failure, respectively. It can be observed that both LWSCC (B3 and B8) and LWVC (B13) beams exhibited a higher number of cracks at failure than NWSCC beams (B1 and B2). This was due to the low stiffness and low modulus of LWA, which generated a high tensile stress at the interface between aggregate and cement matrix, allowing more flexural cracks to propagate during the first stage of loading. Meanwhile, the larger crack widths in NWSCC beams were mainly attributed to the higher vertical load carried by NWSCC beams before failure (compared to lightweight SCC and VC beams), resulting in a higher strain in the tension reinforcement at failure, and hence larger crack widths.

The results also show that fibered-LWSCC and fibered-LWVC beams generally displayed a similar failure mode as their counterpart beams without fibers (shear failure after the formation of the main diagonal crack). However, the inclusion of PVA8 and PVA12 fibers helped the beams to sustain higher shear load associated with higher rate of deformation, which in turn allowed more cracks to propagate prior to shear failure. Moreover, adding 0.3% polymeric fibers effectively helped to reduce the widths of cracks because of the stitching action of fibers; this action controlled the cracking growth by preventing one localized crack from widening and it generated more homogenous and closer microcracks to dissipate the absorbed energy over the entire beam's length. For instance, using 0.3% PVA8 (8 mm) fibers in LWSCC beams helped to reduce the maximum crack width at failure load by an average of 20%, as shown in B4 and B9 compared to B3 and B8, respectively. Less performance was observed with LWSCC beams reinforced with longer polymeric fibers PVA12 (12 mm), in which adding 0.3% PVA12 showed a reduction in

the crack widths by an average of 13.2%, as shown in B5 and B10 compared to B3 and B8, respectively. One possible explanation is that for a given fraction volume, the use of shorter fibers (PVA8) provided a higher number of single fibers dispersed in the concrete matrix compared to longer fibers (PVA12). This may increase the possibility of single fibers being oriented perpendicularly to the shear cracks, which allows better stitching action of fibers and better crack widening control along crack faces.

Finally, at the end of the test it was visually observed that, among all beams containing LC, the failure diagonal crack passed through the LC in some parts while it went around them and passed through the cement paste in other parts of the fractured surface. This observation indicates that the expanded slate lightweight aggregates used in this investigation proved to be relatively strong (compared to other types of LWA), as they were not entirely fractured along the diagonal crack surface.

5.5.3 Load-deflection response

The load-deflection relationships for all tested beams are shown in Figure 5-3. In general, all tested beams seem to have a common elastic behavior from the start of the load application up to the initiation of the first flexural crack. With the increase of applied load beyond the first crack, the stiffness (the slope of load-deflection curve beyond the first crack) of the beams relatively decreased due to the formation of more flexural cracks, and hence the curves experienced linear relationship with a slightly lower slope. With further loading afterwards, the stiffness of the tested beams sharply decreased with the occurrence of diagonal shear cracks, and hence the curves exhibited a nonlinear relationship. In

addition, the beams experienced a higher rate of deformation until the ultimate load. After the peak point, the applied load sharply decreased and mostly remained constant at about 60% to 80% of the ultimate load.

It can be seen from Figure 5-3 that replacing either coarse or fine normal-weight particles with coarse or fine expanded slate aggregates, respectively, appeared to enhance the deformability of tested beams at a certain load. This is clear from the low slope of the load-deflection curves of LWSCC and LWVC beams with respect to NWSCC beams due to the reduction in beam stiffness. These observations can be related to the substitution of conventional aggregates with LWA that have relatively low stiffness and low modulus of elasticity, which in turn reduced the overall stiffness of the tested LWSCC and LWVC beams. On the other hand, replacing normal-weight aggregates with either coarse or fine expanded slate lightweight aggregates in order to reduce the mixtures' density by about 15% showed a reduction in the normalized shear load (V_{nz}) by an average of 16%, as shown in B3 and B8 compared to B1 and B2, respectively. As reported by Taylor (1974), the shear transfer in concrete beams without shear reinforcement along the diagonal fractured surface mainly develops from the contribution of compression shear zone, the dowel action of longitudinal reinforcement, and aggregate interlock mechanism. Therefore, this reduction in the shear capacity of LWSCC beams can be attributed to the use of relatively weak expanded slate coarse aggregate (compared to conventional aggregate) that may have fractured along the diagonal crack surface and reduced the degree of interlocking among the particles (which contributes to transferring up to 50% of the shear strength capacity of beams) (Taylor, 19974; Sherwood et al., 2007), resulting in less frictional resistance along

the failure plane. The results also showed that the lightweight beams with LF (B8) exhibited higher normalized shear load compared to its counterpart beams with LC (B3). This can be related to the fact that in B3, the normal-weight coarse aggregates (which have a higher contribution to transferring the shear strength in beams) were replaced by weaker LC, whereas in B8, the normal-weight sand (which has less contribution to transferring the shear strength) was replaced by LF.

Figure 5-3 also shows that the inclusion of PVA fibers considerably improved the shear capacity and the deformability of fibered-LWSCC beams. For example, by comparing B4 to B3 and B9 to B8, it can be observed that using 0.3% PVA8 fibers increased the ultimate shear load (V_u) and maximum deflection at ultimate load by an average of 19% and 28.5%, respectively. This increase in shear capacity and deformability of fibered-LWSCC beams can be related to the role of fibers in restricting the diagonal cracks from opening wider, which improved the friction and aggregate interlock along the diagonal crack and hence increased the shear resistance and allowed the beam to sustain more load accompanied with larger deformations. This also indicates the beneficial effect of polymeric fibers in improving the energy absorption of the tested beams (the area under the load-deflection curve up to failure load). The results also showed that the addition of shorter fibers (PVA8) showed more pronounced improvement in the V_u and ultimate deformation capacity of tested beams compared to longer fibers (PVA12), as shown in B4 and B5 compared to the control beam with no fibers (B3) (see Table 5-3). This performance could be attributed to the higher dispersion of shorter fibers (PVA8) in the concrete matrix for the same fiber volume compared to longer fibers (PVA12), which increases the probability that individual

fibers will be oriented perpendicularly to the diagonal cracks, as indicated before. Increasing the fiber content resulted in further improvements in the shear capacity and deformability of tested beams. Increasing the fiber content to 0.5% (in B7 and B12) significantly increased the shear capacity (V_{nz}) of LWSCC beams (up to 37% higher than non-fibered beams B3 and B8), and even reached values higher than those exhibited by counterpart NWSCC beams (B7 and B12 compared to B1 and B2, respectively).

It is worth noting that because of the absence of SCC fresh properties restrictions (especially passing ability) in LWVC, it was possible to develop all-lightweight vibrated concrete beams (B13 and B14) with higher volume of LC. This higher volume of LC not only contributed to reducing the beams' density (up to 1711 kg/m^3) but also helped to improve the shear strength of the beams. Although B13 (LWVC) had lower density and lower compressive strength compared to B3 (SCC), the presence of higher volume of expanded slate coarse aggregate in B13 (using C/F aggregate ratio of 1.5) contributed to boosting the degree of interlocking among the particles and allowed extra shear stresses to be transferred along the diagonal cracks. In terms of fibered-LWVC beams, although the inclusion of a high volume of PVA8 fibers (up to 1%) in B14 negatively affected the compressive strength of the concrete mixture, the addition of fiber continued to enhance the shear strength and deformation capacity of LWVC beams (Table 5-3).

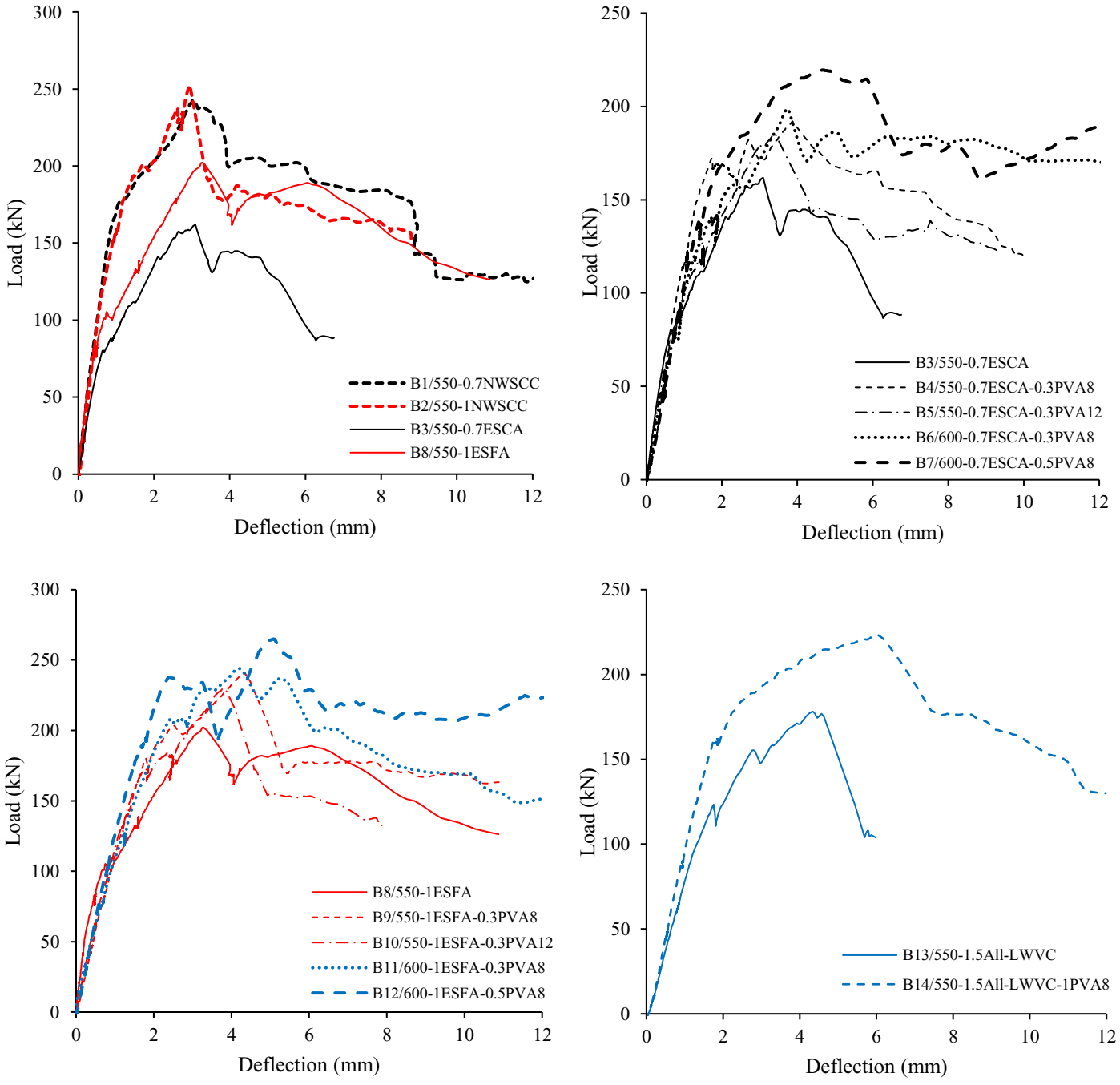

Figure 5-3: Experimental load-midspan deflection responses.

5.5.4 Post-diagonal cracking resistance

Table 5-3 shows the first diagonal cracking load (which was visually observed and confirmed by the sudden jump in the reading of the LVDT) for all tested beams. The post-diagonal cracking resistance indicates the maximum resistance the beam can withstand after the formation of the first diagonal crack. Table 5-3 also presents the values of the post-diagonal cracking resistance for all tested beams, which were calculated using a formula of [(Max failure load – First diagonal cracking load)/Max failure load].

It can be observed from Table 5-3 that the post-diagonal cracking resistance of B8 with LF (the beam developed with the lowest density using LF) was found to be 49% higher than that observed in B3 with LC (the beam developed with the lowest density using LC). This can be attributed to the presence of high-strength crushed granite stones in LWSCC-LF mixtures, which have higher aggregate interlock resistance than partially fractured LC in B3. Increasing the C/F aggregate ratio in LWVC mixtures allowed the beam (B13) to exhibit higher post-diagonal cracking resistance compared to the beam with lower C/F ratio (B3). This result confirms the good strength of the expanded slate aggregates used in this investigation, which showed some contribution toward aggregate interlock along the cracked surface.

Table 5-3 also shows that the addition of polymeric fibers obviously enhanced the post-diagonal cracking resistance of both fibered-LWSCC and fibered-LWVC beams. Regarding fibered-LWSCC beams, using 0.3% PVA8 fibers increased the post-diagonal cracking resistance by 13.3%, while adding longer fibers (PVA12) revealed less improvement and reached up to 9.8%, as shown in B9 and B10 compared to B8. Such

results could be related to the same reasons explained earlier for the ultimate shear load results. Further, increasing the fiber content up to 1% in B14 showed the maximum improvement in the post-diagonal cracking resistance, which reached up to 28%.

5.5.5 Energy absorption

Figure 5-4 shows the energy absorption capacity of all developed beams, which is graphically evaluated by measuring the area under the load-deflection curve up to the peak point (Younis et al., 2017; Joshi et al., 2018) (shown in Figure 5-3). An expected reduction in the energy absorption capacity of tested beams was observed due to replacing normal-weight aggregate with expanded slate lightweight aggregate. However, LWSCC beams containing LF exhibited relatively higher energy absorption capacity compared to that exhibited by LWSCC-LC beams (see B8-12 compared to B3-7). This is due to the higher ultimate shear load resisted by LWSCC-LF compared to LWSCC-LC beams, which was accompanied by a relatively higher rate of deformation.

As mentioned earlier, adding PVA fibers allowed LWSCC beams to experience a higher rate of deformation and higher shear load. Consequently, a larger area was enclosed by the load-deflection curve, indicating higher energy absorbed by the tested beams before failure. In fibered-LWSCC beams, at the same fiber volume of 0.3%, use of PVA8 showed an increase in the energy absorption capacity by an average of 60.3%, while the addition of PVA12 increased the energy absorption capacity by only 27.8% (on average), as shown in B4-5 compared to B3 and B9-10 compared to B8. In addition, increasing the fiber content led to further improvements in the ability of tested beams to absorb more energy until

failure. For example, in the fibered-LWVC beam (B14), the possibility of adding 1% PVA8 fibers exhibited maximum increase in the energy absorption capacity of the beam, reaching up to 97%, higher than that of beam B13 (comparable beam with no fibers), as seen in Figure 5-4.

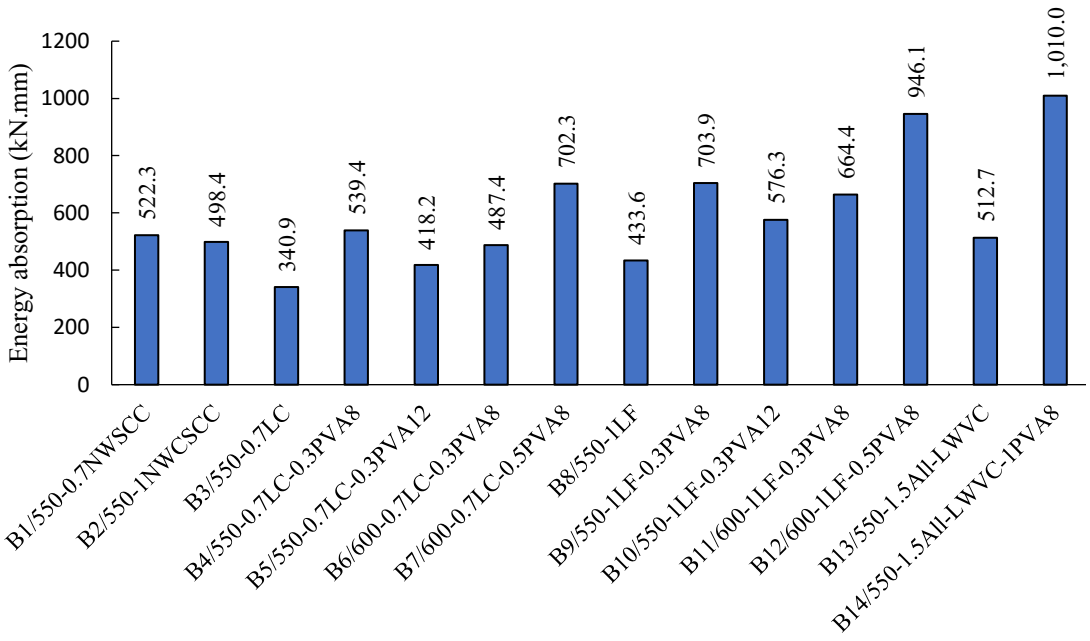

Figure 5-4: Results of energy absorption capacity of all tested beams.

5.5.6 Theoretical predictions of shear strength

The theoretical shear load (V_{pred}) of the tested NWSCC, LWSCC, and LWVC beams was predicted according to the provisions of ACI 318 (2014), CSA A23.3 (2014), AASHTO-LRFD (2017), and Eurocode 2 (2004). However, because these code models do not consider the contribution of fibers in their calculations, these code equations were only used for estimating the shear capacity of the concrete beams without fibers. For all the other tested beams with fibers, six shear strength models (the most available models that consider

the effect of fibers) were extracted from the literature and used in the prediction. Detailed equations of these six models are summarized in Table 5-4.

As indicated in Table 5-4, the four design codes consider a modification factor (λ) to account for the reduced splitting resistance and friction properties of LWC compared to normal-weight concrete of the same compressive strength. Unlike these design codes, the existing models in the literature that were selected to predict the shear strength of fiber-reinforced concrete beams do not consider any modification factor in their calculations. Therefore, I decided to account for the lightweight modification factor by replacing f_c' with $\lambda^2 f_c'$ and τ with $\lambda\tau$ in all six models chosen for fiber-reinforced concrete beams, as recommended by Kang et al. (2011). Here, the factor τ is the average interfacial bond strength of fibers that can be taken as 2.93 MPa for PVA fiber (Hossain et al., 2020). The value of λ was taken as 0.85 for sand-lightweight concrete mixtures and 0.75 for all-lightweight mixtures as recommended by ACI 318 (2014).

The ratio of experimental-to-predicted shear capacity ($V_{\text{exp}}/V_{\text{pred}}$) for each tested beam was calculated and plotted in Figure 5-5 (**a** and **b**). It can be noted from Figure 5-5**a** that all code-based design equations were highly conservative in estimating the shear strength of non-fibered SCC/VC beams without shear reinforcement, showing high $V_{\text{exp}}/V_{\text{pred}}$ ratios. Eurocode 2 (2004), however, showed the closest predictions (most accurate) among all design codes, providing the lowest $V_{\text{exp}}/V_{\text{pred}}$ ratio, which ranged from 1.25 to 1.57. This could be attributed to the different considerations of the modification factor (λ) in the four design codes. ACI 318 (2014), CSA A23.3 (2014), and AASHTO-LRFD (2017) codes

recommend that the factor λ (low-density concrete factor) should be taken as either 0.85 or 0.75, while Eurocode 2 (2004) calculates this factor using the equation $\lambda = 0.4 + 0.6\rho_c/2200$, which generates more numbers (based on the concrete density level [ρ_c]).

By looking at fiber-reinforced concrete beams (Figure 5-5**b**), it can be noted that the model adopted by Mansur et al. (1986) was more conservative in predicting the shear capacity of fibered beams compared to other selected models, presenting $V_{\text{exp}}/V_{\text{pred}}$ ratios in the range of 1.26 to 1.80. On the other hand, the models developed by Imam et al. (1994) and Ashour et al. (1992) appeared to overestimate the shear strength of fiber-reinforced lightweight SCC/VC beams, with $V_{\text{exp}}/V_{\text{pred}}$ ratios in the range of 0.49 to 0.91 and 0.52 to 0.99, respectively. The closest predictions were given by the models developed by Sharma (1986) and Narayanan and Darwish (1987). Although these two models accurately predict the shear strength of LWSCC-LC beams (B4-B7) with $V_{\text{exp}}/V_{\text{pred}}$ ratios in the range of 1.02 to 1.04 and 0.98 to 1.04, respectively, they were more conservative in estimating the shear capacity of LWSCC-LF (B9-B12), indicating relatively higher $V_{\text{exp}}/V_{\text{pred}}$ ratios. This can be related to the estimation of the factor λ, which is taken as 0.85 for both LC and LF mixtures, despite the fact that mixtures with LF exhibited higher concrete density and relatively higher splitting tensile strength. Therefore, further investigations are needed to accurately estimate the modification factor that accounts for the properties of concrete with fine lightweight aggregates.

Table 5-4: Theoretical models of the shear strength for beams without shear reinforcement and with/without fibers.

Code	Model
ACI 318 (2014)	$V_c = \left(0.158\,\lambda\sqrt{f_c'} + 17\,\rho\frac{d}{a}\right) bd \;\leq 0.29\sqrt{f_c'}bd$ Where f_c' = cylinder compressive strength (MPa) λ = lightweight concrete modification factor (1.0 for normal-weight concrete, 0.85 for sand-lightweight concrete, and 0.75 for all-lightweight concrete) ρ = longitudinal flexural reinforcement ratio d = effective depth of beam (mm) a = shear span (mm) b = width of concrete section (mm)
CSA A23.3 (2014)	$V_c = \lambda\,\beta\sqrt{f_c'}bd_v$ β = factor accounting for shear resistance of cracked concrete d_v = effective shear depth (the greater of $0.9d$ or 0.72 of the beam height)
AASHTO-LRFD (2017)	$V_c = 0.083\beta\,\lambda\sqrt{f_c'}bd_v$
Eurocode 2 (2004)	$V_c = [C_{Rd,c}\eta\,K(100\rho f_c')^{1/3}]b_w\,d$ $C_{Rd,c}$= 0.18 for NWC and 0.15 for LWC η = factor to account for lightweight concrete ($\eta = 0.4+0.6\rho_c/2200$); and ρ_c is the upper limit of the dry density for the relevant class K = size effect factor (K=1+$\sqrt{200/\mathrm{d}} \leq 2.0$)
Investigator	Model
Sharma (1986)	$v_u = \frac{2}{3}f_t'\left(\frac{d}{a}\right)^{0.25}$ f_t' = split-cylinder tensile strength of concrete (MPa)
Mansur et al. (1986)	$v_u = \left[\left(0.16\sqrt{f_c'} + 17.2\rho\frac{d}{a}\right) + 0.41\,\tau F\right]$ Where F= fiber factor = [$V_f\,(l_f/d_f)\,D_f$] *Here,* V_f= fiber volume; l_f/d_f = fiber aspect ratio; and D_f = the bond factor dependent on the shape of the fibers (taken as 0.5 for PVA fiber) τ= fiber–matrix interfacial bond strength, taken as 2.93 MPa based on recommendations of Hossain et al. (2020)

Narayanan and Darwish (1987)	$v_u = \left[2.8\frac{d}{a}\left(0.24\left(\frac{f_c'}{20-\sqrt{F}}+0.7+\sqrt{F}\right)+80\rho\frac{d}{a}\right)+0.41\,\tau F\right]$ For $a/d \leq 2.8$
Ashour et al. (1992)	$v_u = \left[\left(0.7\sqrt{f_c'}+7F\right)\frac{d}{a}+17.2\,\rho\frac{d}{a}\right]$ ACI Code Modification
Imam et al. (1994)	$v_u = \left[0.6\,\Psi\sqrt[3]{\omega}\left((f_t')^{0.44}+275\sqrt{\frac{\omega}{\left(\frac{a}{d}\right)^{0.44}}}\right)\right]$ Since $\Psi = \frac{1+\sqrt{5.08/d_a}}{\sqrt{1+d/(25\,d_{a)}}}$ = size effect; d_a is maximum aggregate size in mm; and ω = reinforcement factor = $\rho\,(1+4F)$
RILEM (2003)	$v_u = \left[0.15\sqrt[3]{\frac{3d}{a}}\,k(100\rho f_c')^{1/3}+k_1\,(0.5\left(\frac{d}{a}\right)f_{e,3})\right]$ Where k=1+$\sqrt{200/\mathrm{d}} \leq 2.0$ and $k_1 = \frac{1600-d}{1000} \geq 1.0$ $f_{e,3}$ = equivalent flexural strength

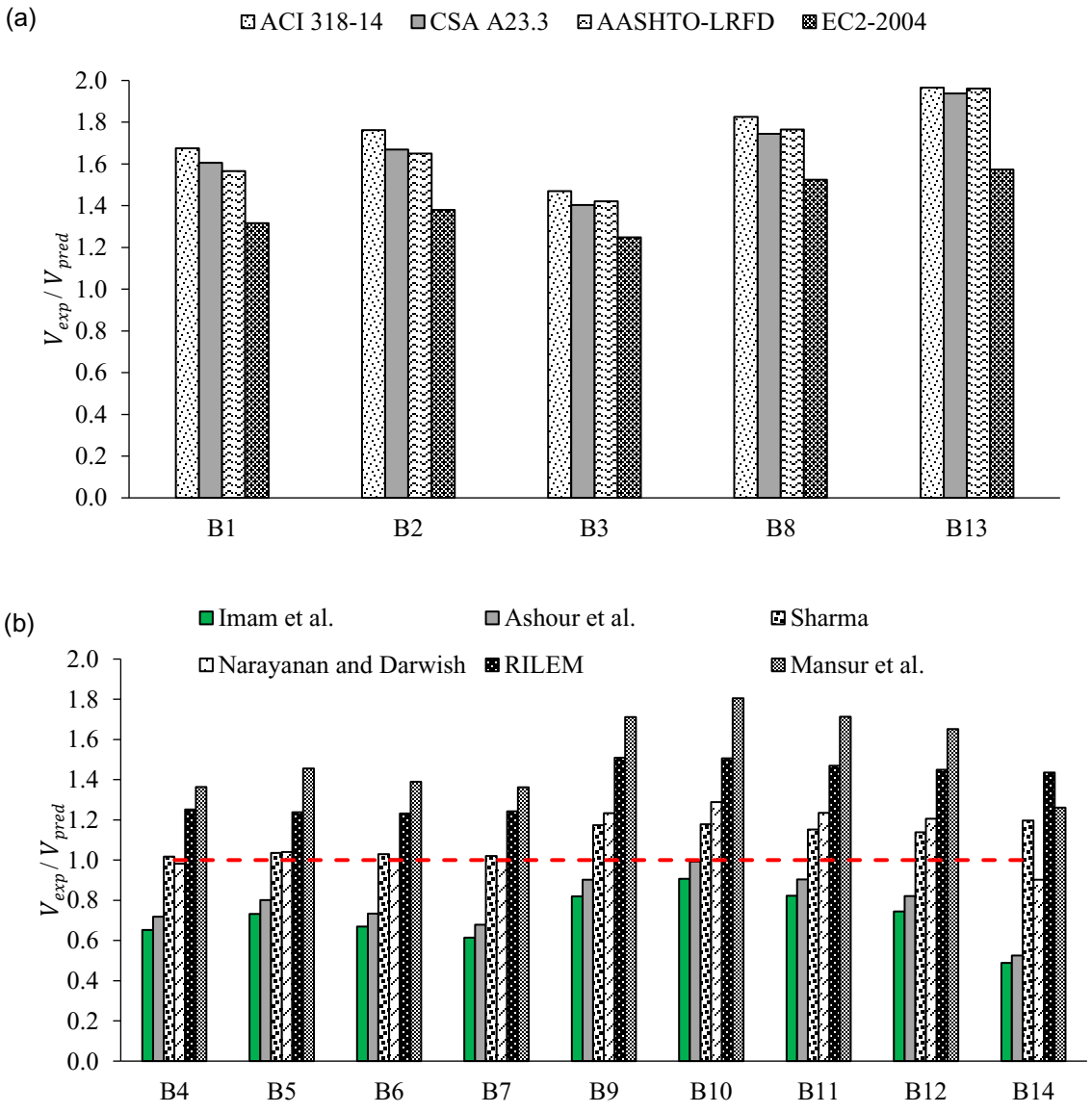

Figure 5-5: Ratio of experimental shear strength to shear strength predicted by (a) code design equations, (b) researchers' models.

5.6 Conclusions

This chapter evaluates the structural performance of a number of lightweight SCC beams under shear load. A total of 14 concrete mixtures (two NWSCC, ten LWSCC, and two LWVC) were developed to cast 14 concrete beams without shear reinforcement. The performance of tested beams was evaluated in terms of cracking pattern, failure mode, load-deflection response, load-carrying capacity, post-diagonal cracking resistance, and energy absorption capacity. Based on the results presented in this chapter, the following conclusions were drawn.

1. Using PVA fibers in the developed LWSCC generally improved the shear resistance and cracking behavior of LWSCC beams. For example, adding 0.3% PVA8 (8 mm) fibers to LWSCC beams showed improvements in the ultimate shear load, post-diagonal cracking resistance, energy absorption capacity, and deformation capacity by about 19%, 17%, 60.3%, and 28.5%, respectively, compared to counterpart beams without fibers.
2. A maximum of 0.3% PVA fibers was possible to use in the development of successful LWSCC mixtures with 550 kg/m^3 binder content. However, increasing the binder content to 600 kg/m^3 allowed using up to 0.5% PVA fibers. This increase in the fiber content (from 0.3% to 0.5%) significantly increased the normalized shear load (V_{nz}) of the tested LWSCC beams by about 37% compared to counterpart beams without fibers.
3. In fibered-LWSCC beams, the inclusion of shorter PVA fibers (PVA8) appeared to have a more positive effect, compared to longer PVA fibers (PVA12), on improving

the performance of LWSCC beams in terms of load-carrying capacity, post-diagonal cracking resistance, deformability, energy absorption capacity, and cracking behavior. For example, using 0.3% PVA8 increased the ultimate shear load and the energy absorption capacity by about 19% and 60.3%, respectively, while the addition of 0.3% PVA12 showed an increase of 14% and 27.8%, respectively.

4. The addition of PVA fibers to LWSCC beams greatly enhanced the cracking behavior and helped the beams to experience higher deformation before failure, reaching up to 6.03 mm compared to 4.34 mm in non-fibered counterpart beam. The cracking behavior of LWSCC with PVA fibers was characterized by a propagation of a higher number of vertical-flexural and inclined-shear cracks with smaller widths prior to failure compared to beams without fibers.
5. LWSCC beams with LF showed relatively higher ultimate shear load, post-diagonal cracking resistance, and energy absorption capacity than LWSCC beams with LC. This was attributed to the presence of higher-strength normal-weight coarse aggregates (mixed with fine lightweight aggregates) in the development of LWSCC-LF beams, which had higher interlock resistance along the diagonal crack compared to partially fractured expanded slate coarse aggregates in LWSCC-LC beams.
6. Because of the absence of the fresh properties' restrictions of SCC, it was possible to use up to 1% PVA fibers in LWVC beams. This increase in fiber content contributed to achieving the maximum improvements in the ultimate shear load,

post-diagonal cracking resistance, energy absorption capacity, and deformation capacity, which reached up to 25.5%, 28%, 97%, and 39%, respectively, compared to the control beam without fibers.

7. All code-based design equations (ACI 318-14, CSA A23.3, AASHTO-LRFD, and EC 2) were highly conservative in estimating the ultimate shear strength of SCC/VC beams without fibers. EC2, however, showed the closest predictions among all design codes, providing the lowest $V_{\text{exp}}/V_{\text{pred}}$. On the other hand, the models developed by Sharma (1986) and Narayanan and Darwish (1987) provided the best predictions for the shear strength of lightweight SCC/VC beams with PVA fibers compared to all other investigated models.

5.7 References

Aashto (Association of State Highway and Transportation Officials) LRFD. (2017). Bridge Design Specifications and Commentary, SI Units. *Aashto*, Washington, DC, USA.

AbdelAleem, B. H., & Hassan, A. A. (2019). Influence of synthetic fibers' type, length, and volume on enhancing the structural performance of rubberized concrete. *Construction and Building Materials*, *229*, 116861.

AbdelAleem, B. H., Ismail, M. K., & Hassan, A. A. (2017). Properties of self-consolidating rubberised concrete reinforced with synthetic fibres. *Magazine of Concrete Research*, *69*(10), 526-540.

Abouhussien, A. A., Hassan, A. A., & Ismail, M. K. (2015). Properties of semi-lightweight self-consolidating concrete containing lightweight slag aggregate. *Construction and Building Materials*, *75*, 63-73.

ACI (American Concrete Institute). (2014). ACI 318R-14: Building code requirements for structural concrete and commentary. *ACI*, Farmington Hills, MI, USA.

Afroughsabet, V., Biolzi, L., & Ozbakkaloglu, T. (2016). High-performance fiber-reinforced concrete: a review. *Journal of materials science*, *51*(14), 6517-6551.

Ahari, R. S., Erdem, T. K., & Ramyar, K. (2015). Effect of various supplementary cementitious materials on rheological properties of self-consolidating concrete. *Construction and Building Materials*, *75*, 89-98.

Arain, M. F., Wang, M., Chen, J., & Zhang, H. (2019). Study on PVA fiber surface modification for strain-hardening cementitious composites (PVA-SHCC). *Construction and Building Materials*, *197*, 107-116.

Ashour, S. A., Hasanain, G. S., & Wafa, F. F. (1992). Shear behavior of high-strength fiber reinforced concrete beams. *Structural Journal*, *89*(2), 176-184.

Aslani, F., & Kelin, J. (2018). Assessment and development of high-performance fibre-reinforced lightweight self-compacting concrete including recycled crumb rubber aggregates exposed to elevated temperatures. *Journal of Cleaner Production*, *200*, 1009-1025.

Behrooyan, M., & Ahmadian, H. R. (2013). Effects of Polyvinyl Alcohol fibers on fracture energy of concrete. *Int. Research J. Appl. Basic Sciences*, *6*, 484-491.

Bogas, J. A., Gomes, A., & Pereira, M. F. C. (2012). Self-compacting lightweight concrete produced with expanded clay aggregate. *Construction and Building Materials*, *35*, 1013-1022.

Campana, S., Fernández Ruiz, M., Anastasi, A., & Muttoni, A. (2013). Analysis of shear-transfer actions on one-way RC members based on measured cracking pattern and failure kinematics. *Magazine of concrete research*, *65*(6), 386-404.

Chai, Y. H. (2016). Service performance of long-span lightweight aggregate concrete box-girder bridges. *Journal of Performance of Constructed Facilities*, *30*(1), 04014196.

Cho, S. H., & Kim, Y. I. (2003). Effects of steel fibers on short beams loaded in shear. *Structural journal*, *100*(6), 765-774.

Corinaldesi, V., & Moriconi, G. (2015). Use of synthetic fibers in self-compacting lightweight aggregate concretes. *Journal of building engineering*, *4*, 247-254.

CSA (Canadian Standards Association). (2014). CSA A23.3-14: Design of concrete structures. *CSA*, Rexdale, ON, Canada.

Ding, J. T., & Li, Z. (2002). Effects of metakaolin and silica fume on properties of concrete. *Materials Journal*, *99*(4), 393-398.

Dymond, B. Z., Roberts-Wollmann, C. L., & Cousins, T. E. (2010). Shear strength of a lightweight self-consolidating concrete bridge girder. *Journal of Bridge Engineering*, *15*(5), 615-618.

EFNARC. (2005). The European Guidelines for Self-Compacting Concrete Specification, Production and Use. *European Federation for Specialist Construction Chemicals and Concrete Systems*, English ed. Norfolk, UK.

Eurocode 2 (2004). Design of Concrete Structures – Part 1-1: General Rules and Rules for Buildings. *European Committee for Standardization*, Brussels, Belgium.

Hassan, A. A. A., Hossain, K. M. A., & Lachemi, M. (2008). Behavior of full-scale self-consolidating concrete beams in shear. *Cement and Concrete Composites*, *30*(7), 588-596.

Hassan, A. A., Ismail, M. K., & Mayo, J. (2015). Mechanical properties of self-consolidating concrete containing lightweight recycled aggregate in different mixture compositions. *Journal of Building Engineering*, *4*, 113-126.

Hassan, A. A., Ismail, M. K., & Mayo, J. (2015). Shear behavior of SCC beams with different coarse-to-fine aggregate ratios and coarse aggregate types. *Journal of Materials in Civil Engineering*, *27*(11), 04015022.

Haug, A. K., & Fjeld, S. (1996). A floating concrete platform hull made of lightweight aggregate concrete. *Engineering Structures*, *18*(11), 831-836.

Hossain, K. M. A., Hasib, S., & Manzur, T. (2020). Shear behavior of novel hybrid composite beams made of self-consolidating concrete and engineered cementitious composites. *Engineering Structures*, *202*, 109856.

Hossain, K. M. A., Lachemi, M., Sammour, M., & Sonebi, M. (2013). Strength and fracture energy characteristics of self-consolidating concrete incorporating polyvinyl alcohol, steel and hybrid fibres. *Construction and Building Materials*, *45*, 20-29.

Imam, M., Vamdewalle, L., & Mortelmans, F. (1994). Shear capacity of steel fiber high-strength concrete beams. *Special Publication*, *149*, 227-242.

Ismail, M. K., & Hassan, A. A. (2021). Influence of fibre type on the shear behaviour of engineered cementitious composite beams. *Magazine of Concrete Research*, *73*(9), 464-475.

Joshi, S. S., Thammishetti, N., & Prakash, S. S. (2018). Efficiency of steel and macro-synthetic structural fibers on the flexure-shear behaviour of prestressed concrete beams. *Engineering Structures*, *171*, 47-55.

Jun Li, J., gang Niu, J., jun Wan, C., Jin, B., & liu Yin, Y. (2016). Investigation on mechanical properties and microstructure of high performance polypropylene fiber reinforced lightweight aggregate concrete. *Construction and Building Materials*, *118*, 27-35.

Kang, T. H., Kim, W., Kwak, Y. K., & Hong, S. G. (2011). Shear testing of steel fiber-reinforced lightweight concrete beams without web reinforcement. *ACI Structural Journal*, *108*(5), 553.

Khayat, K. H., Paultre, P., & Tremblay, S. (2001). Structural performance and in-place properties of self-consolidating concrete used for casting highly reinforced columns. *Materials Journal*, *98*(5), 371-378.

Kılıç, A., Atiş, C. D., Yaşar, E., & Özcan, F. (2003). High-strength lightweight concrete made with scoria aggregate containing mineral admixtures. *Cement and Concrete Research*, *33*(10), 1595-1599.

Kowalsky, M. J., Priestly, M. N., & Seible, F. (1999). Shear and flexural behavior of lightweight concrete bridge columns in seismic regions. *ACI structural journal*, *96*, 136-148.

Lotfy, A., Hossain, K. M., & Lachemi, M. (2016). Mix design and properties of lightweight self-consolidating concretes developed with furnace slag, expanded clay and expanded shale aggregates. *Journal of Sustainable Cement-Based Materials*, *5*(5), 297-323.

MacGregor, J. G., Wight, J. K., Teng, S., & Irawan, P. (1997). *Reinforced concrete: Mechanics and design* (Vol. 3). New Jersey: Prentice Hall.

Mansur, M. A., Ong, K. C. G., & Paramasivam, P. (1986). Shear strength of fibrous concrete beams without stirrups. *Journal of structural engineering*, *112*(9), 2066-2079.

Narayanan, R., & Darwish, I. Y. S. (1987). Use of steel fibers as shear reinforcement. *Structural Journal*, *84*(3), 216-227.

Nehdi, M., & Ladanchuk, J. D. (2004). Fiber synergy in fiber-reinforced self-consolidating concrete. *Materials Journal*, *101*(6), 508-517.

NRMCA (National Ready Mixed Concrete Association). (2003). CIP 36-Structural Lightweight Concrete. *NRMCA,* Washington, DC.

Omar, A. T., & Hassan, A. A. (2019). Use of polymeric fibers to improve the mechanical properties and impact resistance of lightweight SCC. *Construction and Building Materials*, *229*, 116944.

Omar, A. T., Ismail, M. K., & Hassan, A. A. (2020). Use of polymeric fibers in the development of semilightweight self-consolidating concrete containing expanded slate. *Journal of Materials in Civil Engineering*, *32*(5), 04020067.

RILEM. (2003). RILEM-TC-162-TDF: Test and design methods for steel fibre reinforced concrete, stress-strain design method. *Final recommendation. Materials and Structures 36*, pp. 560–567.

Sharma, A. K. (1986). Shear strength of steel fiber reinforced concrete beams. In *Journal Proceedings* (Vol. 83, No. 4, pp. 624-628).

Sherwood, E. G., Bentz, E. C., & Collins, M. P. (2007). Effect of aggregate size on beam-shear strength of thick slabs. *ACI Structural Journal*, *104*(2), 180.

Szydlowki, R., & Mieszcak, M. (2017). Study of application of lightweight aggregate concrete to construct post-tensioned long-span slabs. *Procedia Engineering*, *172*, 1077-1085.

Taylor, H. P. (1974). The fundamental behavior of reinforced concrete beams in bending and shear. *Special Publication*, *42*, 43-78.

Topçu, I. B., & Uygunoğlu, T. (2010). Effect of aggregate type on properties of hardened self-consolidating lightweight concrete (SCLC). *Construction and Building Materials*, *24*(7), 1286-1295.

Wild, S., Khatib, J. M., & Jones, A. (1996). Relative strength, pozzolanic activity and cement hydration in superplasticised metakaolin concrete. *Cement and concrete research*, *26*(10), 1537-1544.

Yang, K. H., & Ashour, A. F. (2011). Aggregate interlock in lightweight concrete continuous deep beams. *Engineering Structures*, *33*(1), 136-145.

Yang, K. H., Sim, J. I., Kang, J. H., & Ashour, A. F. (2012). Shear capacity of monolithic concrete joints without transverse reinforcement. *Magazine of Concrete Research*, *64*(9), 767-779.

Younis, A., Ebead, U., & Shrestha, K. C. (2017). Different FRCM systems for shear-strengthening of reinforced concrete beams. *Construction and Building Materials*, *153*, 514-526.

6. Flexural performance of fiber-reinforced SCC beams containing expanded slate lightweight aggregates

6.1 Abstract

This chapter intends to investigate the structural performance of large-scale fiber-reinforced lightweight self-consolidating concrete (LWSCC) as well as lightweight vibrated concrete (LWVC) beams made with expanded slate aggregates under flexure loads. A total of fourteen reinforced concrete beam specimens were tested under a four-point bending configuration until failure. Two different binder contents (550 - 600 kg/m^3), two types of lightweight aggregates (coarse and fine expanded slate aggregates), two PVA fiber lengths (8 - 12 mm), and three fraction volumes of fibers (0.3%, 0.5%, and 1%) were considered in this investigation. The structural performance of the tested beam specimens was assessed in terms of load-deflection response, cracking behavior, energy absorption, displacement ductility, cracking moment, and ultimate flexural strength. This chapter also investigated the performance of design code provisions in predicting the cracking and ultimate moment capacities of all tested specimens. The results indicated that using shorter PVA fibers seemed to better improve the structural performance of LWSCC beams in terms of deformability, energy absorption, ductility, and ultimate flexural capacity than using longer PVA fibers. Using up to 1% PVA8 fibers in lightweight concrete beams made with expanded slate aggregates proved to completely compensate for the drop in ultimate flexural strength that resulted from the use of low-density aggregates and further helped the beams to experience much higher rates of deformation. The results also showed that

the model proposed by Henager and Doherty well predicted the ultimate moment capacity of LWSCC/LWVC beams reinforced with PVA fibers.

6.2 Introduction

The use of lightweight aggregates in modern construction industry has gained interest due to the global move towards developing sustainable structures. Expanded lightweight aggregates constitute a sustainable substitute to natural aggregates because of their significant role in conserving natural resources and recycling by-product materials (Nes & Øverli, 2016; Alqahtani et al., 2017; Muñoz-Ruiperez et al., 2018). In addition, using lightweight aggregates (LWA) to produce structural lightweight concrete (LWC) can significantly reduce the self-weight of concrete structures, affording a substantial reduction in design loads. This allows minimized concrete dimensions, providing a smaller seismic demand, and introduces potential savings in construction costs (NRMCA, 2003; Kayali, 2008). Moreover, LWC can reach high levels of strength, attaining a convenient strength-to-weight ratio (Omar et al., 2020; Du et al., 2022). Consequently, this type of concrete has been successfully applied in various structural applications, including post-tensioned concrete ceilings and long-span bridges (Rodriguez, 2004; Kwon et al., 2018).

Lightweight self-consolidating concrete (LWSCC) is a novel type of high-performance concrete that combines the structural benefits of LWC and the desired properties of self-consolidating concrete (SCC). Properly designed LWSCC can spread thoroughly under its own weight without segregation, completely fill the formwork, and encapsulate the reinforcement with no vibration effort, which significantly reduces construction time and

labor demand (Shi & Wu, 2005). Recently, the application of LWSCC in construction projects has gradually increased, specifically in the area of offshore and marine structures, in rehabilitation and strengthening of existing buildings, and in the precast industry (Jiang et al., 2004; Shi et al., 2005; Iqbal et al., 2016). In recent years, extensive investigations have been conducted to study the influence of material properties and mix proportions on the fresh and mechanical properties of LWSCC. Most of these studies indicated that using high binder content and minimizing the coarse aggregate volume were required to improve the rheological characteristics of the LWSCC (Lotfy et al., 2016; Assaad & Issa, 2018; Law Yim Wan et al., 2018). Furthermore, supplementary cementing materials (SCMs) such as fly ash (FA), metakaolin (MK), and silica fume are commonly used to achieve acceptable flowability and enhance segregation resistance of the mixtures (Abouhussien et al., 2015; Sadek et al., 2020).

Despite the environmental and structural benefits of using LWC, the application of this concrete is somewhat limited for use in large-scale structural elements. It is well recognized that LWC generally has a lower elastic modulus and more brittle characteristics than NWC (Chi et al., 2003). Hence, LWC members typically express larger deformation, faster crack propagation, and a steeper descending portion of the stress-strain curve compared to their NWC counterparts (Yang et al., 2014; Carmo et al., 2017). In addition, looking through the literature, it is frequently pointed out that LWC members exhibit inferior flexural ductility due to the reduced fracture toughness and more localized crack propagation through the low-density particles (Carmo et al., 2017). This was also proved by Sin et al. (2011) when testing the structural performance of LWC members under flexure loading. Their study

investigated 21 simply supported beams made with different volumes of lightweight expanded clay aggregates and different binder contents. Test results indicated that the ultimate strengths of LWC beams were quite similar to those of NWC beams, but less ductility was observed in LWC. On the other hand, structural members should not only provide acceptable strength but also ensure adequate ductility under unexpected overloading. It is, therefore, imperative to improve the structural behavior and ductility of LWC members in order to extend their use in multiple structural applications.

Adding fibers into LWSCC can also be an effective technique to compensate for the low fracture toughness that results from the use of low-density aggregates. Adjusting the fiber's parameters in the matrix significantly improves the impact resistance, toughness, ductility, energy absorption, and cracking performance of concrete (AbdelAleem & Hassan, 2019; Çelik Z, Bingöl, 2020; Omar & Hassan, 2021). The fibers' bridging mechanism allows tensile stresses to transfer at crack interferences, affording residual strength to the concrete composite (Nes & Øverli, 2016; de Alencar Monteiro et al., 2018; Cardoso et al., 2019). Meanwhile, the stitching action of fibers plays an influential role in delaying the initiation of cracks and limiting their propagation (AbdelAleem et al., 2017). Steel fibers and synthetic fibers are the most commonly used fibers in concrete mixtures. Steel fibers have high modulus of elasticity and stiffness; hence, better enhancement in concrete's compressive strength and toughness can be achieved. However, the addition of synthetic fibers, especially polymeric fibers, into concrete mixtures showed some advantages over steel fibers. Polymeric fibers have lower density and superior corrosion resistance than steel fibers (Corinaldesi & Moriconi, 2015; Jun Li et al., 2016). Over the last decade, many

researchers have investigated the influence of using polymeric fibers on the structural performance of concrete elements. For example, Bastami (2019) studied the effects of macro-polypropylene fibers on the shear and flexural behavior of high-strength concrete beams subjected to static and dynamic loads. The results of this study indicated that the bridging effect of fibers contributed to improving the overall behavior of the beams by delaying shear failure. Moreover, the combined use of polypropylene fibers and sufficient shear reinforcement was found to enhance the flexural ductility and cracking behavior.

Despite the benefit of using polymeric fibers in LWSCC mixtures, there is no sufficient information about the structural performance of beams made with optimized LWSCC mixtures containing polymeric fibers. This chapter attempts to develop LWSCC beams (concrete density ranged from 1628 to 1983 kg/m^3) with improved structural performance using fine and coarse expanded slate lightweight aggregates and different lengths and volumes of polyvinyl alcohol (PVA) fibers. The studied parameters include the type of LWA, binder content, LWA content (concrete density), and fiber length and volume.

6.3 Research Significance

Using LWC in structural members proved to have a desired characteristics in terms of reducing the design loads, seismic demand and saving in the construction costs. However, the brittle behavior and lower elastic modulus of LWC still showing some challenges in the application of such concrete in large-scale structural elements. Adding fibers to LWC, especially polymeric fibers, can help to alleviate the brittle behaviour of LWC and enhance the structural performance while maintaining the desired low density of LWC. In addition, developing LWC as SCC allows engineers to obtain a sustainable material for applications

requiring high compactability and reduced self-weight. However, there is a lack of information in the literature available regarding the in-situ properties and structural behavior of fiber reinforced LWSCC members, which makes it challenging to accomplish a rational design with confidence, especially when fibers are introduced. Hence, this investigation attempts to address this lack of knowledge by presenting an extensive investigation into the flexural performance and ductility of fiber-reinforced concrete beams with optimized LWSCC mixtures. This chapter also highlights the expected challenges and structural benefits that resulted from combining PVA fibers and the maximum possible volume of expanded slate LWA in the production of LWSCC.

6.4 Experimental Program

6.4.1 Mix proportions and specimen details

The experimental investigation was conducted on 14 concrete mixtures (14 large-scale beams) including: 10 LWSCC and fiber-reinforced LWSCC; two lightweight vibrated concrete (LWVC) and fibered LWVC; and two normal-weight self-consolidating concrete (NWSCC) mixtures. Table 6-1 provides the mixture proportions of all developed mixtures/beams. All tested mixtures/beams were labeled by the binder content level, C/F ratio, LWA type (LC or LF), fiber percentage, and type of PVA fiber (refer to Table 6-1). For instance, a fiber-reinforced LWSCC mixture containing a total binder content of 550 kg/m^3, 0.7 C/F ratio, lightweight coarse aggregate (LC), and reinforced with 0.3% PVA8 fiber was labeled as 550-0.7LC-0.3PVA. While a fiber-reinforced LWVC mixture optimized with a binder content of 550 kg/m^3, both LC and LF aggregates at a C/F ratio of 1.5, and 1% PVA8 would be labeled as 550-1.5All-LWVC-1PVA8.

All tested beam specimens were 2440 mm in length and had a square cross-section of 250 x 250 mm. The tension zone was reinforced with two 25M steel rebars, while two 10M steel rebars were placed in the compression zone. Sufficient transverse reinforcement was provided (10M stirrups arranged at 155 mm) to avoid shear failure before flexural failure. Figure 6-1 shows the details of specimen geometry and reinforcement layout of all tested beams.

6.4.2 Fresh and Mechanical properties tests

The fresh properties tests were conducted to evaluate the flowability and passing ability of NWSCC and LWSCC mixtures with and without PVA fibers. Slump flow test and L-box test were performed according to EFNARC guidelines (2005). The results of fresh properties tests are presented in Table 6-2. After 28 days, the compressive strength (f'_c) and splitting tensile strength (*STS*) tests were performed on three identical concrete cylinders (200 mm height x 100 mm diameter) as per ASTM C39 and C496, respectively. The Flexural strength test (FS) was conducted on three prisms (100X100 mm cross section and 400 mm length) as per ASTM C78. The modulus of elasticity (*ME*) of a typical concrete cylinder under compression loading was also assessed for all tested mixtures. All tested concrete cylinders and prisms were cast without external consolidation and moist-cured in the open air at room temperature (about 20 ^{o}C) to simulate the actual conditions of the tested beam specimens. The results of f'_c, *STS*, FS and *ME* of the tested mixtures are included in Table 6-2.

Table 6-1: Mixture proportions of NWSCC, LWSCC, and LWVC with/without fibers.

Beam/Mix #	Mixture designation	Cement (kg/m^3)	SCMs (Type)	SCMs (kg/m^3)	Aggregate					Fiber (%)	Water (kg/m^3)
					C/F ratio	NC (kg/m^3)	NF (kg/m^3)	LC (kg/m^3)	LF (kg/m^3)		
1	550-0.7NWSCC	275	FA+MK	165+110	0.7	620.3	886.1	-	-	-	220
2	550-1NWSCC	275	FA+MK	165+110	1.0	753.2	753.2	-	-	-	220
3	550-0.7LC	275	FA+MK	165+110	0.7	-	689.2	482.4	-	-	220
4	550-0.7LC-0.3PVA12	275	FA+MK	165+110	0.7	-	685.6	480.0	-	0.3	220
5	550-0.7LC-0.3PVA8	275	FA+MK	165+110	0.7	-	685.6	480.0	-	0.3	220
6	600-0.7LC-0.3PVA8	300	FA+MK	180+120	0.7	-	640.3	448.2	-	0.3	240
7	600-0.7LC-0.5PVA8	300	FA+MK	180+120	0.7	-	638.0	446.6	-	0.5	240
8	550-1LF	275	FA+MK	165+110	1.0	617.3	-	-	617.3	-	220
9	550-1LF-0.3PVA12	275	FA+MK	165+110	1.0	614.1	-	-	614.1	0.3	220
10	550-1LF-0.3PVA8	275	FA+MK	165+110	1.0	614.1	-	-	614.1	0.3	220
11	600-1LF-0.3PVA8	300	FA+MK	180+120	1.0	573.6	-	-	573.6	0.3	240
12	600-1LF-0.5PVA8	300	FA+MK	180+120	1.0	571.4	-	-	571.4	0.5	240
13	550-1.5All-LWVC	275	FA+MK	165+110	1.5	-	-	566.8	377.9	-	220
14	550-1.5All-LWVC-1PVA8	275	FA+MK	165+110	1.5	-	-	557.1	371.4	1.0	220

Note: SCMs = supplementary cementing materials; FA = fly ash; MK = metakaolin; C/F = coarse-to-fine ratio; NC = normal-weight coarse aggregate; NF = normal-weight fine aggregate; LC = Lightweight coarse aggregate; and LF = Lightweight fine aggregate.

Table 6-2: Fresh and Mechanical properties of tested mixtures.

Mix #	Mixture ID	T_{50}, (Sec)	L-box ratio (H2/H1)	f'_c (MPa)	*STS* (MPa)	*ME* (GPa)	FS (MPa)	*Dry density* (kg/m^3)
1	550-0.7NWSCC	2.05	0.97	68.9	4.08	30.57	5.76	2259.4
2	550-1NWSCC	2.3	0.91	67.1	3.97	30.41	5.84	2261.2
3	550-0.7LC	2.75	0.92	51.6	2.90	23.21	4.19	1909.1
4	550-0.7LC-0.3PVA12	3.96	0.8	48.9	3.42	21.83	5.13	1907.8
5	550-0.7LC-0.3PVA8	3.48	0.82	50.3	3.61	22.58	5.22	1904.2
6	600-0.7LC-0.3PVA8	3.2	0.91	52.6	3.69	22.34	5.44	1898.1
7	600-0.7LC-0.5PVA8	4.12	0.82	49.3	4.11	20.75	6.09	1893.2
8	550-1LF	2.1	0.95	52.1	3.09	24.87	4.89	1982.8
9	550-1LF-0.3PVA12	2.8	0.82	49.0	3.73	23.46	5.93	1978.2
10	550-1LF-0.3PVA8	2.41	0.85	50.4	3.93	23.89	6.15	1979.7
11	600-1LF-0.3PVA8	2.1	0.88	51.9	4.05	23.91	6.33	1970.6
12	600-1LF-0.5PVA8	2.7	0.83	48.7	4.45	22.04	7.03	1965.3
13	550-1.5All-LWVC	--	--	42.1	2.33	19.36	3.7	1630.6
14	550-1.5All-LWVC-1PVA8	--	--	34.7	3.25	16.92	5.6	1628.2

6.4.3 Instrumentation and test setup

A four-point bending test was adopted to investigate the structural behavior of the beams under flexure loads (see **Figure 6-1**). A single vertical load was applied using a 500 kN hydraulic actuator and then distributed using a distributive steel girder into two points acting on the top face of the beam. A linear variable differential transducer (LVDT) was used to monitor the vertical deflection at the mid-span of each beam. In addition, two strain gauges were attached to the tensile steel to monitor the steel strain during testing. The beam specimens were loaded gradually with a constant loading rate through three steps (50%, 75%, and 100% of the theoretically calculated failure load) until failure. After each load step, the development of cracks on one surface of the beam was detected and their widths were determined using a crack detection microscope. During the test, the load carrying capacity, mid-span deflection and strain measurements were continuously monitored and automatically recorded with a data acquisition system. At failure stage, the failure mechanism was observed, and cracking patterns were sketched for all tested beams. The results attained from the four-point loading test are introduced in Table 6-3.

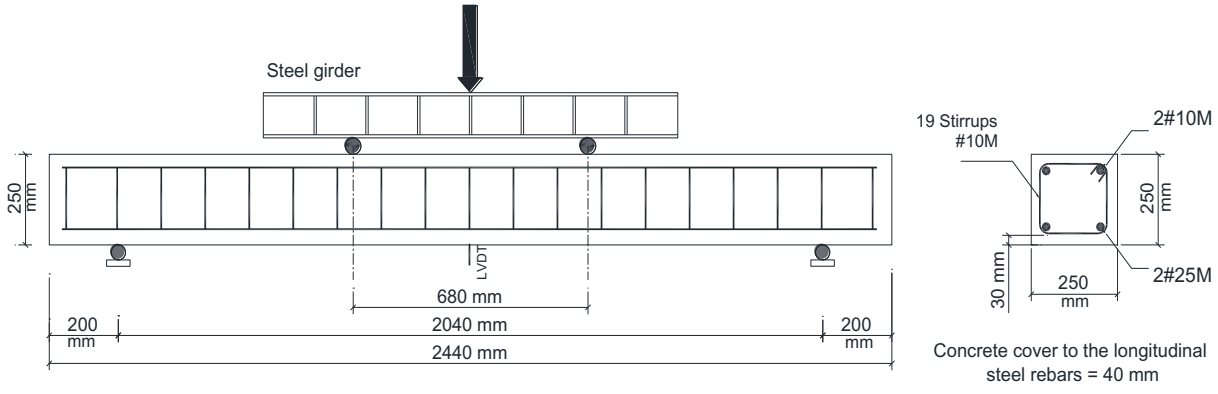

Figure 6-1: Loading configuration and details of test beams.

6.5 Results and Discussion

6.5.1 Load-deflection curves

Table 6-3 provides a summary of the flexure test results for all tested beams. Figure 6-2 represents the load-deflection relationships for all tested beams. From the figure, it can be seen that the load-deflection curves of all tested beams followed a typical pattern. The curves appeared to be linear, with a low deflection rate, up to the formation of the first flexural crack. With further loading in the post-cracking stage, the stiffness of the beams decreased because of the initiation of more flexural cracks; hence, the load-deflection responses remained reasonably linear, with a slightly lower slope until yielding of the reinforcements. After the rebars' yielding, the beams' central deflection rapidly increased, showing a slight increase in the applied load up to the peak load.

Figure 6-2**a** shows the load-midspan deflection curves of the minimum-density SCC beams with either coarse (B3) or fine (B8) expanded slate aggregates and the counterpart NWSCC beams with similar C/F aggregate ratios (B1 and B2). It can be seen that LWSCC beams with minimum possible density exhibited lower pre- and post-cracking flexural stiffnesses than the corresponding NWSCC beams. The use of expanded slate particles that have a low modulus of elasticity and low stiffness, compared to the replaced conventional normal-weight aggregates, can explain this reduction in flexural stiffness of LWSCC beams. It can also be noted that the LWSCC beam made with LF (B8) experienced approximately 16% higher ultimate deflection (δ_u = the deflection value at 85% of the ultimate load in the post-peak portion of the load-deflection curve) than the beam made with LC (B3). A possible explanation is that using low stiffness lightweight fine aggregates in the production of

LWSCC-LF mixtures made the cement mortar more deformable than the conventional cement mortar containing natural sand (which was used in LWSCC-LC). This contributed to the initiation of a great number of micro-cracks in the cement mortar, which helped the LWSCC-LF beam express a high rate of deformation prior to failure. This can also explain the decline in the rate of strength degradation after the LWSCC-LF beam reached its peak load, indicating more ductile failure.

Figure 6-2 (**b** and **c**) show the effect of adding PVA fibers on the flexural behavior of LWSCC beams. From the figure, it can be seen that including PVA fibers slightly increased the flexural stiffness of tested beams. This is mainly attributed to the potential of fibers to control the opening of cracks and restrain their propagation. Moreover, the ultimate deformation capacity of tested beams also increased when fibers were added. For instance, using 0.3% PVA12 fibers increased the ultimate deflection of the LWSCC-LC beam by about 19.9% (B4 compared to B3). The results also indicated that the inclusion of shorter fibers (PVA8) appeared to show better improvement in the beam stiffness and deformability compared to using longer fibers (PVA12). For example, replacing PVA12 with PVA8 at a 0.3% volume fraction increased the ultimate deflection by about 4%, as shown in B5 compared to B4. Due to the shorter length of PVA8 compared to PVA12, a greater number of single fibers was dispersed throughout the concrete matrix (at a similar fraction of fiber). This increased the probability of single fibers being oriented perpendicularly to the crack interfaces, which in turn allows better stitching action of fibers and, consequently, increases the beams' load-carrying capacity and deflection.

Table 6-3: Experimental summary for all tested beams under flexure loads.

Beam #	Beam/Mixture	Moment capacity (kN.m)		Deflection (mm)		Ductility index (μ)	Absorbed energy (kN.m)	Cracking at failure stage	
		1st crack	Ultimate	Yield (δ_y)	Ultimate (δ_u)			Number	Max. width (mm)
B1	550-0.7NWSCC	11.89	91.36	11.50	35.77	3.11	7.84	19	4.85
B2	550-1NWSCC	11.76	92.78	11.52	36.23	3.15	8.07	18	5.00
B3	550-0.7LC	7.42	86.92	11.22	31.58	2.81	6.45	21	3.10
B4	550-0.7LC-0.3PVA12	8.09	90.00	11.36	37.95	3.34	7.80	23	3.30
B5	550-0.7LC-0.3PVA8	8.68	90.51	11.38	39.35	3.46	7.96	24	3.40
B6	600-0.7LC-0.3PVA8	8.86	91.18	11.45	39.97	3.49	8.12	24	3.35
B7	600-0.7LC-0.5PVA8	9.47	93.81	11.50	41.77	3.63	8.53	27	3.60
B8	550-1LF	8.33	88.74	11.45	36.46	3.18	7.58	20	2.50
B9	550-1LF-0.3PVA12	9.00	91.43	11.50	42.08	3.66	8.82	22	2.80
B10	550-1LF-0.3PVA8	9.91	92.82	11.72	45.85	3.91	9.45	24	2.95
B11	600-1LF-0.3PVA8	10.09	93.40	11.60	45.70	3.93	9.60	24	2.90
B12	600-1LF-0.5PVA8	10.95	96.39	11.80	47.62	4.04	10.18	26	3.20
B13	550-1.5All-LWVC	5.16	82.35	11.09	27.64	2.49	5.22	22	3.15
B14	550-1.5All-LWVC-1PVA8	6.81	92.68	12.65	45.55	3.60	9.15	26	3.55

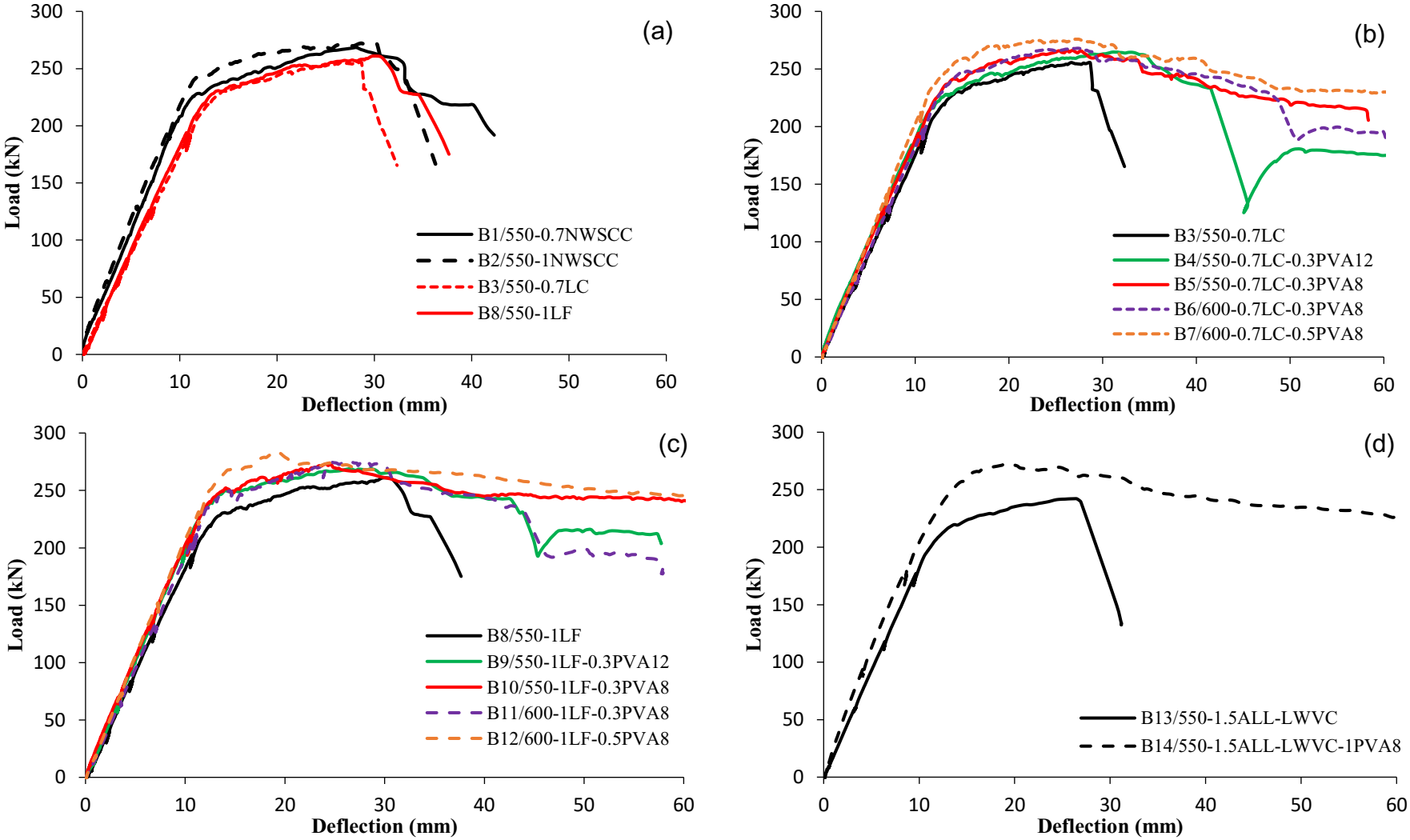

Figure 6-2: Experimental load-midspan deflection responses.

Using higher binder content up to 600 kg/m^3 showed a slight increase in the beams' stiffness and deflection, while the concrete density remained nearly at the same level. It should also be noted that increasing the binder content from 550 kg/m^3 to 600 kg/m^3 allowed for a higher percentage of PVA8 fibers (0.5%) to be used safely in SCC mixtures (see fresh properties results in Table 6-2). This higher volume fraction of fibers (0.5%) further improved the flexural stiffness and beam deformability, achieving an increase of 4.4% (on average) in the ultimate deflection compared to the corresponding beam with only 0.3% PVA fibers (B7 compared to B6, and B12 compared to B11).

Although using more coarse to fine expanded slate aggregates ratio (LC/LF ratio of 1.5) in B13 (vibrated concrete without fibers) allowed a LWVC mixture with minimum density to be developed, using this high content of lightweight aggregates decreased the stiffness and deformation capacity of the beam. For instance, the LWVC beam with minimum density (B13) experienced an ultimate deflection of 27.64 mm, which is about 12.5% lower than that exhibited by the minimum-density counterpart beam in SCC (B3). On the other hand, since vibrated concrete does not have workability restrictions, it was possible to use a higher volume fraction of PVA8 fibers (1%) in the mixture used in B13 to achieve a mixture with maximized fiber content and minimized density (B14). This led to better cracking control, further enhancement in beams' stiffness, and encouraged the beams to undergo greater deflections prior to failure, as shown in B14 compared to B13 (See Figure 6-2**d**).

6.5.2 Cracking behavior

All tested beams exhibited similar cracking pattern characteristics, indicating a typical flexural failure mode. Figure 6-3 shows, schematically, the crack patterns at failure for all tested beams. Figure 6-4 illustrates the failure pattern of tested beams. The number of cracks and the values of the maximum crack width at failure are summarized in Table 6-3. A higher cracking activity can be observed in LWSCC beams made with either coarse or fine expanded slate aggregates compared to counterpart NWSCC beams. The cracking pattern of LWSCC beams was dominated by a greater number of cracks, which is associated with reduced crack openings. For instance, replacing NC with LC (at the same C/F ratio of 0.7) increased the number of cracks from 19 to 21 cracks, while the opening of the main crack decreased by about 36%. One possible explanation is that the reduction in concrete tensile strength allowed more flexural cracks to propagate throughout the beam's length rather than continuing to widen one localized crack.

As mentioned before, adding PVA fibers contributed towards reaching more significant deflection prior to failure compared to that reached by the control beam without fibers. This increase in the beam's deformation capacity encouraged more flexural cracks to propagate before failure, accompanied by wider crack widths at failure. For example, using 0.3% PVA12 fibers with LWSCC-LC beams increased the primary flexural crack width from 3.10 mm to 3.30 mm and raised the number of cracks from 21 to 23 cracks (B4 versus B3). Higher cracking activity was observed with the LWSCC-LC beam reinforced with shorter fibers, in which adding 0.3% PVA8 fibers raised the number of cracks from 21 to 24 cracks (B5 compared to B3). As previously discussed, the better enhancement in the

deformation capacity resulting from using PVA8 compared to PVA12 can explain this latter performance. A similar performance was observed in fiber-reinforced LWSCC-LF beams (B9 and B10 compared to B8). It was also noted that increasing the fiber content continued to increase the number of cracks and crack widths at failure stage. For instance, using a higher dosage of PVA fibers (up to 0.5%) raised the number of cracks from 24 to 27 cracks and increased the maximum crack opening at failure from 3.35 mm to 3.60 mm, compared to the corresponding beam with only 0.3% PVA fibers (B7 compared to B6).

Based on the cracking patterns detected in different stages of loading, it was observed that all fiber-reinforced beams experienced increased crack widths at failure stage compared to the control beam with no fibers. This can be related to the higher load carrying capacity of fiber reinforced concrete beams accompanying with higher deflection at failure stage, which led the beams to experience increased crack widths compared to control beam with no fibers. The results also showed that the inclusion of PVA fibers contributed to further narrow the crack width under service load (taken 40% of the estimated failure load [Gholamreza et al., 2009]).

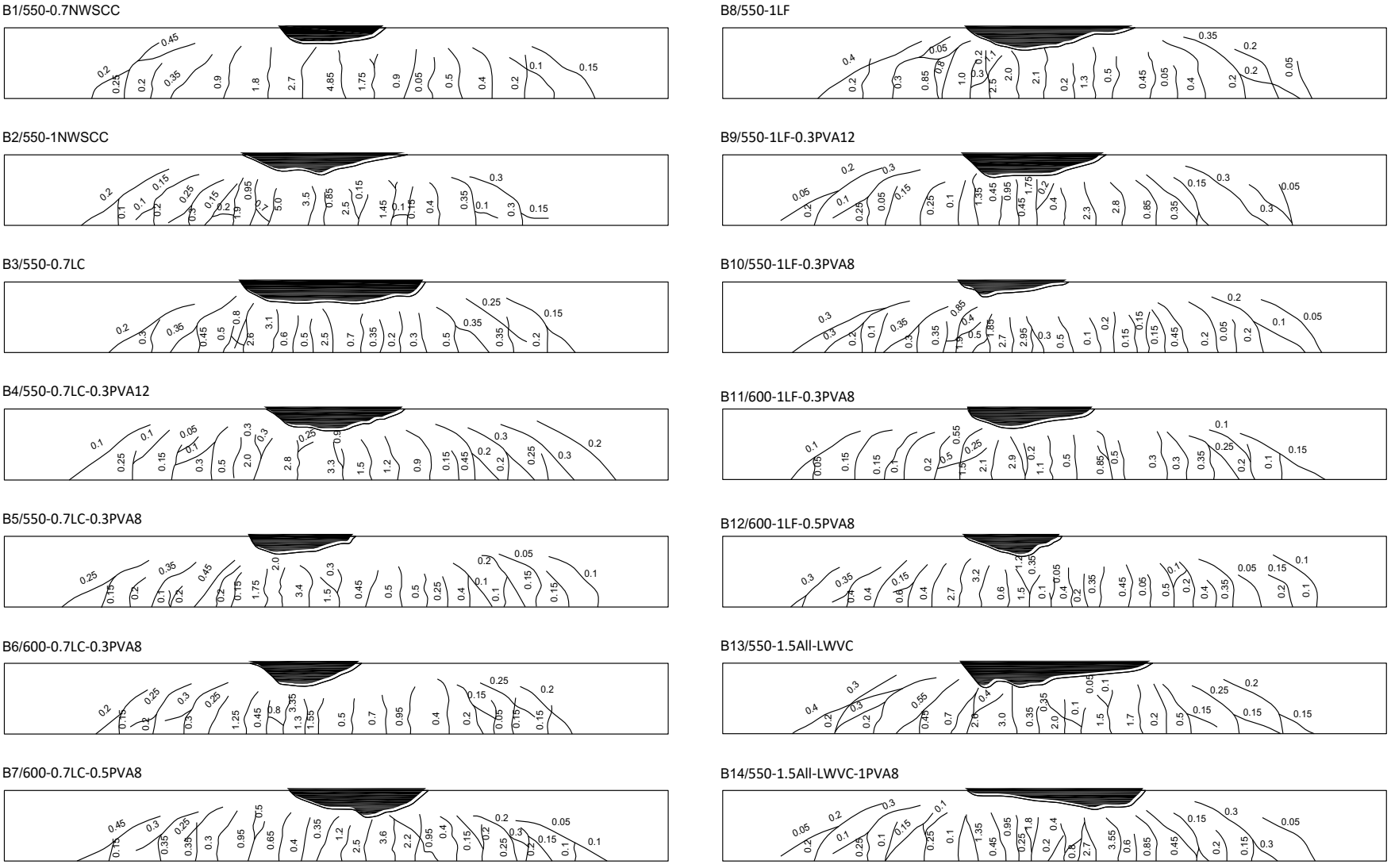

Figure 6-3: Crack patterns for all tested beams at failure stage (crack widths in mm).

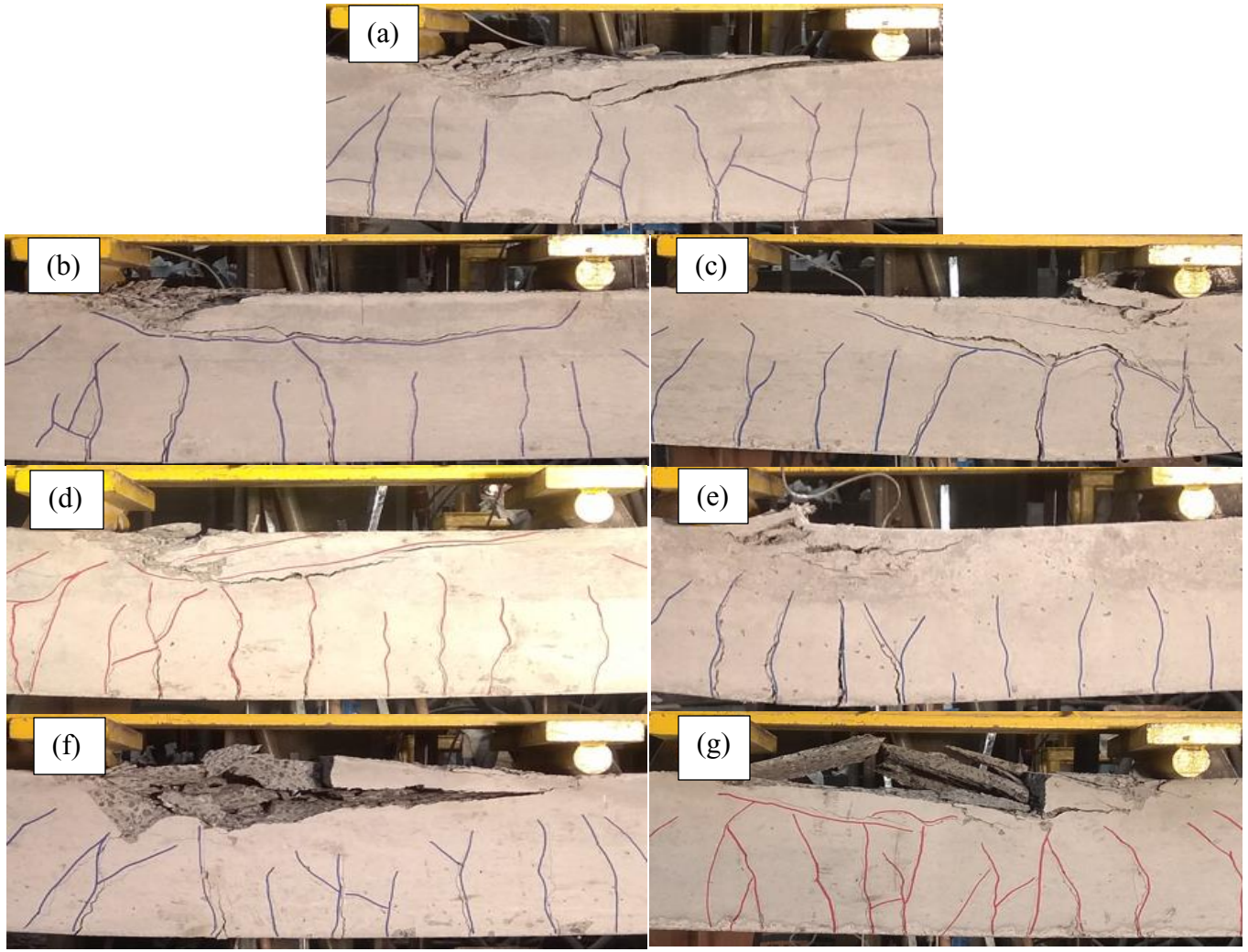

Figure 6-4: Failure pattern of tested beams: (a) 550-1NWSCC; (b) 550-0.7LC; (c) 600-0.7LC-0.5PVA8; (d) 550-1LF; € 600-1LF-0.5PVA8; (f) 550-1.5All-LWVC; (g) 550-1.5All-LWVC-1PVA.

6.5.3 Ductility and energy absorption capacity

In this study, the displacement ductility index (μ) was adopted to evaluate the deformation capability of the tested beams. For each tested beam, the deflection at the yield load (δ_y), the ultimate deflection (δ_u) (the deflection corresponding to 85% of the ultimate load at the post-peak portion of the load deflection curve) (Carmo et al., 2013; Anvari et al., 2021), and the ductility index ($\mu = \delta_u/\delta_y$) were calculated (see Table 6-3). This study also evaluated the energy absorption capacity of each tested beam by calculating the area underneath the load-deflection curve up to the failure point (the point at the post-peak portion corresponding to 85% of ultimate load). The obtained ductility indexes and energy absorption values are presented in Table 6-3.

Replacing the NF in beam B2 with LF (B8) did not show an apparent change in the ductility and absorbed energy. This can be attributed to the large deflection expressed by the LWSCC-LF beam (B8) before failure due to the low stiffness of the cement matrix. In contrast, replacing NC with LC in the LWSCC-LC beam (B3) lowered the ductility ratio and energy absorption capacity. This beam showed values for μ and energy absorption of 2.81 and 6.45 kN.m, respectively, which is about 9.6% and 17.7% lower than that offered by the corresponding NWSCC beam (B3 compared to B1). This reduction in displacement ductility and absorbed energy can be explained by the reduced ultimate deflection showed by the LWSCC-LC beam and the significant drop in the flexural strength after reaching the peak.

Table 6-3 also displays the effect of fiber length and volume on the ductility index and energy absorption of LWSCC/LWVC beams. As expected, the ductility index and absorbed energy of tested beams generally increased with the inclusion of fibers. Using 0.3% PVA12 somewhat increased the μ and energy absorption of the LWSCC beams, with an average increase of 16.9% and 18.6%, respectively, compared to non-fibered beams (B4 versus B3 and B9 versus B8). These results were owing to the stitching mechanism of fibers, which allows transferring higher tensile stresses across the crack faces. This in turn helped the beam to sustain more flexure load accompanied with a higher rate of deformations, and hence improved ductility and higher energy absorption. As previously mentioned, shorter fibers contributed to increasing the chance of having more individual fibers dispersed throughout the concrete matrix (at the same volume fraction of fibers). This helped the beams to sustain higher loads and undergo larger deflection, which further improve the energy absorption and displacement ductility. For example, replacing PVA12 fibers (in B4 and B9) with PVA8 fibers (in B5 and B10) at the same fiber content increased the values of μ and energy absorption capacity of tested specimens by about 5% and 4.6%, respectively.

Increasing the volume fraction of fiber to 0.5% further increased the displacement ductility and absorbed energy of LWSCC beams (reached up to 28.1% and 33.2%, respectively, higher than their reference beams without fibers) (B7 versus B3 and B12 versus B8). In addition, using 0.5% fiber volume seemed to completely compensate for the reduction in ductility resulting from replacing strong normal-weight aggregates with low stiffness expanded slate aggregates. Furthermore, the possibility of adding 1% PVA8 fibers in

LWVC beams showed the greatest improvement in displacement ductility and energy absorbed until failure, reaching up to 44.5% and 75%, respectively, higher than that of the comparable beam without fibers (B14 compared to B13).

6.5.4 Initial Stiffness and Cracking Analysis

Table 6-4 shows the experimental uncracked beam stiffness $(EI_g)_{exp}$ and theoretical uncracked beam stiffness $(EI_g)_{theo}$ calculated based on ACI 318 (2014) code equation. From Table 6-4, it can be seen that the code equation showed a good prediction of $(EI_g)_{theo}$ compared to the experimental value of uncracked stiffness $(EI_g)_{exp}$ for NWSCC beams. For example, NWSCC (B1) exhibited a theoretical to experimental uncracked stiffness ratio $((EI_g)_{theo}/(EI_g)_{exp})$ of 1.09, showing inconsiderable difference between the theoretical and experimental uncracked stiffness. On the othe hand, by looking at LWC beams, it can be seen that the code equation generally overestimates the uncracked stiffness of LWC beams. For example, LWSCC-LC and LWSCC-LF beams (B3 and B8) showed $((EI_g)_{theo}/(EI_g)_{exp})$ ratio of 1.2 and 1.1, respectively, while this ratio reached up to 1.25 in LWVC beam (B13). This can be related to the fact that the calculations of uncracked stiffness according to ACI code depend on the concrete modulus of elasticity predicted by the code empirical equation. This equation is function of the compressive strength and concrete density ($E = W_c^{1.5}\ 0.043\ \sqrt{f_c'}$). And since the concrete density does not account for the type/modulus of elasticity of the lightweight aggregate used (different lightweight aggregates have different strengths/modulus of elasticities), the ACI equation showed higher overestimation of uncracked stiffness for this type of lightweight aggregate (Stalite). The results also indicated that beams with LC exhibited higher overestimation of code equation for

uncracked stiffness compared to beam with LF. This could be related to the fact that LC expanded slate aggregate is expected to be weaker than LF as LC may have more voids due to its higher volume. The reduced strength of LC compared to LF maybe the main reason behind the lower uncracked experimental stiffness values of LC compared to LF. Table 6-4 also showed that ACI code generally underestimate the uncracked stiffness of LWC beams reinforced with fibers. This can be confirmed by the values of ((EIg)theo/(EIg)exp) ratio, in which the ((EIg)theo/(EIg)exp) ratios for beams B4-B7 and B9-B12 are less than 1. In addition, the ((EIg)theo/(EIg)exp) ratio of LWC beams reinforced with fibers decreases as the fiber percentage increases, indicating a higher under estimation of uncracked stiffness as the fiber volume increased. This can be attributed to the effect of fibers on enhancing the experimental concrete stiffness, while this effect is not considered in the code prediction of concrete stiffness.

Table 6-4 also shows the number of cracks and maximum crack width for all tested beams at service load. The theoretical maximum crack width at service load was calculated using Gergely-Lutz (1968) equation, eq. (1), (adopted in early provisions of ACI 318 code) and Frosch model (1999), eq. (2), (adopted in the new crack control calculation in ACI 318). These equations were used to study the prediction accuracy of such equations to calculate the maximum crack width at service load for LWC beams.

$$\omega = 11x\ 10^{-6}\ \beta\ f_s\ \sqrt[3]{d_c A} = 11x10^{-6}\beta z \qquad (1)$$

Where z = $f_s\ \sqrt[3]{d_c A}$; ω is the maximum crack width in mm; f_s is the longitudinal reinforcement stress in MPa; β is the distance from the neutral axis to the bottom fibers

divided by the distance from neutral axis to the centre of tensile reinforcement; d_c is the distance from the centre of the tension reinforcement bar to the extreme tension fiber in mm; A is the concrete effective area surrounding the tension reinforcement with same centroid as tension reinforcement, divided by the number of reinforcement bars in mm^2

$$\omega = 2\frac{f_s}{E_s}\,\beta\,\sqrt{d_c^2 + \left(\frac{s}{2}\right)^2} \qquad (2)$$

Where ω is the maximum crack width in mm; f_s is the steel reinforcement stress in MPa; E_s is the steel modulus of elasticity in MPa; β is a factor depend on d_c and can be calculated from an empirical equation = $1+0.0031d_c$ (Frosch, 1999); d_c is the distance from the centre of the tension reinforcement bar to the extreme tension fiber in mm; s is the spacing of tension reinforcement from center-to-center.

The results of the theoretical maximum cracking width calculated by Eqs. (1) and (2) for all tested beams are presented in Table 6-4. From the table, it can be seen that the Gergely-Lutz (1968) equation generally gave higher values of maximum crack width compared to the experimental values. For example, in NWSCC beams, the predicted crack width by Gergely-Lutz equation showed a higher value reached up to 1.2 times compared to the experimental crack width. It should be noted that in this investigation relatively shallow beams were tested (250 mm depth). Since the factor β in Gergely-Lutz equation has an inverse relationship with the beam depth (according to the definition of β factor), the calculated crack widths of the tested beams were relatively high compared to the experimental ones. The results also showed that the predicted values of maximum crack width compared to experimental crack width were higher in LWC beams (B3, B8, and

B13) compared to NWSCC beams. This can be related to the lower tensile strength of LWC beams which encouraged the beam to initiate higher number of cracks with smaller crack widths. This in turn contributed to increase the difference between the theoretical and experimental crack widths in LWC beams. In the meantime, futher increase in the difference between the theoretical and experimental crack width was observed in LWC beams reinforced with fibers (B4-B7, B9-B12, B14) compared to beams without fibers. Moreover, as the percentage of fibers increases the difference between the predicted and experimental crack width increases. This can be attributed to the effect of fiber is reducing the crack width by stitching mechanism, which in turn resulted in narrower experimental crack width. Similar behaviour was observed in Forsch's model equation but with more close prediction to the experimental values, especially for NWSCC beams. Therefore, the later version of ACI 318 (2014) code is adopting the Forsch's model (1999).

It should be noted that for the benefits of the long-term durability requirements, the design codes set restrictions on the maximum crack width under service load. Table 6-3 indicates that, at service load level, the measured maximum crack width for all tested specimens is well within the acceptable limiting crack width for exterior exposure conditions proposed by ACI 318-14 (0.33 mm), CSA A23.3-14 (0.33 mm), and BS 8110 (0.30 mm).

Table 6-4: Initial Stiffness and Cracking Analysis for tested beams.

Beam #	Beam/Mixture	Experimental initial stiffness ($KN.m^2$)	Theoretical initial stiffness ($KN.m^2$)	Theoretical to experimental initial stiffness	Number of cracks at service load	Max. crack width at service load (mm)	Deflection at service load (mm)	Calculated maximum crack width at service load (Gergely-Lutz equation) (mm)	Calculated maximum crack width at service load (Frosch equation) (mm)
B1	550-0.7NWSCC	10026.1	10974.2	1.09	12	0.25	5.27	0.30	0.24
B2	550-1NWSCC	10317.7	10922.8	1.06	10	0.26	4.55	0.29	0.23
B3	550-0.7LC	7147.3	8607.2	1.2	15	0.22	5.77	0.40	0.31
B4	550-0.7LC-0.3PVA12	8475.8	8162.3	0.96	17	0.2	5.8	0.45	0.35
B5	550-0.7LC-0.3PVA8	9186.0	8404.1	0.91	18	0.2	5.85	0.48	0.37
B6	600-0.7LC-0.3PVA8	9331.4	8326.8	0.89	19	0.19	5.92	0.49	0.39
B7	600-0.7LC-0.5PVA8	9224.4	7813.7	0.85	22	0.18	6.04	0.55	0.44
B8	550-1LF	8273.6	9141.9	1.1	15	0.26	5.95	0.49	0.42
B9	550-1LF-0.3PVA12	9492.9	8687.8	0.92	18	0.2	6.01	0.52	0.44
B10	550-1LF-0.3PVA8	10050.3	8826.3	0.88	19	0.19	6.1	0.58	0.46
B11	600-1LF-0.3PVA8	10355.3	8832.7	0.85	21	0.19	6.15	0.59	0.47
B12	600-1LF-0.5PVA8	10230.2	8230.0	0.8	23	0.17	6.32	0.64	0.50
B13	550-1.5All-LWVC	5896.9	7364.5	1.25	14	0.22	5.22	0.40	0.31
B14	550-1.5All-LWVC-1PVA8	7872.6	6574.3	0.84	19	0.18	5.7	0.46	0.35

6.5.5 Cracking moment analysis

6.5.5.1 Experimental cracking moment capacity

At an early stage of loading, the first crack(s) was observed between the loading points (maximum moment region). Table 6-3 presents the cracking moment values ($M_{cr}^{exp.}$) corresponding to the first flexural crack for all tested beams. A predictable reduction in the $M_{cr}^{exp.}$ of tested beams was observed due to the use of expanded slate aggregates as a replacement for conventional normal-weight aggregates. As seen in beams B3 and B8 as opposed to B1 and B2, respectively, LWSCC beams developed with either LC or LF showed an average of 25.2% lower first crack moment capacities than the normal-weight control beams. This reduction can be attributed to the substantial decline in the tensile strength of LWSCC mixtures as a result of using low stiffness expanded slate lightweight aggregates (refer to Table 6-3). Table 6-3 also shows that using 0.3% fraction volume of polymeric fibers effectively increased the $M_{cr}^{exp.}$ of LWSCC beams. The performance of shorter fibers was more evident at boosting the beams' cracking moment capacity when compared to longer fibers. Using 0.3% PVA8 increased the $M_{cr}^{exp.}$ by about 18%, while using PVA12 increased the $M_{cr}^{exp.}$ by only 8.5%, as indicated in B4-B5 versus B3 and B9-B10 versus B8. Using 0.5% PVA8 fibers showed further improvement in the $M_{cr}^{exp.}$ of tested beams. Since the $M_{cr}^{exp.}$ is directly affected by tensile strength, these improvements in the $M_{cr}^{exp.}$ can be attributed to the enhancement in the tensile strength of the concrete mixtures due to the addition of fibers (see results of *STS* shown in Table 6-2).

Although using a higher LC to LF aggregate ratio in the development of LWVC allowed to achieve a concrete dry density of 1630 kg/m^3 (B13), LWVC beam made with this mixture experienced lower cracking moment than counterpart beams in SCC with minimum possible density (B3 and B8). However, adding 1% fibers to the mixture with both LC and LF aggregates exhibited maximum increase in the $M_{cr}^{exp.}$, reaching up to 32%, higher than that of beam B13 (B14 with 1% fibers compare to its counterpart B13 beam with no fibers). It should also be highlighted that LWSCC beams containing LF (either with or without fibers) showed slightly higher $M_{cr}^{exp.}$ than their counterpart beams with LC. This can be related to the greater tensile strength exhibited by LWSCC-LF mixtures compared to LWSCC-LC mixtures (see Table 6-2).

6.5.5.2 Theoretical predictions of cracking moment

The theoretical cracking moment ($M_{cr}^{theo.}$) for all tested beams was calculated based on the code provisions recommended by the ACI 318 (2014), CSA A23.3 (2014), and Eurocode 2 (EC2, 2004).

According to ACI 318 (2014):

$$M_{cr}^{theo.} = f_r \frac{I_g}{y_t} \quad (1)$$

where f_r (MPa) $= 0.62\lambda\sqrt{f_c'}$, in which λ is a reduction factor that accounts for LWC (λ = 1.0 for NWC, for sand-lightweight concrete is taken as 0.85, and for all-lightweight concrete is taken as 0.75); f_c' = the specified concrete compressive strength in MPa; I_g = the gross second moment of area; and y_t = the distance from the centroid to the outermost tension fiber.

As per CSA A23.3 (2014):

CSA code adopts the same equation (Equation 1) provided by ACI code but used f_r (MPa) $= 0.6\lambda\sqrt{f_c'}$, in which λ = 1 for NWC, 0.85 for structural semi-lightweight concrete, and 0.75 for structural lightweight concrete.

As per EC2 (2004):

$$M_{cr}^{theo.} = f_{ctm}\frac{I_e}{(h-x_u)} \quad (2)$$

where f_{ctm}(MPa) = the average tensile strength of concrete ($f_{ctm} = 0.3\eta f_{ck}^{0.67}$), in which, $\eta = 0.4 + 0.6\rho_c/2200$ is a modification factor accounting for the dry density (ρ_c) of LWC and f_{ck} = the characteristic compressive strength of concrete; I_e = the moment of inertia of the uncracked transformed section; h is the cross-sectional height; and x_u = the distance between the neutral axis and the outermost concrete compression fiber.

Figure 6-5**a** shows the experimental-to-theoretical cracking moment ratio ($M_{cr}^{exp.}/M_{cr}^{theo.}$) for all tested beams. From that figure, it can be observed that the equations proposed by all investigated design codes generally appeared to overestimate the beams' cracking moment, even the normal-weight SCC beams (B1 and B2). The overestimation of the cracking moment seemed to be more evident in LWSCC beams containing LC as opposed to beams containing LF. For example, the LWSCC beam with minimum possible density containing LC (B3) showed a $M_{cr}^{exp.}/M_{cr}^{theo.}$ ratio ranging from 0.64 to 0.75, while in the counterpart beam with LF (B8) the $M_{cr}^{exp.}/M_{cr}^{theo.}$ ratio ranged from 0.70 to 0.84. These results can be attributed to the lower tensile strength of the LWSCC mixtures made with LC (refer to Table 6-2). From Figure 6-5**a**, it can be observed that the polymeric fiber additives obviously increased the $M_{cr}^{exp.}/M_{cr}^{theo.}$ ratio, indicating better estimation for the cracking

moment. The $M_{cr}^{exp.}/M_{cr}^{theo.}$ ratio seemed to be higher in beams with PVA8 in comparison with counterpart beams with PVA12. For instance (B9 compared to B10), in the LWSCC beam with 0.3% PVA12, $M_{cr}^{exp.}/M_{cr}^{theo.}$ ranged from 0.75 to 0.90, while in the counterpart beam with PVA8 this range was 0.81 to 0.98. These results can be related to the better enhancement in $M_{cr}^{exp.}$ with the inclusion of shorter fibers (PVA8) compared to longer fibers (PVA12). Meanwhile, the $M_{cr}^{theo.}$ was almost the same for beams with either shorter or longer fibers as it was calculated based on the value of f_c', which is insignificantly affected by fiber length. Figure 6-5**a** also shows that increasing the fiber amount in LWSCC/LWVC specimens further increased the $M_{cr}^{exp.}/M_{cr}^{theo.}$ ratio.

Because the cracking moment capacity ($M_{cr}^{exp.}$) is more influenced by the concrete tensile strength than its compressive strength, the accuracy of the codes' expressions can be generally improved by replacing the concrete tensile strength derived proportionally from the compressive strength with that obtained from the experiments (*STS*). Figure 6-5**b** indicates that using the values of *STS* (included in Table 6-2) to calculate the cracking moment ($M_{cr}^{theo.}$) gave better predictions, specifically with the equations provided by CSA and ACI codes. The CSA and ACI showed conservative predictions for the cracking moment of tested beams, providing $M_{cr}^{exp.}/M_{cr}^{theo.}$ ratios ranging from 1.04 to 1.25. In contrast, EC2's performance was slightly improved but still overestimated the beams' cracking moment capacity, showing $M_{cr}^{exp.}/M_{cr}^{theo.}$ ratio in the range of 0.58 to 0.70. This can be related to the fact that, unlike the American and Canadian codes, EC2 considered the contribution of longitudinal steel rebars in the calculation of the inertia moment of the

uncracked concrete section, which in turn yielded higher predictions for the $M_{cr}^{theo.}$ of tested beams.

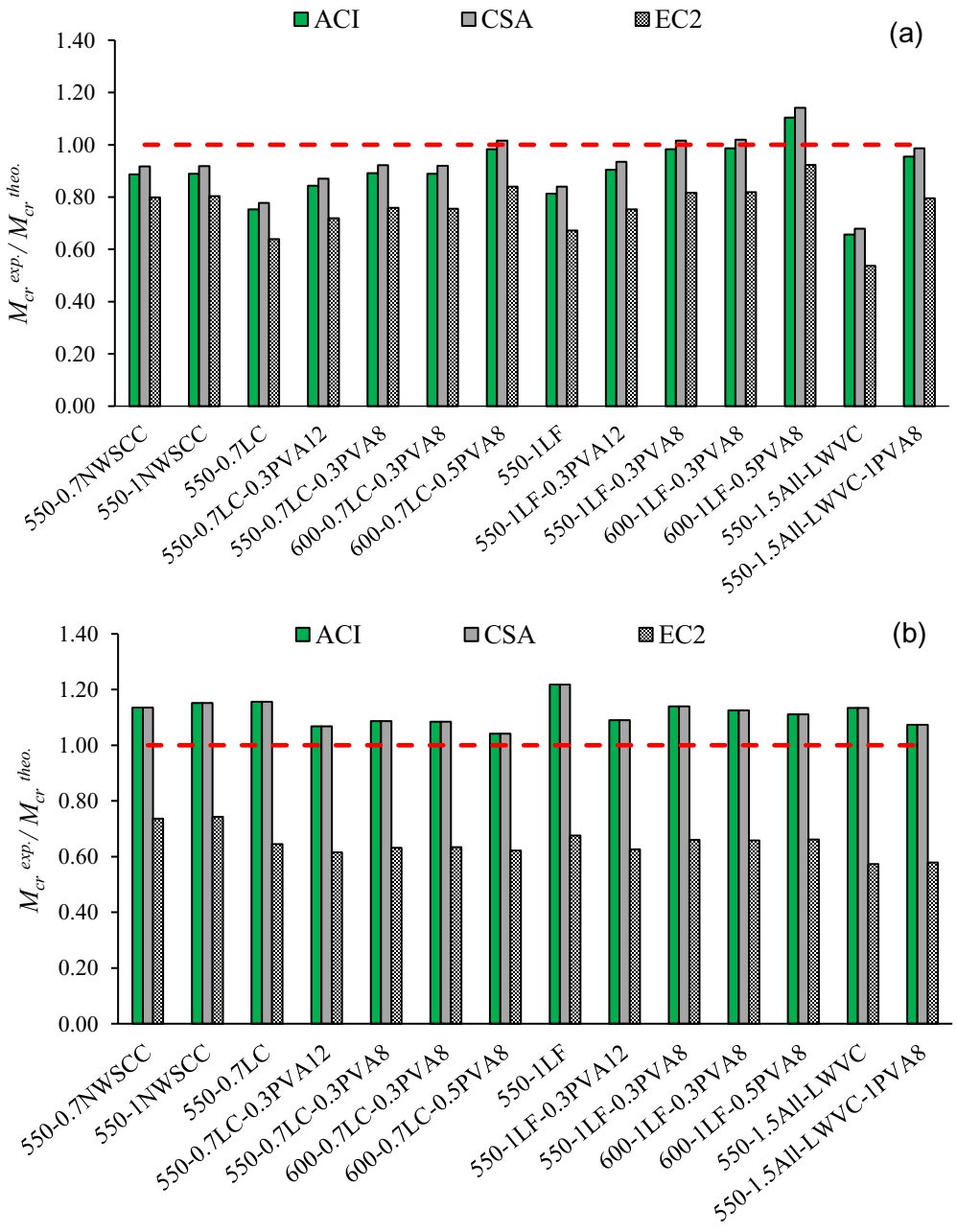

Figure 6-5: Experimental-to-predicted cracking moment ratios on the basis of: (a) tensile strength proportionally calculated from the compressive strength relationship; (b) tensile strength obtained from the experiments.

6.5.6 Ultimate moment capacity

6.5.6.1 Experimental bending moment capacity

The flexural moment capacity ($M_u^{exp.}$) results of all tested beams are given in Table 6-3. By looking at this table, it is found that the $M_u^{exp.}$ values of the control NWSCC beams were 91.36 and 92.78 kN.m, respectively. The attempt to achieve minimum possible SCC density (by substituting normal-weight particles with either fine or coarse expanded slate aggregates) slightly reduced the ultimate failure moment of these developed beams, reaching 4.8% lower than that of corresponding NWSCC beams (B3 and B8 versus B1 and B2, respectively). This reduction was expected given the drop in compressive strength as a result of the reduction in concrete density, which in turn reduced the lever arm between tension and compression forces (due to an increase in the neutral axis depth).

Adding randomly distributed polymeric fibers into LWSCC/LWVC beams generally improved the bending moment capacity. For instance, using 0.3% PVA12 with LWSCC beams inconsiderably boosted the $M_u^{exp.}$ by 3%; while adding shorter fibers (PVA8), at the same fiber volume, showed a slight improvement in the $M_u^{exp.}$ reached up to 4.6%, as indicated in B9 and B10 compared to the control beam without fibers (B8). The better improvement seen with PVA8 compared to PVA12 can be related to the same reasons discussed in the previous sections. Increasing the level of binder content (up to 600 kg/m^3) insignificantly affected the $M_u^{exp.}$ of tested beams. However, using higher binder content allowed for higher fraction volume (0.5% instead of 0.3%) of PVA8 fibers to be used safely in SCC mixtures, resulting in further improvements in the $M_u^{exp.}$ of LWSCC beams. Using

high LC/LF aggregate ratio in the production of LWVC mixtures (reaching lower concrete density than that obtained in SCC) further decreased the ultimate flexural strength. However, combining high amount of PVA8 (1%) with higher volumes of expanded slate aggregates seemed to compensate for the reduction in the ultimate flexural strength, achieving $M_u^{exp.}$ comparable to the NWSCC beams. For example, employing 1% PVA8 in the production of LWVC beam increased the $M_u^{exp.}$ by 12.6% in comparison with the LWVC beam without fibers (B14 versus B13). This increase in the beam bending moment capacity reached around 99% of the $M_u^{exp.}$ of the control NWSCC beams (B14 compared to B1 and B2).

6.5.6.2 Prediction of flexural moment capacity

In this section, the experimental flexural capacities ($M_u^{exp.}$) of LWSCC/LWVC beam with/without polymeric fibers were compared with the obtained theoretical design moments ($M_u^{theo.}$) calculated based on the rectangular stress block analysis, as recommended by the ACI 318 (2014), CSA A23.3 (2014), and Eurocode 2 (EC2, 2004). The rectangular stress block recommended by all design codes is specified with a width of "$\alpha f_c'$" and a height of "βc", where α and β are the stress block coefficients. Eqs. (3) to (8) present the values of stress block coefficients specified by each design code. The ACI 318 (2014) assumes that a concrete strain value of 0.003 at the extreme compression fiber of the member is required to reach the nominal flexural capacity of this member, while the CSA code (2014) and EC2 (2004) specify a higher value of 0.0035 for ultimate concrete strain.

Table 6-5: Comparison of experimental and predicted bending moment capacities.

Beam #	Beam/Mixture	Ultimate moment capacity, $M_u^{exp.}$ (kN.m)	Predicted ultimate moment $M_u^{theo.}$ (kN.m)				Experimental-to-predicted ultimate moment			
			ACI	CSA	EC2	Henager & Doherty	ACI	CSA	EC2	Henager & Doherty
B1	550-0.7NWSCC	91.36	73.65	72.95	74.31	-	1.24	1.25	1.23	-
B2	550-1NWSCC	92.78	73.46	72.75	74.19	-	1.26	1.27	1.25	-
B3	550-0.7LC	86.92	71.56	70.96	72.88	-	1.21	1.22	1.19	-
B4	550-0.7LC-0.3PVA12	90.00	-	-	-	75.78	-	-	-	1.19
B5	550-0.7LC-0.3PVA8	90.51	-	-	-	79.52	-	-	-	1.14
B6	600-0.7LC-0.3PVA8	91.18	-	-	-	79.94	-	-	-	1.14
B7	600-0.7LC-0.5PVA8	93.81	-	-	-	84.50	-	-	-	1.11
B8	550-1LF	88.74	72.11	71.52	73.30	-	1.23	1.24	1.21	
B9	550-1LF-0.3PVA12	91.43	-	-	-	76.37	-	-	-	1.20
B10	550-1LF-0.3PVA8	92.82	-	-	-	80.17	-	-	-	1.16
B11	600-1LF-0.3PVA8	93.40	-	-	-	80.43	-	-	-	1.16
B12	600-1LF-0.5PVA8	96.39	-	-	-	85.13	-	-	-	1.13
B13	550-1.5All-LWVC	82.35	70.02	69.45	71.38	-	1.18	1.19	1.15	-
B14	550-1.5All-LWVC-1PVA8	92.68	-	-	-	90.35	-	-	-	1.03

ACI 318 (2014):

$$\alpha = 0.85 \tag{3}$$

$$\beta = 0.85 - 0.05(f_c' - 28)/7 \text{ since } 0.65 \leq \beta \leq 0.85 \tag{4}$$

CSA A23.3 (2014):

$$\alpha = 0.85 - 0.0015 f_c' \geq 0.67 \tag{5}$$

$$\beta = 0.97 - 0.0025 f_c' \geq 0.67 \tag{6}$$

EC2 (2004):

$$\alpha = 1.0 - (f_c' - 50)/200 \ \leq 1.0 \tag{7}$$

$$\beta = 0.8 - (f_c' - 50)/400 \ \leq 0.8 \tag{8}$$

Since the code equations neglect the contribution of fibers in transferring tension stresses along the cracked section, the above formulas were only used to predict the ultimate moment capacity of the non-fibered concrete beam specimens. For all the other tested beams with fibers, based on Henager and Doherty's model (1976), ACI 544.4R (1988) suggested the following equations to predict the nominal flexural moment of fiber-reinforced concrete beams with reinforcing steel bars.

$$M_n = A_s f_y \left(d - \frac{a}{2}\right) + A_s' f_s \left(\frac{a}{2} - d'\right) + \sigma_t \, b \, (h - e) \left(\frac{h}{2} + \frac{e}{2} - \frac{a}{2}\right) \tag{9}$$

$$e = (\varepsilon_{fibers} + 0.003)c/0.003 \tag{10}$$

$$\sigma_t = 0.00772 \left(\frac{l_f}{d_f}\right) V_f F_{be} \text{ (MPa)} \tag{11}$$

where A_s denotes the tensile reinforcement area; A_s' = compression reinforcement area; f_y = yield strength of reinforcement; f_s = stress of compression reinforcement; d = effective

depth; b = beam width; h = beam height; a = depth of rectangular stress block; c = depth of neutral axis; e = distance from top of tensile stress block of fiber-reinforced concrete to the extreme compression fiber of concert section; ε_{fibers} = strain in fibers; σ_t = tensile stress in fibrous concrete; d_f = fiber diameter; V_f = volume fraction of fibers; and F_{be} = bond efficiency of the fiber.

On the other hand, the coefficient 0.00772 specified in equation (11) was calculated based on the typical bond strength of steel fibers with normal-strength concrete (Hasgul et al., 2018). Since this study adopted the use of PVA fibers (which have different bond characteristics compared to steel fibers) in the development of concrete mixtures, equation (12), proposed by Ahmed and Pama (1992), was used in order to better represent the bond characteristics between PVA fiber and concrete.

$$\sigma_t = 2\eta_o\eta_b\eta_l V_f \tau_f \left(\frac{l_f}{d_f}\right) \text{ (MPa)} \quad (12)$$

where η_o is the fiber orientation factor (η_o= 0.41 for randomly oriented fibers [Oh, 1992]); η_b is the bond efficiency factor (1.0 for smooth fibers [Dwarakanath & Nagaraj, 1992]); η_l is the length efficiency factor (taken as 0.97 based on the numerical calculations proposed by Oh, [1992]); and τ_f is the fiber-matrix interfacial bond strength (for PVA fiber, τ_f = 2.93 MPa [Hossain et al., 2020]).

The $M_u^{exp.}/M_u^{theo.}$ ratio for each tested beam was calculated and tabulated in Table 6-5. It can be noted from the table that the design codes considered herein (ACI, CSA, and EC2) were conservative in estimating the ultimate moment capacity of non-fibered SCC/VC beams, showing $M_u^{exp.}/M_u^{theo.}$ ratio in the range of 1.15 to 1.27. The reduction in concrete

density exhibited a general decrease in the $M_u^{exp.}/M_u^{theo.}$ ratio, which indicates a lower margin of safety. This could be attributed to the calculation of the equivalent stress block coefficients for LWC members, which only considered the concrete compressive strength as a factor. However, the unit weight of concrete also deserves consideration as a primary factor together with the concrete compressive strength (Yang et al., 2020). By looking at fiber-reinforced concrete beams (B4-B7, B9-B12, and B14), it can be observed that applying equation (12) with Henager and Doherty's model showed good predictions, in which the $M_u^{exp.}/M_u^{theo.}$ ratio ranged from 1.03 to 1.19. Similar to non-fibered beams, reducing the concrete density appeared to reduce the safety margin of the proposed model, as shown in B14 (with a dry density of 1628 kg/m^3) compared to B4 (with a concrete density of 1907 kg/m^3).

6.6 Conclusions

This chapter evaluated the flexural performance of large-scale lightweight self-consolidating concrete reinforced with PVA fibers. A total of 14 reinforced concrete beams with different aggregate types, fiber lengths, and fiber volumes were constructed and tested. The performance of tested beams was evaluated in terms of load-deflection response, cracking behavior, energy absorption, ductility, cracking moment, and ultimate moment capacity. The performance of code provisions in predicting the cracking moment and ultimate moment capacity was also assessed. From the experimental results presented in this chapter, the following conclusions were drawn.

1. Using expanded slate coarse or fine aggregates in the production of LWSCC mixtures achieved a minimum mixtures' density of approximately 15% lighter than with conventional normal-weight concrete. However, beams made with the minimum-density SCC showed a drop in cracking moment, ultimate moment capacity, and energy absorption by about 25.2%, 4.8%, and 17.7%, respectively, compared to normal-weight concrete beams.
2. It was possible to use up to a maximum of 0.3% PVA fibers in the production of successful LWSCC with a binder content level of 550 kg/m^3. The addition of these fibers generally enhanced the flexural performance and cracking activity of tested LWSCC beams. For instance, using 0.3% of PVA8 (8 mm) fibers improved the deformability, ductility, absorbed energy, cracking moment capacity, and ultimate flexural strength of tested beams by about 24.6%, 23.1%, 24%, 18%, and 4.6%.
3. Developing LWSCC with higher binder content (600 kg/m^3 compared to 550 kg/m^3) allowed higher percentage of PVA fibers (0.5% compared to 0.3% in 550 kg/m^3 binder) to be used successfully in the mixture. Using higher percentage of PVA fibers (0.5%) completely compensated for the reduction in flexural strength of LWSCC beams resulting from using lightweight aggregates, and the beams achieved much higher ductility and absorbed energy compared to non-fibered beams.
4. The inclusion of shorter fibers (PVA8) more obviously improved the performance of LWSCC beams in terms of deformability, cracking moment capacity, ultimate

flexural strength, ductility, energy absorption, and cracking behavior when compared to the use of longer PVA fibers (PVA12).

5. LWSCC beams made with fine aggregates expanded slate (mixed with normal-weight coarse aggregate) experienced higher deformations at failure than their counterpart beams made with coarse aggregates expanded slate (mixed with normal-weight sand), indicating more ductile failure. In addition, beams with fine expanded slate aggregates showed relatively better structural performance in terms of deformability, ductility index, absorbed energy, and cracking moment capacity compared to beams with expanded slate coarse aggregates.
6. Adding polymeric fibers to LWSCC beams generally improved the cracking activity and helped the beams to undergo a high rate of deformation at the failure stage. Shorter fibers were more efficient at enhancing the cracking activity of tested beams compared to longer fibers, exhibiting a maximized number of cracks and wider cracks at failure.
7. Because of the absence of SCC workability restrictions, it was feasible to produce LWVC with a maximized volume of LWA, using up to 1.5 C/F ratio of both coarse and fine expanded slate aggregates. However, the beam made with this maximized volume of lightweight aggregates showed a substantial decrease in the bending moment capacity. Using 1% PVA8 (maximized dosage of PVA fibers) in this beam compensated for this decrease, achieving around 99% ultimate moment capacity compared to the control NWSCC beams. This combination of maximized volumes

of LWA and PVA fibers contributed towards reaching concrete dry density of 1628 kg/m^3.

8. The equivalent stress block recommended by the three investigated design codes (ACI 318-14, CSA A23.3, and EC2) conservatively estimated the ultimate moment capacity for all tested beams without fibers, presenting experimental-to-theoretical ratios ($M_u^{exp.}/M_u^{theo.}$) in the range of 1.15 to 1.27. In contrast, the model developed by Henager and Doherty well predicted the ultimate moment capacity of LWSCC/LWVC beams with PVA fibers.

6.7 References

AbdelAleem, B. H., & Hassan, A. A. (2019). Influence of synthetic fibers' type, length, and volume on enhancing the structural performance of rubberized concrete. *Construction and Building Materials*, *229*, 116861.

AbdelAleem, B. H., Ismail, M. K., & Hassan, A. A. (2017). Properties of self-consolidating rubberised concrete reinforced with synthetic fibres. *Magazine of Concrete Research*, *69*(10), 526-540.

Abouhussien, A. A., Hassan, A. A., & Ismail, M. K. (2015). Properties of semi-lightweight self-consolidating concrete containing lightweight slag aggregate. *Construction and Building Materials*, *75*, 63-73.

ACI (American Concrete Institute). (2014). ACI 318R-14: Building code requirements for structural concrete and commentary. *American Concrete Institute*, Farmington Hills, MI, USA.

ACI Committee 544. (1988). Design considerations for steel fiber reinforced concrete (ACI 544.4R-88). *American Concrete Institute*, Farmington Hills, MI.

Ahmed, H. I., & Pama, R. P. (1992, July). Ultimate flexural strength of reinforced concrete beams with large volumes of short randomly oriented steel fibres. In *Rilem Proceedings* (pp. 467-467). Chapman & Hall.

Alqahtani, F. K., Ghataora, G., Khan, M. I., & Dirar, S. (2017). Novel lightweight concrete containing manufactured plastic aggregate. *Construction and Building Materials*, *148*, 386-397.

Anvari, A., Ghalehnovi, M., De Brito, J., & Karimipour, A. (2021). Improved bending behaviour of steel-fibre-reinforced recycled aggregate concrete beams with a concrete jacket. *Magazine of Concrete Research*, *73*(12), 608-626.

Assaad, J. J., & Issa, C. A. (2018). Stability and Bond Properties of Latex-Modified Semi-Lightweight Flowable Concrete. *ACI Materials Journal*, *115*(4).

Bastami, R. (2019). *Structural Performance of High-Strength Reinforced Concrete Beams Built with Synthetic Fibers* (Doctoral dissertation, Université d'Ottawa/University of Ottawa).

Canadian Standards Association (CSA). (2014). Design of Concrete Structures for Buildings (CSA-A23.3 M-14). *Canadian Standards Association*, Rexdale, ON.

Cardoso, D. C., Pereira, G. B., Silva, F. A., Silva Filho, J. J., & Pereira, E. V. (2019). Influence of steel fibers on the flexural behavior of RC beams with low reinforcing ratios: Analytical and experimental investigation. *Composite Structures*, *222*, 110926.

Carmo, R. N. D., Costa, H., Gomes, G., & Valença, J. (2017). Experimental evaluation of lightweight aggregate concrete beam–column joints with different strengths and reinforcement ratios. *Structural Concrete*, *18*(6), 950-961.

Carmo, R. N. F., Costa, H., Simões, T., Lourenço, C., & Andrade, D. (2013). Influence of both concrete strength and transverse confinement on bending behavior of reinforced LWAC beams. *Engineering structures*, *48*, 329-341.

Çelik, Z., & Bingöl, A. F. (2020). Fracture properties and impact resistance of self-compacting fiber reinforced concrete (SCFRC). *Materials and Structures*, *53*(3), 1-16.

Chi, J. M., Huang, R., Yang, C. C., & Chang, J. J. (2003). Effect of aggregate properties on the strength and stiffness of lightweight concrete. *Cement and Concrete Composites*, *25*(2), 197-205.

Corinaldesi, V., & Moriconi, G. (2015). Use of synthetic fibers in self-compacting lightweight aggregate concretes. *Journal of building engineering*, *4*, 247-254.

de Alencar Monteiro, V. M., Lima, L. R., & de Andrade Silva, F. (2018). On the mechanical behavior of polypropylene, steel and hybrid fiber reinforced self-consolidating concrete. *Construction and Building Materials*, *188*, 280-291.

Du, Y., Qi, H. H., Jiang, J., & Liew, J. Y. (2022). Experimental study on the dynamic behaviour of expanded-shale lightweight concrete at high strain rate. *Materials and Structures*, *55*(1), 1-17.

Dwarakanath, H. V., & Nagaraj, T. S. (1992). Deformational behavior of reinforced fiber reinforced concrete beams in bending. *Journal of Structural Engineering*, *118*(10), 2691-2698.

EFNARC. (2005). The European Guidelines for Self-Compacting Concrete Specification, Production and Use. *European Federation for Specialist Construction Chemicals and Concrete Systems*, English ed. Norfolk, UK.

Eurocode 2 (2004). Design of Concrete Structures – Part 1-1: General Rules and Rules for Buildings. *European Committee for Standardization*, Brussels, Belgium.

Fathifazl, G., Razaqpur, A. G., Isgor, O. B., Abbas, A., Fournier, B., & Foo, S. (2009). Flexural Performance of Steel-Reinforced Recycled Concrete Beams. *ACI Structural Journal*, *106*(6).

Frosch, R. J. (1999). Another look at cracking and crack control in reinforced concrete. *Structural Journal*, *96*(3), 437-442.

Gergely, P., & Lutz, L. A. (1968). Maximum crack width in reinforced concrete flexural members. *Special Publication*, *20*, 87-117.

Hasgul, U., Turker, K., Birol, T., & Yavas, A. (2018). Flexural behavior of ultra-high-performance fiber reinforced concrete beams with low and high reinforcement ratios. *Structural Concrete*, *19*(6), 1577-1590.

Henager, C. H., & Doherty, T. J. (1976). Analysis of reinforced fibrous concrete beams. *Journal of the Structural Division*, *102*(1), 177-188.

Hossain, K. M. A., Hasib, S., & Manzur, T. (2020). Shear behavior of novel hybrid composite beams made of self-consolidating concrete and engineered cementitious composites. *Engineering Structures*, *202*, 109856.

Iqbal, S., Ali, A., Holschemacher, K., Bier, T. A., & Shah, A. A. (2016). Strengthening of RC beams using steel fiber reinforced high strength lightweight self-compacting concrete (SHLSCC) and their strength predictions. *Materials & Design*, *100*, 37-46.

Jiang, D., Wang, G., Montaruli, B. C., & Richardson, K. L. (2004, May). Concrete offshore LNG terminals-A viable solution and technical challenges. In *Offshore Technology Conference*. OnePetro.

Jun Li, J., gang Niu, J., jun Wan, C., Jin, B., & liu Yin, Y. (2016). Investigation on mechanical properties and microstructure of high performance polypropylene fiber reinforced lightweight aggregate concrete. *Construction and Building Materials*, *118*, 27-35.

Kayali, O. (2008). Fly ash lightweight aggregates in high performance concrete. *Construction and building materials*, *22*(12), 2393-2399.

Kwon, S. J., Yang, K. H., & Mun, J. H. (2018). Flexural tests on externally post-tensioned lightweight concrete beams. *Engineering Structures*, *164*, 128-140.

Law Yim Wan, D. S., Aslani, F., & Ma, G. (2018). Lightweight self-compacting concrete incorporating perlite, scoria, and polystyrene aggregates. *Journal of Materials in Civil Engineering*, *30*(8), 04018178.

Lotfy, A., Hossain, K. M., & Lachemi, M. (2016). Mix design and properties of lightweight self-consolidating concretes developed with furnace slag, expanded clay and expanded shale aggregates. *Journal of Sustainable Cement-Based Materials*, *5*(5), 297-323.

Muñoz-Ruiperez, C., Rodríguez, Á., Junco, C., Fiol, F., & Calderon, V. (2018). Durability of lightweight concrete made concurrently with waste aggregates and expanded clay. *Structural Concrete*, *19*(5), 1309-1317.

Nes, L. G., & Øverli, J. A. (2016). Structural behaviour of layered beams with fibre-reinforced LWAC and normal density concrete. *Materials and Structures*, *49*(1), 689-703.

NRMCA (National Ready Mixed Concrete Association). (2003). CIP 36-Structural Lightweight Concrete. *NRMCA,* Washington, DC.

Oh, B. H. (1992). Flexural analysis of reinforced concrete beams containing steel fibers. *Journal of structural engineering*, *118*(10), 2821-2835.

Omar, A. T., & Hassan, A. A. (2021). Behaviour of expanded slate semi-lightweight SCC beams with improved cracking performance and shear capacity. In *Structures* (Vol. 32, pp. 1577-1588). Elsevier.

Omar, A. T., Sadek, M. M., & Hassan, A. A. (2020). Impact resistance and mechanical properties of lightweight self-consolidating concrete under cold temperatures. *ACI Materials Journal*, *117*(5), 81-91.

Rodriguez, S. (2004). Design of long span concrete box girder bridges: Challenges and solutions. In *Structures 2004: Building on the Past, Securing the Future* (pp. 1-11).

Sadek, M. M., Ismail, M. K., & Hassan, A. A. (2020). Stability of lightweight self-consolidating concrete containing coarse and fine expanded slate aggregates. *ACI Materials Journal*, *117*(3), 133-143.

Shi, C., & Wu, Y. (2005). Mixture proportioning and properties of self-consolidating lightweight concrete containing glass powder. *ACI Materials Journal*, *102*(5), 355.

Shi, C., Yang, X., Yu, Z., & Khayat, H. (2005, May). Design and application of self-compacting lightweight concretes. In *SCC'2005-China: 1st International Symposium on Design, Performance and Use of Self-Consolidating Concrete* (pp. 55-64). RILEM Publications SARL.

Sin, L. H., Huan, W. T., Islam, M. R., & Mansur, M. A. (2011). Reinforced Lightweight Concrete Beams in Flexure. *ACI Structural Journal*, *108*(1).

Standard, British. (1997). BS 8110 Part 1, Structural use of concrete part 1. Code of practice for design and construction. *British Standard Institution*, London, UK.

Yang, K. H., Mun, J. H., & Lee, J. S. (2014). Flexural tests on pre-tensioned lightweight concrete beams. *Proceedings of the Institution of Civil Engineers-Structures and Buildings*, *167*(4), 203-216.

Yang, K. H., Mun, J. H., Hwang, S. H., & Song, J. K. (2020). Flexural capacity and ductility of lightweight concrete T-beams. *Structural Concrete*, *21*(6), 2708-2721.

7. Performance of Stalite Lightweight SCC Beam-Column Joints under Reversed Cyclic Loading

7.1 Abstract

This chapter investigates the structural performance of expanded slate (Stalite) lightweight self-consolidating concrete (LWSCC) beam-column joints under quasi-static reversed cyclic loading. Six beam-column joints made with different lightweight aggregate types (coarse and fine Stalite lightweight aggregates) and designed with/without joint shear reinforcement were cast and tested. The performance of tested specimens was assessed in terms of failure mode, hysteretic response, deformation, strength degradation, ductility, brittleness index, and energy dissipation capacity. The applicability and accuracy of design code provision in predicting the shear and flexural strengths of the tested joints were also investigated. The results indicated that it is possible to design Satlite LWSCC mixtures with a density ranging from 1888-1966 kg/m^3, having a sufficient structural performance under cyclic loading. Properly designed LWSCC beam-column joints made with Satlite aggregates showed slight reductions in the load-carrying capacity of around 8.5% and ductility and dissipated energy of around 11.4% and 15.8% compared to NWSCC specimen. Despite the brittle nature of Stalite lightweight aggregates, LWSCC joints with sufficient hoops exhibited satisfactory cyclic performance and experienced ductile flexural beam failure. The results also indicated that LWSCC specimens containing Stalite fine aggregates showed better structural performance in terms of load-carrying capacity,

strength degradation, ductility, brittleness index, and energy dissipation capacity compared to counterpart specimens with Stalite coarse aggregates.

7.2 Introduction

Seismic events over the years have shown severe damage and lateral instability for reinforced concrete (RC) structures that led to catastrophic collapses. One of the guiding principles in designing an earthquake-resistant construction is to minimize the structure's self-weight (Agrawal & Shrikhande, 2006). The use of lightweight concrete (LWC) in construction practices can effectively decrease gravity loads acting on the structure, which contributes toward reaching reduced structural dimensions and thus reduces the seismic inertial mass of building structures (Kayali, 2008; Bogas & Gomes, 2013). Besides the reduced weight, LWC can be developed with high strength levels, achieving a convenient strength-to-weight ratio and superior durability properties (Mitchell & Marzouk, 2007; Omar et al., 2020). Consequently, this type of concrete became an attractive material for multiple structural applications such as long-span bridges, high-rise buildings, and ocean platforms (Yu et al., 2015; Mousa et al., 2018). Despite the advantages of using lightweight aggregate in concrete, LWC generally exhibits a lower modulus of elasticity, lower shear resistant capacity, and more brittle fracture characteristics, when compared to conventional normal-weight concrete (NWC) (Chi et al., 2003; Wu et al., 2018). This still poses some concerns among designers/engineers regarding the feasibility of using this material in structural applications, especially in seismically active regions.

Expanded slate (Stalite) lightweight aggregate has been successfully employed in the production of lightweight concrete. The superior mechanical characteristics of this

aggregate, compared to all other types of lightweight aggregates (LWA), contribute to developing concrete mixtures with a high strength-to-weight ratio and improved impact and abrasion resistance (Omar & Hassan, 2019; Sadek & Hassan, 2021). Reinforced LWC beams made with expanded slate aggregate also showed higher shear resistance and better post-cracking resistance, compared to LWC made with other types of LWA (Hassan et al., 2015). However, the performance of expanded slate LWC elements under reversed cyclic loads is not well documented and needs further investigation.

Beam-column joints (BCJs) are one of the most crucial components in RC frame structures under seismic loading that plays a significant role in maintaining structural integrity and overall stability of the structural system. Under intense earthquake events, BCJs are typically subjected to large shear forces that may lead to large deformations and hence serious damage or global collapse of the structures. Although many research studies have been carried out on NWC beam-column joints, research on the seismic performance of BCJs made with LWC is limited. Forzani et al. (1979) investigated the structural behaviour of four interior BCJs made with LWC and NWC under monotonic and reversed cyclic loading. In their research, lightweight expanded shale aggregate was used to develop LWC mixtures with a comparable compressive strength to the control NWC mixture (31–35 MPa) and a dry density of 1874 kg/m^3. The authors reported that, under monotonic loading, NWC and lightweight expanded shale joints' performance were very similar, with no apparent change in the load-displacement curves. However, when subjected to cyclic loading, lightweight expanded shale specimens demonstrated lower load-carrying capacity associated with more noticeable strength degradation when compared to NWC

counterparts. The authors attributed that to the early bond deterioration that occurred in lightweight expanded shale specimens at relatively small story drifts that caused pinching of the hysteresis diagram. Contradictory findings were reported by Rabbat et al. (1986), when testing 16 full-scale BCJs made with either expanded clay or expanded shale aggregates under reversed cyclic loads. Their results showed that LWC joints performed similar to their counterparts NWC joints in terms of strength, strength deterioration, and dissipated energy.

From the perspective of seismic design, structures should not only withstand earthquake force but also assure sufficient ductility and energy dissipation characteristics under major seismic events. This allows the structure to undergo large plastic deformations and dissipate the energy the structure receives from the earthquake without a substantial loss of strength. In this scope, the American codes (ACI 352R, 2002; ACI 318, 2019) adopt the concept of a strong column/weak beam in designing BCJs, so that plastic hinges are likely to be formed in the beam rather than in the column. In order to assure such concept, closely spaced hoops should be provided within the joint core to prevent the early shear strength degradation and improve the ductility of BCJs. Closely spaced hoops' detailing however, usually leads to steel congestion in the joint. This risks formation of honeycombing within the joint and requires more challenge to achieve a proper consolidation of concrete in this region. Self-consolidating concrete (SCC) is an ideal choice in this situation due to its high flowability and stability, which can overcome the compaction difficulties and reduce the risk of segregation in such highly congested regions (Paultre et al., 2005).

Lightweight self-consolidating concrete (LWSCC) is a good choice in multiple structural applications requiring high compactability and reduced self-weight. However, the development of this innovative concrete material is challenging due to the risk of aggregate floating in such flowable mixture and the high-water absorption of lightweight aggregates during mixing (Bogas et al., 2012). Although the fresh and mechanical properties of some LWSCC mixtures have been investigated in the literature (Lotfy et al., 2016; Nepomuceno et al., 2018; Hilal et al., 2021), no studies have examined the performance of LWSCC beam-column joints made with Stalite lightweight aggregates under cyclic loads. Due to the growing interest towards using LWSCC in construction, this research was conducted to study the performance of LWSCC beam-column joints made with two different LWA stalite aggregates (either coarse or fine Stalite aggregate) under reversed cyclic loading. The study also evaluates the contribution of joint shear reinforcement on enhancing the performance of the tested LWSCC joints in terms of degradation in load-carrying capacity, deformability, ductility, and energy dissipation capacity.

7.3 Research Significance

The use of lightweight concrete (LWC) in construction practices can effectively reduce seismic hazards. Incorporating LWA in SCC mixtures combines the desired properties of SCC, especially in highly congested areas, with the advantage of LWC in structural applications. However, there is a lack of information in the literature regarding the cyclic performance of LWSCC members, which makes it challenging to achieve a rational design with confidence. In addition, despite the high strength and quality of Stalite lightweight aggregates compared to all other LWAs (Abouhussien et al., 2015; Omar & Hassan, 2021),

insufficient studies were carried out to evaluate the structural performance of concrete members containing this type of lightweight aggregate under reversed cyclic loading. Therefore, this chapter aims to address this knowledge gap by presenting a comprehensive investigation covering the structural performance of lightweight self-consolidating concrete beam-column joints made with coarse/fine lightweight Stalite aggregates under reversed cyclic loading.

7.4 Experimental Program

7.4.1 Concrete mixtures and specimen details

Three concrete mixtures, selected from the developed mixtures in the first stage, were investigated in this stage. The mixture proportions of all developed mixtures are summarized in **Table 7-1**. Mixtures 1-2 were designed with the maximum volume of Stalite aggregate (either LC or LF) that can be used safely to develop successful SCC mixtures with a binder content of 550 kg/m^3. While mixture three was developed as NWSCC to be compared with mixtures 1-2, in order to evaluate the effect of replacing strong normal-weight aggregates with low-density aggregates on the structural performance of BCJs under cyclic loading. The author aimed to maintain a similar water-to-binder ratio and similar binder content in both lightweight and normal weight mixtures.

The fresh properties of NWSCC and LWSCC mixtures were assessed in terms of slump flow, V-funnel, and L-box tests as per EFNARC guidelines (2005). After 28 days, the compressive strength (f'_c) and splitting tensile strength (*STS*) tests were performed on three identical concrete cylinders (200 mm height x 100 mm diameter) as per ASTM C39 and

C496, respectively. The modulus of elasticity (*ME*) of a typical concrete cylinder under compression loading was also measured for all tested mixtures. The fresh and mechanical properties of the tested mixtures are summarized in

Table 7-2.

In this investigation, a total of six BCJs were cast and tested under quasi-static reversed cyclic loading. The experimental program was divided into two series as follows:

- Series I (weak joints): in this series, the three developed mixtures (NWSCC and two LWSCC mixtures with LC and LF) were used to cast three beam-column joint specimens. These specimens were designed according to the strong-beam/weak-column concept (shear-deficient specimens), in which no transverse hoops (shear reinforcement) were placed in the joint core, as shown in Figure 7-1**a**. This concept was adopted to assess the failure mode, shear strength, and energy dissipation capacity of LWSCC joints compared to NWSCC joints under reversed cyclic loads.
- Series II (strong joints): the specimens in this series (NWSCC and two LWSCC mixtures with LC and LF) were designed to follow the concept of strong-column/weak-beam as per recommendations of ACI 352R (2002). Sufficient shear reinforcement was added into the joint panel to study the effect of stirrups confinement on improving the performance of LWSCC joints under seismic excitation.

Both weak and strong joints were cast with identical concrete dimensions and were designed according to ACI 318 (2019). The lengths of the beam and column in this study were selected to be about one-third of the full-size joints (assuming a 3-m typical column height). L-shape bars with adequate developmental lengths were provided at the top and bottom of the beam to avoid bond/slip failure. Figure 7-1 shows the typical concrete dimensions and joint reinforcement details of specimens in series I and II.

Joints in series I were labelled by the concrete type (NWSCC or LWSCC), LWA type (LC or LF) if existing, and "WJ" that represents the weak joint design concept. While "SJ" was added to the designation of joints in series II to indicate that these specimens were designed as strong joint specimens.

Table 7-1: Mixture proportions for tested mixtures.

Mixture ID	Cement (kg/m^3)	MK (kg/m^3)	FA (kg/m^3)	Aggregates					HRWRA (kg/m^3)	Fresh density (kg/m^3)
				C/F ratio	NC (kg/m^3)	NF (kg/m^3)	LC (kg/m^3)	LF (kg/m^3)		
NWSCC	275	110	165	1.0	753.2	753.2	-	-	3.40	2276.4
LWSCC-LF	275	110	165	0.7	492.6	-	-	703.7	3.75	1966.3
LWSCC-LC	275	110	165	1.0	-	559.0	559.0	-	3.55	1888.1

Note: FA = fly ash; MK = metakaolin; C/F = coarse-to-fine ratio; NC = normal-weight coarse aggregate; NF = normal-weight fine aggregate; LC = Lightweight coarse aggregate; LF = Lightweight fine aggregate; and HRWRA = High-range water reducer admixtures.

Table 7-2: Fresh and mechanical properties for tested mixtures.

Mixture designation	T_{50} (sec)	V-funnel (sec)	L-box ratio (H_2/H_1)	f'_c (MPa)	*STS* (MPa)	*ME* (GPa)
NWSCC	2.15	12.64	0.86	67.1	3.91	30.41
LWSCC-LF	1.80	8.90	0.92	52.3	2.82	23.25
LWSCC-LC	2.65	17.12	0.80	48.1	2.54	22.05

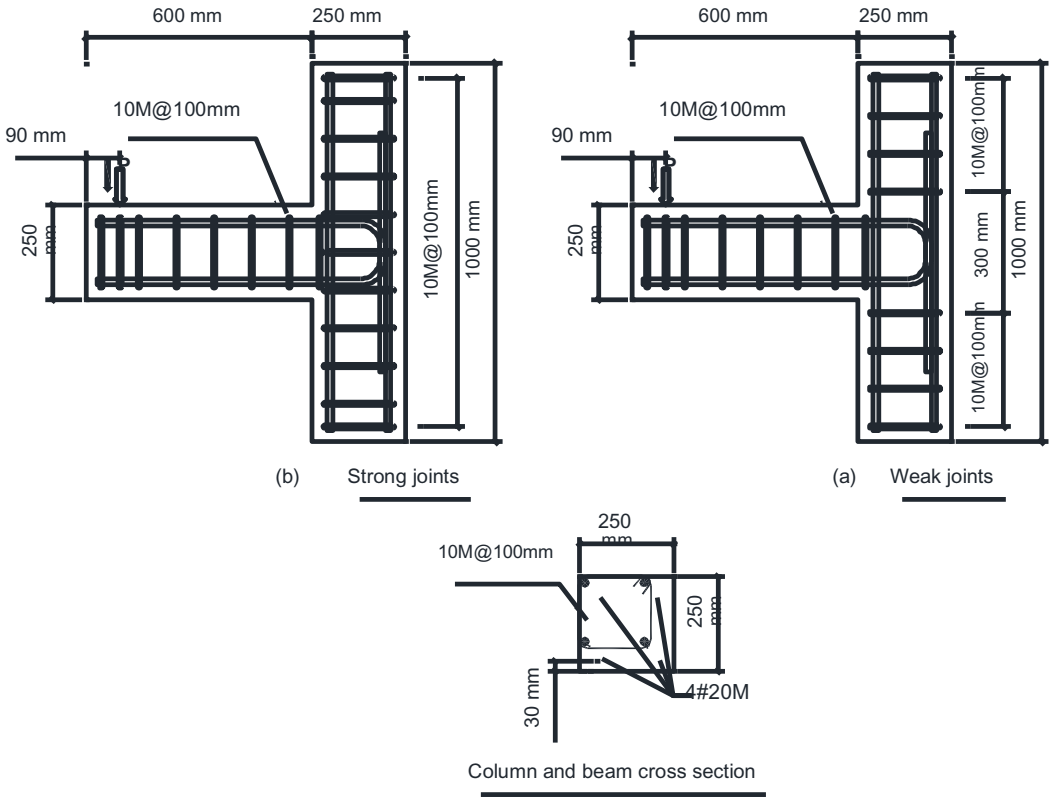

Figure 7-1: Geometry and reinforcing details of specimens.

7.4.2 Test setup and loading procedure

The configuration of the test setup adopted in this study is shown in Figure 7-2. The column was initially loaded with 10% of its nominal compressive capacity using a hydraulic jack to represent the gravity loads. The axial load acting on the column remained constant throughout the test and was monitored using a data acquisition system. All tested specimens were subjected to reversed cyclic vertical displacement loading applied at the beam's tip (90 mm away from the beam's end [Figure 7-1]) using a double-acting hydraulic actuator with a 500 kN-load capacity.

Figure 7-2: Test setup *(Note: 1 mm = 0.039 in.).*

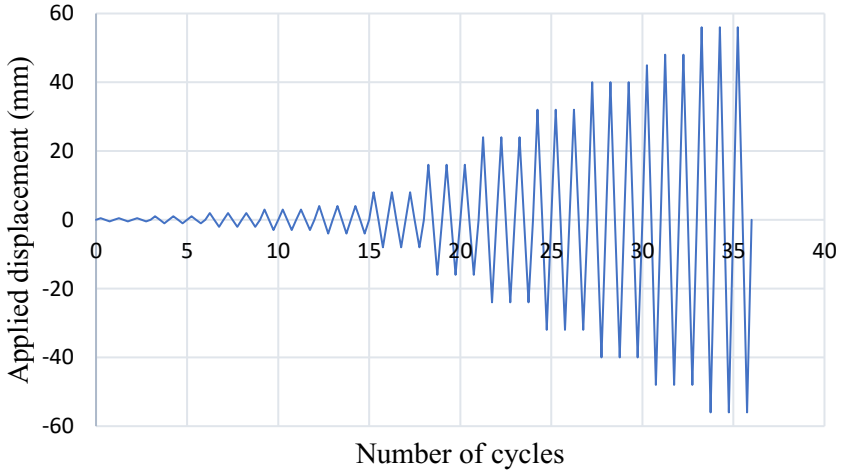

Figure 7-3: Sequence of applied displacement.

A quasi-static displacement-controlled loading procedure (Figure 7-3) was adopted following the ACI 2006 guidelines for moment-resisting frames. The displacement was applied with increasing amplitude in different load steps. Each load step had three full

reversed cycles with a frequency of 0.08 Hz. All tested specimens were suitably instrumented with a linear variable differential transducer (LVDT) to monitor the deflection at the beam's tip and beam's mid-span. In addition, the strains at the section of the maximum moment were recorded using two electrical resistance strain gauges affixed to the bottom and top longitudinal beam's reinforcement. Crack propagation after each loading step was closely observed and sketched. The loading process was stopped when a significant drop in the load-carrying capacity was observed. Throughout the test history, the measurements of load cells, LVDTs, and strain gauges were continuously monitored and automatically recorded with a data acquisition system. The data obtained from the tests were collected and analyzed to obtain the failure modes, hysteresis response, ultimate load, ductility, brittleness index, and energy dissipation capacity.

7.5 Results and Discussion

7.5.1 Failure modes and general cracking behavior

Four different modes of failure are expected in beam-column joints when subjected to reversed cyclic load: (i) beam yielding failure—"B-mode" (in which the longitudinal steel bars in the beam yield without any visual sign of shear cracks in the joint up to failure); (ii) joint shear failure after beam's rebars yields—"BJ-mode" (in which the diagonal shear cracking in the joint core zone occurs after yielding of beam's longitudinal steel reinforcement); (iii) joint shear failure without beam yields—"J-mode" (in which the joint shear stress due to applied loads exceeds the joint shear strength before the longitudinal steel bars in beam reach yield, and the failure occur due to widening of the major diagonal crack in the joint core zone); and (iv) compressive flexural failure at beam end—"CB-

mode" (occurs when concrete crushes under cyclic load before beam reinforcement yield and the joint shear strength is greater than the joint shear stress).

7.5.1.1 Weak Joint Specimens

Figure 7-4 shows, schematically, the cracking pattern of beam-column joints in series I (designed with a strong beam-weak joint concept) at the failure stage. By monitoring the specimens throughout the test history, it was observed that fine visible flexural cracks were initiated at the beam-column interface at the early stage of loading. By increasing the applied load, the flexural cracks at the beam-column interface continued to propagate rapidly through the whole depth of the beam section. The yielding of beam reinforcement was experimentally detected for all tested specimens in this series at a load of approximately 51 to 59% of the peak load. The initiation of diagonal shear cracks in the joint zone of LWSCC specimens (S2-S3) was observed just after the beam reinforcement reached the yield stress (58% and 64% of the ultimate load in S2 and S3, respectively). In contrast, in the NWSCC specimen (S1), the initiation of diagonal shear cracks within the joint was initiated later at 85% of the ultimate load. This can be related to the higher shear strength of the NWSCC beam-column joint compared to LWSCC joints.

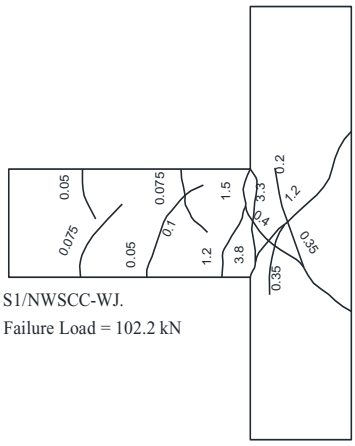

S1/NWSCC-WJ.
Failure Load = 102.2 kN

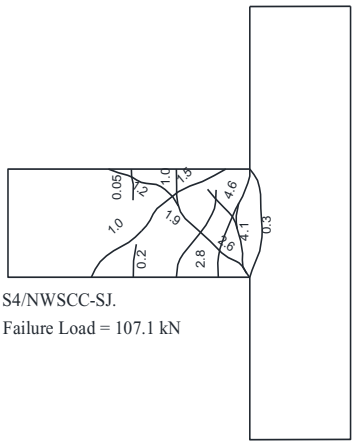

S4/NWSCC-SJ.
Failure Load = 107.1 kN

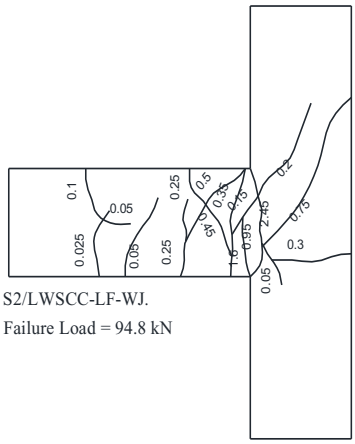

S2/LWSCC-LF-WJ.
Failure Load = 94.8 kN

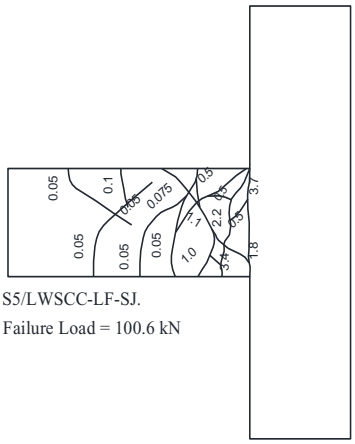

S5/LWSCC-LF-SJ.
Failure Load = 100.6 kN

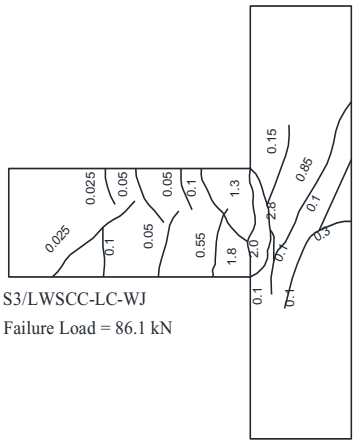

S3/LWSCC-LC-WJ
Failure Load = 86.1 kN

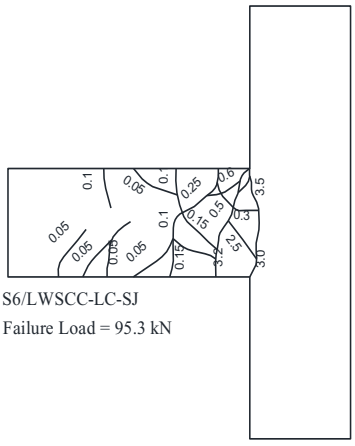

S6/LWSCC-LC-SJ
Failure Load = 95.3 kN

Figure 7-4: Crack patterns of tested beam-column joints at failures.

After the initiation of the diagonal shear cracks in series I (S1-S3), a further increase in the applied load led to extending the diagonal shear crack to the outermost parts of the column with continuing increase in the crack opening up to the peak load. All tested specimens in this series (whether NWSCC or LWSCC) failed in a BJ-mode, in which the beam longitudinal reinforcement reached yield first (as indicated by the strain gauges attached to the steel bars at the beam-column interface) and then diagonal cracks in the joint zone were formed (refer to Figure 7-4).

7.5.1.2 Strong Joint Specimens

Providing sufficient transverse reinforcement in the joint region of NWSCC and LWSCC specimens (series II) showed a change in failure mode from BJ-mode to B-mode (S4-S6), in which the beam longitudinal reinforcement reached yield with no formation of shear cracks in the joint zone up to failure (refer to Figure 7-4). This proves the potential of transverse hoops to restrict the damage in the joint during cyclic load actions. Figure 7-4 and Table 7-3 also illustrate the cracking pattern, maximum crack width at the beam-column interface, and maximum crack width within the panel of beam-column joints. From the figure, it can be seen that LWSCC joints generally exhibited higher cracking activity compared to NWSCC specimens, demonstrating a higher number of cracks with smaller crack widths at the beam-column interface and within the joint region. This may be related to the lower concrete tensile strength of LWSCC (due to the use of low-density aggregate), which encouraged new flexural and shear cracks to initiate rather than continuing to widen existing cracks.

Table 7-3: Results of reversed cyclic loading.

	Joint #	Specimen ID	Ultimate load (kN)	Deflection at ultimate load (mm)	Failure Mode	Initial Stiffness (kN/mm)	Crack width	
							At beam-column interface (mm)	Within joint panel (mm)
Series I	S1	NWSCC-WJ	102.2	12.95	BJ-mode	19.23	3.8	1.2
	S2	LWSCC-LF-WJ	94.8	13.02	BJ-mode	16.36	2.45	0.75
	S3	LWSCC-LC-WJ	86.1	12.22	BJ-mode	14.70	2.8	0.85
Series II	S4	NWSCC-SJ	107.1	22.12	B-mode	20.17	4.6	-
	S5	LWSCC-LF-SJ	100.6	22.72	B-mode	16.53	3.7	-
	S6	LWSCC-LC-SJ	95.3	21.15	B-mode	15.03	3.5	-

It is worthy to mention that specimens cast with a strong joint concept showed a higher number of cracks along the beam associated with greater crack widths at the beam-column interface when compared to counterpart specimens cast as weak joint. For example, the LWSCC specimen made with LF and designed as a strong joint exhibited a maximum crack width at the interface of 3.7mm, while the counterpart specimen designed with a weak joint exhibited a maximum crack width of 2.45mm (refer to Table 7-4). This is due to the relatively higher deformation accompanied with a higher ultimate load of strong joint specimens compared to weak joint specimens.

7.5.2 Load-deformation envelope curves

7.5.2.1 Weak Joint specimens

Figure 7-5 shows the envelop load-tip deflection curves for all tested beam-column joints. The load-deflection envelop curves were drawn using the points of maximum load with their corresponding deflection from the first cycle in each load step from hysteresis loops. From the figure, it can be seen that the tested specimens showed a similar pattern in the push and pull directions with a slight difference in the values of the peak load. This can be due to the geometrical imperfections and steel bars disposition during casting concrete in beam-column joints. Table 7-3 shows the results of ultimate deflection (the deflection value corresponding to 85% of the ultimate load in the descending branch of the load-deflection envelope curve). From the table, it can be indicated that in the pre-peak stage, LWSCC specimens with either coarse or fine expanded slate aggregates showed a lower stiffness compared to counterpart NWSCC specimens. This is clear from the lower slope of the ascending branch of load-deflection curves of LWSCC specimens compared to NWSCC

specimen. Such findings can be related to the low modulus of elasticity and low stiffness of expanded slate particles compared to the conventional normal-weight aggregates, which led to the initiation of earlier micro-cracks, and in turn, reduced the initial stiffness of the tested beam-column joints.

Figure 7-5 and Table 7-3 also showed that, in weak joints, replacing normal weight coarse/fine aggregate with LF and LC, in attempt to reduce the concrete density by an average of 15.3%, reduced the load-carrying capacity of beam-column joint by 7.8% and 18.7% respectively. Since these specimens exhibited BJ-failure, their load-carrying capacity is directly proportional to the joint shear strength and flexural strength of the beam section. The drop in compressive strength (due to using lower density aggregate) reduced the shear strength of tested specimens. In the meantime, lower concrete strength resulted in increasing the compression stress block depth in the beam section at the interface (location of the plastic hinge), and thus reduced the lever arm between tension and compression forces. The small lever arm correspondingly reduces the bearing moment capacity of the beam and hence the overall load-carrying capacity of the BCJs. It should be noted that using LWSCC-LC showed a more pronounced reduction in the load-carrying capacity than LWSCC-LF when compared to NWSCC beam-column joint. This may be related to the lower interlock resistance of LC in resisting higher shear stress compared to the normal weight aggregate used in the LWSCC-LF joint (Omar & Hassan, 2021). This, in turn, contributed to weaken the joint shear strength of the LWSCC-LC joint and hence resulted in a pronounced decreased load-carrying capacity.

In the post-peak stage, the LWSCC-LC specimen (S3) deteriorated more rapidly compared to the NWSCC specimen (S1), exhibiting a steeper descending portion of the load-deflection (more brittle failure) (see Figure 7-5**a** and Table 7-3). This can be attributed to the crack path in LWC, which go through the coarse aggregate particles rather than around them, demonstrating a brittle failure with a faster crack propagation and increased rate of strength degradation. On the other hand, the use of LF as a replacement for normal-weight sand (in order to obtain minimum density SCC) exhibited a slightly lower rate of strength degradation compared to NWSCC beam-column joint. Such results can be related to the fact that using low stiffness lightweight fine aggregates in the development of LWSCC-LF mixtures made the cement mortar more deformable than the conventional cement mortar containing natural sand. This encouraged more cracks to initiate through the cement matrix, and hence improved the deformability of the joint prior to failure.

7.5.2.2 Strong joints vs. weak joints

Figure 7-5**b** shows the load-deflection curves of beam-column joints reinforced with adequate transverse hoops within the joint zone (strong joints). From the figure, it can be observed that the addition of transverse hoops in the joint slightly increased the load-carrying capacity of the tested specimens. For example, the NWSCC specimen cast with sufficient transverse hoops (S4) sustained a reversed cyclic load up to 107.1 kN, which is 5.1% higher than that resisted by the counterpart specimen without transverse shear reinforcement (weak joint-S1). In addition, placing lateral hoops within the joint panel alleviated the reduction in load-carrying capacity resulted from using lower density aggregates. As shown in Table 7-3, replacing normal-weight aggregates with either LC/LF

aggregates showed a reduction in the ultimate load capacity of strong joint specimens by an average of 8.5% (S5 and S6 compared to S4), while a reduction of 13.3% (on average) was observed in weak joint specimens (S2 and S3 compared to S1). Despite the slight effect of transverse hoops on load-carrying capacity, they helped to significantly improve the deformation capability of tested specimens. For instance, specimens S4, S5, and S6 showed displacements corresponding to ultimate load reached up to 1.7, 1.75, and 1.73 times higher than those of beam-column joints without transverse reinforcement S1, S2, and S3, respectively (see Table 7-3). Moreover, joints reinforced with transverse hoops in the joint zone (S4, S5, and S6) exhibited increased ultimate deflection of 45%, 40%, and 57%, higher than those of S1, S2, and S3, respectively (counterpart specimens without hoops). This behaviour can be related to the change in the failure mode of tested specimens after using transverse shear reinforcement within the joint. All tested strong joints (S4-S6) also experienced a lower rate of strength degradation than counterpart specimens designed as weak joints (S1-S3). This can be related to the fact that, in the post-peak stage, flexural plastic hinges formed in the beams with no formation of shear cracks in the joint panel of the tested specimens (S4-S6). This resulted in higher cracking activity along the beam length, and hence higher rate of deformation with a gradual decrease in strength until failure.

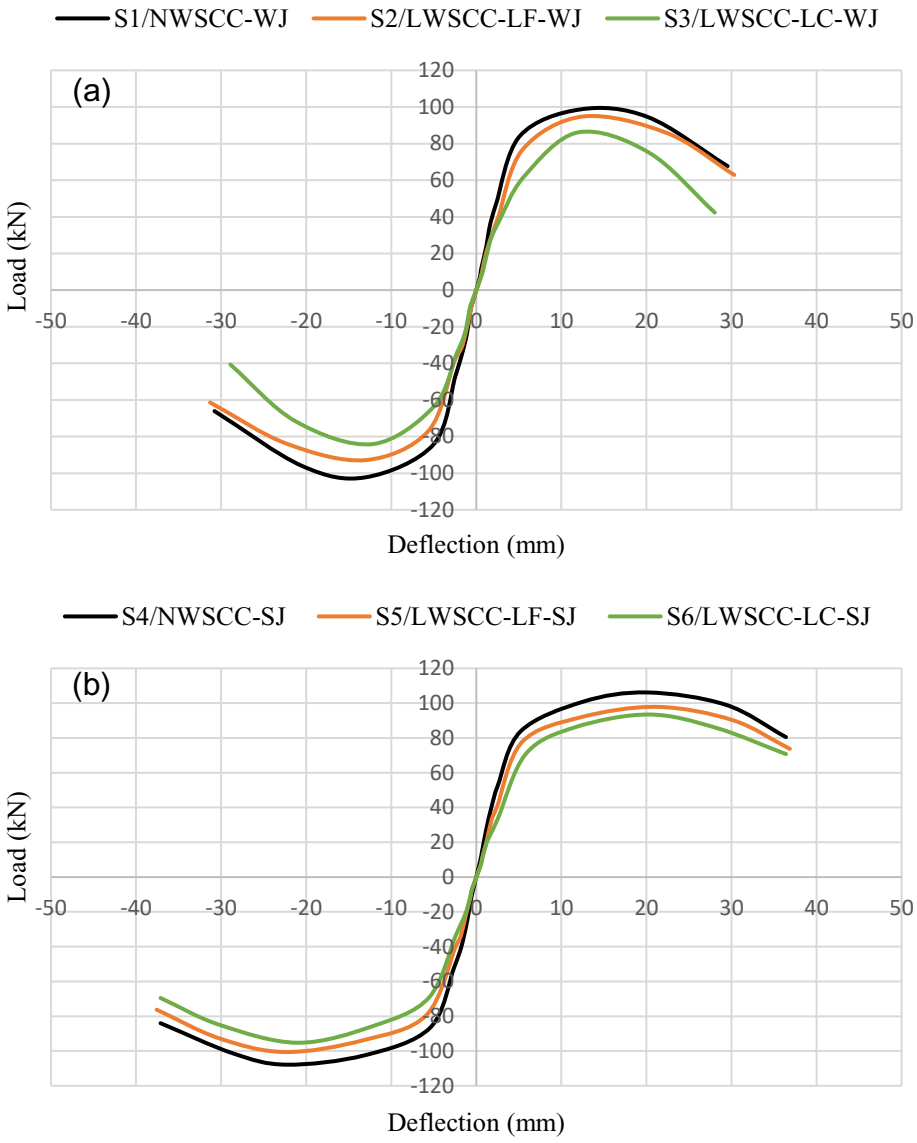

Figure 7-5: Load deflection envelop curves (a) joints without transverse hoops and (b) joints with transverse hoops.

7.5.3 Ductility and brittleness

Ductility is a desirable structural property that reflects the ability of any structure to undergo large inelastic deformations before failure. Table 7-4 and Figure 7-6 show the calculated displacement ductility for all tested beam-column joints, which is defined by the

ratio between the ultimate deflection (Δ_u) and the yield deflection (Δ_y). The load-tip deflection envelop curves were used to determine the ultimate and yield deflections. Ultimate deflection Δ_u was defined as the deflection value that corresponding to the intersection between the horizontal line at 85% of the ultimate load and the descending branch of the load-deflection envelop curve. Meanwhile, yield deflection Δ_y was taken as the deflection value corresponding to the point of intersection between the horizontal line at 85% of the ultimate load and the extension of the line that passes through the origin and 50% of the ultimate load (Shannag et al., 2002). The brittleness index (BI) was also calculated in this study to evaluate the ductility and deformability of the tested joints (refer to Table 7-4 and Figure 7-6). BI of concrete joints can be defined as the ratio of the recovered deformation energy obtained before fracture to the irreversible plastic energy consumed during the failure (A2/A1 in Figure 7-7) (Topcu, 1997).

Table 7-4: Yield deflection, ultimate deflection, ductility, and brittleness index.

	Joint #	Specimen ID	Yield deflection Δ_y (mm)	Ultimate deflection Δ_u (mm)	ductility index (μ)	Brittleness index (BI)
Series I	S1	NWSCC	4.75	23.20	4.88	0.40
	S2	LWSCC-LF	5.20	24.80	4.77	0.41
	S3	LWSCC-LC	5.35	20.70	3.87	0.48
Series II	S4	NWSCC-JR	5.15	33.65	6.53	0.34
	S5	LWSCC-LF-JR	5.40	34.60	6.41	0.35
	S6	LWSCC-LC-JR	5.65	32.70	5.79	0.38

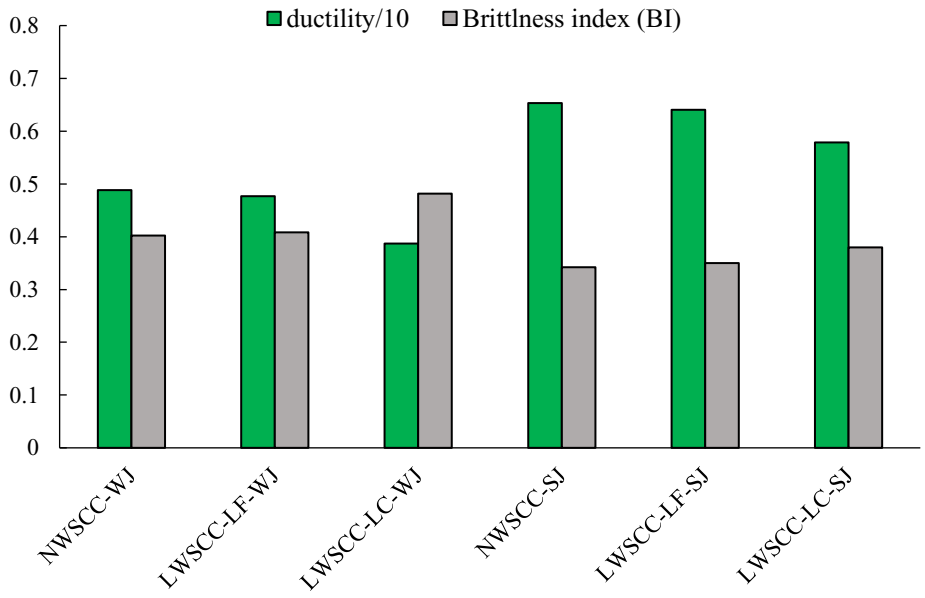

Figure 7-6: Results of ductility and brittleness index.

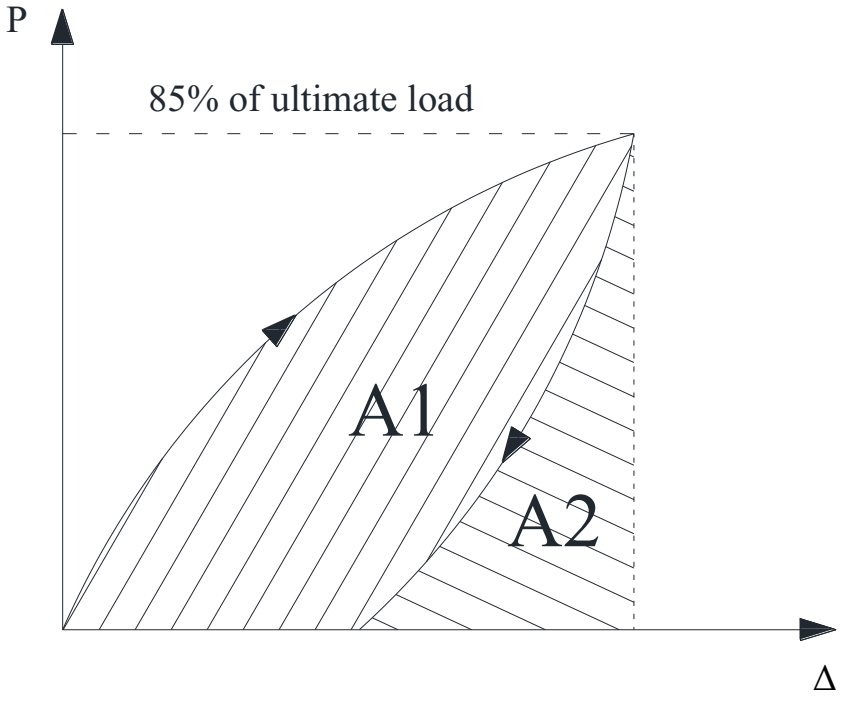

Figure 7-7: Definition of brittleness index.

7.5.3.1 Weak Joint specimens

By looking at Table 7-4, it can be seen that replacing the normal-weight coarse aggregate in NWSCC (S1) with LC in S3, in an attempt to reduce the concrete density by about 17%, lowered the ductility ratio by about 20.8% and increased the BI by 17.9%. This reduction in ductility (increase in BI) can be explained by the higher yield deflection and the lower ultimate deflection (Δu) of LWSCC-LC, which decreases the ductility ratio of LWSCC-LC compared to NWSCC. In contrast, replacing the normal-weight sand with LF in the development of LWSCC-LF (S2) (achieving a reduction in the mixtures' density by about 13.6%) did not show a significant change in the ductility ratio or BI (difference less than 3%). This can be related to the fact that despite the slightly higher yield deflection of LWSCC-LF compared to NWSCC (due to lower initial stiffness), the relatively higher ultimate deflection of LWSCC-LF (compared to NWSCC) resulted in a comparable ductility of the two mixtures (LWSCC-LF and NWSCC).

7.5.3.2 Strong Joint Specimens

The results also showed that the addition of transverse hoops within the joint in series II (strong joints) efficiently mitigated the reduction in ductility that resulted from replacing normal-weight coarse aggregate with LC Stalite aggregates (see Table 7-4 and Figure 7-6). For example, in strong joints, replacing normal-weight coarse aggregate by LC Stalite aggregate (S6 compared to S4) reduced the ductility by 11.4%, while this reduction was 20.8% in weak joints (S3 compared to S1). This can be attributed to the role of joint hoops in enhancing the joint shear strength, which improves the strength degradation by

restricting crack propagation, resulting in higher ultimate deflection (Δ_u) prior to failure. It should be noted that a minimum ductility index (μ) of 3 is considered imperative to ensure the redistribution of moments, especially in the areas of seismic design (Ashour, 2000; Sin et al., 2011). Accordingly, despite the reduced ductility of LWSCC joints compared to NWSCC ones, LWSCC joints proved to have an adequate ductile behaviour that can be considered for structural elements subjected to large deformations caused by earthquakes.

7.5.4 Energy dissipation

The hysteretic energy dissipation capacity is a measure to estimate the energy dissipated of beam-column joints in the post-elastic zone during the cyclic load history. In this study, the hysteretic energy dissipation capacity was computed by summing up the energy dissipated in successive load-tip displacement loops during the test. Figure 7-8 shows the hysteretic cycles for all tested joints (S1-S6). The dissipated energy for a load step can be calculated by finding the area enclosed by the hysteresis loops of the load step in the load-displacement diagram. The energy dissipated for each load step and cumulative energy dissipation for all tested specimens is presented in Table 7-5 and Figure 7-9.

From Table 7-5, it can be seen that, at the initial loading stage (up to step 6), all tested specimens showed low energy dissipated at each load step. After specimens entered the elastic-plastic stage, an obvious increase in the energy dissipation capacity can be observed for all tested specimens with further loading. This can be related to the rapid propagation of flexural cracks along the beam section after the yield of longitudinal reinforcement. Figure 7-9 indicates that although the LWSCC-LF specimen (S2) had a lower concrete

density than the NWSCC specimen (S1) by about 13.6%, both joints (S1 and S2) showed a comparable energy dissipation capacity under reversed cyclic loading (difference of 1.9%). One possible explanation is that although the LWSCC-LF joint sustained a slightly lower ultimate load than the NWSCC joint, it experienced a relatively higher ultimate deflection prior to failure. On the other hand, the energy dissipation capacity of the LWSCC-LC specimen (S3) was lower than that of the LWSCC-LF specimen (S2) by about 25.1%. This behaviour can be attributed to the lower joint shear strength of LWSCC specimens developed with LC compared to that containing LF. The reduced joint shear strength had an undesirable pinching effect (see Figure 7-8), which limited the load-carrying capacity and deformability of tested specimens and hence reduced the energy dissipation capacity.

Providing sufficient hoops within the joint zone (strong joints) significantly enhanced the ability of all tested specimens (S1-S6) to dissipate energy under reversed cyclic loading. The cumulative absorbed energy for NWSCC, LWSCC-LF, and LWSCC-LC specimens was found to be enhanced by 1.82, 1.86, and 2.10 times, respectively, compared to counterpart specimens in series I without hoops (S4-S6 compared to S1-S3) (refer to Figure 7-9). The addition of hoops into the strong joints changed the mode of failure from BJ-mode to B-mode, providing higher load-carrying capacity/deformability for these tested specimens prior to failure, and hence, increasing the energy dissipation capacity.

It can also be noted that the use of transverse hoops in the joint alleviated the reduction in energy dissipation capacity that resulted from replacing normal-weight aggregate with LC. For example, replacing normal-weight coarse aggregate with LC in the development of

LWSCC decreased the energy dissipation capacity of the tested joint by about 26.9% in the absence of transverse hoops, while this reduction was only 15.8% when transverse hoops were provided. Figure 7-8 indicates that weak joints with LWSCC (LC or LF) showed an undesirable pinching effect at the post-peak stage. However, using sufficient hoops within the joint (strong joint) eliminated this effect which helped these specimens to reach high ductility levels and dissipate higher energy without losing the structural integrity.

Table 7-5: Cumulative energy dissipation.

Step #	S1	S2	S3	S4	S5	S6
	E (kN.mm)	E (kN.mm)	E (kN.mm)	E (kN.mm)	E (kN.mm)	E (kN.mm)
1	1.02	0.99	0.93	1.40	1.07	0.97
2	3.34	3.41	3.26	4.50	3.52	3.14
3	17.70	17.33	13.53	20.71	12.85	12.51
4	36.9	35.4	27.5	47.7	36.9	28.0
5	71.7	67.5	55.8	93.8	73.0	57.2
6	276.9	272.7	201.7	279.7	247.5	234.5
7	1686.9	1505.2	1195.6	1641.0	1614.6	1246.5
8	4281.3	3879.2	3206.8	4321.2	4325.8	3295.4
9	6097.0	5981.8	4457.1	7640.1	7850.4	6317.9
10				11105.2	11077.0	9280.2

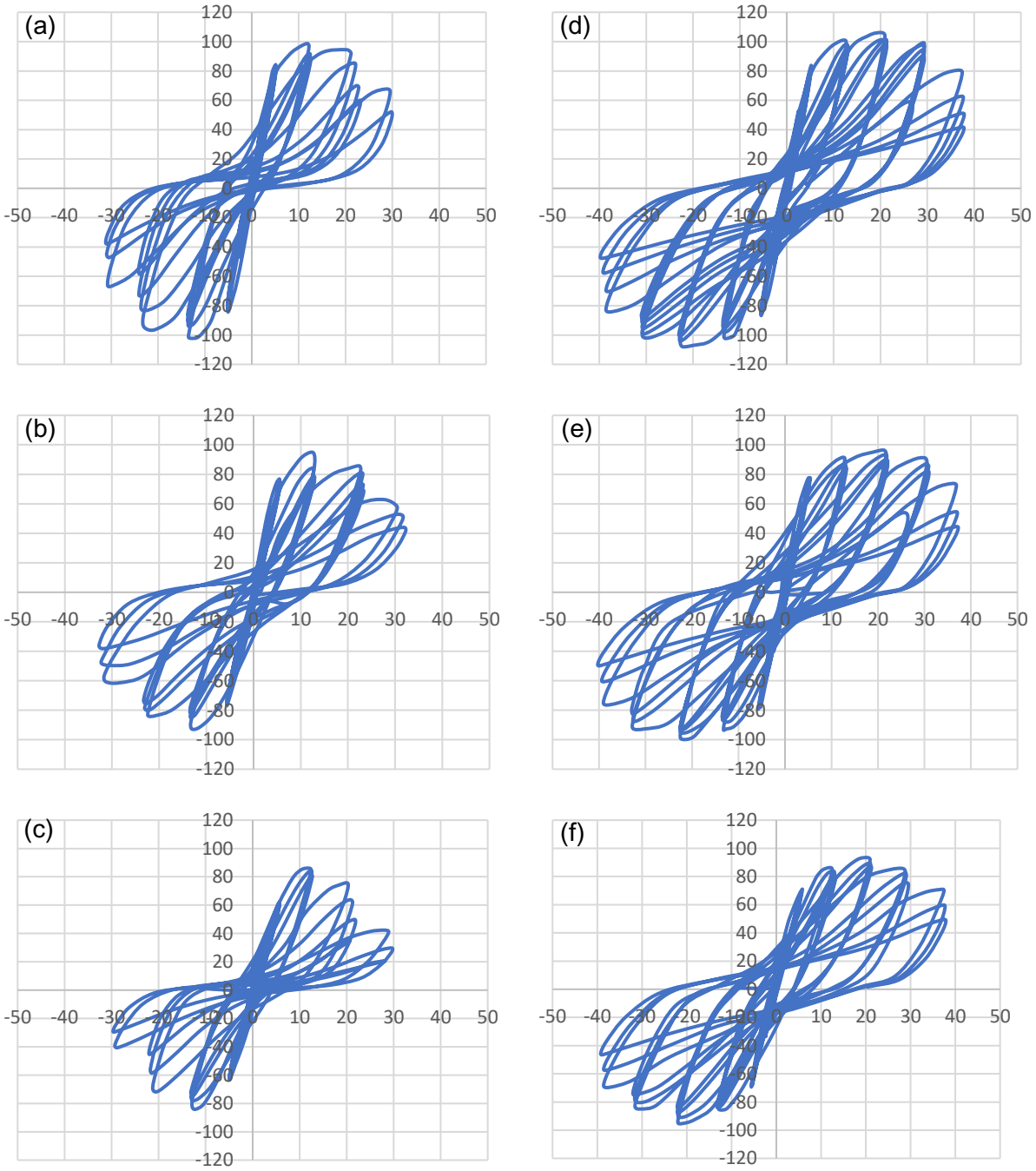

Figure 7-8: Hysteretic responses for (a) NWSCC-WJ, (b) LWSCC-LF-WJ, (c) LWSCC-LC-WJ, (d) NWSCC-SJ, (e) LWSCC-LF-SJ, and (f) LWSCC-LC-SJ specimens.

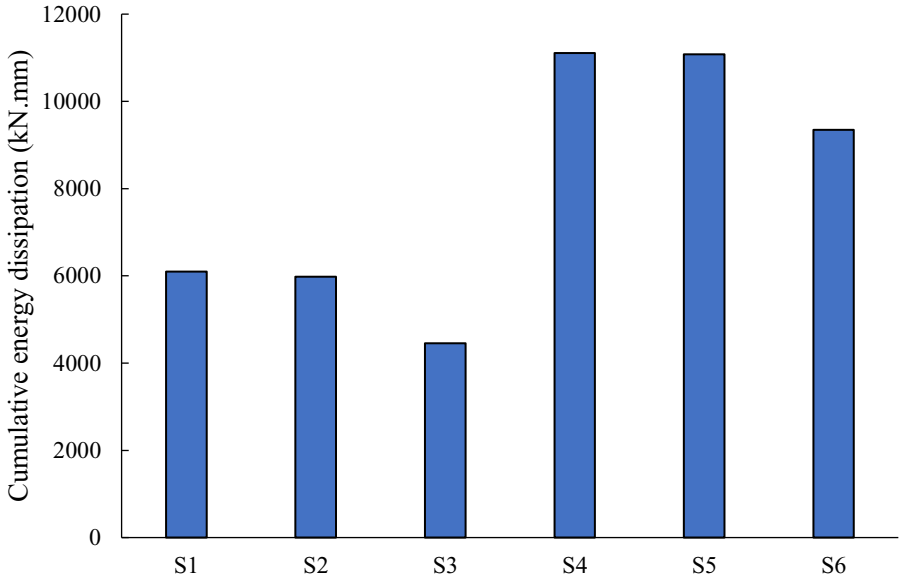

Figure 7-9: Energy dissipation.

7.5.5 Comparison with design codes

7.5.5.1 Beam flexural strength

The experimental ultimate bending moment (M_{exp}) resisted by the beam section was compared to the theoretical ultimate bending moment (M_{theo}) calculated using the rectangular stress block analysis as recommended by the ACI 318-19 code. The experimental-to-theoretical (M_{exp}/M_{theo}) ratio was calculated and presented in Table 7-6. For tested specimens in series I (weak joints), it can be noted that although using the ACI code equation normally gives a lower theoretical moment compared to experimental, the theoretical moment of LWSCC joints (S2-S3) showed higher values compared to the experimental. This is because the observed mode of failure of LWSCC joints was BJ mode (combined shear and flexural failure) and not a pure bending failure.

By looking at Table 7-6, series II with hoops (strong joints) (S5-S6), the experimental moment values of tested specimens exceeded the theoretical moment capacity predicted by the ACI code. These results confirmed the observed B mode of failure, in which the experimental moment exceeded the flexural capacity of the beam section. This also highlights the role of proper detailing of the joint core in changing the brittle failure (BJ mode) of LWSCC beam-column joints to a ductile flexure failure (B mode) in the beam.

Table 7-6: Experimental and predicted results.

Joint #	Failure Mode	Beam strength			Joint strength	
		M_{exp} (kN.m)	M_{theo} (kN.m)	M_{exp}/M_{theo}	V_j (kN)	V_{exp}/V_{pred} EC2
S1	BJ	52.12	50.10	1.04	291.72	1.07
S2	BJ	48.34	48.70	0.99	264.91	1.25
S3	BJ	43.91	47.50	0.92	241.46	1.18
S4	B	54.621	50.10	1.09	-	-
S5	B	51.306	48.70	1.05	-	-
S6	B	48.603	47.50	1.02	-	-

7.5.5.2 Joint shear strength

In this section, the experimental shear capacities of weak joints (joints that experienced BJ-failure) were compared to the design joint shear strength predicted by EC2 (2004) design codes. It should be noted that, in strong joints, no sign of shear failure was observed within the joint core and the detected failure was a B-mode failure. This means that specimens S4-S6 did not reach the joint failure shear strength. Therefore, S4-S5 were excluded from this discussion. In the following section, the experimental shear force in the joint (V_{jh}) is calculated based on the equilibrium principle in the horizontal direction (Eq. 1) as follows:

$$V_{jh} = T - V_{col} = \frac{PL_b}{0.9d_b} - \frac{P(L_b+0.5h_c)}{L_c} \quad (1)$$

where T is the tensile force in the beam reinforcement; V_{col} is the shear force of the column; P is the applied force at the beam end; L_b is the distance from the column face to the point of load application; d_b is the effective depth of the beam; h_c is the column depth; and L_c is the column length.

In EC 2 (2004), the beam-column joint can be considered as a part of the column within the beam depth. And the shear strength of the column can be calculated as follows:

$$V = \left[\tau_R k(1.2 + 40\rho_1) + 0.15\sigma_{cp}\right]bd + A_{sw}f_{yw}(0.9d/s) \quad (2)$$

where τ_R is the basic shear strength of concrete in MPa; $k = (1.6 - d)$, in which d is the effective depth of the column in (m); ρ_1 is the longitudinal reinforcement ratio in the column; σ_{cp} is the compression stress in the column (N/mm^2); A_{sw} is the area of transverse reinforcement (mm^2); s is the spacing between stirrups; and f_{yw} is the yield strength of stirrups (MPa).

It should be noted that, since the seismic design codes (i.e., ACI 352R, 2002; Eurocode 8, 2004) specify a sufficient number of lateral hoops to be provided within the joint panel, they should not be used to predict the joint shear strength of weak joint (without hoops).

Table 7-6 presents the experimental joint shear force (V_{jh}) and the ratio between the experimental shear force and the predictions of code equations for all tested weak joint specimens. By looking at the table, it can be noted that EC 2 conservatively predicts the shear strength of tested weak beam-column joints, providing a safety margin in the range of 1.07-1.25.

7.6 Conclusions

This chapter evaluates the behaviour of beam-column joints made with different types of aggregates (normal-weight and Stalite lightweight aggregates) under reversed cyclic loading. The performance of tested specimens was assessed in terms of load-carrying capacity, stiffness degradation, ductility, brittleness index, and energy dissipation capacity. The accuracy of design code provisions in predicting the shear and flexural strength of beam-column joints was also ascertained. Based on the experimental results obtained from this investigation, the following conclusions may be drawn:

1. Lightweight Stalite coarse/fine aggregates can be used to develop SCC mixtures with a concrete density of around 15.3% lighter than NWC. A properly detailed beam-column joint made with these LWSCC mixtures showed slightly lower load-carrying capacity under reversed cyclic loads of around 8.5% and ductility and dissipated energy of around 11.4% and 15.8% compared to NWSCC specimen.
2. Despite the brittle characteristics of Stalite lightweight aggregates that clearly observed in LWSCC beam-column joints without sufficient transverse reinforcement (weak joints), properly detailed Stalite LWSCC beam-column joints (strong joints) exhibited more ductile failure (ductile flexural beam failure, B-mode).
3. Designing LWSCC beam-column joints as a strong joint (with sufficient hoops) helped to alleviate the reduction in load-carrying capacity, rate of strength degradation, ductility, brittleness index, and energy dissipation capacity that resulted from using Stalite LWA when compared to NWSCC. For example, in

strong joints, using Stalite LWA showed a reduction in the load-carrying capacity of 8.5% (on average) compared to NWSCC joint, while this reduction reached up to 13.3% (on average) when comparing weak joints to NWSCC joint.

4. LWSCC beam-column joints made with Stalite fine aggregates appeared to have relatively better structural performance under cyclic loads compared to LWSCC with Stalite coarse aggregates. For example, using LF as a replacement of normal-weight sand reduced the load-carrying capacity, ductility index, and dissipated energy of tested weak beam-column joint by about 7.8%, 2.4%, and 1.9%, respectively (S2 compared to S1), while these reductions reached up to 18.7%, 20.8%, and 25.1%, respectively (S3 compared to S1), when LC was used.
5. The developed Stalite LWSCC mixtures in this investigation, especially those made with LF, proved to be a good candidate for lightweight structural members subjected to large deformations caused by earthquakes. This is because a minimum ductility index (μ) of 3 was recommended by previous researchers in the seismic areas (to ensure the redistribution of moments), while the developed Stalite LWSCC in this investigation had a high ductility index of 6.41.
6. The theoretical prediction of bending moment capacity of ACI design code did not show accurate results in Stalite LWSCC beam-column joints designed with a weak joint concept. This is because weak Stalite LWSCC joints in this investigation failed in BJ mode (combined shear and flexural failure) rather than a pure bending failure. On the other hand, in beam-column joints with sufficient hoops (strong joints), the theoretical prediction of the ACI code was conservative in estimating

the bending moment capacity. This confirms the observed mode of failure (B mode) in strong Stalite LWSCC joints.

7.7 References

Abouhussien, A. A., Hassan, A. A., and Hussein, A. A. (2015). Effect of expanded slate aggregate on fresh properties and shear behaviour of lightweight SCC beams. *Magazine of Concrete Research*, *67*(9), 433-442.

ACI Committee 318. (2019). Building Code Requirements for Structural Concrete (ACI 318-19) and Commentary. *American Concrete Institute, Farmington* Hills, MI.

ACI Committee 352. (2002). Recommendations for design of beam-column connections in monolithic reinforced concrete structures (ACI 352R-02). *American Concrete Institute*, Farmington Hills, MI.

Agrawal, P., and Shrikhande, M. (2006). *Earthquake resistant design of structures*. PHI Learning Pvt. Ltd..

Ashour, S. A. (2000). Effect of compressive strength and tensile reinforcement ratio on flexural behavior of high-strength concrete beams. *Engineering structures*, *22*(5), 413-423.

Bogas, J. A., and Gomes, A. (2013). Compressive behavior and failure modes of structural lightweight aggregate concrete–Characterization and strength prediction. *Materials & Design*, *46*, 832-841.

Bogas, J. A., Gomes, A., and Pereira, M. F. C. (2012). Self-compacting lightweight concrete produced with expanded clay aggregate. *Construction and Building Materials*, *35*, 1013-1022.

Chi, J. M., Huang, R., Yang, C. C., and Chang, J. J. (2003). Effect of aggregate properties on the strength and stiffness of lightweight concrete. *Cement and Concrete Composites*, *25*(2), 197-205.

EFNARC (2005). European Guidelines for Self-compacting Concrete Specification, Production and Use. European Federation for Specialist Construction Chemicals and Concrete Systems: Farnham, UK.

Eurocode 2. (2004). Design of Concrete Structures – Part 1-1: General Rules and Rules for Buildings. *European Committee for Standardization*, Brussels, Belgium.

Eurocode 8. (2004). Design of structures for earthquake resistance part 1: general rules, seismic actions and rules for buildings. *European Committee for Standardization,* Brussels, Belgium.

Forzani, B., Popov, E. P., and Bertero, V. V. (1979). *Hysteretic behavior of lightweight reinforced concrete beam-column subassemblages*. Berkeley, CA, USA: University of California, Earthquake Engineering Research Center.

Hassan, A. A., Ismail, M. K., and Mayo, J. (2015). Shear behavior of SCC beams with different coarse-to-fine aggregate ratios and coarse aggregate types. *Journal of Materials in Civil Engineering*, *27*(11), 04015022.

Hilal, N., Hamah Sor, N., and Faraj, R. H. (2021). Development of eco-efficient lightweight self-compacting concrete with high volume of recycled EPS waste materials. *Environmental Science and Pollution Research*, *28*(36), 50028-50051.

Kayali, O. (2008). Fly ash lightweight aggregates in high performance concrete. *Construction and building materials*, *22*(12), 2393-2399.

Lotfy, A., Hossain, K. M., and Lachemi, M. (2016). Durability properties of lightweight self-consolidating concrete developed with three types of aggregates. *Construction and Building Materials*, *106*, 43-54.

Mitchell, D. W., and Marzouk, H. (2007). Bond characteristics of high-strength lightweight concrete. *ACI Structural Journal*, *104*(1), 22.

Mousa, A., Mahgoub, M., and Hussein, M. (2018). Lightweight concrete in America: presence and challenges. *Sustainable Production and Consumption*, *15*, 131-144.

Nepomuceno, M. C., Pereira-de-Oliveira, L. A., and Pereira, S. F. (2018). Mix design of structural lightweight self-compacting concrete incorporating coarse lightweight expanded clay aggregates. *Construction and Building Materials*, *166*, 373-385.

Omar, A. T., and Hassan, A. A. (2019). Use of polymeric fibers to improve the mechanical properties and impact resistance of lightweight SCC. *Construction and Building Materials*, *229*, 116944.

Omar, A. T., and Hassan, A. A. (2021). Behaviour of expanded slate semi-lightweight SCC beams with improved cracking performance and shear capacity. In *Structures, 32,* 1577-1588.

Omar, A. T., and Hassan, A. A. (2021). Shear Behavior of Lightweight Self-Consolidating Concrete Beams Containing Coarse and Fine Lightweight Aggregates. *ACI Structural Journal*, *118*(3).

Omar, A. T., Sadek, M. M., and Hassan, A. A. (2020). Impact Resistance and Mechanical Properties of Lightweight Self-Consolidating Concrete under Cold Temperatures. *ACI Materials Journal*, *117*(5).

Paultre, P., Khayat, K. H., Cusson, D., and Tremblay, S. (2005). Structural performance of self-consolidating concrete used in confined concrete columns. *ACI structural journal*, *102*(4), 560-568.

Rabbat, B. G., Daniel, J. I., Weinmann, T. L., and Hanson, N. W. (1986). Seismic behavior of lightweight and normal weight concrete columns. In *Journal Proceedings* (Vol. 83, No. 1, pp. 69-79).

Sadek, M. M., and Hassan, A. A. (2021). Abrasion and Scaling Resistance of Lightweight Self-Consolidating Concrete Containing Expanded Slate Aggregate. *ACI Materials Journal*, *118*(2), 31-42.

Sin, L. H., Huan, W. T., Islam, M. R., and Mansur, M. A. (2011). Reinforced Lightweight Concrete Beams in Flexure. *ACI Structural Journal*, *108*(1).

Topcu, İ. B. (1997). Assessment of the brittleness index of rubberized concretes. *Cement and Concrete Research*, *27*(2), 177-183.

Wu, T., Wei, H., and Liu, X. (2018). Shear strength of interior beam–column joints with lightweight aggregate concrete. *Magazine of Concrete Research*, *70*(3), 109-128.

Yu, Q. L., Spiesz, P., and Brouwers, H. J. H. (2015). Ultra-lightweight concrete: Conceptual design and performance evaluation. *Cement and Concrete Composites*, *61*, 18-28.

8. Cyclic behavior of expanded slate lightweight SCC beam-column joints containing different lengths of PVA fibers

8.1 Abstract

This chapter investigates the structural performance of lightweight self-consolidating concrete (LWSCC) and lightweight vibrated concrete (LWVC) beam-column joints reinforced with PVA fibers under quasi-static reversed cyclic loading. A total of eight exterior beam-column joints with different lightweight aggregate types (coarse and fine expanded slate aggregates), different PVA fiber lengths (8 - 12 mm), and different percentages of fibers (0.3% and 1%) were casted and tested. The structural performance of the tested joints was assessed in terms of failure mode, hysteretic response, stiffness degradation, ductility, brittleness index, and energy dissipation capacity. The results revealed that LWSCC specimens made with expanded slate fine aggregates (LF) appeared to have better structural performance under reversed cyclic load compared to that containing expanded slate coarse aggregates (LC). Shorter length of PVA fibers proved to have a better enhancement in the structural performance of LWSCC-beam-column joints (BCJs) in terms of initial stiffness, load-carrying capacity, ductility, cracking activity, and energy dissipation capacity compared to longer fiber. The results also indicated that Using 1% PVA8 fibers in LWVC joint with high LC/LF aggregate content helped to develop joint with significant enhancement in load-carrying capacity, ductility, and energy dissipation, while maintaining reduced self-weight of 28% lower than normal-weight concrete.

8.2 Introduction

One of the guiding principles in designing an earthquake-resistant construction is to minimize the structure's mass (Agrawal & Shrikhande, 2006). Utilizing lightweight concrete (LWC) in construction practices can significantly diminish the gravity load and cross-sectional areas of structural elements and thus effectively reduce the seismic action on buildings (Kayali, 2008; Bogas & Gomes, 2013). Accordingly, LWC has been widely adopted with great success in multiple structural applications such as long-span bridges, high-rise buildings, and ocean platforms (Yu et al., 2015; Mousa et al., 2018). Meanwhile, it was pointed out that the mechanical characteristics and failure modes of LWC are quite different from that of normal-weight concrete (NWC). Unlike NWC, LWC normally exhibits a lower modulus of elasticity, steeper descending branch in the stress-strain curve, inferior shear resistant capacity, and more brittle fracture characteristics (Chi et al., 2003; Carmo et al., 2017; Wu et al., 2018). Also, the cracks initiate in the coarse aggregates of LWC during failure states, results in faster crack propagation and a significant drop in load-carrying capacity (Yang et al., 2014).

Among different types of lightweight aggregates, expanded slate (Stalite) lightweight aggregate is characterized by low density, dimensional stability, and high strength. The superior mechanical characteristics of this aggregate allowed to obtain concrete mixtures with high strength-to-weight ratio and improved impact and abrasion resistance (Omar & Hassan, 2019; Sadek & Hassan, 2021). Reinforced LWC beams made with expanded slate aggregate also exhibited higher shear resistance and better post-cracking resistance, compared with LWC beams made with other types of lightweight aggregates (Hassan et

al., 2015). However, the structural performance of expanded slate LWC members under reversed cyclic loads is not well documented and needs further investigation. By looking at the literature, it can be indicated that there is a contradiction in presenting the structural behavior of LWC under reversed cyclic loading. For example, four interior beam-column joints (BCJs) made with LWC and NWC were tested by Forzani et al. (1979) to evaluate their structural performance under monotonic and reversed cyclic loading. In their study, Lightweight expanded shale aggregate was adopted to produce LWC mixtures with a dry density of 1874 kg/m^3 and a compressive strength in the range of 31–35 MPa. The results obtained from their investigation indicated that the load-displacement curves obtained for NWC and LWC joints were quite similar under monotonic loading. However, when subjected to cyclic loading, LWC joints exhibited lower load-carrying capacity associated with more noticeable strength degradation and pinching of the hysteresis diagram compared to NWC specimens. On the contrary, Rabbat et al. (1986) reported in their study that LWC joints made with expanded shale and expanded clay performed similarly to their counterparts NWC joints in terms of strength, strength degradation, and energy dissipation. Beam-column joints are considered one of the weakest components in RC frame structures under seismic loading. Under strong earthquake events, BCJs are normally subjected to horizontal and vertical shear forces accompanied by large deformations that may lead to serious damage or global collapse of the structures. The catastrophic collapse observed, over the years, in RC structures during severe earthquakes demonstrated the crucial importance of ensuring proper ductility and damage tolerance of such structures during seismic events. Ductility is a desirable structural property that reflects the ability of any

structure to undergo significant deformations and dissipate the earthquake's energy without a substantial loss of strength (Rashid & Mansur, 2005). In order to provide adequate ductility for BCJs, seismic design codes (ACI 352R, 2002; ACI 318, 2019) recommend the use of closely spaced hoops within the joint core to prevent the early shear strength degradation of the connection. Nevertheless, closely spaced hoops' detailing usually leads to steel congestion in the joint, which causes difficulties in placing and consolidating the concrete in this region and thus risks formation of honeycombing within the joint. Furthermore, dense arrangements of transverse hoops may result in improper bonding between concrete and reinforcing bars, which may lead to a premature failure of the joint. Self-consolidating concrete (SCC) is an ideal choice in the situation of closely spaced hoops within the BCJs due to its high flowability and stability. SCC can overcome the compaction difficulties and reduce the risk of segregation, in such highly congested regions (Paultre et al., 2005). Lightweight self-consolidating concrete (LWSCC) is a novel type of high-performance concrete that can be adopted in multiple structural applications requiring high compactability and reduced self-weight. Another innovative solution in designing BCJs is the use of fiber-reinforced concrete. Adding fibres into concrete has proven to significantly improve the shear strength, ductility, stiffness degradation, energy dissipation, and damage tolerance of BCJs subjected to reverse cyclic loading (Ganesan et al., 2013; AbdelAleem & Hassan, 2019; Cardoso et al., 2019). The fibers' bridging mechanism effectively helps to transfer stress across crack interferences, providing residual strength to the concrete composite in post-peak stage (Cardoso et al., 2019; Çelik Z, Bingöl, 2020). Meanwhile, the stitching action of fibers plays an effective role in arresting cracks, thus

effectively delaying the initiation of cracks and limiting their propagation (AbdelAleem et al., 2017). Adding fibers into LWSCC has been found to alleviate the reduction in shear strength and other mechanical properties that results from using low-density aggregates (Omar & Hassan, 2021).

This chapter aims to investigate the performance of exterior BCJs made with fiber reinforced LWSCC and lightweight vibrated concrete (LWVC) mixtures containing coarse and fine expanded slate aggregates under reversed cyclic loading. This research also attempts to improve the performance of exterior LWSCC/LWVC beam-column joints by using different lengths and volumes of polyvinyl alcohol (PVA) fibers.

8.3 Research significance

Lightweight concrete proved to have several economic benefits in terms of reducing the structural elements self-weight and size in addition to reducing the seismic demand especially for structural elements that responsible to resisting seismic lateral loads. However, the brittle characteristics of lightweight aggregates in LWC impose a big challenge to employ such concrete in structures that requires high ductility and energy-absorption capacity. Using fibers especially polymeric fibers proved to have a significant effect on enhancing the load-carrying capacity, ductility, cracking activity, and energy dissipation capacity of concrete without a considerable increase in the self-weight of concrete. Combining the desired properties of polymeric fibers (PVA fibers) with the economic benefits of LWC can be considered as an effective technique to develop a concrete composite with a minimized self-weight and high level of ductility.

The structural behavior of LWC reinforced with polymeric fibers under the action of cyclic loading is not well demonstrated in the available literature, especially when expanded slate lightweight aggregates were used. Despite the outstanding performance of expanded slate lightweight aggregates compared to all other lightweight aggregates, insufficient studies were conducted to examine the performance of concrete members containing this type of lightweight aggregate under reversed cyclic loading. Therefore, this chapter attempts to address this lack of knowledge by presenting a comprehensive investigation into the structural performance of fiber reinforced LWC-BCJs subjected to reversed cyclic loading.

8.4 Experimental Program

8.4.1 Materials and properties

Type I portland cement, type F fly ash (FA), and class N metakaolin (MK) were used to develop the concrete mixtures investigated in this study. Graded crushed granite stones (10 mm maximum aggregate size) and natural sand (passing through 4.75 mm IS sieve) were used as normal-weight coarse (NC) and fine (NF) aggregates, respectively. Both aggregates (NC and NF) had a specific gravity of 2.6 and absorption ratio of 1%. Expanded slate lightweight coarse aggregate (LC) and expanded slate lightweight fine aggregate (LF) were used to optimize the LWSCC mixtures. The specific gravities of Stalite LC and LF aggregates were 1.53 and 1.80, respectively. Expanded slate (Stalite) aggregates were provided by the Carolina Stalite Company (Salisbury, NC, USA), which were prepared by expanding slate rocks in a rotary kiln at temperatures over 1000°C. Two types of commercial PVA fibers were used: PVA8 (8 mm long and 38 μm in diameter) and PVA12 (12 mm long and 100 μm in diameter) (see Figure 8-1). The tensile strengths of PVA8 and

PVA12 were 1600 and 1300 MPa, respectively, and both fibers had a specific gravity of 1.3. A high-range water-reducing admixture was utilized during mixing to obtain the required slump flow for the developed mixtures.

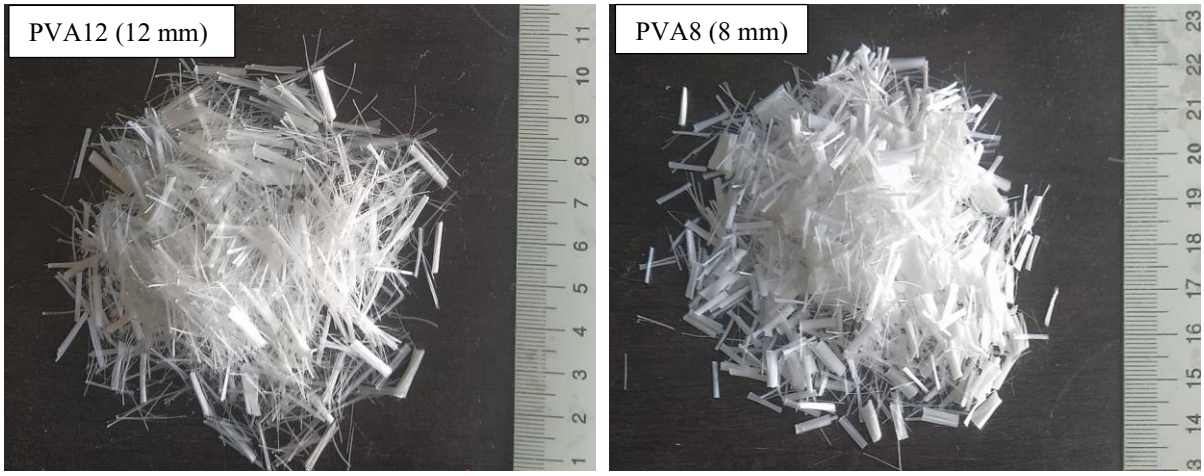

Figure 8-1: Polyvinyl alcohol (PVA) fibers used in this work.

8.4.2 Concrete mixtures, casting, and specimen details

This investigation contained a total of eight mixtures (eight beam-column joints) including: 5 LWSCC and fiber-reinforced LWSCC; two lightweight vibrated concrete (LWVC) and fibered LWVC; and one normal-weight self-consolidating concrete (NWSCC) mixtures. Table 8-1 provides the mixture proportions of all developed mixtures.

All tested joints were cast with identical concrete dimensions and were designed to fail in flexure with a ductile behavior according to ACI 318 (2019). L-shape bars with adequate developmental lengths were provided at the top and bottom of the beam to avoid bond/slip failure. Figure 8-2**a** shows the typical concrete dimensions and reinforcement details of all tested specimens.

Table 8-1: Mixture proportions of NWSCC, LWSCC, and LWVC mixtures with/without fibers.

Mix/ Joint #	Mixture ID	Cement (kg/m^3)	SCMs (Type)	SCMs (kg/m^3)	Aggregate					Fiber (%)
					C/F ratio	NC (kg/m^3)	NF (kg/m^3)	LC (kg/m^3)	LF (kg/m^3)	
S1	NWSCC	275	FA+MK	165+110	1.0	753.2	753.2	-	-	-
S2	LWSCC-LC	275	FA+MK	165+110	0.7	-	689.2	482.4	-	-
S3	LWSCC-LC-0.3PVA12	275	FA+MK	165+110	0.7	-	685.6	480.0	-	0.3
S4	LWSCC-LC-0.3PVA8	275	FA+MK	165+110	0.7	-	685.6	480.0	-	0.3
S5	LWSCC-LF	275	FA+MK	165+110	1.0	617.3	-	-	617.3	-
S6	LWSCC-LF-0.3PVA8	275	FA+MK	165+110	1.0	614.1	-	-	614.1	0.3
S7	All-LWVC	275	FA+MK	165+110	1.5	-	-	566.8	377.9	-
S8	All-LWVC-1PVA8	275	FA+MK	165+110	1.5	-	-	557.1	371.4	1.0

Note: All mixtures have a 0.4 w/b ratio; MK = metakaolin; FA = fly ash; C/F = coarse-to-fine aggregate ratio (by weight); NC = normal-weight coarse aggregate; NF = normal-weight fine aggregate; LC = lightweight coarse aggregate; and LF = lightweight fine aggregate.

8.4.3 Fresh and mechanical properties tests

The fresh properties of NWSCC and LWSCC mixtures were assessed in terms of slump flow, V-funnel, and L-box tests as per EFNARC guidelines (2005). During the casting of each BCJ, six identical concrete cylinders (200 mm height x 100 mm diameter) were poured. After 28 days, the compressive strength (f'_c) and splitting tensile strength (*STS*) tests were performed on these concrete cylinders (three cylinders for each property) as per ASTM C39 and C496, respectively. All tested cylinders were cast without external consolidation and exposed to a curing regime similar to that of the tested BCJs. The fresh and mechanical properties of the tested mixtures are summarized in Table 8-2.

Table 8-2: Fresh and mechanical properties for tested mixtures.

Mixture designation	T_{50} (sec)	V-funnel (sec)	L-box ratio (H_2/H_1)	f'_c (MPa)	*STS* (MPa)	*Dry density* (kg/m^3)
NWSCC	2.30	7.75	0.92	67.5	3.95	2261.2
LWSCC-LC	2.75	10.80	0.89	51.8	2.88	1909.1
LWSCC-LC-0.3PVA12	3.95	13.10	0.79	48.9	3.40	1907.5
LWSCC-LC-0.3PVA8	3.51	11.30	0.82	50.5	3.62	1905.2
LWSCC-LF	2.10	5.90	0.95	52.3	3.10	1982.8
LWSCC-LF-0.3PVA8	2.45	6.45	0.85	50.7	3.92	1978.2
All-LWVC	-	-	-	43.1	2.36	1630.8
All-LWVC-1PVA8	-	-	-	36.7	3.35	1627.5

Note: f'_c = 28-day compressive strength; and *STS* = splitting tensile strength.

8.4.4 Test setup and loading procedure

Figure 8-2**b** shows the configuration of the test setup adopted in this investigation. The column was vertically positioned in the testing frame and firmly fixed under the application of about 10% of its nominal compressive capacity using a hydraulic jack to represent the gravity loads. The axial load acting on the column remained constant throughout the test

and was monitored using a data acquisition system. All tested specimens were subjected to reversed cyclic vertical displacement loading applied at the beam's tip (90 mm away from the beam's end [Figure 8-2]) using a 500 kN servo-hydraulic dynamic actuator. A quasi-static displacement-controlled loading procedure (Figure 8-3) was adopted, following the ACI 2006 guidelines for moment-resisting frames. The displacement was applied with increasing amplitude in different load steps. Each load step had three full reversed cycles with a frequency of 0.08 Hz. In order to monitor the deflection at the beam's tip and beam's mid-span, all tested specimens were suitably instrumented with a linear variable differential transducer (LVDT). In addition, the strains at the section of the maximum moment were recorded using two electrical resistance strain gauges affixed to the bottom and top longitudinal beam's reinforcement. The crack propagation after each loading step was closely observed and sketched. The loading process was stopped when a significant drop in the load-carrying capacity was observed. Throughout the test history, the measurements of load cells, LVDTs, and strain gauges were continuously monitored and automatically recorded with a data acquisition system. Finally, based on the readings obtained from this test, the performance of tested joints was assessed in terms of failure modes, hysteresis response, ductility, brittleness index, energy dissipation capacity, and stiffness degradation.

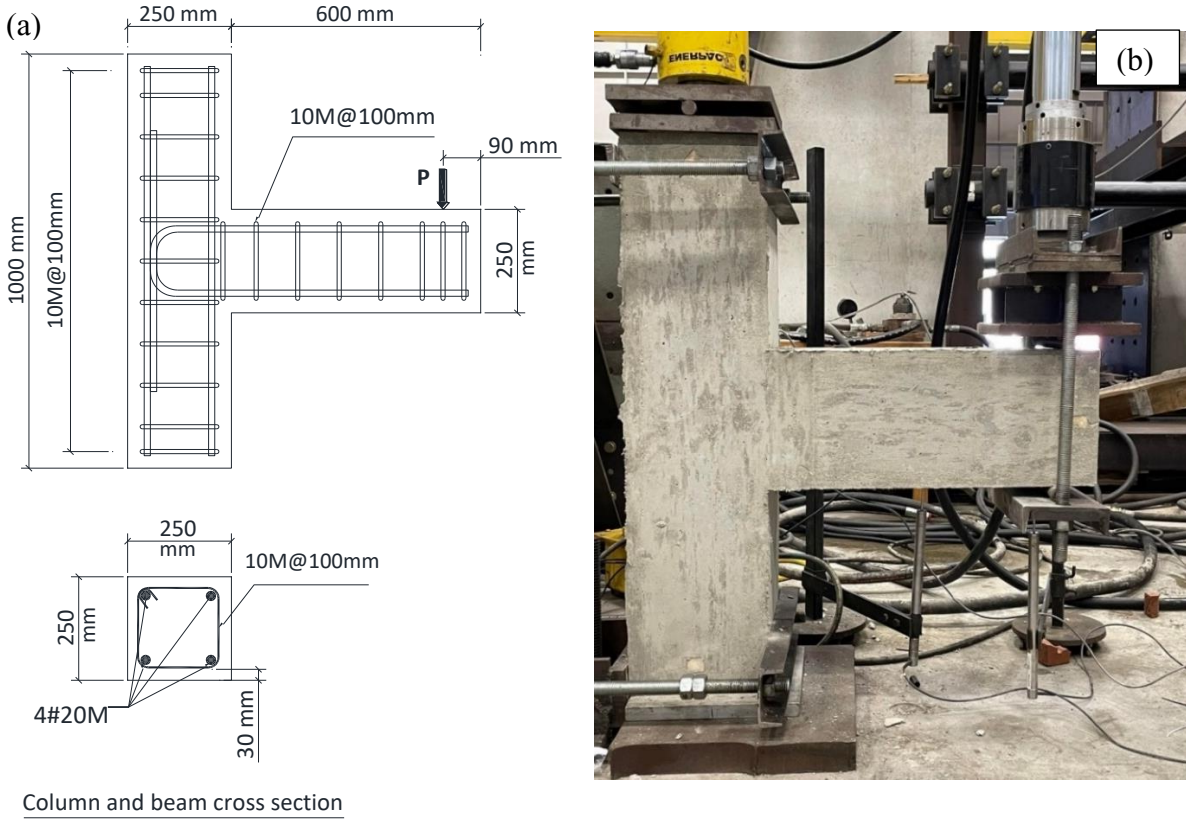

Figure 8-2: Configuration of: (a) Specimen dimensions and reinforcement details; and (b) test setup.

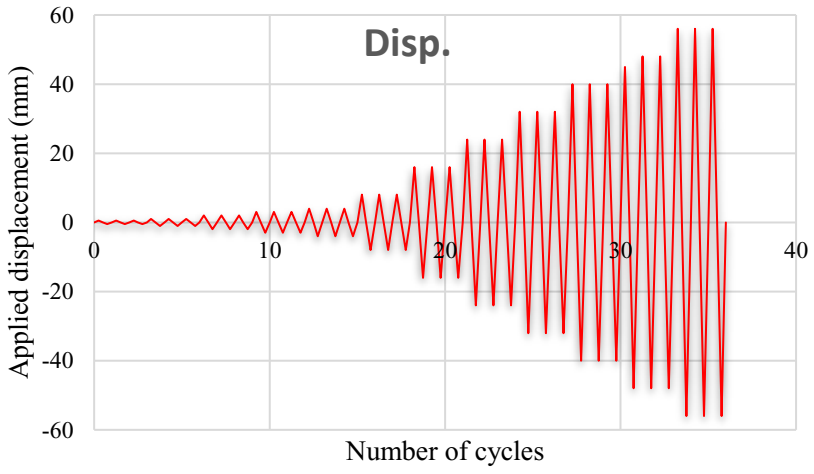

Figure 8-3: Sequence of applied displacement.

8.5 Results and discussion

8.5.1 Failure modes

Figure 8-4 shows, schematically, the cracking pattern of all tested beam-column joints at the failure stage. Table 8-3 also presents the failure mode for all tested specimens under cyclic loading. It can be observed that LWSCC joint made with LF (S5) exhibited failure mode (B-mode) similar to NWSCC joint (S1), in which the beam longitudinal reinforcement reached yield (as confirmed by the strain gauges attached to the steel rebars) with no formation of shear cracks in the joint panel up to failure (Figure 8-4). On the other hand, LWSCC joint made with LC (S2) exhibited BJ-mode at failure stage, in which the beam longitudinal reinforcement reached yield first and then diagonal cracks in the joint zone were formed (see Figure 8-4). The lower tensile strength and reduced aggregate interlock resistance of LWSCC-LC mixture, compared to that made with LF (which was mixed with strong normal weight coarse aggregate), were the main reason behind the initiation of the shear crack within the S2 joint core.

Table 8-3 shows that the inclusion of PVA fibers into LWSCC-LC specimens succeeded to change the failure mode from a combined shear/flexural failure (BJ-mode) (S2) to pure bending failure (B-mode) (S3-S4). In the meantime, all fibred-LWSCC joints exhibited failure mode similar to that observed in control specimens without fibers (B-mode). This behavior can be related to the role of fibers in arresting cracks by stitching action, which improved the joint shear strength, and in turn changed the failure mode to B-mode failure. The results also indicated that LWVC beam-column joints (S7) with all lightweight aggregates, exhibited a BJ-mode of failure. This may be related to the excessive reduction

in the compressive strength resulted from using high percentages of lightweight aggregate (in attempt to reach a concrete dry density of 1630 kg/m^3), which negatively affects the joint shear strength. The possibility of using up to 1% fiber volume in S8 (with a density level similar to S7) contributed to changing the latter failure mode to B-mode. The results of strain gauges glued at the surface of the rebar also confirmed that the upper and lower steel rebars at the beam-column interface section reached yield before failure for all tested specimens.

8.5.2 Cracking analysis

Figure 8-4 and Table 8-3 show the cracking pattern, maximum crack width at beam-column interface, and maximum crack width within the beam-column joint. All crack widths in Figure 8-4 are in mm and their values are corresponding to the failure load at cycle 21 (load step 7). By comparing LWSCC to NWSCC specimens, it can be seen that the cracking pattern of LWSCC joints was dominated by a higher number of cracks with reduced crack openings at beam-column interface. For example, replacing NF with LF (at the same C/F ratio of 1.0) increased the number of cracks from 8 to 11 cracks, while the maximum crack width at the interface decreased by about 23.4% (S5 compared to S1). This behavior can be related to the reduction in concrete tensile strength (due to the use of low-density aggregate), encouraging more flexural cracks to initiate throughout the beam's length rather than continuing to widen existing cracks.

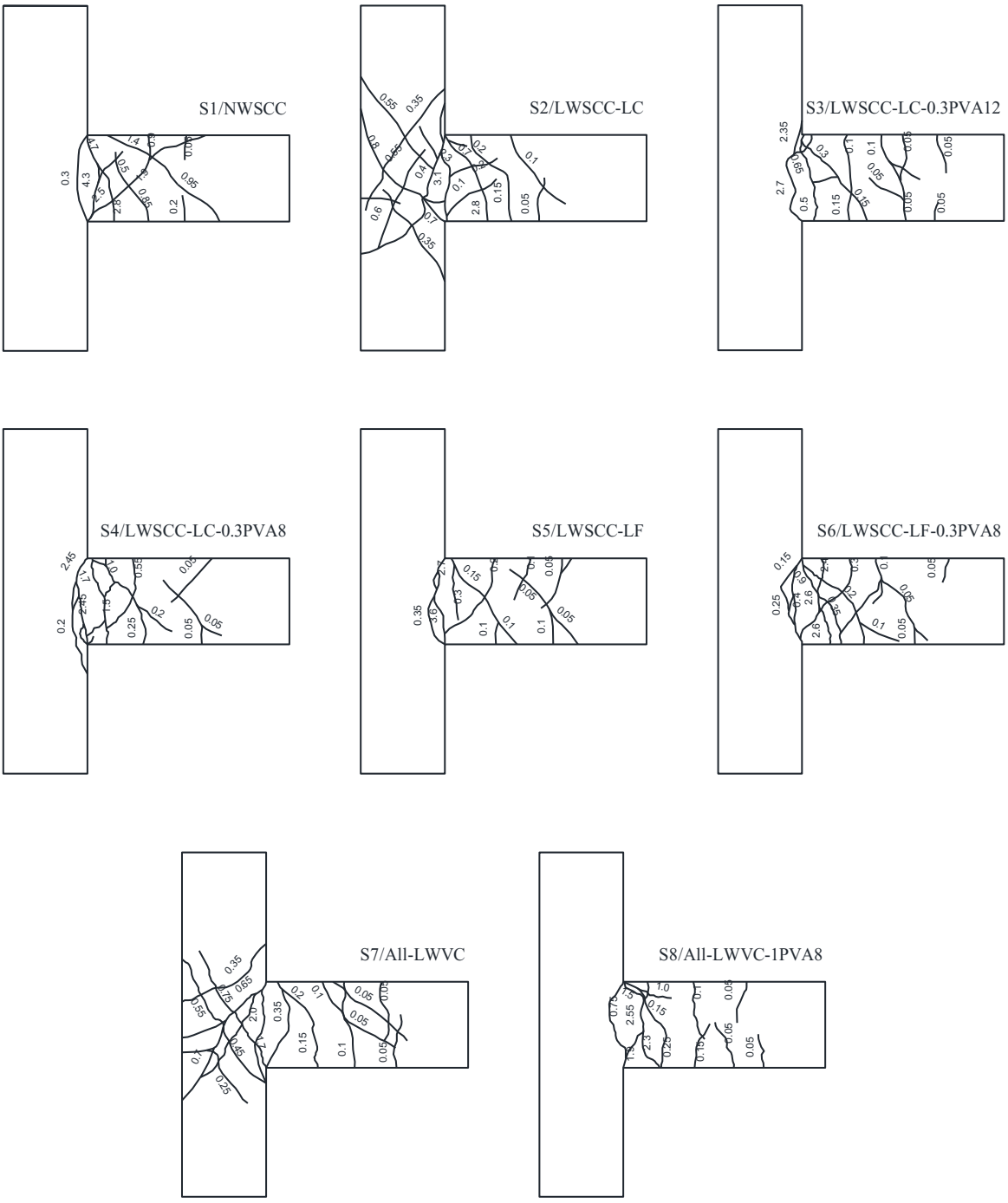

Figure 8-4: Crack patterns of tested beam-column joints at failure.

Table 8-3: Results of reversed cyclic loading.

Joint #	Specimen ID	1st Crack load (kN)	Ultimate load (kN)	Initial Stiffness (kN/mm)	Failure Mode	Number of cracks	Crack width	
							At beam-column interface (mm)	Within joint panel (mm)
S1	NWSCC	29.8	108.3	13.27	B-mode	8	4.70	-
S2	LWSCC-LC	19.3	92.5	11.33	BJ-mode	13	3.10	0.80
S3	LWSCC-LC-0.3PVA12	24.1	99.7	12.03	B-mode	11	2.70	-
S4	LWSCC-LC-0.3PVA8	25.6	104.8	12.99	B-mode	10	2.45	-
S5	LWSCC-LF	21.5	97.6	12.65	B-mode	11	3.60	-
S6	LWSCC-LF-0.3PVA8	28.3	107.8	13.98	B-mode	11	2.60	-
S7	All-LWVC	16.7	83.2	10.26	BJ-mode	14	2.35	0.75
S8	All-LWVC-1PVA8	23.5	101.3	15.06	B-mode	9	2.55	-

From Figure 8-4 and Table 8-3, it can also be observed that LWSCC joints reinforced with PVA fibers exhibited relatively reduced crack openings under cyclic loading, when compared to non-fibered LWSCC counterparts. For instance, the possibility of using 0.3% PVA12 fibers with LWSCC-LC joints reduced the maximum crack width at beam-column interface by about 13% compared to control specimen without fibers (S3 versus S2). This is related to the role of fibers in stitching the cracks and limited their opening. Further reduction in the maximum crack width at the interface was observed when shorter fibers were used instead of longer fibers. For example, using PVA8 fibers reduced the maximum crack width at beam-column interface by about 21% compared to control specimen without fiber (compared to 13% reduction when PVA 12 was used). It should be noted that, at a given percentage of fibers, using shorter fibers ensures a higher number of single fibers dispersed within matrix. This improves the fiber stitching mechanism and, hence, helps to better control the crack widening. By looking at LWVC joints with all lightweight aggregates (S7-S8), it can be observed that the inclusion of 1% PVA8 fibers in S8 succeeded to compensate for the reduction in joint shear strength that resulted from using LC and LF aggregate with high lightweight aggregate ratio. The inclusion of such high percentage of PVA fibers (1%) helped to arrest the initiation of cracks within the beam-column joint and reduced the number of cracks at beam-column interface (S8 vs. S7).

8.5.3 Load-displacement envelope curves

The envelop load-tip deflection curves for all tested beam-column joints are shown in Figure 8-5. The envelop curves were drawn using the points of maximum load with their corresponding deflection from the first cycle in each load step from hysteresis loops. From

the figure, it can be noticed that although all tested specimens showed a similar pattern in the push and pull directions, there is a slight difference in the values of the peak load in each direction. This can be due to the geometrical imperfections and steel bars disposition during casting concrete in BCJs. Table 8-4 shows the results of deflection corresponding to ultimate load and ultimate deflection, which defined as the deflection value at 85% of the ultimate load in the post-peak portion of the load-deflection envelope curve. From the table, it can be indicated that replacing normal weight coarse aggregate with LC, in attempt to reduce the concrete density by about 15.5%, reduced the ultimate deflection and the deflection corresponding to ultimate load of tested BCJs by 16% and 4% respectively. The higher reduction in the ultimate deflection can be related to the steep slope of the descending portion of load-deflection envelop curve, which resulted in a lower ultimate deformation that corresponding to 85% of the ultimate load. The crack paths in LWC usually go through the coarse aggregate particles rather than around them, demonstrating a brittle failure with a faster crack propagation, and thus increases the stiffness degradation in the post-peak portion of load-deflection curve. On the other hand, employing LF as a replacement to normal-weight sand (in attempt to obtain minimum density of 12.3% lower than NWSCC) showed an enhanced stiffness degradation in the post-peak stage of loading compared to counterpart LWSCC-LC sample. A possible explanation is that using low stiffness expanded slate fine aggregates in the production of LWSCC-LF mixtures made the cement mortar more deformable than the conventional cement mortar containing conventional sand. This contributed to the initiation of a great number of micro-cracks in

the cement mortar, and hence improved the deformability of the LWSCC-LF joint prior to failure.

Figure 8-5 (**b** and **c**) and Table 8-4 also showed that the possibility of developing successful LWSCC mixtures with 0.3% PVA fibers in this study helped to increase the deformability of tested LWSCC-BCJs under reversed cyclic loading. For instance, using 0.3% PVA12 fibers increased the ultimate deflection and the deflection corresponding to ultimate load of the LWSCC-LC specimens by about 38.9% and 4%, respectively (S3 compared to S2). The results also indicated that S4 joint reinforced with shorter fibers (PVA8) showed better improvements in terms of ultimate deflection and deflection at ultimate load reached up to 44.8% and 5.9%, respectively (S4 compared to S2). The better results of shorter fibers compared to longer fibers could be attributed to the better dispersion of shorter fibers as mentioned earlier in the cracking analysis section. It should be noted that the better enhancement in the ultimate deflection compared to deflection corresponding to ultimate load can be related to the effect of fibers in reducing the rate of strength degradation in post-peak stage. This in turn helped to significantly increase the ultimate deflection (deflection corresponding to 85% of ultimate load) compared to deflection corresponding to ultimate load in joints reinforced with fibers.

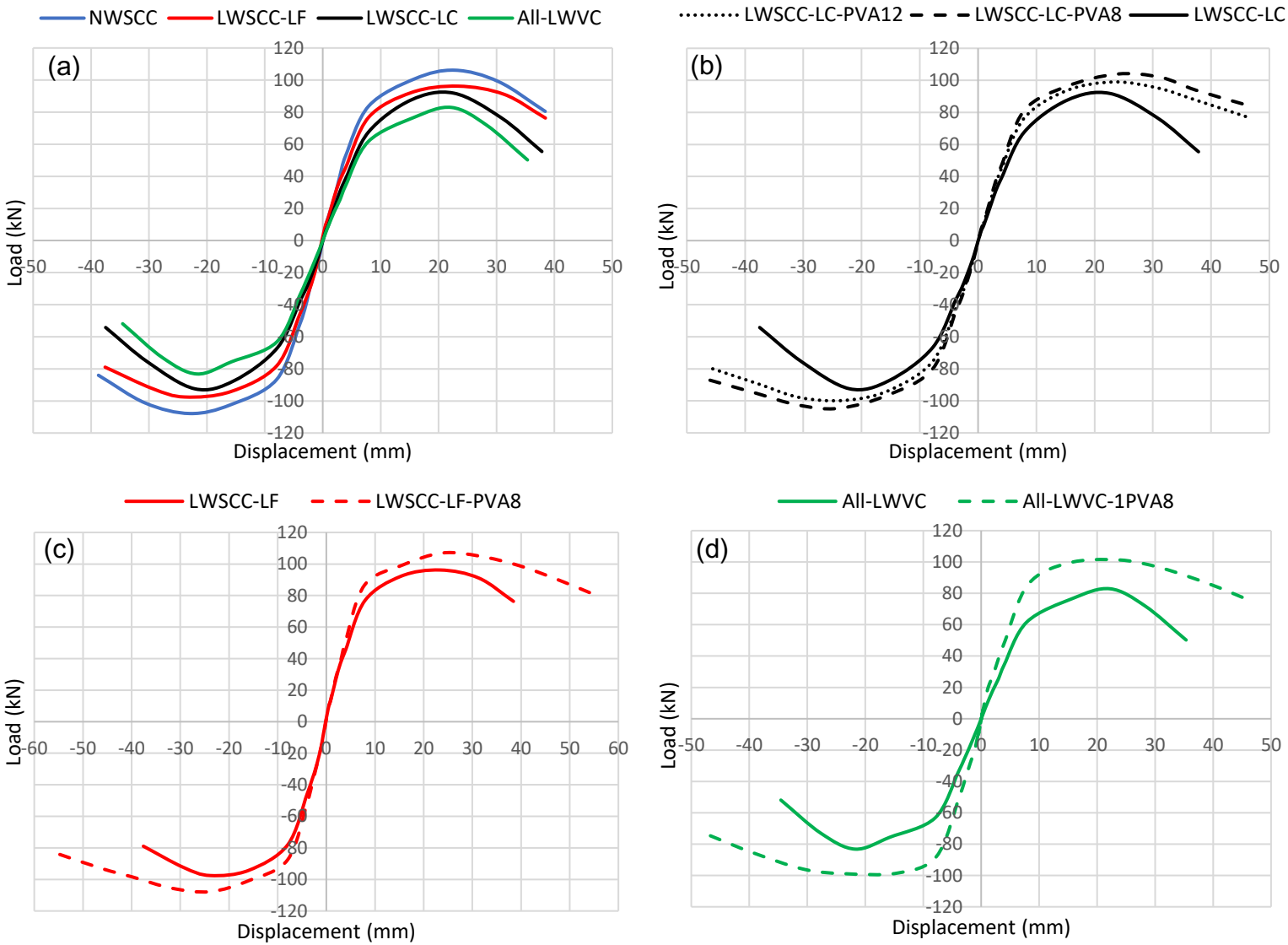

Figure 8-5: Load-displacement envelop curves for all tested joints.

Figure 8-5**d** shows the load-deflection envelope curves for LWVC joints developed with maximized volume of expanded slate aggregates (achieving a reduction of 28% in the concrete density) and maximized fraction of PVA fibers (1%). Looking at Figure 8-5**d** and Table 8-4, it can be seen that although the development of S7 mixture allowed to reach a LWVC with minimum density of 1630 kg/m^3 and suitable strength (Table 8-2), this joint exhibited a significant reduction in deformability. However, adding a high-volume fraction of PVA8 fibers (1%) to this mixture in joint S8 compensated for this reduction and helped to achieve joint with higher deformability without affecting the concrete density.

8.5.4 First crack load and ultimate load

The first crack load was observed visually, at an early stage of loading. Table 8-3 presents the first crack load and ultimate load results for all tested joints. Replacing normal weight coarse aggregate with LC, in attempt to reduce the concrete density by about 15.5%, reduced the first crack load and ultimate load of BCJs by about 35.2% and 14.6%, respectively. Meanwhile, using LF as a replacement of normal-weight sand reduced the first crack load and ultimate load of BCJs by about 27.8% and 9.8%, respectively. The reduction in first crack load of tested LWSCC joints can be explained by the substantial decline in the tensile strength of LWSCC mixtures as a result of using low stiffness expanded slate lightweight aggregates (refer to Table 8-2). In the meantime, the reduction in load-carrying capacity can be attributed to the drop in compressive strength (due to using lower density aggregate), which in turn reduced the joint shear strength and flexural strength of beam section It can also be noted that using LC showed a more pronounced reduction in the ultimate load capacity of LWSCC-BCJs compared to LF (see Table 8-3).

This may be related to the lower interlock resistance of LC in resisting higher shear stress compared to the normal weight aggregate used in the LWSCC-LF joint (Omar & Hassan, 2021b). This, in turn, contributed to weaken the joint shear strength of the LWSCC-LC joint and hence resulted in a pronounced decreased load-carrying capacity.

Table 8-3 also showed that optimizing successful expanded slate LWSCC mixtures with 0.3% PVA8 seemed to greatly increase the first cracking load and load carrying capacity of LWSCC joints by about 32.6% and 13.4%, respectively, compared with joint without fibers (S4 compared with S2). This performance can be related to the mechanism of PVA fibers in delaying the initiation of cracks and forcing the cracks to take an irregular path, demanding more energy for further propagation and in turn increasing the first cracking load and ultimate load capacity of tested specimens. The results also indicated that adding longer fibers (PVA12), at the same fiber volume, slightly improved the first crack load and load carrying capacity compared with shorter fibers (PVA8). Combining high percentage of PVA8 fibers (1%) with maximized lightweight aggregate ratio in S8 helped to recovering the reductions in the first crack load and ultimate load resulted from using high lightweight aggregate ratio and achieving a strength comparable to NWSCC joint with maintaining minimized density reached to 1627.5 kg/m^3.

8.5.5 Ductility and brittleness

Ductility is a crucial factor for any structural element, especially in regions of seismic activity. Ductility reflects the ability of the structural element to undergo significant deformations beyond the yield point and before failure. In this study, the displacement ductility index (μ) for all tested beam-column joints was expressed in terms of μ = the

ultimate deflection (Δ_u)/the yield deflection (Δ_y). Ultimate deflection Δ_u was defined as the deflection value corresponding to 85% of the maximum load in post-peak branch of the load-deflection envelop curve. Meanwhile, yield deflection Δ_y was taken as the deflection value corresponding to the point of intersection between the horizontal line at 85% of the ultimate load and the extension of the line that passes through the origin and 50% of the ultimate load (Shannag et al., 2002). The brittleness index (BI) was also calculated in this study to evaluate the ductility and deformability of the tested joints. BI of concrete joints can be defined as the ratio of the recovered deformation energy obtained before fracture to the irreversible plastic energy consumed during the failure (A2/A1 in Figure 8-6) (Topcu, 1997). The ductility index (μ) and brittleness index (BI) of all tested beams are presented in Table 8-4 and Figure 8-7.

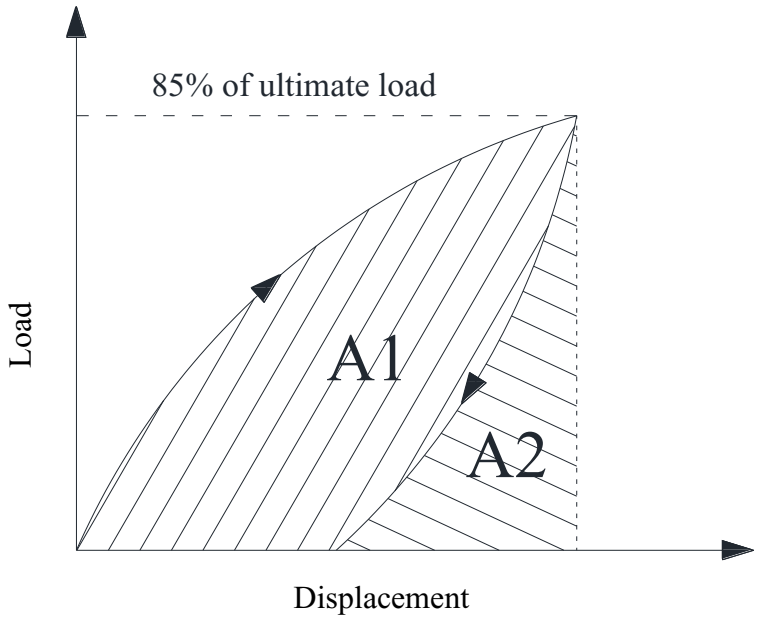

Figure 8-6: Definition of brittleness index.

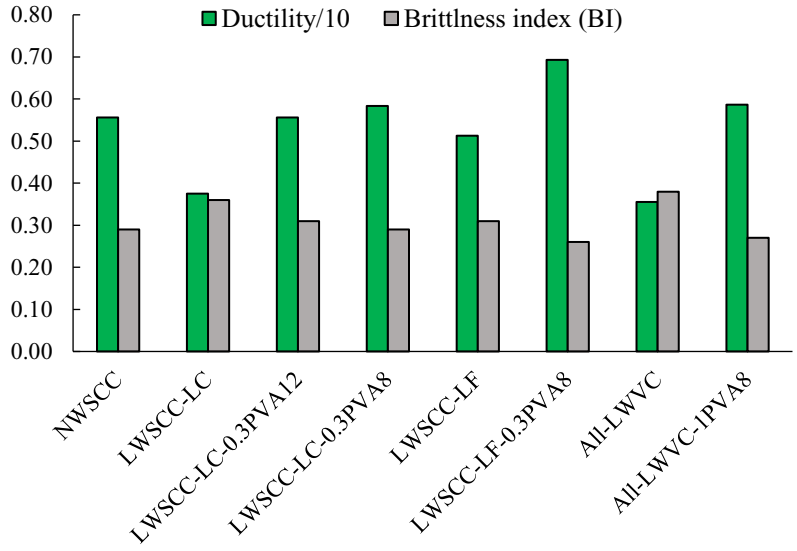

Figure 8-7: Results of ductility and brittleness index.

Table 8-4: Yield deflection, ultimate deflection, ductility, and brittleness index.

Joint #	Specimen ID	Yield deflection Δ_y (mm)	Deflection at peak load (mm)	Ultimate deflection Δ_u (mm)	ductility index (μ)	Brittleness index (BI)
S1	NWSCC	6.40	22.93	35.60	5.56	0.29
S2	LWSCC-LC	7.95	22.08	29.80	3.75	0.36
S3	LWSCC-LC-0.3PVA12	7.50	22.97	41.20	5.49	0.31
S4	LWSCC-LC-0.3PVA8	7.40	23.38	43.15	5.83	0.29
S5	LWSCC-LF	7.00	22.85	35.90	5.13	0.31
S6	LWSCC-LF-0.3PVA8	6.85	23.87	47.45	6.93	0.26
S7	All-LWVC	8.10	21.75	28.75	3.59	0.38
S8	All-LWVC-1PVA8	6.70	23.74	39.30	5.87	0.27

Replacing the normal-weight coarse aggregate in NWSCC (S1) with LC in S2 (achieving a reduction in the mixtures' density by about 15.5%) lowered the ductility ratio by about 32.6% and increased the BI by 24.1%. This reduction in ductility (increase in BI) can be explained by the change in failure mode from B-mode to BJ-mode due to using LC, which resulted in lower ultimate deflection (Δu) and hence decreased the ductility of LWSCC-

LC joint compared to NWSCC counterpart. In contrast, replacing the normal-weight sand with LF in the development of LWSCC-LF (S5), in an attempt to reduce the concrete density by about 12.3%, showed a relatively slight reduction in the ductility of tested joints (compared to joint with LC, which showed a higher reduction). By comparing LWSCC-LF joint (S5) to NWSCC joint (S1), it can be noted that the ductility ratio decreased by 7.7%, while the BI increased by about 6.9%. Such findings can be related to the high rate of deformation exhibited by LWSCC-LF joint prior to failure (compared to the low ultimate deflection experienced by counterpart LWSCC-LC joint) which resulted in a slight reduction in the ductility of LWSCC-LF joints compared to NWSCC one.

Table 8-4 also illustrates the ductility index and BI of LWSCC beam-column joints reinforced with PVA fibers. From the table, it can be noted that the ductility of tested joints generally increased with the addition of fibers. In particular, optimizing successful expanded slate LWSCC mixtures with 0.3% PVA fibers efficiently mitigated the reduction in ductility that resulted from replacing normal-weight coarse aggregate with LC (see Table 8-4 and Figure 8-7). For example, incorporating PVA12 exhibited an increase in the ductility index of LWSCC-LC joints by about 46.6% and reduced the BI by about 13.9%, compared to control joint without fiber (S3 compared to S2), achieving a ductility comparable to NWSCC joint. Meanwhile, the use of PVA8 more obviously improved the ductility of tested LWSCC-BCJs, exhibiting an increase in the μ by about 55.6% and a reduction in the BI by 19.4%, compared to LWSCC joint without fiber (S4 compared to S2). Similar performance was observed with LWSCC-LF joints, in which the inclusion of 0.3% PVA8 fibers helped the tested joints to reach a ductility index of 6.93. It should be

noted that a minimum ductility index (μ) of 3 is considered imperative to ensure the redistribution of moments, especially in the areas of seismic design (Sin et al., 2011; Eurocode 2, 2004). Accordingly, fibered-LWSCC joints proved to have an adequate ductile behaviour that can be considered for structural elements subjected to large deformations caused by earthquakes.

Table 8-4 also showed that a significant reduction in the self-weight by 28% was observed when normal-weight coarse and fine aggregate were replaced by Stalite LC and LF aggregate in the production of LWVC joint (reaching a concrete dry density of 1630 kg/m^3). However, the ductility of this LWVC joint (S7) was also significantly reduced by 35.4%. In this study, the development of successful expanded slate LWVC mixture with up 1% PVA8 fibers (S8) helped to compensate for the reduction in the joint ductility, achieving ductility comparable to NWSCC mixture with maintaining a minimized self-weight reached up to 28% lower than NWSCC joint.

8.5.6 Energy dissipation capacities

The nonlinear behavior of BCJs during the cyclic load history has been evaluated by calculating the hysteretic energy dissipation capacity. This property is a measure to estimate the energy dissipated of beam-column joints in the post-elastic stage of loading. In this study, the hysteretic energy dissipation capacity was computed by summing up the area enclosed by all hysteresis loops in the load-displacement diagram. The hysteretic cycles of the load-deflection curve for all tested joints (S1-S8) are shown in Figure 8-8, while Figure 8-9 presents the cumulative energy dissipation results for all tested specimens.

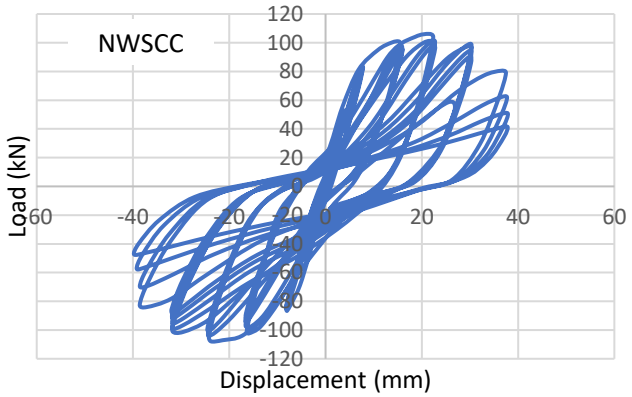
NWSCC
Load (kN)
Displacement (mm)
120
100
80
60
40
20
0
-20
-40
-60
-80
-100
-120
-60
-40
-20
0
20
40
60

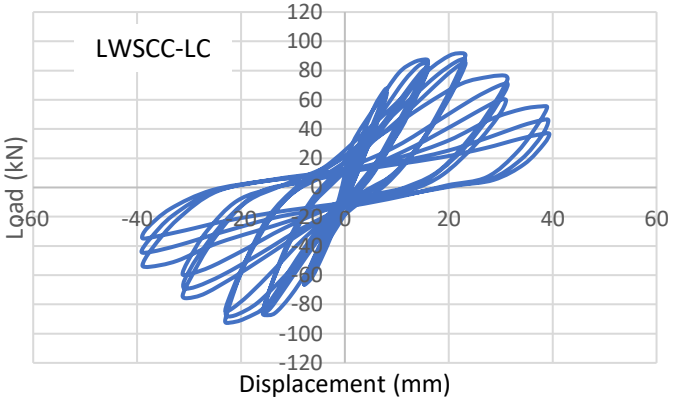
LWSCC-LC
Load (kN)
Displacement (mm)
120
100
80
60
40
20
0
-20
-40
-60
-80
-100
-120
-60
-40
-20
0
20
40
60

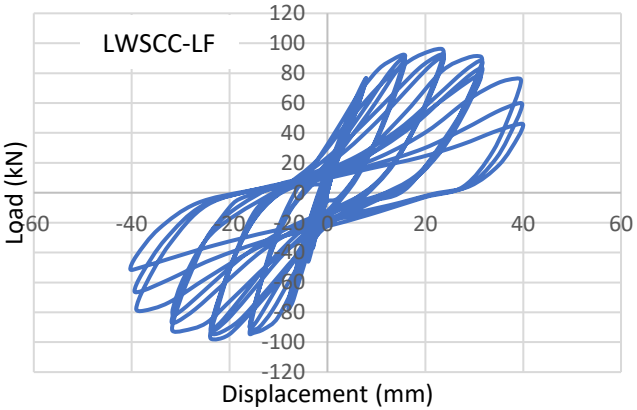
LWSCC-LF
Load (kN)
Displacement (mm)
120
100
80
60
40
20
0
-20
-40
-60
-80
-100
-120
-60
-40
-20
0
20
40
60

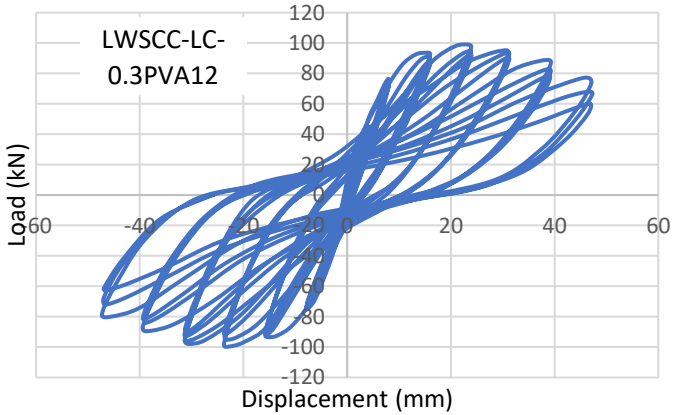
LWSCC-LC-
0.3PVA12
Load (kN)
Displacement (mm)
120
100
80
60
40
20
0
-20
-40
-60
-80
-100
-120
-60
-40
-20
0
20
40
60

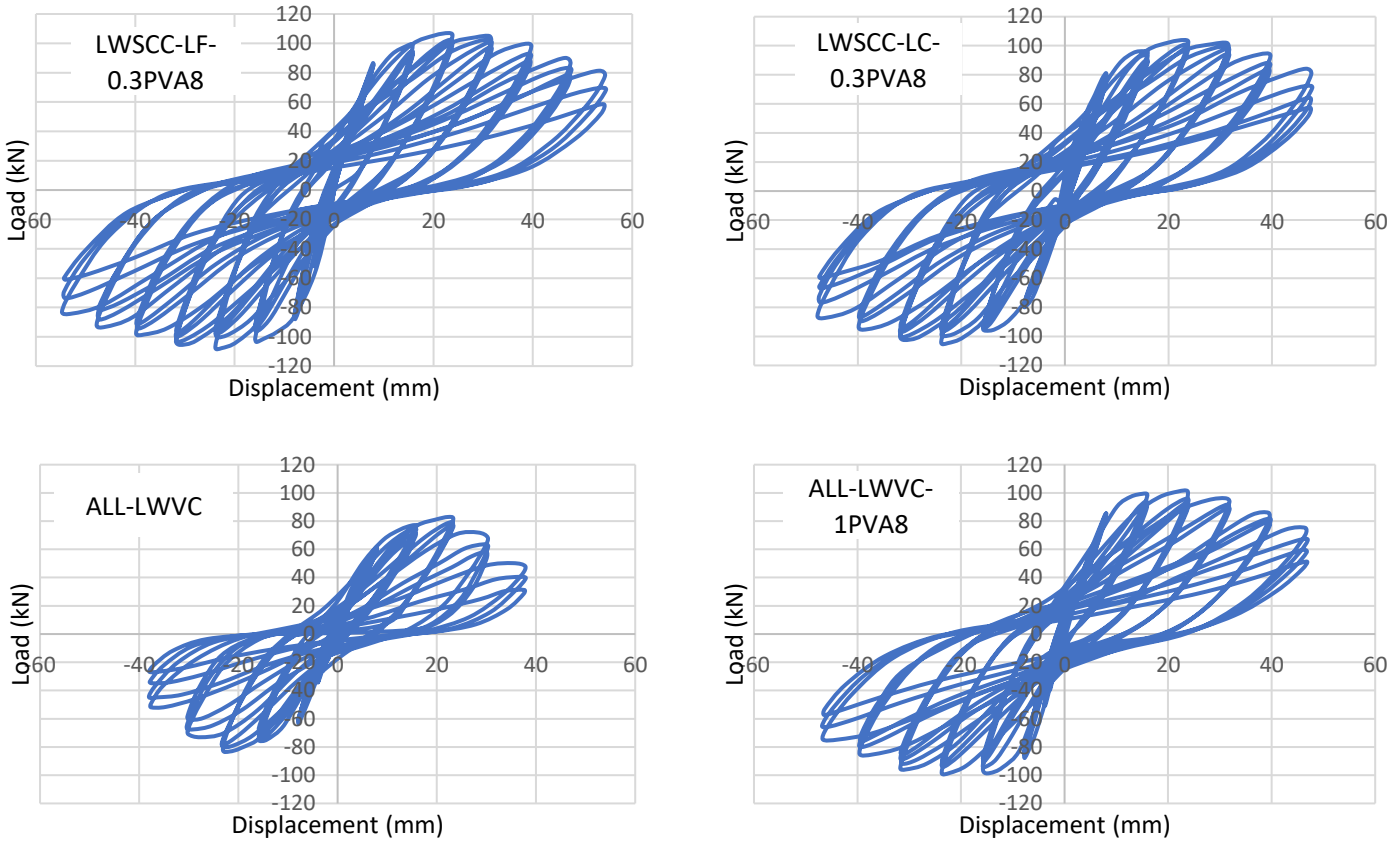

Figure 8-8: Hysteretic responses for all tested specimens.

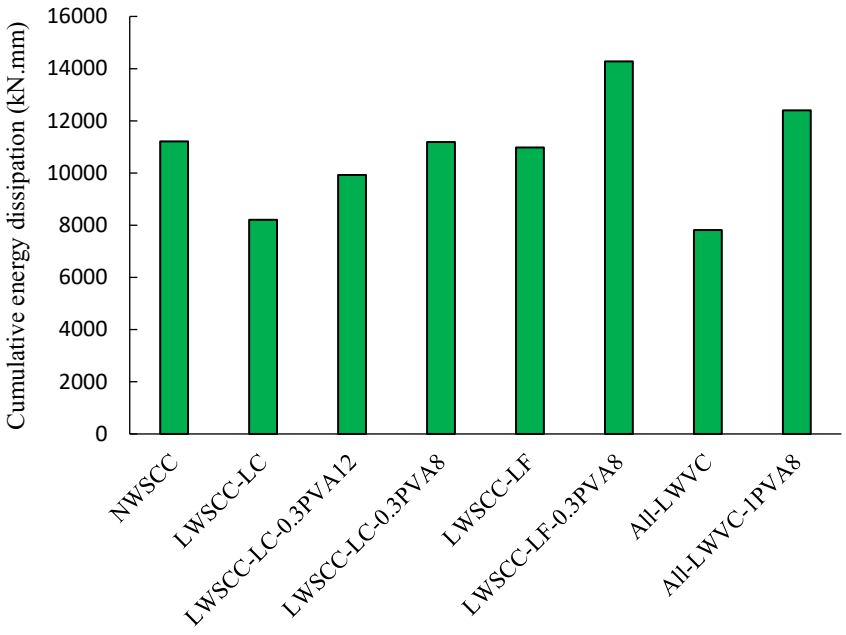

Figure 8-9: Energy dissipation.

Figure 8-9 indicates that the use of LF as a full replacement to normal sand in LWSCC-LF joint (S5) succeeded to reduce the self-weight of concrete by 12.3% and dissipate a comparable hysteretic energy to NWSCC under reversed cyclic loading (difference less than 3%). This can be attributed to the high rate of deformation expressed by LWSCC-LF specimen (S5) prior to failure. In contrast, the energy dissipation capacity of the LWSCC-LC specimen (S2) was lower than that of NWSCC specimen (S1) by about 26.9%. This performance can be ascribed to the lower joint shear strength of LWSCC specimens developed with LC compared to NWSCC joint. The reduced joint shear strength had an undesirable pinching effect (see Figure 8-8), which limited the load-carrying capacity and deformability of tested specimens and hence reduced the energy dissipation capacity.

The addition of PVA fibers generally helped to increase the energy dissipation capacity of tested LWSCC joints, and even compensated for the reduction resulted from using low

density aggregates (especially in LWSCC-LC joints). This is due to the improvement in load-carrying capacity and deformability of LWSCC joints after the addition of fibers. The results also indicated that the inclusion of PVA8 in LWSCC joint contributed to dissipate higher energy compared to the joint cast with PVA12. For instance, LWSCC-LC specimen reinforced with PVA8 (S4) exhibited 12.7% higher energy dissipation compared to its counterpart joint reinforced with PVA12 (S3).

Figure 8-9 also shows that despite the significant reduction in the self-weight observed in LWVC joint which reached up to 28% lower than NWSCC joint, LWVC joint had an energy dissipation capacity of 30.3% lower than NWSCC joint. This is due to the considerable reduction in joint shear strength of LWVC that forced the joint to fail in BJ-mode, demonstrating low load-carrying capacity and reduced ultimate deflection and hence reduced the cumulative dissipated energy. Optimizing expanded slate LWVC mixture with up to 1% PVA fibers in this study succeeded to fully recover the latter reduction in the energy dissipation capacity resulted from using LC and LF aggregates, achieving an energy dissipation capacity even higher than NWSCC joint by 10.5 %. The potential of fibers in enhancing the joint shear strength by stitching mechanism may explain this behavior. Therefore, this improvement in joint shear strength helped the joint to sustain higher ultimate load and experience larger deformation, leading to higher energy dissipation capacity.

8.5.7 Stiffness degradation

The stiffness of the beam-column joints was assessed using the secant stiffness coefficient determined from each complete hysteresis loop. This coefficient was calculated by dividing the maximum load of first cycle in each load step by its corresponding displacement. The variations of stiffness throughout the loading history for each of the tested joints are shown in Figure 8-10. It can be seen from the figure that, in the initial loading stage (up to 15 cycles), no apparent change in the stiffness of tested joints can be observed. This can be explained such that at early stages of loading (up to 15 cycles) the crack width in each of the tested joints did not exceed 0.1 mm width, which does not have a significant effect on the joints' stiffness. As the loading stages proceeded, the cracks in the joints started to open wider and reduced the overall stiffness of tested joints. It can be also noted that LWSCC joints S2 and S5 showed lower initial stiffness (14.7% and 4.7% less, respectively) than NWSCC specimen (S1). This can be related to the low stiffness of expanded slate aggregate that used in the production of LWSCC mixtures, thus reduced the initial stiffness of the composite.

The stiffness degradation trend of LWSCC Specimen made with LF (S5) seems to be much slower than that of the counterpart specimen with LC (S2), as shown in Figure 8-10**a**. This may be attributed to the fact that, as mentioned earlier, the failure plane of LWSCC-LC mixtures usually occurs at both the aggregate boundary and across the aggregate itself, which in turn reduces the amount of shear forces that can be transmitted through the joint core by aggregate interlocking. This results in a significant drop in load carrying capacity and hence increases the rate of strength/stiffness degradation. In contrast, the failure plane

in LWSCC-LF specimens mainly occurred at the aggregate boundaries (due to the presence of strong normal-weight granite coarse aggregate mixed with LF). This ensures the transmission of sufficient magnitude of shear forces across the failure plane by aggregate interlocking with a slight reduction in load carrying capacity, demonstrating ductile failure with lower rate of stiffness degradation after peak.

The results presented in Figure 8-10 and Table 8-3 indicate that optimizing successful SCC expanded slate mixtures with PVA fibers in this study generally increased the initial stiffness of LWSCC beam-column joints. For example, adding 0.3% PVA8 to LWSCC-LC mixture increased the initial stiffness of tested joint by about 14.7% compared to the control mixture without fibers (S4 compared to S2). The results also indicated that changing the fibers' length did not show a significant effect on the initial stiffness of tested beam-column joints. It can be also observed from Figure 8-10 that adding 0.3% of PVA fibers succeeded to reduce the rate of stiffness degradation after peak, demonstrating more gradual loss of strength. This indicates that LWSCC specimens reinforced with PVA fibers have a higher ability to maintain sufficient loading beyond failure and exhibit more ductile failure.

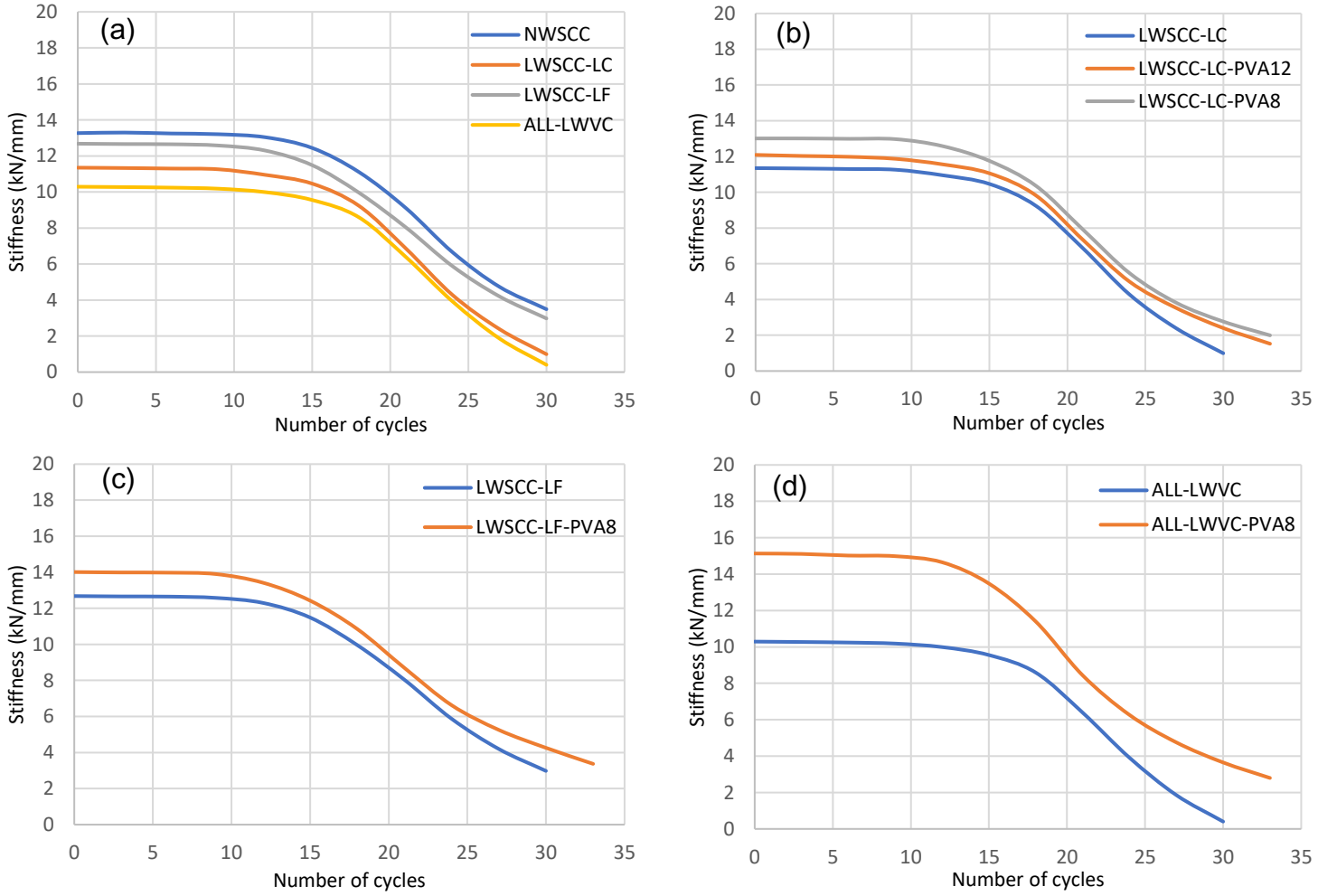

Figure 8-10: Stiffness degradation of tested specimens.

Figure 8-10**a** also show the stiffness variation of LWVC mixture with all lightweight slate aggregates throughout the loading history. From the figure, it is obviously seen that the initial stiffness of S7 joint is low (lower than LWSCC S2 joint by about 9.3%), which is expected because of the higher content of low stiffness Stalite aggregates (LC and LF). Maximizing the content of lightweight aggregate and the percentage of PVA fibers (up to 1%) in the development of successful expanded slate LWVC mixture in this study (S8) helped to significantly increase the initial stiffness of LWVC joints and decreased the rate of stiffness degradation. For instance, as shown in Figure 8-10**d**, adding 1% PVA8 fibers to LWVC mixtures increased the initial stiffness by 46.7% compared with the control joint without fibers (S8 compared to S7).

8.6 Conclusions

This chapter evaluates the behaviour of exterior beam-column joints made with fiber-reinforced LWSCC under reversed cyclic loading. Different types of aggregates (normal-weight and expanded slate lightweight aggregates) and different lengths and volumes of PVA fibers were investigated in this study. The results obtained from this investigation discussed the performance of tested specimens in terms of failure mode, load-displacement envelope curves, ductility, brittleness index, stiffness degradation, and energy dissipation capacity. According to the experimental results obtained from this work, the following conclusions can be drawn:

7. Expanded slate coarse/fine lightweight aggregates can be used to develop SCC mixtures with a minimum possible density of approximately 15% lighter than NWC. However, BCJs made with some optimized slate LWSCC mixtures in this

study (density ranges from 84.5 to 87.7% of conventional NWC) showed a drop in the initial stiffness, load-carrying capacity, and ductility by an average of 9.7%, 12.2%, and 20.1%, respectively, compared to NWSCC ones.

8. Using LF in the development of LWSCC showed some advantages over using LC. Although optimized mixtures with LC reached lower density compared to mixtures with LF (15.5% lighter than NWC compared to 12.3% in the case of LF), BCJs made with optimized LWSCC-LF had less reductions in terms of initial stiffness (4.7% compared to 14.7% in LC joint), load-carrying capacity (9.8% compared to 14.6% in LC joint), ductility (7.7% compared to 32.6% in LC joint), and dissipation energy (2.1% compared to 26.9% in LC joint), when compared to NWSCC joint.
9. Using optimized expanded slate LWSCC mixture with PVA fibers in BCJs helped to significantly enhance the joint's structural performance. For example, BCJ with LWSCC-LC and PVA8 fibers achieved a comparable load carrying capacity, ductility, and energy dissipation capacity to that of NWSCC joint.
10. Joint made with LF exhibited B-mode of failure while joint made with LC exhibited BJ-mode. The brittle characteristics of LC aggregate (compared to LF) was the main reason for the reduction of the joint's shear strength which caused the brittle mode of failure. However, adding PVA fibers to LWSCC-LC helped to alleviate the LC joint brittleness and changed its failure mode from BJ-mode to a ductile flexural failure (B-mode).
11. By comparing different lengths of PVA fibers, it can be revealed that the highest improvement in the cyclic behavior of LWSCC BCJs in terms of first crack load,

initial stiffness, load-carrying capacity, ductility, cracking activity, and energy dissipation capacity was observed when shorter fibers were used.

12. Using high percentage of PVA fibers (1%) in LWVC compensated for the significant reduction in load-carrying capacity that resulted from using high lightweight aggregate content and helped to improve the overall cyclic performance of BCJs. This improvement allowed to develop BCJ with significant enhancement in ductility, stiffness, cracking activity, and energy dissipation, while maintaining a considerable reduction in the self weight reached up to 28% lower than NWSCC.

8.7 References

AbdelAleem, B. H., & Hassan, A. A. (2019). Influence of synthetic fibers' type, length, and volume on enhancing the structural performance of rubberized concrete. *Construction and Building Materials*, *229*, 116861.

AbdelAleem, B. H., Ismail, M. K., & Hassan, A. A. (2017). Properties of self-consolidating rubberised concrete reinforced with synthetic fibres. *Magazine of Concrete Research*, *69*(10), 526-540.

ACI Committee 318. (2019). Building Code Requirements for Structural Concrete (ACI 318-19) and Commentary. *American Concrete Institute, Farmington* Hills, MI.

ACI Committee 352. (2002). Recommendations for design of beam-column connections in monolithic reinforced concrete structures (ACI 352R-02). *American Concrete Institute*, Farmington Hills, MI.

Agrawal, P., and Shrikhande, M. (2006). *Earthquake resistant design of structures*. PHI Learning Pvt. Ltd..

Bogas, J. A., and Gomes, A. (2013). Compressive behavior and failure modes of structural lightweight aggregate concrete–Characterization and strength prediction. *Materials & Design*, *46*, 832-841.

Cardoso, D. C., Pereira, G. B., Silva, F. A., Silva Filho, J. J., & Pereira, E. V. (2019). Influence of steel fibers on the flexural behavior of RC beams with low reinforcing ratios: Analytical and experimental investigation. *Composite Structures*, *222*, 110926.

Carmo, R. N. D., Costa, H., Gomes, G., & Valença, J. (2017). Experimental evaluation of lightweight aggregate concrete beam–column joints with different strengths and reinforcement ratios. *Structural Concrete*, *18*(6), 950-961.

Çelik, Z., & Bingöl, A. F. (2020). Fracture properties and impact resistance of self-compacting fiber reinforced concrete (SCFRC). *Materials and Structures*, *53*(3), 1-16.

Chi, J. M., Huang, R., Yang, C. C., and Chang, J. J. (2003). Effect of aggregate properties on the strength and stiffness of lightweight concrete. *Cement and Concrete Composites*, *25*(2), 197-205.

EFNARC (2005). European Guidelines for Self-compacting Concrete Specification, Production and Use. European Federation for Specialist Construction Chemicals and Concrete Systems: Farnham, UK.

Eurocode 2. (2004). Design of Concrete Structures – Part 1-1: General Rules and Rules for Buildings. *European Committee for Standardization*, Brussels, Belgium.

Eurocode 8. (2004). Design of structures for earthquake resistance part 1: general rules, seismic actions and rules for buildings. *European Committee for Standardization*, Brussels, Belgium.

Forzani, B., Popov, E. P., and Bertero, V. V. (1979). *Hysteretic behavior of lightweight reinforced concrete beam-column subassemblages*. Berkeley, CA, USA: University of California, Earthquake Engineering Research Center.

Ganesan, N., Raj, B., & Shashikala, A. P. (2013). Behavior of self-consolidating rubberized concrete beam-column joints. *ACI Materials Journal*, *110*(6), 697.

Hassan, A. A., Ismail, M. K., and Mayo, J. (2015). Shear behavior of SCC beams with different coarse-to-fine aggregate ratios and coarse aggregate types. *Journal of Materials in Civil Engineering*, *27*(11), 04015022.

Kayali, O. (2008). Fly ash lightweight aggregates in high performance concrete. *Construction and building materials*, *22*(12), 2393-2399.

Mousa, A., Mahgoub, M., and Hussein, M. (2018). Lightweight concrete in America: presence and challenges. *Sustainable Production and Consumption*, *15*, 131-144.

Omar, A. T., & Hassan, A. A. (2021a). Behaviour of expanded slate semi-lightweight SCC beams with improved cracking performance and shear capacity. In *Structures* (Vol. 32, pp. 1577-1588). Elsevier.

Omar, A. T., & Hassan, A. A. (2021b). Shear behavior of lightweight self-consolidating concrete beams containing coarse and fine lightweight aggregates. *ACI Structural Journal*, *118*(3), 175-186.

Omar, A. T., and Hassan, A. A. (2019). Use of polymeric fibers to improve the mechanical properties and impact resistance of lightweight SCC. *Construction and Building Materials*, *229*, 116944.

Omar, A. T., and Hassan, A. A. (2019). Use of polymeric fibers to improve the mechanical properties and impact resistance of lightweight SCC. *Construction and Building Materials*, *229*, 116944.

Paultre, P., Khayat, K. H., Cusson, D., and Tremblay, S. (2005). Structural performance of self-consolidating concrete used in confined concrete columns. *ACI structural journal*, *102*(4), 560-568.

Rabbat, B. G., Daniel, J. I., Weinmann, T. L., and Hanson, N. W. (1986). Seismic behavior of lightweight and normal weight concrete columns. In *Journal Proceedings* (Vol. 83, No. 1, pp. 69-79).

Rashid, M. A., & Mansur, M. A. (2005). Reinforced high-strength concrete beams in flexure. *ACI Structural Journal*, *102*(3), 462.

Sadek, M. M., and Hassan, A. A. (2021). Abrasion and Scaling Resistance of Lightweight Self-Consolidating Concrete Containing Expanded Slate Aggregate. *ACI Materials Journal*, *118*(2), 31-42.

Shannag, M. J., Barakat, S., & Abdul-Kareem, M. (2002). Cyclic behavior of HPFRC-repaired reinforced concrete interior beam-column joints. *Materials and Structures*, *35*(6), 348-356.

Sin, L. H., Huan, W. T., Islam, M. R., & Mansur, M. A. (2011). Reinforced Lightweight Concrete Beams in Flexure. *ACI Structural Journal*, *108*(1).

Topçu, İ. B. (1997). Assessment of the brittleness index of rubberized concretes. *Cement and Concrete Research*, *27*(2), 177-183.

Wu, T., Wei, H., and Liu, X. (2018). Shear strength of interior beam–column joints with lightweight aggregate concrete. *Magazine of Concrete Research*, *70*(3), 109-128.

Yang, K. H., Mun, J. H., & Lee, J. S. (2014). Flexural tests on pre-tensioned lightweight concrete beams. *Proceedings of the Institution of Civil Engineers-Structures and Buildings*, *167*(4), 203-216.

Yu, Q. L., Spiesz, P., and Brouwers, H. J. H. (2015). Ultra-lightweight concrete: Conceptual design and performance evaluation. *Cement and Concrete Composites*, *61*, 18-28.

9. Summary and recommendations

9.1 Summary

In the current thesis, an experimental program was established to investigate the influence of using different polymeric fibers on the development of LWSCC mixtures with minimum possible density and improved mechanical properties. The investigation examined different replacement levels of normal-weight fine or coarse aggregates by fine and coarse lightweight expanded slate (Stalite) aggregates to optimize these mixtures. Different types of aggregates (normal-weight and coarse/fine expanded slate lightweight aggregates), binder contents (550 kg/m^3 and 600 kg/m^3), coarse-to-fine aggregate (C/F) ratios (0.7, 1.0, and 1.5), fiber types (PVA and PP fibers), fiber lengths (8 mm, 12 mm, and 19 mm), and fiber volumes (0.3%, 0.5%, and 1%) were used to optimize the fresh and mechanical properties of the developed mixtures. The thesis also investigates the effect of using different polymeric fibers' types, lengths, and volumes on enhancing the shear and flexural performance of large-scale reinforced-concrete beams made with these optimized mixtures. Moreover, the effect of combining PVA fibers and the maximum possible volume of Stalite aggregates on the cyclic performance of exterior beam-column joints was also discussed. Based on the experimental results obtained from this research work, the following conclusions may be drawn:

9.1.1 Use of polymeric fibers to optimize the fresh properties, stability, strength of LWSCC mixtures containing expanded slate aggregate (First stage)

- It was possible to optimize successful expanded slate LWSCC mixtures with a dry density ranging from 1848-1982 kg/m^3 and a compressive strength range of 49.1-53.8 MPa using a minimum binder content of 550 kg/m^3. Further increase in the coarse aggregate slate significantly reduced the passing ability, while increasing the content of expanded slate sand resulted in an increased risk of segregation. Increasing the binder content from 550 kg/m^3 to 600 kg/m^3, however, helped to increase the amount of LWA in the mixture, achieving concrete mixtures with lower density and slightly improved compressive strength.
- With 550 kg/m^3 binder content, it was only possible to use up to 0.3% polymeric fibers to develop acceptable LWSCC mixtures. Combining fibers and LWA in SCC mixtures seemed to heighten the inter-particle friction and blockage, which reduced the passing ability of the mixtures. Nevertheless, increasing the binder content to 600 kg/m^3 improved the flowability and passing ability of the developed mixtures, allowing a maximum of 0.5% fibers to be used safely with acceptable SCC fresh properties.
- The inclusion of polymeric fibers significantly enhanced the segregation resistance, STS, FS, and impact resistance of the developed mixtures, however, the compressive strength and ME were insignificantly affected. Using PVA8 fibers appeared to be the most effective type of polymeric fibers at improving the FS, STS, impact resistance of the LWSCC mixtures, followed by PVA12 and then PP19. For example, the

improvement in impact resistance when using PVA8 fibers reached up to 64% compared to a 50% and 30% increase (on average) when using PVA12 and PP19.

- Under drop-weight impact test (recommended by ACI-544), adding polymeric fibers to LWSCC mixtures immensely increased the difference between the number of blows for ultimate failure and initial cracks, indicating a significant enhancement in the ductility and post-cracking behavior of the developed mixtures.
- LWSCC mixtures developed with expanded slate fine aggregate exhibited better results in terms of flowability, passing ability, compressive strength, STS, FS, and impact resistance capacity, when compared to their counterpart mixtures developed with expanded slate coarse aggregate.

9.1.2 Impact resistance and mechanical properties of lightweight SCC under cold temperatures (Second stage)

- LWSCC mixtures exhibited a noticeable increase in the mechanical properties and impact resistance capacity when tested under cold temperatures. Greater enhancement was observed as the temperature decreased, however, all tested specimens appeared to fail in a more brittle manner compared to when they were tested at room temperature.
- Under cold temperatures, LWSCC mixtures made with LC showed more pronounced improvements in the mechanical properties and impact resistance compared to counterpart mixtures containing LF. Also, employing higher volume of expanded slate aggregate in LWSCC mixtures showed further enhancement in the mechanical properties and impact resistance under cold temperatures.

- The use of PVA fibers in LWSCC mixtures helped to boost the enhancing effect of cold temperatures on the mechanical properties and impact resistance of the developed mixtures. Moreover, under drop-weight test, adding 0.3% PVA fibers to LWSCC mixtures helped to further increase the difference between the number of blows for ultimate failure and initial cracks, indicating more ductile failure under cold temperature.

9.1.3 Effect of using different types and volumes of polymeric fibers on improving the shear strength and flexural performance of large-scale LWSCC beams (Third stage)

- Adding 0.3% PVA8 (8 mm) fibers to LWSCC beams not only compensated for the reduction in the ultimate shear load resulted from using low-stiffness aggregate, but also showed improvements in the post-diagonal cracking resistance, energy absorption capacity, and deformation capacity by about 17%, 60.3%, and 28.5%, respectively, compared to counterpart beams without fibers. In addition, using 0.3% of PVA8 fibers improved the deformability, ductility, absorbed energy, cracking moment capacity, and ultimate flexural strength of tested beams by about 24.6%, 23.1%, 24%, 18%, and 4.6%.
- The possibility of using up to 0.5% PVA8 fibers with 600 kg/m^3 binder content in the production of LWSCC mixtures helped to significantly increase the normalized shear load of the tested LWSCC beams by about 37% compared to counterpart beams without fibers. Also, this contributed to alleviating the reduction in flexural strength of LWSCC beams resulting from using lightweight aggregates. In the meantime, further

enhancement in the cracking activity, post-diagonal cracking resistance, energy absorption capacity, and ductility was also observed.

- The inclusion of shorter PVA fibers (PVA8) more obviously improved the performance of LWSCC beams under shear and flexure loads in terms of ultimate load, post-diagonal cracking resistance, deformability, ductility, absorbed energy, and cracking behavior when compared to the use of longer PVA fibers (PVA12).
- In general, LWSCC beams developed with LF (mixed with normal-weight coarse aggregate) showed relatively higher ultimate shear load, post-diagonal cracking resistance, flexural capacity, ductility index, and energy absorption capacity, when compared to counterpart beams developed with LC (mixed with normal-weight sand). In addition, beams with LF experienced more gradual descending portion (under flexure loads) accompanied with higher deformations at failure than their counterpart beams containing LC.
- Despite the noticeable reduction in the shear strength resulted from employing both LC and LF with C/F ratio of 1.5 in the development of LWVC mixtures (reaching a 28% reduction in concrete dry density), combining high fraction volume of PVA8 (1%) fibers with high content of LWAs completely compensated for this reduction. This combination also helped to achieve great improvements in the post-diagonal cracking resistance, energy absorption capacity, and deformation capacity, which reached up to 28%, 97%, and 39%, respectively, compared to the control beam without fibers.

9.1.4 Cyclic behavior of large-scale LWSCC beam-column joints with/without polymeric fibers (Fourth stage)

- Lightweight expanded slate coarse/fine aggregates can be used to develop SCC mixtures with a concrete density of approximately 15% lighter than NWC. A properly detailed beam-column joint (with sufficient hoops) made with these LWSCC mixtures showed slightly lower load-carrying capacity, ductility and dissipated energy, when compared to NWSCC specimen.
- Using LF in the development of LWSCC showed some advantages over using LC. Although optimized mixtures with LF reached lower density compared to mixtures with LF (15.5% lighter than NWC compared to 12.3% in the case of LF), LWSCC beam column joints made with LF had less reductions (compared to NWSCC specimen) in terms of initial stiffness (4.7% compared to 14.7% in LC joint), load-carrying capacity (9.8% compared to 14.6% in LC joint), ductility (7.7% compared to 32.6% in LC joint), and dissipation energy (2.1% compared to 26.9% in LC joint).
- The developed slate LWSCC mixtures in this research work, especially those made with LF, proved to be a good candidate for lightweight structural members subjected to large deformations caused by earthquakes. This is because a minimum ductility index (μ) of 3 is considered imperative to ensure the redistribution of moments in such regions, while the developed LWSCC in this investigation had a high ductility index of 6.41.
- Using optimized expanded slate LWSCC mixture with PVA fibers in BCJs helped to significantly enhance the joint's structural performance. For example, BCJ with

LWSCC-LC and PVA8 fibers achieved a comparable load carrying capacity, ductility, and energy dissipation capacity to that of NWSCC joint.

- Joint made with LF exhibited B-mode of failure while joint made with LC exhibited BJ-mode. The brittle characteristics of LC (compared to LF) was the main reason for the reduction of the joint's shear strength which caused the brittle mode of failure. However, the inclusion of PVA fibers into LWSCC-LC specimens helped to alleviate the joint brittleness and changed its failure mode from shear/flexural failure (BJ-mode) to a ductile flexural failure (B-mode).
- By comparing different lengths of PVA fibers, it can be revealed that the highest improvement in the cyclic behavior of LWSCC BCJs in terms of first crack load, initial stiffness, load-carrying capacity, ductility, cracking activity, and energy dissipation capacity was observed when shorter fibers were used.
- Using high percentage of PVA fibers (1%) in LWVC compensated for the significant reduction in load-carrying capacity that resulted from using high lightweight aggregate content and helped to improve the overall cyclic performance of BCJs. This improvement allowed to develop BCJ with significant enhancement in ductility, stiffness, cracking activity, and energy dissipation, while maintaining a considerable reduction in the self weight reached up to 28% lower than NWSCC.
- In general, the use of Stalite LWSCC in beam-column joints in this study resulted in a slight reduction in the load-carrying capacity, ductility, and energy dissipation capacity. However, the fact that the Stalite LWSCC used in this study had up to 15.3% reduction in the self-weight compared to NWC should also be considered. The reduction in self-

weight can not only reduce the cross-sectional dimension and lead to more economical design but also reduce the seismic demand of the structure. Designer/engineers should consider the cost and benefits associated with the use of each concrete type (LWC vs. NWC), in the light of their available behaviors, to make their appropriate decision.

9.2 Research contribution and potential applications

- LWSCC mixtures developed with expanded slate and PVA fibers exhibited adequate impact resistance under cold temperatures, making these mixtures a good solution in offshore structures, especially in Arctic region.
- The developed LWSCC mixtures in this research work, especially those made with LF, proved to be a good candidate for lightweight structural members subjected to large deformations caused by earthquakes. Large-scale concrete elements made with these mixtures high ductility index reached up to 6.41.
- Mixture (LWSCC-LF-0.3PVA8) is recommended to be used in multiple structural applications that require high impact resistance, ductility, shear strength, and good compactability. Also, mixture (All-LWVC-1PVA) showed the highest reduction in concrete density with acceptable mechanical properties and adequate structural performance.
- Using PVA fibers helped to alleviate the reduction in the load carrying capacity and ductility of the beam-column joint that resulted from using high volume of LWA. In addition to further enhancing the structural behavior of beam-column joints under cyclic loading.

9.3 Recommendations for Future Research

- Further investigations are needed to examine the durability of LWSCC mixtures reinforced with polymeric fibers against abrasion, freezing-thawing action, chloride and sulfate attacks.
- Evaluating the possibility of using expanded slate fine aggregate (LF) in the development of engineered cementitious composite (ECC) as a replacement for normal-weight sand, which may result in a cementitious composite with convenient strain hardening response and reduced self-weight.
- Using advanced methods to test the impact resistance of fiber-reinforced LWSCC, to provide more accurate and consistent results (full scale LWSCC beams under impact loading, for example).
- Evaluating the behavior of full-scale LWSCC elements subjected to flexural, shear, and cyclic loading under arctic conditions.

9.4 Limitations of research

The results obtained from this study were typically affected by the properties of the used materials. Therefore, any changed in the physical and/or chemical properties of the fine aggregate, coarse aggregate, cement, SCMs, admixtures, and fibers may affect the mixtures' properties in the fresh and hardened states. In the structural stage (Chapters 5, 6, 7, and 8), comparative investigations were conducted to evaluate the benefits of combining high content of expanded slate aggregate with high percentage of polymeric fibers on the shear, flexural, and cyclic performance of reinforced concrete beams/beam-column joints

neglecting the effect of changing in the specimens' size, longitudinal reinforcement ratio, and shear span-to-effective depth ratio. At materials and structural level, all tests were conducted based on the available facilities in Memorial University's labs. However, in some tests, such as the impact test, using advanced instruments may result in better measurements with further details. Also, in cyclic load test the available testing frame limits the dimensions of concrete specimens that can be tested to one third of full-scale concrete joint.

Bibliography

Aashto (Association of State Highway and Transportation Officials) LRFD. (2017). Bridge Design Specifications and Commentary, SI Units. *Aashto*, Washington, DC, USA.

AbdelAleem, B. H., & Hassan, A. A. (2018). Development of self-consolidating rubberized concrete incorporating silica fume. *Construction and Building Materials*, *161*, 389-397.

AbdelAleem, B. H., & Hassan, A. A. (2019). Cyclic Behavior of Rubberized Beam-Column Joints Reinforced with Synthetic Fibers. *ACI Materials Journal*, *116*(2), 105-118.

AbdelAleem, B. H., & Hassan, A. A. (2019). Influence of synthetic fibers' type, length, and volume on enhancing the structural performance of rubberized concrete. *Construction and Building Materials*, *229*, 116861.

AbdelAleem, B. H., Ismail, M. K., & Hassan, A. A. (2017). Properties of self-consolidating rubberised concrete reinforced with synthetic fibres. *Magazine of Concrete Research,* 69(10), 526-540.

AbdelAleem, B. H., Ismail, M. K., & Hassan, A. A. (2018). The combined effect of crumb rubber and synthetic fibers on impact resistance of self-consolidating concrete. *Construction and Building Materials*, *162*, 816-829.

AbdelAleem, B. H., Ismail, M. K., & Hassan, A. A. (2018). The combined effect of crumb rubber and synthetic fibers on impact resistance of self-consolidating concrete. *Construction and Building Materials*, *162*, 816-829.

Abouhussien, A. A., Hassan, A. A. A., & Hussein, A. A. (2015). Effect of expanded slate aggregate on fresh properties and shear behaviour of lightweight SCC beams. *Magazine of Concrete Research*, 67(9), 433-442.

Abouhussien, A. A., Hassan, A. A. A., & Ismail, M. K. (2015). Properties of semi-lightweight self-consolidating concrete containing lightweight slag aggregate. *Construction and Building Materials*, 75, 63-73.

ACI (American Concrete Institute). (2014). ACI 318R-14: Building code requirements for structural concrete and commentary. *ACI*, Farmington Hills, MI, USA.

ACI 544.2R-89 (1999) Measurement of properties of fiber reinforced concrete. *ACI Committee 544*, West Conshohocken, PA, USA.

ACI Committee 318. (2019). Building Code Requirements for Structural Concrete (ACI 318-19) and Commentary. *American Concrete Institute, Farmington* Hills, MI.

ACI Committee 352. (2002). Recommendations for design of beam-column connections in monolithic reinforced concrete structures (ACI 352R-02). *American Concrete Institute*, Farmington Hills, MI.

ACI Committee 544. (1988). Design considerations for steel fiber reinforced concrete (ACI 544.4R-88). *American Concrete Institute*, Farmington Hills, MI.

Afroughsabet, V., Biolzi, L., & Ozbakkaloglu, T. (2016). High-performance fiber-reinforced concrete: a review. *Journal of materials science*, *51*(14), 6517-6551.

Agrawal, P., and Shrikhande, M. (2006). *Earthquake resistant design of structures*. PHI Learning Pvt. Ltd..

Ahari, R. S., Erdem, T. K., & Ramyar, K. (2015). Effect of various supplementary cementitious materials on rheological properties of self-consolidating concrete. *Construction and Building Materials*, *75*, 89-98.

Ahmed, H. I., & Pama, R. P. (1992, July). Ultimate flexural strength of reinforced concrete beams with large volumes of short randomly oriented steel fibres. In *Rilem Proceedings* (pp. 467-467). Chapman & Hall.

Alqahtani, F. K., Abotaleb, I. S., & Harb, S. (2021). LEED Study of Green Lightweight Aggregates in Construction. *Sustainability*, 13(3), 1395.

Alqahtani, F. K., Ghataora, G., Khan, M. I., & Dirar, S. (2017). Novel lightweight concrete containing manufactured plastic aggregate. *Construction and Building Materials*, *148*, 386-397.

Andiç-Çakır, Ö., & Hızal, S. (2012). Influence of elevated temperatures on the mechanical properties and microstructure of self consolidating lightweight aggregate concrete. *Construction and building materials*, *34*, 575-583.

Anvari, A., Ghalehnovi, M., De Brito, J., & Karimipour, A. (2021). Improved bending behaviour of steel-fibre-reinforced recycled aggregate concrete beams with a concrete jacket. *Magazine of Concrete Research*, *73*(12), 608-626.

Arain, M. F., Wang, M., Chen, J., & Zhang, H. (2019). Study on PVA fiber surface modification for strain-hardening cementitious composites (PVA-SHCC). *Construction and Building Materials*, *197*, 107-116.

Ashour, S. A. (2000). Effect of compressive strength and tensile reinforcement ratio on flexural behavior of high-strength concrete beams. *Engineering structures*, *22*(5), 413-423.

Ashour, S. A., Hasanain, G. S., & Wafa, F. F. (1992). Shear behavior of high-strength fiber reinforced concrete beams. *Structural Journal*, *89*(2), 176-184.

Aslani, F., & Kelin, J. (2018). Assessment and development of high-performance fibre-reinforced lightweight self-compacting concrete including recycled crumb rubber aggregates exposed to elevated temperatures. *Journal of Cleaner Production*, *200*, 1009-1025.

Assaad, J. J., & Issa, C. A. (2018). Stability and Bond Properties of Latex-Modified Semi-Lightweight Flowable Concrete. *ACI Materials Journal*, *115*(4).

ASTM C127. (2015). Standard test method for relative density (specific gravity) and absorption of fine aggregate. *ASTM International*, West Conshohocken, PA, USA.

ASTM C150 / C150M. (2012). Standard Specification for Portland Cement. *ASTM International*, West Conshohocken, PA, USA.

ASTM C1609 / C1609M. (2012). Standard Test Method for Flexural Performance of Fiber-Reinforced Concrete (Using Beam with Third-Point Loading). *ASTM International*, West Conshohocken, PA, USA.

ASTM C231 / C231M. (2014). Standard Test Method for Air Content of Freshly Mixed Concrete by the Pressure Method. *ASTM International*, West Conshohocken, PA, USA.

ASTM C39 / C39M. (2011). Standard Test Method for Compressive Strength of Cylindrical Concrete Specimens. *ASTM International*, West Conshohocken, PA, USA.

ASTM C494 / C494M. (2013). Standard Specification for Chemical Admixtures for Concrete. *ASTM International*, West Conshohocken, PA, USA.

ASTM C618. (2012). Standard Specification for Coal Fly Ash and Raw or Calcined Natural Pozzolan for Use in Concrete. *ASTM International*, West Conshohocken, PA, USA.

ASTM C78 / C78M. (2018). Standard Test Method for Flexural Strength of Concrete (Using Simple Beam with Third-point Loading). *ASTM International*, West Conshohocken, PA, USA.

Azmee, N. M., & Shafiq, N. (2018). Ultra-high performance concrete: From fundamental to applications. *Case Studies in Construction Materials*, *9*, e00197.

Balendran, R. V., Zhou, F. P., Nadeem, A., & Leung, A. Y. T. (2002). Influence of steel fibres on strength and ductility of normal and lightweight high strength concrete. *Building and environment*, *37*(12), 1361-1367.

Banthia, N., & Gupta, R. (2006). Influence of polypropylene fiber geometry on plastic shrinkage cracking in concrete. *Cement and concrete Research*, *36*(7), 1263-1267.

Bastami, R. (2019). *Structural Performance of High-Strength Reinforced Concrete Beams Built with Synthetic Fibers* (Doctoral dissertation, Université d'Ottawa/University of Ottawa).

Behrooyan, M., & Ahmadian, H. R. (2013). Effects of Polyvinyl Alcohol fibers on fracture energy of concrete. *Int. Research J. Appl. Basic Sciences*, *6*, 484-491.

Beirnes, M., Dagenais, M. A., & Wight, G. (2019). Cold temperature effects on the impact resistance of thin, lightweight UHPFRC panels. *International Journal of Impact Engineering*, *127*, 110-121.

Bogas, J. A., and Gomes, A. (2013). Compressive behavior and failure modes of structural lightweight aggregate concrete–Characterization and strength prediction. *Materials & Design*, *46*, 832-841.

Bogas, J. A., Gomes, A., & Pereira, M. F. C. (2012). Self-compacting lightweight concrete produced with expanded clay aggregate. *Construction and Building Materials*, *35*, 1013-1022.

Campana, S., Fernández Ruiz, M., Anastasi, A., & Muttoni, A. (2013). Analysis of shear-transfer actions on one-way RC members based on measured cracking pattern and failure kinematics. *Magazine of concrete research*, *65*(6), 386-404.

Cardoso, D. C., Pereira, G. B., Silva, F. A., Silva Filho, J. J., & Pereira, E. V. (2019). Influence of steel fibers on the flexural behavior of RC beams with low reinforcing ratios: Analytical and experimental investigation. *Composite Structures*, *222*, 110926.

Carmo, R. N. D., Costa, H., Gomes, G., & Valença, J. (2017). Experimental evaluation of lightweight aggregate concrete beam–column joints with different strengths and reinforcement ratios. *Structural Concrete*, *18*(6), 950-961.

Carmo, R. N. F., Costa, H., Simões, T., Lourenço, C., & Andrade, D. (2013). Influence of both concrete strength and transverse confinement on bending behavior of reinforced LWAC beams. *Engineering structures*, *48*, 329-341.

Çelik, Z., & Bingöl, A. F. (2020). Fracture properties and impact resistance of self-compacting fiber reinforced concrete (SCFRC). *Materials and Structures*, *53*(3), 1-16.

Chai, Y. H. (2016). Service performance of long-span lightweight aggregate concrete box-girder bridges. *Journal of Performance of Constructed Facilities*, *30*(1), 04014196.

Chi, J. M., Huang, R., Yang, C. C., & Chang, J. J. (2003). Effect of aggregate properties on the strength and stiffness of lightweight concrete. *Cement and Concrete Composites*, *25*(2), 197-205.

Cho, S. H., & Kim, Y. I. (2003). Effects of steel fibers on short beams loaded in shear. *Structural journal*, *100*(6), 765-774.

Choi, J., Zi, G., Hino, S., Yamaguchi, K., & Kim, S. (2014). Influence of fiber reinforcement on strength and toughness of all-lightweight concrete. *Construction and Building Materials*, 69, 381-389.

Choi, Y. W., Kim, Y. J., Shin, H. C., & Moon, H. Y. (2006). An experimental research on the fluidity and mechanical properties of high-strength lightweight self-compacting concrete. *Cement and Concrete Research*, 36(9), 1595-1602.

Choi, Y., & Yuan, R. L. (2005). Experimental relationship between splitting tensile strength and compressive strength of GFRC and PFRC. *Cement and Concrete Research*, 35(8), 1587-1591.

Corinaldesi, V., & Moriconi, G. (2015). Use of synthetic fibers in self-compacting lightweight aggregate concretes. *Journal of Building Engineering*, 4, 247-254.

CSA (Canadian Standards Association). (2014). CSA A23.3-14: Design of concrete structures. *CSA*, Rexdale, ON, Canada.

Cyr, M., & Mouret, M. (2003). Rheological characterization of superplasticized cement pastes containing mineral admixtures: consequences on self-compacting concrete design. *Proceedings of seventh CANMET/ACI International Conference on Superplasticizers and Other Chemical Admixtures in Concrete, American Concrete Institute*, Farmington Hills, Michigan, USA.

Dahmani, L., Khenane, A., & Kaci, S. (2007). Behavior of the reinforced concrete at cryogenic temperatures. *Cryogenics*, *47*(9-10), 517-525.

de Alencar Monteiro, V. M., Lima, L. R., & de Andrade Silva, F. (2018). On the mechanical behavior of polypropylene, steel and hybrid fiber reinforced self-consolidating concrete. *Construction and Building Materials*, *188*, 280-291.

Ding, J. T., & Li, Z. (2002). Effects of metakaolin and silica fume on properties of concrete. *Materials Journal*, *99*(4), 393-398.

Du, Y., Qi, H. H., Jiang, J., & Liew, J. Y. (2022). Experimental study on the dynamic behaviour of expanded-shale lightweight concrete at high strain rate. *Materials and Structures*, *55*(1), 1-17.

Dwarakanath, H. V., & Nagaraj, T. S. (1992). Deformational behavior of reinforced fiber reinforced concrete beams in bending. *Journal of Structural Engineering*, *118*(10), 2691-2698.

Dymond, B. Z., Roberts-Wollmann, C. L., & Cousins, T. E. (2010). Shear strength of a lightweight self-consolidating concrete bridge girder. *Journal of Bridge Engineering*, *15*(5), 615-618.

EFNARC (2005). European Guidelines for Self-compacting Concrete Specification, Production and Use. European Federation for Specialist Construction Chemicals and Concrete Systems: Farnham, UK.

Eurocode 2 (2004). Design of Concrete Structures – Part 1-1: General Rules and Rules for Buildings. *European Committee for Standardization*, Brussels, Belgium.

Eurocode 8. (2004). Design of structures for earthquake resistance part 1: general rules, seismic actions and rules for buildings. *European Committee for Standardization,* Brussels, Belgium.

Fathifazl, G., Razaqpur, A. G., Isgor, O. B., Abbas, A., Fournier, B., & Foo, S. (2009). Flexural Performance of Steel-Reinforced Recycled Concrete Beams. *ACI Structural Journal*, *106*(6).

Fernandez, R. P., & Pardo, M. L. (2013). Offshore concrete structures. *Ocean Engineering*, *58*, 304-316.

Floyd, R. W., Hale, W. M., & Bymaster, J. C. (2015). Effect of aggregate and cementitious material on properties of lightweight self-consolidating concrete for prestressed members. *Construction and Building Materials*, *85*, 91-99.

Forzani, B., Popov, E. P., and Bertero, V. V. (1979). *Hysteretic behavior of lightweight reinforced concrete beam-column subassemblages*. Berkeley, CA, USA: University of California, Earthquake Engineering Research Center.

Frosch, R. J. (1999). Another look at cracking and crack control in reinforced concrete. *Structural Journal*, *96*(3), 437-442.

Ganesan, N., Raj, B., & Shashikala, A. P. (2013). Behavior of self-consolidating rubberized concrete beam-column joints. *ACI Materials Journal*, *110*(6), 697.

Gergely, P., & Lutz, L. A. (1968). Maximum crack width in reinforced concrete flexural members. *Special Publication*, *20*, 87-117.

Grabois, T. M., Cordeiro, G. C., & Toledo Filho, R. D. (2016). Fresh and hardened-state properties of self-compacting lightweight concrete reinforced with steel fibers. *Construction and Building Materials*, *104*, 284-292.

Hasgul, U., Turker, K., Birol, T., & Yavas, A. (2018). Flexural behavior of ultra-high-performance fiber reinforced concrete beams with low and high reinforcement ratios. *Structural Concrete*, *19*(6), 1577-1590.

Hassan, A. A. A., Hossain, K. M. A., & Lachemi, M. (2008). Behavior of full-scale self-consolidating concrete beams in shear. *Cement and Concrete Composites*, *30*(7), 588-596.

Hassan, A. A. A., Ismail, M. K., & Mayo, J. (2015). Mechanical Properties of Self-Consolidating Concrete Containing Lightweight Recycled Aggregate in Different Mixture Compositions. *Journal of Building Engineering*, 4, 113-126.

Hassan, A. A., Ismail, M. K., & Mayo, J. (2015). Shear behavior of SCC beams with different coarse-to-fine aggregate ratios and coarse aggregate types. *Journal of Materials in Civil Engineering*, *27*(11), 04015022.

Hassan, A. A., Lachemi, M., & Hossain, K. M. (2012). Effect of metakaolin and silica fume on the durability of self-consolidating concrete. *Cement and concrete composites*, *34*(6), 801-807.

Hassanpour, M., Shafigh, P., & Mahmud, H. B. (2012). Lightweight aggregate concrete fiber reinforcement–A review. *Construction and Building Materials*, *37*, 452-461.

Haug, A. K., & Fjeld, S. (1996). A floating concrete platform hull made of lightweight aggregate concrete. *Engineering Structures*, *18*(11), 831-836.

Henager, C. H., & Doherty, T. J. (1976). Analysis of reinforced fibrous concrete beams. *Journal of the Structural Division*, *102*(1), 177-188.

Hilal, N., Hamah Sor, N., and Faraj, R. H. (2021). Development of eco-efficient lightweight self-compacting concrete with high volume of recycled EPS waste materials. *Environmental Science and Pollution Research*, *28*(36), 50028-50051.

Hossain, K. M. A., Hasib, S., & Manzur, T. (2020). Shear behavior of novel hybrid composite beams made of self-consolidating concrete and engineered cementitious composites. *Engineering Structures*, *202*, 109856.

Hossain, K. M. A., Lachemi, M., Sammour, M., & Sonebi, M. (2013). Strength and fracture energy characteristics of self-consolidating concrete incorporating polyvinyl alcohol, steel and hybrid fibres. *Construction and Building Materials*, *45*, 20-29.

Imam, M., Vamdewalle, L., & Mortelmans, F. (1994). Shear capacity of steel fiber high-strength concrete beams. *Special Publication*, *149*, 227-242.

Iqbal, S., Ali, A., Holschemacher, K., & Bier, T. A. (2015). Mechanical Properties of Steel Fiber Reinforced High Strength Lightweight Self-Compacting Concrete (SHLSCC). *Construction and Building Materials*, 98, 325-333.

Iqbal, S., Ali, A., Holschemacher, K., Bier, T. A., & Shah, A. A. (2016). Strengthening of RC beams using steel fiber reinforced high strength lightweight self-compacting concrete (SHLSCC) and their strength predictions. *Materials & Design*, *100*, 37-46.

Ismail, M. K., & Hassan, A. A. (2016). Use of metakaolin on enhancing the mechanical properties of self-consolidating concrete containing high percentages of crumb rubber. *Journal of Cleaner Production*, *125*, 282-295.

Ismail, M. K., & Hassan, A. A. (2017). Use of Steel Fibers to Optimize Self-Consolidating Concrete Mixtures Containing Crumb Rubber. *ACI Materials Journal*, *114*(4).

Ismail, M. K., & Hassan, A. A. (2021). Influence of fibre type on the shear behaviour of engineered cementitious composite beams. *Magazine of Concrete Research*, *73*(9), 464-475.

Ismail, M. K., & Hassan, A. A. A. (2015). Influence of mixture composition and type of cementitious materials on enhancing the fresh properties and stability of self-consolidating rubberized concrete. *Journal of Materials in Civil Engineering*, 28(1), 04015075.

Ismail, M. K., Hassan, A. A., & Lachemi, M. (2018). Effect of Fiber Type on Impact and Abrasion Resistance of Engineered Cementitious Composite. *ACI Materials Journal*, *115*(6).

Jiang, D., Wang, G., Montaruli, B. C., & Richardson, K. L. (2004, May). Concrete offshore LNG terminals-A viable solution and technical challenges. In *Offshore Technology Conference*. OnePetro.

Joshi, S. S., Thammishetti, N., & Prakash, S. S. (2018). Efficiency of steel and macro-synthetic structural fibers on the flexure-shear behaviour of prestressed concrete beams. *Engineering Structures*, *171*, 47-55.

Jun Li, J., gang Niu, J., jun Wan, C., Jin, B., & liu Yin, Y. (2016). Investigation on mechanical properties and microstructure of high performance polypropylene fiber reinforced lightweight aggregate concrete. *Construction and Building Materials*, *118*, 27-35.

Jun Li, J., jun Wan, C., gang Niu, J., feng Wu, L., & chao Wu, Y. (2017). Investigation on flexural toughness evaluation method of steel fiber reinforced lightweight aggregate concrete. *Construction and Building Materials*, *131*, 449-458.

Kang, T. H., Kim, W., Kwak, Y. K., & Hong, S. G. (2011). Shear testing of steel fiber-reinforced lightweight concrete beams without web reinforcement. *ACI Structural Journal*, *108*(5), 553.

Karahan, O., Hossain, K. M., Ozbay, E., Lachemi, M., & Sancak, E. (2012). Effect of metakaolin content on the properties self-consolidating lightweight concrete. *Construction and Building Materials*, *31*, 320-325.

Kayali, O. (2008). Fly ash lightweight aggregates in high performance concrete. *Construction and building materials*, *22*(12), 2393-2399.

Kayali, O., Haque, M. N., & Zhu, B. (2003). Some characteristics of high strength fiber reinforced lightweight aggregate concrete. *Cement and Concrete Composites*, *25*(2), 207-213.

Khayat, K. H., Kassimi, F., & Ghoddousi, P. (2014). Mixture Design and Testing of Fiber-Reinforced Self-Consolidating Concrete. *ACI Materials Journal*, 111(2), 143-151.

Khayat, K. H., Paultre, P., & Tremblay, S. (2001). Structural performance and in-place properties of self-consolidating concrete used for casting highly reinforced columns. *Materials Journal*, *98*(5), 371-378.

Kılıç, A., Atiş, C. D., Yaşar, E., & Özcan, F. (2003). High-strength lightweight concrete made with scoria aggregate containing mineral admixtures. *Cement and Concrete Research*, *33*(10), 1595-1599.

Kim, H. K., Jeon, J. H., & Lee, H. K. (2012). Workability, and mechanical, acoustic and thermal properties of lightweight aggregate concrete with a high volume of entrained air. *Construction and Building Materials*, *29*, 193-200.

Kim, M. J., Yoo, D. Y., Kim, S., Shin, M., & Banthia, N. (2018). Effects of fiber geometry and cryogenic condition on mechanical properties of ultra-high-performance fiber-reinforced concrete. *Cement and Concrete Research*, *107*, 30-40.

Kim, Y. J., Choi, Y. W., & Lachemi, M. (2010). Characteristics of self-consolidating concrete using two types of lightweight coarse aggregates. *Construction and Building Materials*, *24*(1), 11-16.

Ko, D., & Choi, H. (2013). Truss rail method for punching shear strength of flat-plate slab-column using high-strength lightweight concrete. *Magazine of Concrete Research*, 65(10), 589–599.

Kowalsky, M. J., Priestly, M. N., & Seible, F. (1999). Shear and flexural behavior of lightweight concrete bridge columns in seismic regions. *ACI structural journal*, *96*, 136-148.

Kwon, S. J., Yang, K. H., & Mun, J. H. (2018). Flexural tests on externally post-tensioned lightweight concrete beams. *Engineering Structures*, *164*, 128-140.

Lachemi, M., Hossain, K. M., Lambros, V., & Bouzoubaa, N. (2003). Development of cost-effective self-consolidating concrete incorporating fly ash, slag cement, or viscosity-modifying admixtures. ACI Materials Journal, 100(5), 419-425.

Law Yim Wan, D. S., Aslani, F., & Ma, G. (2018). Lightweight self-compacting concrete incorporating perlite, scoria, and polystyrene aggregates. *Journal of Materials in Civil Engineering*, *30*(8), 04018178.

Lee, G. C., Shih, T. S., & Chang, K. C. (1988). Mechanical properties of concrete at low temperature. *Journal of cold regions engineering*, *2*(1), 13-24.

Li, J., Wan, C., Niu, J., Wu, L., & Wu, Y. (2017). Investigation on flexural toughness evaluation method of steel fiber reinforced lightweight aggregate concrete. *Construction and Building Materials*, 131, 449-458.

Libre, N. A., Shekarchi, M., Mahoutian, M., & Soroushian, P. (2011). Mechanical properties of hybrid fiber reinforced lightweight aggregate concrete made with natural pumice. *Construction and Building Materials*, 25(5), 2458-2464.

Liu, C. (2011). Experimental investigation on mechanical property of concrete exposed to low temperatures. *master's thesis, Tsinghua University, Beijing, PR China*.

Liu, X., Zhang, M. H., Chia, K. S., Yan, J., & Liew, J. R. (2016). Mechanical properties of ultra-lightweight cement composite at low temperatures of 0 to− 60° C. *Cement and Concrete Composites*, *73*, 289-298.

Lotfy, A., Hossain, K. M., & Lachemi, M. (2016). Mix design and properties of lightweight self-consolidating concretes developed with furnace slag, expanded clay and expanded shale aggregates. *Journal of Sustainable Cement-Based Materials*, *5*(5), 297-323.

Lotfy, A., Hossain, K. M., & Lachemi, M. (2016). Durability properties of lightweight self-consolidating concrete developed with three types of aggregates. *Construction and Building Materials*, *106*, 43-54.

MacGregor, J. G., Wight, J. K., Teng, S., & Irawan, P. (1997). *Reinforced concrete: Mechanics and design* (Vol. 3). New Jersey: Prentice Hall.

Madandoust, R., & Mousavi, S. Y. (2012). Fresh and Hardened Properties of Self-Compacting Concrete Containing Metakaolin. Construction and Building Materials, 35, 752-760.

Malhotra, V. M., Carette, G. G., & Bilodeau, A. (1994). Mechanical properties and durability of polypropylene fiber reinforced high-volume fly ash concrete for shotcrete applications. *Materials Journal*, *91*(5), 478-486.

Mansur, M. A., Ong, K. C. G., & Paramasivam, P. (1986). Shear strength of fibrous concrete beams without stirrups. *Journal of structural engineering*, *112*(9), 2066-2079.

Marar, K., & Eren, O. (2011). Effect of Cement Content and Water/ Cement Ratio on Fresh Concrete Properties without Admixtures. International Journal of Physical Sciences, 6(24), 5752-5765.

Mazaheripour, H., Ghanbarpour, S., Mirmoradi, S. H., & Hosseinpour, I. (2011). The effect of polypropylene fibers on the properties of fresh and hardened lightweight self-compacting concrete. *Construction and Building Materials*, 25(1), 351-358.

Melby, K., Jordet, E. A., & Hansvold, C. (1996). Long-span bridges in Norway constructed in high-strength LWA concrete. *Engineering structures*, *18*(11), 845-849.

Mitchell, D. W., and Marzouk, H. (2007). Bond characteristics of high-strength lightweight concrete. *ACI Structural Journal*, *104*(1), 22.

Miura, T. (1989). The properties of concrete at very low temperatures. *Materials and Structures*, *22*(4), 243-254.

Montejo, L. A., Sloan, J. E., Kowalsky, M. J., & Hassan, T. (2008). Cyclic response of reinforced concrete members at low temperatures. *Journal of Cold Regions Engineering*, *22*(3), 79-102.

Mousa, A., Mahgoub, M., & Hussein, M. (2018). Lightweight concrete in America: presence and challenges. *Sustainable Production and Consumption*, *15*, 131-144.

Muñoz-Ruiperez, C., Rodríguez, Á., Junco, C., Fiol, F., & Calderon, V. (2018). Durability of lightweight concrete made concurrently with waste aggregates and expanded clay. *Structural Concrete*, *19*(5), 1309-1317.

Narayanan, R., & Darwish, I. Y. S. (1987). Use of steel fibers as shear reinforcement. *Structural Journal*, *84*(3), 216-227.

Nehdi, M., & Ladanchuk, J. D. (2004). Fiber synergy in fiber-reinforced self-consolidating concrete. *Materials Journal*, *101*(6), 508-517.

Nepomuceno, M. C., Pereira-de-Oliveira, L. A., and Pereira, S. F. (2018). Mix design of structural lightweight self-compacting concrete incorporating coarse lightweight expanded clay aggregates. *Construction and Building Materials*, *166*, 373-385.

Nes, L. G., & Øverli, J. A. (2016). Structural behaviour of layered beams with fibre-reinforced LWAC and normal density concrete. *Materials and Structures*, *49*(1), 689-703.

NRMCA (National Ready Mixed Concrete Association). (2003). CIP 36-Structural Lightweight Concrete. *NRMCA,* Washington, DC.

Oh, B. H. (1992). Flexural analysis of reinforced concrete beams containing steel fibers. *Journal of structural engineering*, *118*(10), 2821-2835.

Omar, A. T., & Hassan, A. A. (2019). Use of polymeric fibers to improve the mechanical properties and impact resistance of lightweight SCC. *Construction and Building Materials*, *229*, 116944.

Omar, A. T., & Hassan, A. A. (2021). Shear behavior of lightweight self-consolidating concrete beams containing coarse and fine lightweight aggregates. *ACI Structural Journal*, *118*(3), 175-186.

Omar, A. T., & Hassan, A. A. (2021). Behaviour of expanded slate semi-lightweight SCC beams with improved cracking performance and shear capacity. In *Structures, 32,* 1577-1588.

Omar, A. T., Ismail, M. K., & Hassan, A. A. (2020). Use of polymeric fibers in the development of semilightweight self-consolidating concrete containing expanded slate. *Journal of Materials in Civil Engineering*, *32*(5), 04020067.

Omar, A. T., Sadek, M. M., & Hassan, A. A. (2020). Impact resistance and mechanical properties of lightweight self-consolidating concrete under cold temperatures. *ACI Materials Journal*, *117*(5), 81-91.

Oti, J. E., Kinuthia, J. M., Bai, J., Delpak, R., & Snelson, D. G. (2010). Engineering properties of concrete made with slate waste. *Proceedings of the Institution of Civil Engineers-Construction Materials*, *163*(3), 131-142.

Papanicolaou, C. G., & Kaffetzakis, M. I. (2011). Lightweight aggregate self-compacting concrete: state-of-the-art & pumice application. *Journal of Advanced Concrete Technology*, *9*(1), 15-29.

Passuello, A., Moriconi, G., & Shah, S. P. (2009). Cracking behavior of concrete with shrinkage reducing admixtures and PVA fibers. *Cement and Concrete Composites*, *31*(10), 699-704.

Paultre, P., Khayat, K. H., Cusson, D., & Tremblay, S. (2005). Structural performance of self-consolidating concrete used in confined concrete columns. *ACI structural journal*, *102*(4), 560-568.

Pigeon, M., & Cantin, R. (1998). Flexural properties of steel fiber-reinforced concretes at low temperatures. *Cement and Concrete Composites*, *20*(5), 365-375.

Rabbat, B. G., Daniel, J. I., Weinmann, T. L., and Hanson, N. W. (1986). Seismic behavior of lightweight and normal weight concrete columns. In *Journal Proceedings* (Vol. 83, No. 1, pp. 69-79).

Raithby, K. D., & Lydon, F. D. (1981). Lightweight concrete in highway bridges. *International Journal of Cement Composites and Lightweight Concrete*, *3*(2), 133-146.

Rashid, M. A., & Mansur, M. A. (2005). Reinforced high-strength concrete beams in flexure. *ACI Structural Journal*, *102*(3), 462.

Reda Taha, M. M., El-Dieb, A. S., Abd El-Wahab, M. A., & Abdel-Hameed, M. E. (2008). Mechanical, fracture, and microstructural investigations of rubber concrete. *Journal of materials in civil engineering*, *20*(10), 640-649.

RILEM. (2003). RILEM-TC-162-TDF: Test and design methods for steel fibre reinforced concrete, stress-strain design method. *Final recommendation. Materials and Structures 36*, pp. 560–567.

Rodriguez, S. (2004). Design of long span concrete box girder bridges: Challenges and solutions. In *Structures 2004: Building on the Past, Securing the Future* (pp. 1-11).

Rostasy, F. S., & Wiedemann, G. (1980). Stress-strain-behaviour of concrete at extremely low temperature. *Cement and concrete research*, *10*(4), 565-572.

Sadek, M. M., and Hassan, A. A. (2021). Abrasion and Scaling Resistance of Lightweight Self-Consolidating Concrete Containing Expanded Slate Aggregate. *ACI Materials Journal*, *118*(2), 31-42.

Sadek, M. M., Ismail, M. K., & Hassan, A. A. (2020). Stability of lightweight self-consolidating concrete containing coarse and fine expanded slate aggregates. *ACI Materials Journal*, *117*(3), 133-143.

Sari, D., & Pasamehmetoglu, A. G. (2005). The effects of gradation and admixture on the pumice lightweight aggregate concrete. *Cement and concrete research*, *35*(5), 936-942.

Shafigh, P., Mahmud, H., & Jumaat, M. Z. (2011). Effect of steel fiber on the mechanical properties of oil palm shell lightweight concrete. *Materials & Design*, *32*(7), 3926-3932.

Shannag, M. J., Barakat, S., & Abdul-Kareem, M. (2002). Cyclic behavior of HPFRC-repaired reinforced concrete interior beam-column joints. *Materials and Structures*, *35*(6), 348-356.

Sharma, A. K. (1986). Shear strength of steel fiber reinforced concrete beams. In *Journal Proceedings* (Vol. 83, No. 4, pp. 624-628).

Sherwood, E. G., Bentz, E. C., & Collins, M. P. (2007). Effect of aggregate size on beam-shear strength of thick slabs. *ACI Structural Journal*, *104*(2), 180.

Shi, C., & Wu, Y. (2005). Mixture proportioning and properties of self-consolidating lightweight concrete containing glass powder. *ACI Materials Journal*, *102*(5), 355.

Shi, C., & Yang, X. (2005). Design and application of self-consolidating lightweight concretes. *Proceedings of 1st Int. RILEM Symp. on design, performance and use of self-consolidating concrete*. RILEM Publication SARL, Paris, France, 55-64.

Shi, C., Yang, X., Yu, Z., & Khayat, H. (2005). Design and application of self-compacting lightweight concretes. In *SCC'2005-China: 1st International Symposium on Design, Performance and Use of Self-Consolidating Concrete* (pp. 55-64). RILEM Publications SARL.

Sin, L. H., Huan, W. T., Islam, M. R., & Mansur, M. A. (2011). Reinforced Lightweight Concrete Beams in Flexure. *ACI Structural Journal*, *108*(1).

Singh, M., Saini, B., & Chalak, H. D. (2019). Performance and composition analysis of engineered cementitious composite (ECC)–A review. *Journal of Building Engineering*, *26*, 100851.

Standard, British. (1997). BS 8110 Part 1, Structural use of concrete part 1. Code of practice for design and construction. *British Standard Institution*, London, UK.

Szydlowki, R., & Mieszcak, M. (2017). Study of application of lightweight aggregate concrete to construct post-tensioned long-span slabs. *Procedia Engineering*, *172*, 1077-1085.

Taylor, H. P. (1974). The fundamental behavior of reinforced concrete beams in bending and shear. *Special Publication*, *42*, 43-78.

Ting, T. Z. H., Rahman, M. E., Lau, H. H., & Ting, M. Z. Y. (2019). Recent development and perspective of lightweight aggregates based self-compacting concrete. *Construction and Building Materials*, *201*, 763-777.

Topcu, İ. B. (1997). Assessment of the brittleness index of rubberized concretes. *Cement and Concrete Research*, *27*(2), 177-183.

Topçu, I. B., & Uygunoğlu, T. (2010). Effect of aggregate type on properties of hardened self-consolidating lightweight concrete (SCLC). *Construction and Building Materials*, *24*(7), 1286-1295.

Umehara, H., Uehara, T., Enomoto, Y., & Oka, S. (1994). Development and usage of lightweight high-performance concrete. Proceedings of International Conference on

high Performance Concrete (supplementary papers), Singapore, *American Concrete Institute,* Detroit, USA, 339-53.

Uygunoğlu, T., & Topçu, İ. B. (2009). Thermal expansion of self-consolidating normal and lightweight aggregate concrete at elevated temperature. *Construction and Building Materials*, *23*(9), 3063-3069.

Wang, H. T., & Wang, L. C. (2013). Experimental study on static and dynamic mechanical properties of steel fiber reinforced lightweight aggregate concrete. *Construction and Building Materials*, *38*, 1146-1151.

Wang, S., & Li, V. C. (2007). Engineered cementitious composites with high-volume fly ash. *ACI Materials journal*, *104*(3), 233.

Wild, S., Khatib, J. M., & Jones, A. (1996). Relative strength, pozzolanic activity and cement hydration in superplasticised metakaolin concrete. *Cement and concrete research*, *26*(10), 1537-1544.

Wu, H. C., & Li, V. C. (1994). Trade-off between strength and ductility of random discontinuous fiber reinforced cementitious composites. *Cement and concrete composites*, *16*(1), 23-29.

Wu, T., Wei, H., and Liu, X. (2018). Shear strength of interior beam–column joints with lightweight aggregate concrete. *Magazine of Concrete Research*, *70*(3), 109-128.

Wu, Z., Zhang, Y., Zheng, J., & Ding, Y. (2009). An experimental study on the workability of self-compacting lightweight concrete. *Construction and Building Materials*, 23(5), 2087-2092.

Xie, J., & Yan, J. B. (2018). Experimental studies and analysis on compressive strength of normal-weight concrete at low temperatures. *Structural Concrete*, *19*(4), 1235-1244.

Yamane, S., Kasami, H., & Okuno, T. (1978). Properties of concrete at very low temperatures. *Special Publication*, *55*, 207-222.

Yang, K. H., & Ashour, A. F. (2011). Aggregate interlock in lightweight concrete continuous deep beams. *Engineering Structures*, *33*(1), 136-145.

Yang, K. H., Mun, J. H., & Lee, J. S. (2014). Flexural tests on pre-tensioned lightweight concrete beams. *Proceedings of the Institution of Civil Engineers-Structures and Buildings*, *167*(4), 203-216.

Yang, K. H., Mun, J. H., Hwang, S. H., & Song, J. K. (2020). Flexural capacity and ductility of lightweight concrete T-beams. *Structural Concrete*, *21*(6), 2708-2721.

Yang, K. H., Sim, J. I., Kang, J. H., & Ashour, A. F. (2012). Shear capacity of monolithic concrete joints without transverse reinforcement. *Magazine of Concrete Research*, *64*(9), 767-779.

Yang, L. H., Han, Z., & Li, C. F. (2011). Strengths and flexural strain of CRC specimens at low temperature. *Construction and Building Materials*, *25*(2), 906-910.

Yao, S. X., & Gerwick, B. C. (2006). Development of Self-Compacting Lightweight Concrete for RFP Reinforced Floating Concrete Structures. Technical Report, California, USA.

Younis, A., Ebead, U., & Shrestha, K. C. (2017). Different FRCM systems for shear-strengthening of reinforced concrete beams. *Construction and Building Materials*, *153*, 514-526.

Yu, Q. L., Spiesz, P., and Brouwers, H. J. H. (2015). Ultra-lightweight concrete: Conceptual design and performance evaluation. *Cement and Concrete Composites*, *61*, 18-28.